EXTRACTION OF HEAVY METALS AND PHENOLIC POLLUTANTS FROM ENVIRONMENTAL SYSTEMS UTILIZING DESIGNER GREEN SOLVENTS

IRFAN WAZEER

FACULTY OF ENGINEERING
UNIVERSITI MALAYA
KUALA LUMPUR

2025

EXTRACTION OF HEAVY METALS AND PHENOLIC POLLUTANTS FROM ENVIRONMENTAL SYSTEMS UTILIZING DESIGNER GREEN SOLVENTS

IRFAN WAZEER

THESIS SUBMITTED IN FULFILMENT OF THE

REQUIREMENTS FOR THE DEGREE OF DOCTOR OF

PHILOSOPHY

DEPARTMENT OF CHEMICAL ENGINEERING
FACULTY OF ENGINEERING
UNIVERSITI MALAYA
KUALA LUMPUR

2025

UNIVERSITI MALAYA

ORIGINAL LITERARY WORK DECLARATION

Name of Candidate: **IRFAN WAZEER**

Registration/Matrix No.: **S2042966/1**

Name of Degree: **Doctor of Philosophy**

Title: **EXTRACTION OF HEAVY METALS AND PHENOLIC POLLUTANTS FROM ENVIRONMENTAL SYSTEMS UTILIZING DESIGNER GREEN SOLVENTS.**

Field of Study: **Purification & Separation Processes (NEC 524: Chemical Process)**

I do solemnly and sincerely declare that:

(1) I am the sole author/writer of this Work;
(2) This work is original;
(3) Any use of any work in which copyright exists was done by way of fair dealing and for permitted purposes and any excerpt or extract from, or reference to or reproduction of any copyright work has been disclosed expressly and sufficiently and the title of the Work and its authorship have been acknowledged in this Work;
(4) I do not have any actual knowledge nor do I ought reasonably to know that the making of this work constitutes an infringement of any copyright work;
(5) I hereby assign all and every rights in the copyright to this Work to the University of Malaya ("UM"), who henceforth shall be owner of the copyright in this Work and that any reproduction or use in any form or by any means whatsoever is prohibited without the written consent of UM having been first had and obtained;
(6) I am fully aware that if in the course of making this Work I have infringed any copy- right whether intentionally or otherwise, I may be subject to legal action or any other action as may be determined by UM.

Candidate's Signature Date:11/08/2024

Subscribed and solemnly declared before,

Witness's Signature Date:11/08/2024

Name:

Designation:

EXTRACTION OF HEAVY METALS AND PHENOLIC POLLUTANTS FROM ENVIRONMENTAL SYSTEMS UTILIZING DESIGNER GREEN SOLVENTS

ABSTRACT

Water pollution is a critical and problematic issue that threatens the sustainability of human civilization. Heavy metals such as cadmium and lead are responsible for myriad environmental problems due to their toxicity. In addition, phenol and cresol isomers are classified as priority phenolic pollutants due to their high toxicity to human health and aquatic life. Therefore, these pollutants must be removed from waste streams before they are released into the environment. Several volatile organic compounds (VOCs) that have been used as extractants are toxic, volatile, and flammable. A class of neoteric solvents called hydrophobic deep eutectic solvents (HDES) have recently attracted considerable interest from both academia and industry. HDES are generally immiscible with water solutions and exhibit high extraction efficiency for various target analytes. The objective of this thesis is to investigate the feasibility of HDES for the removal of heavy metals and phenolic contaminants by liquid-liquid extraction (LLE) processes. Conductor-like Screening Model for Real Solvents (COSMO-RS) was used for the possible selection of potential HDES. In addition, different correlations were used to ascertain the reliability of the experimental data. Based on the COSMO-RS screening and the availability of chemicals in the laboratory, some potential HDES were selected for the extraction of phenolic contaminants. The HDES were characterized by measuring their main physical properties such as melting point, stability, viscosity, and density. To understand the formation of intermolecular interactions such as hydrogen bonds between the precursors of HDES, FTIR and ^{1}HNMR analyses were performed. For the removal of cresols, six HDES were experimentally investigated, and all HDES showed very high efficiency in removing cresols from water. The effects of contact time, mass ratio of HDES to water, initial concentration, and molar ratio of HDES were also investigated for the three

selected HDES. The extraction efficiency of > 94% was achieved for the removal of cresol isomers from wastewater with all prepared HDES. For the removal of phenol, the TOPO-based HDES showed higher extraction efficiency (up to 96%). The study also examines the extraction of lead and cadmium with eight HDES. Among eight HDES, thymol:decanoic acid (1:1 molar ratio) showed the highest efficiency: 93.49% for lead at 1000 ppm and 76.70% for cadmium at 100 ppm. Optimization of parameters such as HDES molar ratio, contact time, pH and HDES to water mass ratio further improves performance. Regeneration and reuse of the HDESs has proven effective over multiple cycles, with minimal loss of efficiency. Terpene-based HDESs have also been investigated for the extraction of iron and copper. Thymol:decanoic acid shows an extraction efficiency of 93.91% for iron at 100 ppm, while menthol:decanoic acid achieves an efficiency of 74.69% for copper at 10 ppm. The extraction mechanism is explored using FTIR spectra and the solvents show high reusability and sustainability. In this study, a total of 10 HDES are utilized. The results highlight the effectiveness of HDESs as sustainable and scalable solutions for environmental remediation.

Keywords: HDES, Phenol, Heavy metals, Liquid-liquid extraction, COSMO-RS.

PENGEKSTRAKAN LOGAM BERAT DAN BAHAN PENCEMAR FENOLIK DARI SISTEM ALAM SEKITAR MENGGUNAKAN PELARUT HIJAU DIREKABENTUK

ABSTRAK

Pencemaran air merupakan isu kritikal dan masalah yang mengancam kelestarian tamadun manusia. Logam berat seperti kadmium dan plumbum menjadi punca kepada pelbagai masalah alam sekitar akibat ketoksikan mereka. Selain itu, fenol dan isomer kresol diklasifikasikan sebagai pencemar fenolik yang diberi keutamaan kerana ketoksikan mereka yang tinggi terhadap kesihatan manusia dan kehidupan akuatik. Oleh itu, pencemar ini mesti dikeluarkan daripada aliran sisa sebelum dilepaskan ke alam sekitar. Beberapa sebatian organik mudah meruap (VOC) yang telah digunakan sebagai bahan pengekstrak adalah toksik, mudah meruap, dan mudah terbakar. Satu kelas pelarut baharu yang dikenali sebagai pelarut eutek hidrofobik (HDES) telah menarik minat yang besar dari kalangan akademik dan industri. HDES secara amnya tidak larut dengan larutan berair dan menunjukkan kecekapan pengekstrakan yang tinggi untuk pelbagai bahan analitikal sasaran. Objektif tesis ini adalah untuk menyiasat kebolehlaksanaan HDES untuk penyingkiran logam berat dan pencemar fenolik melalui proses pengekstrakan cecair-cecair (LLE). Model Saringan Seperti Konduktor untuk Pelarut Sebenar (COSMO-RS) telah digunakan untuk pemilihan HDES yang berpotensi. Selain itu, beberapa korelasi digunakan untuk memastikan kebolehpercayaan data eksperimen. Berdasarkan saringan COSMO-RS dan ketersediaan bahan kimia di makmal, beberapa HDES yang berpotensi telah dipilih untuk pengekstrakan bahan pencemar fenolik. HDES tersebut telah dicirikan dengan mengukur sifat fizikal utama mereka seperti takat lebur, kestabilan, kelikatan, dan ketumpatan. Untuk memahami pembentukan interaksi antara molekul seperti ikatan hidrogen antara prekursor HDES, analisis FTIR dan 1H NMR telah dijalankan. Untuk penyingkiran kresol, enam HDES telah disiasat melalui eksperimen,

dan kesemua HDES menunjukkan kecekapan yang sangat tinggi dalam penyingkiran kresol daripada air. Kesan masa sentuhan, nisbah jisim HDES kepada air, kepekatan awal, dan nisbah molar HDES juga telah disiasat untuk tiga HDES yang dipilih. Kecekapan pengekstrakan lebih daripada 94% telah dicapai untuk penyingkiran isomer kresol dari air buangan dengan semua HDES yang disediakan. Untuk penyingkiran fenol, HDES berasaskan TOPO menunjukkan kecekapan pengekstrakan yang lebih tinggi (sehingga 96%). Kajian ini juga meneliti pengekstrakan plumbum dan kadmium dengan lapan HDES. Antara lapan HDES, thymol: asid dekanoik (nisbah molar 1:1) menunjukkan kecekapan tertinggi: 93.49% untuk plumbum pada 1000 ppm dan 76.70% untuk kadmium pada 100 ppm. Pengoptimuman parameter seperti nisbah molar HDES, masa sentuhan, pH, dan nisbah jisim HDES kepada air meningkatkan lagi prestasi. Regenerasi dan penggunaan semula HDES telah terbukti berkesan dalam beberapa kitaran, dengan kehilangan kecekapan yang minimum. HDES berasaskan terpena juga telah disiasat untuk pengekstrakan besi dan tembaga. Thymol: asid dekanoik menunjukkan kecekapan pengekstrakan sebanyak 93.91% untuk besi pada 100 ppm, manakala menthol:asid dekanoik mencapai kecekapan sebanyak 74.69% untuk tembaga pada 10 ppm. Mekanisme pengekstrakan diterokai menggunakan spektra FTIR dan pelarut menunjukkan kebolehgunaan semula dan kelestarian yang tinggi. Dalam kajian ini, sejumlah 10 HDES digunakan. Keputusan ini menonjolkan keberkesanan HDES sebagai penyelesaian lestari dan boleh diskala-besarkan untuk pemulihan alam sekitar.

Keywords: HDES, fenol, logam berat, pengekstrakan cecair-cecair, COSMO-RS.

ACKNOWLEDGEMENTS

Almighty God, Allah S.W.T., I thank You for all the blessings You have bestowed upon me during this doctoral journey and for making it a success.

Secondly, I would like to express my utmost gratitude to my PhD supervisors, Dr. Hanee Farzana Binti Hizaddin, Prof. Mohd Ali Hashim and Dr. Mohamed K. Hadj-Kali. Their unwavering support, invaluable advice and profound knowledge helped me to complete my PhD thesis. Without their mentorship, encouragement and constructive feedback, this journey would not have been possible. I greatly appreciate their commitment to my academic and personal growth.

My heartfelt gratitude goes to my family, especially my parents, brother, and wife, for their unwavering support and prayers. Their unwavering belief in my abilities has been a constant source of motivation. They have always pushed me to bring out the best in me and they have kept faith in me through every challenge. Regardless of time, space and distance, your positivity and determination have been my pillars of strength.

I am also very grateful to my colleagues, lab mates and friends, Dr. Muhammad Omer Aijaz, Engr. Muhammad Shafiq, Dr. Mohammed Abobakr Al-Maari, Dr. Lahssen El Blidi and Dr. Sarwono Mulyono for their constant support. I thank you for all your help in the laboratory, for your insightful advice and for the many discussions that have enriched my research.

I would like to acknowledge the support of my institution for providing me with the necessary resources and environment for my research. In addition, I am grateful to the funding agencies and organizations that have supported my research financially.

Thank you all for being part of this incredible journey. Your support, guidance and encouragement have been indispensable, and I am deeply grateful to each and every one of you.

TABLE OF CONTENTS

LIST OF FIGURES

LIST OF TABLES

LIST OF SYMBOLS AND ABBREVIATIONS

$\gamma\infty$	:	Activity coefficient at infinite dilution
γ_{phenol}^{∞}	:	Activity coefficient of phenol at infinite dilution
γ_{water}^{∞}	:	Activity coefficient of water at infinite dilution
ρ	:	Density
C_0	:	Analyte concentration in the water phase before the extraction
C_1	:	Analyte concentration in the water phase after the extraction
C_{set}	:	Concentration of the extractant phase
C_{phenol}^{∞}	:	Capacity of phenol at infinite dilution
$c_{phenolic}^{initial}$	:	Initial concentration of phenolic pollutant in aqueous phase
$c_{phenolic}^{final}$	:	Final concentration of phenolic pollutant in aqueous phase
V_{set}	:	Volume of the extractant phase
V_0	:	Volume of the initial water phase
$M_{aq,ini}$	:	Initial concentration of metal in the aqueous phase
$M_{aq,eql}$	:	Equilibrium concentration of metal in the aqueous phase
S_{phenol}^{∞}	:	Selectivity of phenol at infinite dilution
σ	:	Sigma
u	:	Standard uncertainty
σhb	:	Specific threshold for hydrogen bonding
μ	:	Viscosity
s	:	Standard deviation of the measurements
n	:	Number of measurements
$D_{phenolic}$	:	Distribution ratio for phenolic pollutants
D_{water}	:	Distribution ratio for water
$x_{phenolic}^{B}$	:	Concentration of phenolic pollutants in bottom phase

$x^{T}_{phenolic}$	:	Concentration of phenolic pollutants in top phase
x^{B}_{water}	:	Concentration of water in bottom phase
x^{T}_{water}	:	Concentration of water in top phase
x_i	:	Composition of each constituent
x'_1	:	Water concentration in water rich-phase
x'_2	:	Phenol concentration in water rich-phase
x'_3	:	HDES concentration in water rich-phase
x''_1	:	Water concentration in HDES rich-phase
x''_2	:	Phenol concentration in HDES rich-phase
x''_3	:	HDES concentration in HDES rich-phase
m_i	:	Mass of each constituent
m_{total}	:	Total mass of the phase
w'_{phenol}	:	Concentration of phenolic pollutant in extract phase
w''_{phenol}	:	Concentration of phenolic pollutant in raffinate phase
w''_{water}	:	Concentration of water in raffinate phase
w'_{HDES}	:	Concentration of water in extract phase
a	:	Intercept constant in Hand correlation
b	:	Slope constant in Hand correlation
c	:	Intercept constant in Othmer-Tobias
d	:	Slope constant in Othmer-Tobias
R^2	:	linear regression
π-π	:	pi-pi noncovalent interactions
^{1}HNMR	:	Proton nuclear magnetic resonance
2-CP	:	2-chlorophenol
3-CP	:	3-chlorophenol

4-CP	:	4-chlorophenol
2,3-CP	:	2,3-chlorophenol
2,4-DCP	:	2,4-dichlorophenol
2,4,6-TCP	:	2,4,6-trichlorophenol
3,4-CP	:	3,4-chlorophenol
4-NP	:	Nitrophenol
AAS	:	atomic absorption spectroscopy
ASA	:	Acetylsalicylic acid
BHB	:	Butyl 4-hydroxybenzoate
BTFA	:	Benzoyltrifluoroacetone
BPA	:	Bisphenol-A
ChCl	:	Choline chloride
CMP	:	Camphor
COSMO-RS	:	Conductor-like Screening Model for Real Solvents
D	:	Distribution ratio
DCA	:	Dichloroacetic acid
DDC	:	1-dodecanol
DdecA	:	Dodecanoic acid
DecA	:	Decanoic acid
DESs	:	Deep eutectic solvents
DHBP	:	2,4-dihydroxybenzophenone
DFT	:	Density functional theory
T_{deg}	:	Degradation temperature
DLLME	:	Dispersive liquid–liquid microextraction
DNP	:	Dinitrophenol
EE	:	Extraction efficiency

EF	:	Enrichment factor
EHB	:	2-Ethylhexyl 4-hydroxybenzoate
ELLME	:	Emulsification liquid-liquid microextraction
ER	:	Extraction recovery
EPA	:	Environmental Protection Agency
ETAAS	:	Electrothermal Atomic Absorption Spectroscopy
EU	:	European Union
FAAS	:	Flame atomic absorption spectrophotometer
FA	:	Formic acid
FTIR	:	Fourier transformation infrared
GC	:	Gas chromatography
GC-FID	:	Gas chromatography–flame ionization detection
GC-MS	:	Gas chromatography–mass spectrometry
HBA	:	Hydrogen bond acceptor
HBD	:	Hydrogen bond donor
HDC	:	Hydrocinnamic acid
HDES	:	Hydrophobic deep eutectic solvents
HMOBP	:	2-hydroxy-4-methoxybenzophenone
HPLC	:	High-performance liquid chromatography
HPLC-DAD	:	High-performance liquid chromatography with a diode-array detector
HPLC-UV	:	High-performance liquid chromatography with ultraviolet detection
HSDME	:	Headspace single-drop microextraction
HSPME	:	Headspace solid-phase microextraction
IBHB	:	Isobutyl 4-hydroxybenzoate
ICP-OES	:	Inductively coupled plasma-optical emission spectrometer

IL	:	Ionic liquids
LLE	:	Liquid-liquid extraction
LLME	:	Liquid-liquid microextraction
LOD	:	Limit of detection
LR	:	Linear range
T_m	:	Melting point
MAA	:	Methyl anthranilate
MBK	:	Methyl isobutylketone
MHB	:	Methyl 4-hydroxybenzoate
MISPE	:	Molecularly imprinted solid-phase extraction
MMF-SPME	:	Multiple monolithic fiber-solid phase microextraction
MNA	:	Mandelic acid
MPD	:	Methyl-2,4-pentanediol
MTOAB	:	Methyltrioctylammonium bromide
MTOAC	:	Methyltrioctylammonium chloride
MW	:	Molecular weight
NonA	:	Nonanoic acid
OctA	:	Octanoic acid
OA	:	Oxalic acid
OHB	:	n-octyl 4-hydroxybenzoate
PA	:	Propionic acid
PAHs	:	Polycyclic aromatic hydrocarbons
p-CP	:	p-chlorophenol
PS	:	Proton Sponge®
PSC	:	Phenyl salicylate
Rec	:	Recovery

RSD	:	Relative standard deviation
SA	:	Salicylic acid
SDME	:	Single drop microextraction
SLM	:	Supported liquid membrane
SPM	:	Spectrophotometer
SPME	:	Solid-phase microextraction
TBAB	:	Tetrabutyl ammonium bromide
TDA	:	Tetradecyl alcohol
THAB	:	Tetraheptylammonium bromide
THPTF	:	Trihexyl (tetradecyl) phosphonium tetrafluoroborate
THF	:	Tetrahydrofuran
TOMC	:	Trioctylmethylammonium chloride
TOPO	:	Trioctylphosphine oxide
TPP	:	Triphenyl phosphate
TZVPD	:	Triple zeta valence potential with diffuse functions
TTFA	:	Thenoyltrifluoroacetone
UAE	:	Ultrasound-assisted extraction
USA-DLLME	:	Ultrasonication assisted dispersive liquid-liquid micro extraction
UV-Vis	:	Ultraviolet–visible spectroscopy
VALLME	:	Vortex-assisted liquid-liquid microextraction
VOCs	:	Volatile organic compounds
WHO	:	World Health Organization

CHAPTER 1: INTRODUCTION

1.1 Background Study

Water is fundamental to life, the ecosystem, and farming, with its quality significantly influencing soil richness and crop production (Molden et al., 2010). The World Health Organization (WHO) predicts that by 2030, water scarcity will impact about 62% of the global populace (Khan et al., 2021). Water contamination is a grave issue and ranks among the top reasons for illness and mortality around the globe. There are many causes of water pollution, including household waste (Galadima et al., 2011), industrial waste (Wang & Yang, 2016), and the use of manure (Loyon, 2017), herbicides, and pesticides in agriculture (Zahoor & Mushtaq, 2023). Many contaminants are found in wastewater, including heavy metals (Akpor & Muchie, 2010; Barakat, 2011), organic solvents (Rashed, 2013; Torres et al., 2003), phenolic compounds (Villegas et al., 2016), and polycyclic aromatic hydrocarbons (PAHs) (Manoli & Samara, 2008; Nasrullah et al., 2019).

In recent years, the exponential growth of industrial processes has led to a significant increase in the volume and toxicity of industrial metal effluents (Zheng et al., 2015). Increased emissions of these metals contribute to both economic and environmental problems. Metals are a vital source of economic benefits and pollution and their consumption is expected to increase in line with global economic standards (Ongondo et al., 2011). However, the gap between supply and demand has led the European Union (EU) to designate certain metals as critical to the EU's continued economic development (Schaeffer et al., 2018). Water contaminated with high concentrations of metal salts becomes undrinkable; for certain metals, (e.g., cadmium, arsenic, lead), even trace amounts in the water are extremely toxic (Al-Mutaz & Wazeer, 2016; Madoni & Romeo, 2006; Martin & Holdich, 1986). Therefore, the removal of metal salts from water is of paramount importance to avoid environmental and health problems. In addition,

extraction of metals from water can be economically viable as some metal salts (e.g., palladium, gold, silver) become rare and expensive.

On the other hand, phenolic compounds are the major contributors to water pollution because of their high toxicity and carcinogenicity (Khan et al., 2021; Wasi et al., 2013). These compounds are primarily formed during various manufacturing processes, (e.g., polymer resins, paints, gasoline, and petrochemicals). They are often released into the atmosphere without being properly treated, resulting in significant water pollution. According to WHO, the environmental requirement for phenol in drinking water should not exceed 0.001 mg L^{-1} (Aghav et al., 2011). International bodies, including the EU and the Malaysian EPA, have set the limit for the discharge of phenol into the atmosphere at 1 ppm (Khan et al., 2021). The maximum amount of phenol that can be discharged from industrial effluents is 5 ppm (Brinda Lakshmi et al., 2013; Chen et al., 2012). Additionally, even discharge to inland or water bodies at quantities as low as 1 ppm are deemed undesirable and harmful (Debadatta & Susmita, 2015). Therefore, it is important to exclude these phenolic compounds from wastewater to meet the strict requirements mentioned above. Bisphenol contamination of water is also a major public health concern, while many organic pollutants of the bisphenol type have been detected in the multiple environmental matrices, (e. g, soil, water, and air) so far (Tsai, 2006; Vasiljevic & Harner, 2021).

Other major pollutants in water samples are PAHs. Due to their mutagenic and carcinogenic properties, PAHs are on the EU and US EPA list of priority pollutants (Wenzl et al., 2006). They are released into the atmosphere during the incomplete combustion of fuels or other organic substances. It is therefore crucial to identify them correctly and to investigate the ways to eliminate them.

1.2 Problem Statement

Water contamination is a critical and troublesome issue that threatens human civilization's sustainability. Water streams contain a variety of primary pollutants that have a detrimental influence on human health and the marine ecosystem. WHO and EPA listed several health toxics chemicals including some toxic heavy metals and phenolic pollutants (Gjineci et al., 2016; Schäfer et al., 2005). Heavy metals such as cadmium and lead subsidize innumerable environmental issues based on their toxicity. Furthermore, owing to their high toxicity for human health and aquatic life, phenol, and cresol isomers are considered as priority phenolic pollutants by WHO. Therefore, these contaminants need to be removed from waste stream fluids before they are released to the environment. Various volatile organic compounds (VOCs) that have been used as extraction agents (e.g., alcohols, chloroform) are toxic, volatile, and flammable. A class of neoteric solvents termed as hydrophobic deep eutectic solvents (HDES) have recently attained considerable interest in both academics and the industrial community. HDES are subclass of deep eutectic solvents that are generally immiscible in water solutions and possess high extraction efficiencies for various target analytes. The aim of this thesis is to examine the feasibility of HDES for the removal of heavy metals and phenolic pollutants by employing liquid-liquid extraction (LLE). The Conductor-like Screening Model for Real Solvents (COSMO-RS) screening tool was employed for the possible selection of potential HDES. Additionally, consistency tests were performed to ascertain the reliability of the experimental data for each system. HDES with higher selectivity and distribution ratio resulted in better extraction of pollutants from aqueous environment.

1.3 Research questions and hypothesis

According to WHO, heavy metals and phenolic pollutants are considered as priority pollutants that are harmful to human health and the environment. Various processes have been used for the separation of these pollutants; however, this thesis focuses on the use

of LLE process for the separation of heavy metals and phenolic compounds from water model solutions. LLE process does not require a high amount of energy or expensive equipment and can be carried out under ambient conditions (Cai et al., 2015). Usually, organic solvents have been used in these processes for the removal of pollutants (Černá, 1995; Chang et al., 2010, 2011); the purpose of this study is to use the neoteric green solvents known as deep eutectic solvents (DESs). DESs are formed by combining a hydrogen bond acceptor (HBA), e.g., a quaternary ammonium halide, with a hydrogen bond donor (HBD), e.g., glycerol, capable of forming a complex with the halide, which contributes to a substantial depression of the freezing point of the mixture. DESs have emerged as a promising alternative for both ionic liquids (ILs) and VOCs. DESs manifest most of the advantages of ILs, including low-melting points, high thermal stability, wide liquid ranges, low volatility, and designable chemical and physical properties. They are also considerably cheaper, less toxic and easier to prepare than traditional ILs. To extract pollutants from water, it is required to use hydrophobic solvents, however, most of the DES are hydrophilic. Hence, one of the major challenges is to find effective HDES for the removal of such contaminants. HDES are class of neoteric solvents that depict low or even negligible water miscibility, low flammability, wide liquid range, low vapor pressure, and high solvation capacity. Therefore, this thesis will focus on the extraction of priority pollutants from water effluent through HDES.

The central question is “How to identify and investigate the best HDES that will provide the separation of heavy metals and phenolic pollutants from the aqueous solutions via LLE”?

The following are sub questions:

1. How to choose the promising HDES before the experimental investigation?
2. What will be the main parameters that will affect the separation process?
3. How to correlate the experimental data?

4. DES with higher hydrophobicity, selectivity, and distribution ratio will result in higher extraction efficiency of pollutants from wastewater.

The hypotheses are sub sectioned as follows:

1. COSMO-RS screening tool will result in the selection of efficient HDES based on the geometry and structure of HDES.
2. HDES with low viscosity will result in better extraction of pollutants from water (Lee et al., 2019).
3. The 1:1 mass ratio between HDES and aqueous phase, and room temperature will give higher distribution ratio and selectivity (Phelps et al., 2018).
4. Consistency tests will result in the reliability of the experimental data (Hadj-Kali et al., 2017).

1.4 Aim and objectives

This thesis aims to examine the feasibility of HDES for the removal of heavy metals and phenolic pollutants by employing LLE process.

The main objectives of this thesis are listed below:

1. To screen and select potential HDES for the efficient extraction of heavy metals and phenolic compounds, utilizing either COSMO-RS or experimental screening.
2. To prepare the selected HDES and perform comprehensive characterization through physical property measurements (e.g., density, viscosity) as well as analysis using ^{1}HNMR and FTIR spectroscopy .
3. To conduct experiments on LLE, focusing on the efficient removal of targeted heavy metals and phenolic pollutants.
4. To analyze the parameters affecting pollutant removal and HDES reusability while validating experimental data using COSMO-RS and correlation models.

1.5 Scope of study

This study focused on the removal of heavy metals and phenolic pollutants from water using HDES via LLE. The following aspects were covered in this study.

1. Selection of appropriate HDES for the removal of heavy metals and phenolic pollutants from water.
2. Characteristics of the selected HDES.
3. Screening of HDES for the removal of phenols.
4. Optimization of LLE process parameters such as solvent concentration, extraction time, DESs to water solution mass ratio, and molar ratio of HDES to achieve maximum efficiency.
5. Characterization of the extracted heavy metals and phenolic pollutants using analytical techniques such as gas chromatography (GC), High-performance liquid chromatography (HPLC) and atomic absorption spectroscopy (AAS).
6. Suggestions for future research and recommendations.

The study aims to provide valuable insights into the potential use of HDES for the removal of heavy metals and phenolic pollutants from water. The findings of this research can be used for the development of effective and sustainable methods for the treatment of polluted water.

CHAPTER 2: LITERATURE REVIEW

2.1 Introduction

This chapter's goal is to provide a critical assessment of the appropriate literature that will help in accomplishing the aims of the study. Figure 2.1 provides an overview of the literature review given in this chapter.

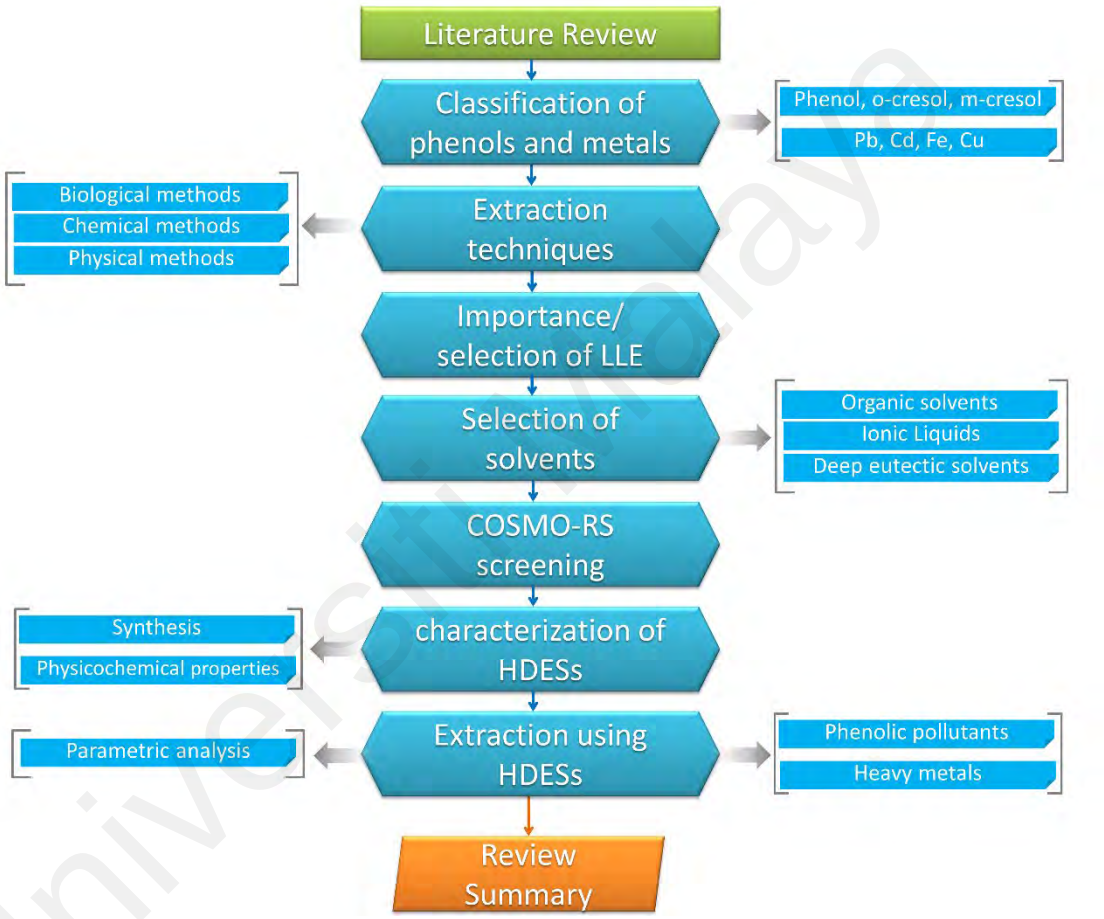

Figure 2.1: Literature review flowchart.

2.2 Classification of pollutants

The volume and toxicity of industrial metal effluents have experienced a notable rise in recent years due to the exponential growth of industrial processes. In the case of certain metals such as cadmium, arsenic, and lead, even small quantities of these substances in the water can be highly poisonous. Hence, the elimination of metal salts from water holds significant impact to mitigate potential environmental and health concerns. On the

contrary, phenolic compounds have been identified as significant contributors to water pollution due to their elevated levels of toxicity and carcinogenic properties (Khan et al., 2021; Wasi et al., 2013). Hence, the exclusion of these phenolic compounds from wastewater is of utmost significance to adhere to the aforementioned stringent criteria.

In this work, lead, cadmium, iron, and copper were chosen because they are often present in industrial effluent and have negative impacts on human health and the environment. In addition, phenol and cresol isomers were chosen as representative phenolic contaminants. Persistent in nature, these heavy metals and phenolic pollutants can build up in both the environment and the food chain, eventually causing harm. Because of the strict regulations imposed by environmental groups, these contaminants have attracted a lot of attention from scientists looking to find new and better treatment options. To guarantee clean and safe water for human use, sustainable and effective technologies for removing harmful contaminants from water are required. The effort is meant to aid in the discovery of efficient strategies for eradicating these contaminants, which has important real-world implications.

2.3 Extraction Techniques

Traditional methods for removing toxic metals and organic pollutants from water include adsorption and extraction (Abbas et al., 2016; Ngo et al., 2015; Tchinsa et al., 2021), reverse osmosis (Wimalawansa, 2013; Yang et al., 2019), filtration (Thirunavukkarasu et al., 2020), membrane processes (Bodzek et al., 2011; Van der Bruggen et al., 2003), ion exchange (Hubicki & Kołodyńska, 2012), ozonation (Wang & Chen, 2020; Xiao et al., 2015), photocatalytic degradation (Khasawneh & Palaniandy, 2021), biological, chemical oxidation or reduction, chemical precipitation, evaporation, and coagulation (Archana et al., 2016; Gunatilake, 2015; Thasneema et al., 2021).

Table 2.1: **Advantages and disadvantages of the current methods used to extract heavy metals from wastewater.**

Method	Advantages	Drawbacks	Refs.
Oxidation/Ion-exchange	Fast kinetic, high removal efficiency, and effective in treating inorganic effluent. No sludge disposal. Low cost of materials	Highly affected by the pH of the solution. Fouling of metals. Suitable for low concentration. Higher capital and operational costs.	(Azimi et al., 2017)
Chemical precipitation	Simple operation and low capital cost. Easily automated treatment method.	Further treatment is needed because of the production of a large amount of sludge. Slow metal precipitation and poor settling. Requires a large number of chemicals to reduce metals to an acceptable level for discharge.	(Barakat, 2011; Joshi et al., 2017)
Membrane treatment	Less energy consumption Easy fabrication, environmentally friendly, and removes both organic and inorganic compounds.	Production of concentrated sludge. Membrane fouling. Higher cost and lower permeate flux.	(Abdullah et al., 2019)
Flotation/Coagulation	Relatively economical and easy operation.	Production of sludge. Incomplete removal of heavy metals.	(Bolisetty et al., 2019)
Electrochemical technologies	Environmentally friendly and rapid process.	Higher electricity cost. Large capital investments. Formation of large particles.	(Chaemiso & Nefo, 2019)
LLE	Relatively low operational costs. Easy operation. Selectivity of exchangers for efficient removal of metals.	Use of large volume of organic solvents. Possible cross-contamination of the aqueous streams.	(Crini & Lichtfouse, 2019)

The petroleum, metallurgical and mining industries generate significant quantities of aqueous solutions contaminated with heavy and light metals (Vardhan et al., 2019). Existing traditional solvent extraction methods for selective recovery/removal of these metal salts are dependent on VOCs and potentially hazardous chemicals such as aliphatic hydrocarbons, sulfuric acid, and organophosphorus extractants (Flett, 2005). Therefore, there is an urgent need to develop new methods for selective extraction of metal salts and purification of water that are more economical and environmentally friendly. Table 2.1 shows the advantages and disadvantages of the various technologies used to remove metals from the water medium.

Extraction is usually measured in terms of extraction efficiency (EE), which can be determined using the following equation:

$$EE(\%) = \frac{C_0 - C_1}{C_0} \times 100 \quad (2.1)$$

Where C_0 is the analyte concentration in the water phase before the extraction, and C_1 is the analyte concentration in the water phase after the extraction.

The distribution ratio (D) of metals can be obtained using the following equation (Ola & Matsumoto, 2019):

$$D = \frac{M_{aq,ini} - M_{aq,eql}}{M_{aq,eql}} \quad (2.2)$$

Where $M_{aq,ini}$ is the initial concentration of metal in the aqueous phase, and $M_{aq,eql}$ is the equilibrium concentration of metal in the aqueous phase.

Like heavy metals, phenolic compounds are also considered pollutants and toxic substances that have harmful effects on the environment and human health even at low concentrations (Anku et al., 2017; Bazrafshan et al., 2016).

Table 2.2: **Advantages and disadvantages of the available phenol removal methods.**

Techniques	Advantages	Disadvantages	Refs.
Chemical methods			
Oxidation	Simple operation No increase in the volume of sludge and wastewater for the gaseous oxidation process.	Requires expensive chemicals. Incomplete phenol oxidation. High pressure and temperature for wet oxidations of phenols.	(Anku et al., 2017; Bandosz et al., 2020; Hernández-Francisco et al., 2017)
Electrochemical treatment	No sludge production. No need for expensive chemicals.	High energy consumption. Expensive equipment is needed.	(Loos et al., 2018)
Photochemical	No sludge production. Great degradation of phenols.	Production of by-products. Expensive equipment.	(Rosman et al., 2018)
Physical methods			
Adsorption	Efficient removal of phenols. Need mild temperature and pressure. Economical and simple operation.	Regeneration step is difficult. Many adsorbents possess low adsorption efficiency. Calcination is needed	(Khan et al., 2021; Yagub et al., 2014)
Membrane filtration	Economically feasible	Concentrated sludge is produced.	(Mohammadi et al., 2015)
LLE	Easy operation. Mild operating conditions.	Use of organic solvents. Sometimes has low selectivity and distribution ratio.	(Sas et al., 2018)
Ion exchange	Adsorbent regeneration.	Not practical for all types of pollutants.	(Caetano et al., 2009)
Biological methods			
Biological degradation	Phenol is consumed by microorganisms and convert them into a harmless compound	Formation of toxic by-products. The problem of growth control. Sludge production.	(Baker & Mayfield, 1980)
Enzyme degradation	Enzymatic reactions take place under moderate pH and temperature. Higher catalytic efficiency.	Enzyme instability and non-reusability.	(Kumar et al., 2005)

Various industries release phenols in their effluents, including refineries, coal processing, pharmaceutical, plastics, and pulp and paper manufacturing (Busca et al., 2008). Due to the toxicity of phenols, these effluents cannot be discharged directly. Without treatment, the emissions can seriously affect the health of humans, animals, and aquatic habitats (Gupta et al., 2008). As a result, a plethora of environmental regulations have been enacted that set discharge limitations. The EPA and the EU have already set a limit for phenolic compounds of 1 mg L-1 (Sas et al., 2020). Various technologies with their advantages and disadvantages for the removal of phenolic pollutants are discussed in Table 2.2.

2.4 Importance of LLE

LLE is a popular physical method used for the removal of phenols and heavy metals from water. Compared to other methods such as chemical and biological methods, LLE offers several advantages. One of the main benefits of LLE is its ability to selectively remove the target pollutants from a complex mixture of contaminants. This means that LLE can be tailored to target specific pollutants in water, which may not be possible with other methods. LLE is also a relatively simple and inexpensive method, making it a cost-effective solution for the treatment of large volumes of water. Furthermore, LLE can be performed on-site, which minimizes the need for transportation of contaminated water to treatment plants. Overall, LLE offers a practical and efficient solution for the removal of phenols and heavy metals from water, especially in cases where the pollutants are present in low concentrations or in complex matrices.

Another advantage of LLE is its ability to achieve high removal efficiencies of the target pollutants. Unlike other physical methods such as adsorption, where the surface area of the adsorbent limits the removal capacity, LLE can achieve high removal efficiencies due to its ability to extract the target pollutants into a separate liquid phase.

This phase separation ensures that the pollutants are effectively removed from the water, leaving behind a clean and safe product. Additionally, LLE can be easily optimized for different operating conditions, such as pH and temperature, which allows for greater control over the treatment process. Moreover, LLE can be combined with other physical and chemical methods, such as precipitation or coagulation, to further enhance the removal efficiency of the target pollutants. In summary, LLE is a reliable and effective physical method for the removal of phenols and heavy metals from water, offering several advantages over other treatment methods.

2.5 Solvent selection

When above separation methods are compared, extraction methods are the most promising extraction and purification methods due to their high performance, low cost, ease of handling, and ability to reuse the extractant (Blanco-Pedrekhon et al., 2021). However, when hydrophobic media are required, toxic organic chemicals (e.g., VOCs) are still mainly used due to the lack of more environmentally friendly hydrophobic alternatives. A trend has evolved in modern chemical engineering toward the replacement of harmful organic solvents with more environmentally friendly solvents that satisfy the requirements for "Green Chemistry" (Dai et al., 2013). One alternative to organic solvents is ionic IL, which has attracted much interest as an "environmentally friendly solvent" due to its environmentally friendly properties such as non-flammability, non-volatility, durability, and negligible vapor pressure (dos Santos Junior et al., 2019; Hadj-Kali et al., 2020; McNeice et al., 2018; Salleh et al., 2019). In the last decade, ILs have attracted great interest in various fields, including biomass pretreatment (Tadesse & Luque, 2011), catalysis and biocatalysis (Vekariya, 2017), organic synthesis (Hajipour & Rafiee, 2015), and carbon capture (Wu et al., 2020). Nevertheless, ILs have drawbacks that limit their use as designer solvents in industrial applications, including their high cost (Sarmad et

al., 2017), flammability (Clark & Tavener, 2007), poor biodegradability, toxicity, and high viscosity (Habibi et al., 2013; Wazeer et al., 2021a).

The use of green solvents is a research priority to achieve the sustainable development goals. DESs are sometimes regarded as a new class of IL analogues (Lima et al., 2021; Verevkin et al., 2015). They have physicochemical and IL -related advantages (Hadj-Kali et al., 2017). DESs are non-toxic, environmentally friendly, inexpensive and easy to prepare (Al-Dawsari et al., 2020; Karimi et al., 2020; Mulyono et al., 2019; Shabani et al., 2020). They consist of two or more compounds that produce a mixture with a melting point lower than that of the individual components (Zhang et al., 2012). In most cases, DESs are prepared by associating a HBA with a HBD, such as glycerol, and forming a complex with a halide, which contributes to a significant decrease in the freezing point of the mixture (Li et al., 2021). Because certain DESs have a glass transition temperature rather than a eutectic point, they are known as low transition mixtures (Francisco et al., 2013). Most of the DESs presented in the literature so far are hydrophilic and unstable in water, which leads to the separation of the two components (Silva et al., 2016). Van Osch et al. (2015) first developed the idea of HDES. The water-insoluble solvents were used to extract water-insoluble VOCs and the extraction yield and efficiency were reported to be high.

Usually, the term HDES refers to DES, which contains a water-soluble quaternary ammonium salt as HBA and a nonpolar, water-insoluble component (such as alcohol or fatty acid) as HBD (Ge et al., 2018; Shi et al., 2020). However, these solvents dissolve in the aqueous phase, resulting in a free solution of fatty acids or alcohol due to the dissolution of the quaternary ammonium salt. Shishov et al. (2020) stated that the mixtures of two or more water-insoluble substances (such as menthol or thymol) and nonpolar fatty acids or alcohols can be considered as "hydrophobic" DESs. When

dissolved in water, such mixtures remain stable and have poor water solubility. Therefore, DESs comprising both water-soluble and insoluble components cannot be termed "hydrophobic". HDES are further divided into ionic and non-ionic HDES. The preparation of ionic HDES generally depends on the formation of a hydrogen bond. Van Osch et al. (2015) prepared the ionic HDES by combining long chain quaternary ammonium salts (HBA) with decanoic acid (DecA) as HBD. HBAs, which are dependent on long-chain ammonium salts, are preferred for HDES synthesis because they confer higher hydrophobicity than short-chain ammonium salts, e.g., choline chloride (ChCl). Due to the scarcity of cheap and readily available organic compounds from which HDES can be synthesized, the number of non-ionic HDES is quite limited. Moreover, it is difficult to distinguish between HBA and HBD in non-ionic HDES. However, some studies suggest that DL-menthol has the properties of HBA, while long-chain and short-chain organic acids and phenolic compounds have the properties of HBD (Makoś et al., 2020). Figure 2.2 shows the structure of some HBA and HBD used to prepare HDES.

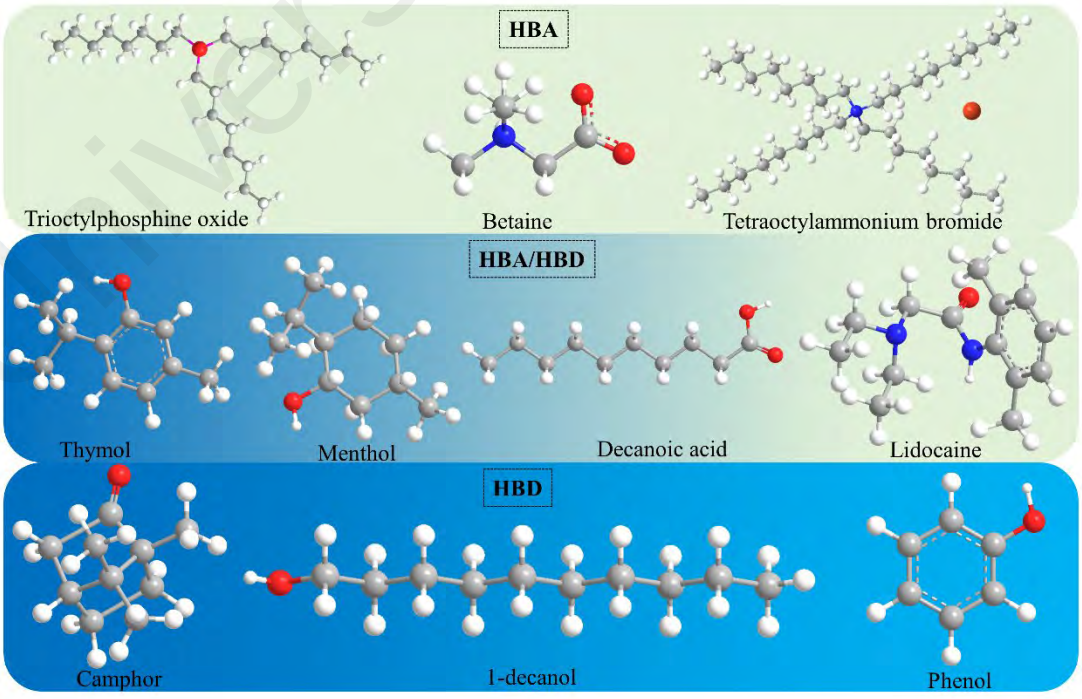

Figure 2.2: Molecular structures of the HBA and HBD used to form HDES.

In extraction methods, there is a growing interest in the use of HDES, and various studies have been published over the last couple of years. Applications of HDES in various fields including extraction have been summarized in Table 2.3. Some recent examples of each application have also been presented in Table 2.3. Several review articles have been published on the properties and applications of DESs in the extraction process (Cunha & Fernandes, 2018; Espino et al., 2016; Lee et al., 2019; Pena-Pereira & Namieśnik, 2014; Shishov et al., 2017; Tang et al., 2015; Wazeer et al., 2021a; Wazeer et al., 2021b; Wazeer et al., 2018a). In most of the studies included in the reviews mentioned above, hydrophilic and water-miscible DESs were used, and the analytes of interest were extracted from solid or non-aqueous liquid samples that could be phase-separated from the DESs. In 2019, few authors have published review articles on the physicochemical properties and applications of HDES. These review articles focused on the extraction of biomolecules and transition metals using HDES.

Table 2.3: Applications of HDES in various fields with some recent examples.

Analyte	Source	Solvent	Analysis	Process	Ref.
Food Safety					
Detection of Pesticides					
Triazoles	Surface water	ChCl:ASA[a] (1:2) Menthol:DCA[d] (1:2)	HPLC[b]	DLLME[c]	(Tomai et al., 2019)
benzoylureas	Water samples	MTOAC[e]:DDC[f] (1:2.5)	HPLC	DLLME	(Yang et al., 2017)
	Tea and fruit juices	THPTF[g]:TDA[h] (1:3)	HPLC	DLLME	(Liu et al., 2020)
Food additives					
UV-531, UV-326, UV-328	Food packaging bags	Menthol:NonA[j] (3:1)	HPLC	LLME	(Wen et al., 2020)
DHBP[k], benzophenone HMOBP[l]	water samples	MTAC:DecA (1:3)	HPLC-UV[m]	Ultrasound-DLLME	(Wang et al., 2017)
Environmental Safety					
Heavy metals					

Table 2.3, continued.

Analyte	Source	Solvent	Analysis	Process	Ref.
Zn^{2+}, Cd^{2+}	Juice	Menthol:sorbitol :MNA[n] (1:2:1)	FAAS[o]	Air-assisted LLME	(Sorouraddin et al., 2021)
Pb^{2+}	Milk	Menthol:sorbitol :MNA (1:2:1)	FAAS	DLLME	(Sorouraddin et al., 2020)
Pb^{2+}	Water	Menthol:PSC[p] (1:1)	ETAAS[q]	LLME	(Abdi et al., 2020)
Cu	Acidic solutions	Menthol:DecA (1:3)	UV-Vis	LLE	(Schaeffer et al., 2018)
Micropollutants					
chlorophenols	Waste water	MTOAC:OctA[s] (1:2)	HPLC	DLLME	(An et al., 2020)
		Menthol:thymol (1:2)	HPLC	LLE	(Adeyemi et al., 2020)
Phenol	Aqueous medium	Menthol:DecA (1:1)	UV-Vis	LLE	(Ji et al., 2020)
Bisphenol A	Aqueous medium	Menthol:acetic acid (1:1)	HPLC	LLE	(An et al., 2020)
Miscellaneous applications					
Bioactive compounds					
Lycopene	Tomato	Menthol:lactic acid (1:8)	UV–Vis	UAE[t]	(Sas et al., 2019)
Terpenes	Spices	TBAB[u]:DDC (1:2)	GC-MS[v]	HSDME[w]	(An & Row, 2021)
Pharmaceuticals compounds					
Ciprofloxacin	Aqueous medium	Menthol: DdecA[y](2:1)	UV–Vis	LLE	(Florindo et al., 2019b)
Azeotropic mixtures					
Butanol, Ethanol	Aqueous medium	DL-Menthol:DdecA (2:1)	^{1}HNMR[z]	LLE	(Verma & Banerjee, 2018)
Bio catalysis					
Glycolipid production	-	Menthol: DecA (1:1)	HPLC	Trans esterification	(Hollenbach et al., 2020)

[a]acetylsalicylic acid, [b]high-performance liquid chromatography, [c]dispersive liquid-liquid microextraction, [d]dichloroacetic acid, [e]methyltrioctylammonium chloride, [f]1-dodecanol, [g]Trihexyl (tetradecyl) phosphonium tetrafluoroborate, [h]tetradecyl alcohol, [i]gas chromatography–flame ionization detection, [j]nonanoic acid, [k]2,4-dihydroxybenzophenone, [l]2-hydroxy-4-methoxybenzophenone, [m]high-performance liquid chromatography with ultraviolet detection, [n]mandelic acid, [o]flame atomic absorption spectrophotometer, [p]phenyl salicylate, [q]Electrothermal Atomic Absorption Spectroscopy, [r]trioctylmethylammonium chloride, [s]octanoic acid, [t]ultrasound-assisted extraction, [u]tetrabutyl ammonium bromide, [v]gas chromatography–mass spectrometry, [w]headspace single-drop microextraction, [x]Spectrophotometer, [y]dodecanoic acid, [z]proton nuclear magnetic resonance

Cao and Su (2021) presented a review on the properties and the general trend of applications of HDES. More importantly, they stated that ongoing development of HDES should be beneficial to proponents of green chemistry as well as practitioners who aim to minimize pollution and improve efficiency. Recently, Zainal-Abidin et al. (2021) published a review paper on HDES. They have thoroughly compared and discussed various critical physicochemical parameters of HDES such as melting points, density, viscosity, thermal stability, and water solubility. In addition, they also investigated the applications of HDES in medicine and removal of pollutants from various media. Therefore, this review evaluates the prospects, current status, limitations, and further R&D needs of water treatment processes based on HDES that could be used to extract metals and organic pollutants from industrial process waters and wastewaters. To expedite the adoption of HDES in the area of green and sustainable chemistry, recent studies on the extraction of metals and organic pollutants from aqueous solutions using HDES are summarized here. An in-depth parametric analysis based on the literature data is also presented that examines the effects of molar ratio of HDES, mass ratio of HDES to water, initial contaminant concentration, and type of HDES components.

2.6 COSMO-RS screening

COSMO-RS is essential for modelling the extraction process. Furthermore, when integrated with sensitivity tests, this predictive model has the potential to save time and money that are commonly invested in the experimental procedure. This modelling technique can provide a quick preliminary estimate in a screening procedure of various solvents for analyte extraction using DESs or ILs.

Adeyemi et al. (2020) demonstrated the use of COSMOThermX and TMoleX software in describing the mechanism of chlorophenols extraction from aqueous solution utilizing

HDES, which was via the hydrophobic interaction and hydrogen bonding between the chlorophenols and the HDES. Additionally, the authors were able to compare 3-chlorophenol extraction efficiency with the COSMOThermX modeling findings and observed that the model provided a decent forecast of chlorophenol extraction efficiency. In another study, Wazeer et al. (2018b) employed the COSMO-RS approach to filter DESs for separating the azeotropic binary mixture of benzene and either methanol or ethanol. After estimating the activity coefficient in each DES at infinite dilution of benzene, ethanol, and methanol, three DESs were chosen as the top performers and experiments were carried out to validate the screening results.

Rodríguez-Llorente et al. (2020) performed a COSMO-RS screening to select the appropriate solvents based on the activity coefficients at infinite dilution of the phenolic contaminants in the solvents. They used COSMOThermX to obtain the sigma profiles of the compounds. The activity coefficients at infinite dilution were plotted for phenol, 2-nitrophenol and 2-chlorophenol (2-CP) in some commercial organic solvents (terpenes, terpenoids, carboxylic acids) and HDES. The largest values of activity coefficients at infinite dilution in natural solvents were obtained for terpenes, which do not contain heteroatoms in their structure. In comparison, phenols contained in terpenoids, and carboxylic acids have lower activity coefficients at infinite dilution, suggesting that these solvents have a higher affinity for phenolic compounds. A similar effect is observed with the commercial solvents, which would be more suitable for the extraction of phenols than toluene due to their greater polarity. Lower activity coefficients were observed for HDES containing terpenoids and medium chain fatty acids. Compared to the two terpenoids used in HDES, menthol has a stronger affinity for extraction of phenolic chemicals than thymol, resulting in lower activity coefficients in menthol-based HDES.

The most typical approach for selecting the proper solvent for extracting desired compounds is via trial and error, especially when working with unfamiliar and understudied solvents such as DES. As a result, improper solvent selection may occur. This can result in poor solvent selection. COSMO-RS is a useful software that can be used to screen the ideal DESs for extracting the target compounds, which clearly saves time, cost and effort that would otherwise be spent on the lengthy experiment.

To the best of our knowledge, there are only a few studies dealing with the modeling of the extraction process of phenols from aqueous media using HDES. In COSMO-RS, the hydrogen bonding threshold is marked at the values of σ=-0.0085 for HBD, and σ=+0.0085 for HBA indicators. This means that, if the species demonstrate peaks at σ<-0.0085, it indicates the presence of hydrogen bond donors, whereas if they demonstrate peaks at σ>+0.0085, it indicates the presence of HBA. As can be seen from the sigma profile of chlorophenols and the HDES constituents in Figure 2.3 which was taken directly from Adeyemi et al. (2020), the chlorophenols show tendencies as HBDs due to the presence of peaks to the left of the threshold i.e., at σ<-0.0085. This would draw them to the HDES constituents (menthol-thymol, menthol-hexanoic acid, menthol-OctA, and menthol-DecA), which show tendencies as HBAs based on their usual peaks to the right of the threshold i.e., at σ>0.0085. Thus, there would be a mechanism for the transfer of chlorophenols from the water phase to the HDES phase based on the formation of hydrogen bonding interaction between the chlorophenols and the HDES constituents. This is also supported by a handful of research groups who have made similar observations that chlorophenols are transferred to hydrophobic IL from the water phase via hydrogen bonds (Brinda Lakshmi et al., 2013; Deng et al., 2011; Fan et al., 2008).

2.7 Characterization of HDES

HDES are generally prepared by the same methods used to prepare DESs. The hydrophobicity of HDES is related to the hydrophobicity of their precursors. Poorly soluble or insoluble components in water are used for the synthesis of HDES. HDES are classified into two categories. The most intensively studied HDES are mainly composed of quaternary ammonium salts with longer alkyl chains. For example, Van Osch et al. (2015) prepared the first type of HDES consisting of a DecA with ammonium salts with long alkyl chains, which exhibit a higher degree of hydrophobicity than short-chain ammonium salts. The solubility of the prepared solvents in water was studied based on the water content of the water-saturated HDES, and the water solubility ranged from 1.8 - 6.9%. The second type is a combination of two or more natural components (HBA or HBD). Ribeiro et al. (2015) introduced the first natural HDES by combining DL -menthol with a natural carboxylic acid. Menthol, an inexpensive natural monoterpene with very poor water solubility, has been used in the pharmaceutical industry to prepare eutectic mixtures with other terpenes (Ribeiro et al., 2015). The hydrogen bonding interactions are weak in this type of combination, resulting in much lower viscosities than the conventional hydrophilic DESs and quaternary- ammonium-based HDES (Smith et al., 2014; Van Osch et al., 2015). Due to the inherent hydrophobic property of menthol, the prepared HDES were hydrophobic and immiscible with water. Their solubility in water was determined to be 1.2 to 1.6%, which is much lower than that of quaternary ammonium-based HDES (Ribeiro et al., 2015).

Compared to hydrophilic DESs, HDES have longer alkyl chains, reducing the weight of hydrophilic domains (e.g., hydroxyl and carboxylate groups) in the chemical structure (Florindo et al., 2019a; J. Wang et al., 2020; X. Wang et al., 2020). This variation in the chemical structure of HDES can lead to a notable change in their physicochemical properties. Like conventional DESs, HDES have a much lower melting point than their

constituents. The melting point of HDES depends on the nature of the HBA/HBD, their molar ratio, and the strength and structure of the interaction between the components of DES. The presence of charged and polar components in hydrophilic DESs and salt-based HDES could lead to a significant decrease in the melting point (Florindo et al., 2018a).

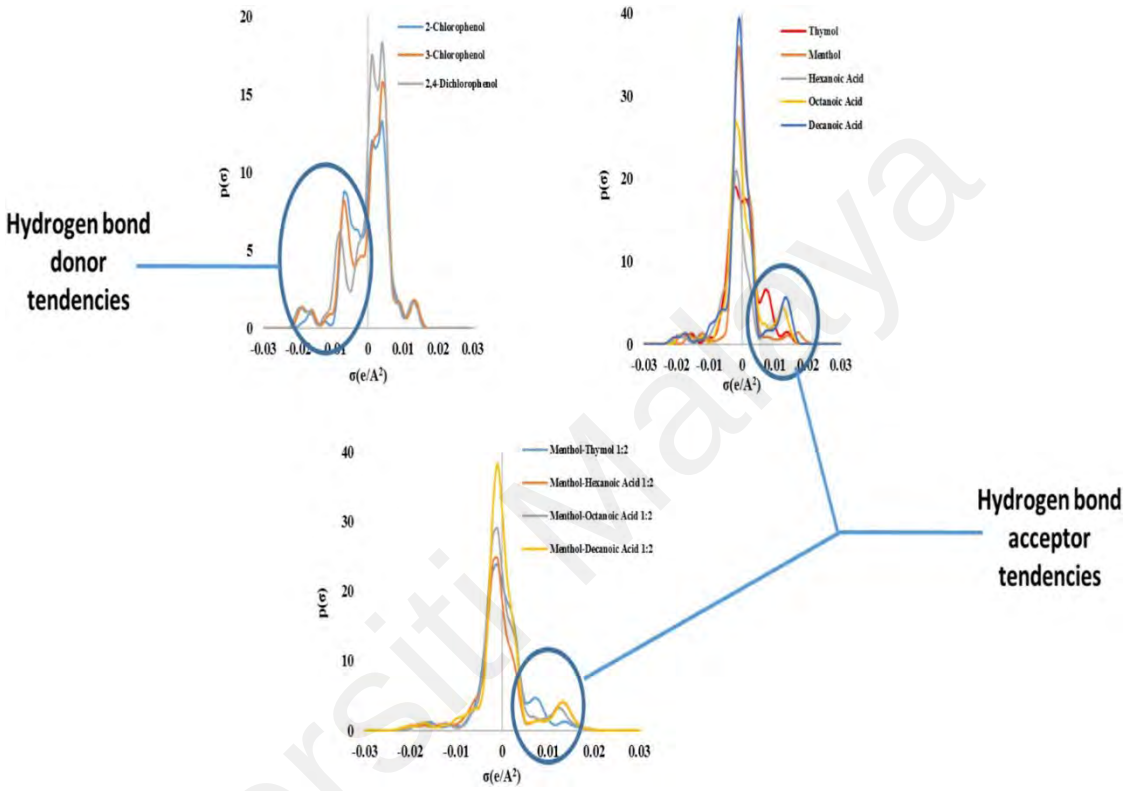

Figure 2.3: Sigma profile of HDES and chlorophenols (Adeyemi et al., 2020).

On the other hand, natural HDES exhibit less melting point depression, resulting in a less viscous type of DES (Haider et al., 2021). The melting point of most HDES is below 25 °C, which allows their use as reaction media or solvents at room temperature (Florindo et al., 2019a; Longeras et al., 2020). The addition of an alkyl chain to the fatty acid component of HBD leads to an increase in the melting point of HDES (Arcon & Franco Jr, 2020). In comparison, increasing the alkyl chain length of the ammonium salt decreases the melting point of HDES.

Because of the difference in density, the effectiveness of DESs depends heavily on their immiscibility with water (Lee et al., 2020). The density of the extractant is crucial in two-

phase extractions because it affects whether the extractant can be collected from the upper or lower liquid phase. From Table 2.4, most HDES have a lower density than water. In addition, HDES exhibit a wide range of viscosity values that are primarily influenced by the type of HBA (Table 2.4), which increases the likelihood that solvents will need to be modified to create task-specific solvents. Since HDES are formed by hydrogen bonds between the original components (Van Osch et al., 2020), these interactions may hinder the movement of HDES molecules, resulting in high viscosity of HDES. Several researchers (Lee et al., 2019; Makoś et al., 2020; Zainal-Abidin et al., 2021) have already compiled some data on the physical properties of HDES. Therefore, Table 2.4 shows only those HDESs that have been used for the removal of contaminants from polluted water. The properties include density (ρ, g.cm^{-3}), viscosity **(**μ, m.Pa.s), and melting point (T_m, °C).

Table 2.4: Physicochemical properties of selected HDES at 25 °C and atmospheric pressure.

HBA	HBD	Ratio	Synthesis	ρ	μ	T_m	Ref.
Lidocaine	DecA	2:1, 3:1, 4:1	heating at 35 ℃	0.958, 0.949, 0.942	237.5, 208.5, 142.0		(Van Osch et al., 2016)
TOMC	MHB[a]	1:1, 1:2, 2:1	heating at 80 ℃ for 30 mins	0.964, 1.01, 0.931	1088, 967, 2437		(Shi et al., 2020)
	BHB[b]	1:1, 1:2, 1:3, 2:1		0.951, 0.983, 1.046, 0.926	1435, 778, 910, 1547		
	IBHB[c]	1:1, 1:2, 1:3, 2:1		0.948, 0.979, 1.005, 0.929	1525, 1807, 2031, 1530		
	EHB[d]	1:1, 1:2, 1:3, 2:1		0.939, 0.963, 0.976, 0.929	1526, 1045, 930, 1491		
	OHB[e]	1:1, 1:2, 1:3,		0.942, 0.964, 0.978,	1680, 1730, 1327,		

Table 2.4, continued.

HBA	HBD	Ratio	Synthesis	ρ	μ	T_m	Ref.
		1:4, 2:1		0.987, 0.928	1490, 1436		
Thymol	MPD[f]	2:1	heating between 60-80 ℃ for 1 h	0.959	32.689	-66.7	(Almustafa et al., 2020)
	1-decanol	2:1		0.915	14.376	-15.2	
Menthol	MPD	2:1		0.900	68.396	-7.4, 13.66	
	1-decanol	2:1		0.870	27.979	-17.9	
MAA[g]	Lidocaine	9:1		1.110	10.880		(Edgecomb et al., 2020)
	ibuprofen	9:1		1.120	10.850		
	PS[h]	9:1		1.120	9.430		
	DL-menthol	9:1		1.110	8.350		
DL-menthol	Lidocaine	5:5		0.900	38.680		
	ibuprofen	7:3		0.940			
	PS	7:3		0.880	24.963	13.3	
Thymol	TOPO[i]	1:1		0.898	69.930		(Schaeffer et al., 2020)
TOPO	DecA	1:1		0.881	44.110		
HDC[j]	DecA	1:1		0.978	11.290		
TOPO	TTFA[k]	2:1		1.100	28.100	19.2	(Hanada & Goto, 2021)
	BTFA[l]	2:1		1.050	13.200	24.8	
TTFA	TPP[m]	2:1		1.320	11.600	20.5	
BTFA	TPP	2:1				25.2	
DdecA[n]	OctA	1:3	heating at 40 ℃	0.901	7.085		(Florindo et al., 2018b)
	NonA	1:3		0.897	8.636		
	DecA	1:2		0.894	10.756		
DL-menthol	OctA	1:1	heating at 70 ℃	0.902	12.540		(Sas et al., 2019)
	DecA	1:1		0.896	15.980		
DdecA	OctA	1:3		0.901	6.848		
	DecA	1:2		0.889	10.570		
TOMC	DecA	2:1, 1:1, 1:2	heating at 75 ℃ for 30 mins	0.896, 0.893, 0.891	288, 1214, 2515	-2, 13, 1	(Li et al., 2020)
	Ketoprofen	2:1, 1:1, 1:2		1.024, 0.989, 0.988	4915, 4717, 4670		
	Gemfibroz-il	1:2, 1:1		0.923, 0.942	3034, 3040		
TBAB	Thymol	1:2		0.910	420	≤ 20	(Faraji et al., 2020)
	OctA	1:2		0.920	125	≤ -10	

[a]Methyl 4-hydroxybenzoate, [b]butyl 4-hydroxybenzoate, [c]isobutyl 4-hydroxybenzoate, [d]2-Ethylhexyl 4-hydroxybenzoate, [e]n-octyl 4-hydroxybenzoate, [f]methyl-2,4-pentanediol, [g]Methyl anthranilate, [h]Proton Sponge®, [i]Trioctylphosphine oxide, [j]Hydrocinnamic acid, [k]Thenoyltrifluoroacetone, [l]benzoyltrifluoroacetone, [m]triphenyl phosphate, [n]dodecanoic acid.

2.8 Extraction using HDES

2.8.1 Removal of heavy metals

The first study on the transfer of metallic species from aqueous media into HDES was reported by Tereshatov et al. (2016). HDES were prepared by mixing tetraheptylammonium chloride as HBA with different HBD (i.e., ibuprofen, oleic acid, and DecA) and DL -menthol (HBA) with lauric acid (HBD) for the extraction of indium from aqueous media by LLEs. HDES based on tetraalkylammonium salt showed efficient and rapid extraction of indium in the range of 1×10^{-7}-8×10^{-1} M oxalic acid (OA) and 0.001-10.2 M HCl in the aqueous phase. For tetraalkylammonium-based HDES, ion pair formation was the most critical step in the extraction of indium from aqueous environments. Moreover, DL-menthol-based HDES efficiently extracted the metal from aqueous streams with low acidity (pH ≈ 3). In another study (Edgecomb et al., 2020), the same group prepared non-ionic HDES based on mixtures of active pharmaceutical and food ingredients to extract indium. DL -menthol:lidocaine, DL -menthol: PS, MAA:lidocaine, MAA:PS demonstrated distribution coefficients of 2-800 in 0.05 M HCl. Previously reported HDES also exhibited distribution ratios higher than 1 in 0.05 M HCl (Tereshatov et al., 2016). The HDES with lidocaine and PS as HBDs exhibited EE above 99% in some systems to extract indium ions from hydrochloric acid solutions.

The molar ratio of HBA to HBD plays a vital role in the extraction of metals from aqueous media. Figure 2.4 shows the effect of DecA:lidocaine HDES molar ratio on the distribution coefficient. For almost all metals, the higher the concentration of DecA in DecA:lidocaine HDES, the higher the decrease in distribution ratio. This could be due to an increase in hydrophobicity caused by an increase in DecA in the DES. It has also been suggested that the extraction process occurs by an ion exchange mechanism in which positively charged metal ions are exchanged with protonated lidocaine. A new class of HDES was prepared by mixing quaternary ammonium salt with parabens, and the effect

of the molar ratio of HDES was evaluated to extract the toxic heavy metal Cr (VI) from water (Shi et al., 2020). TOMC was mixed with BHB, IBHB, OHB and EHB at different molar ratios. For each HDES, the EE of Cr (VI) increased when the molar ratio was increased from 0.5:1 (HBA:HBD) to 1:2, indicating that the EE increased with increasing content of parabens in the HDES. For example, the EE of Cr (VI) increased from ~50 to ~95% when the molar ratio of TOMC:BHB HDES was changed from 0.5:1 to 1:2.

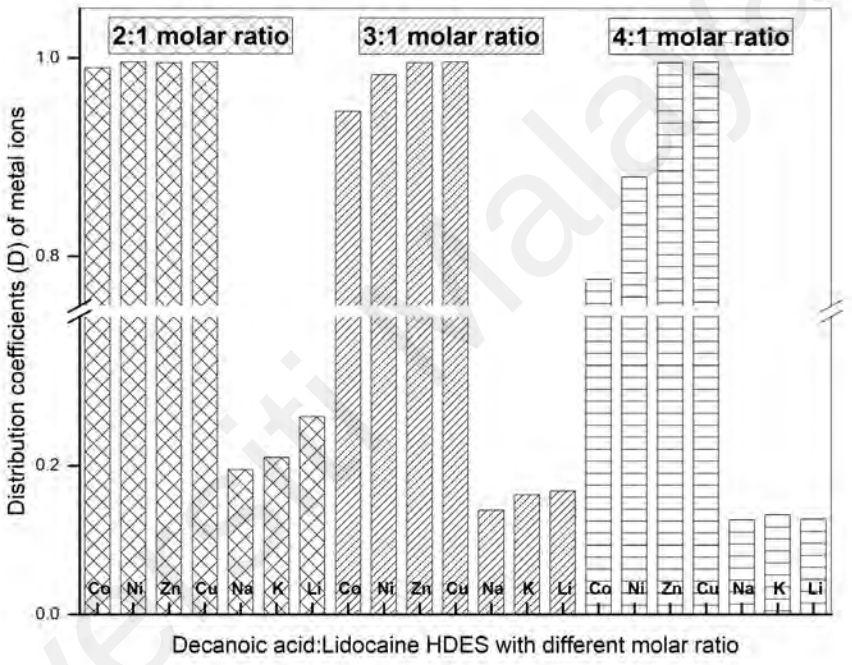

Figure 2.4: Effect of HDES' molar ratio on the distribution coefficient of metal ions. Data are taken from (Van Osch et al., 2016).

Another significant factor affecting the extraction of metal ions is the nature of HBA/HBD of HDES. Liu et al. (2021) studied the effect of HBD of HDES on the extraction of Pt(IV) from chloride solution. TOPO was mixed with 1-butanol, 1-hexanol and L-menthol in a molar ratio of 1:1. The effect of HBD in the HDES on the extraction efficiency of Pt(IV) was ordered as follows: TOPO:1-butanol (98.9%) > TOPO:1-hexanol (98.3%) > TOPO:L-menthol (94.4%) for 5.6 mmol L^{-1} chloride solution. This could be due to the fact that the reagents TOPO and HBD have different hydrogen bonding energy. There are also differences in ion binding energy between the extracting

extractant and $PtCl^{62-}$. Terpene-based HDES have been investigated for the extraction of Cu(II) by mixing menthol or thymol with carboxylic acids (Schaeffer et al., 2018). The extraction of Cu(II) was investigated at compositions near to the eutectic as a function of the carboxylic acid's alkyl chain length. The extraction efficiency decreased steadily when the alkyl chain length of the carboxylic acid was increased from 8 to 18 in terpene-based HDES. Schaeffer et al. (2020) studied the effect of HBA of non-ionic HDES for the separation of metals from aqueous streams. Non-ionic HDES were prepared by mixing TOPO and HDC as HBAs with DecA as HBD in 1:1 molar ratio. DecA:TOPO HDES showed excellent extraction of metals than DecA:HDC HDES at a concentration of 2 M HCl, as shown in Figure 2.5. No significant metal extraction was observed when DecA:HDC HDES was used as extraction solvent. The lack of metal extraction in the DecA:HDC system was attributed to the unfavorable electrostatic interactions between the anionic platinate and palladate chlorocomplexes and the carboxylate ligands. The enhanced extraction of most metals in the eutectic DecA:TOPO is due to the formation of their respective neutral complexes in aqueous solution.

The pH of the solution affects the existing form of the target contaminant present and consequently the efficiency of removal of the target contaminant. Ola and Matsumoto (2019) investigated the effect of pH on the extractability of Fe(III) and Mn(II) ions using HDES. The results showed that the change in pH was much more significant for a metal solution that was in contact with lidocaine solution than for the solution that was in contact with DecA. This finding indicates that lidocaine protonation happened. In Fe(III), the ion pair reaction between Fe^{3+} and the decanoic anion was observed at pH less than 2 during the extraction process. In contrast, precipitation occurred at a higher pH in the aqueous phase, and the influence of pH could not be assessed. The same phenomenon was observed for Mn(II) at pH less than 2.2 and more than 3.5. For Mn(II), pH between

2.2 and 3.5, the cation exchange reaction between Mn^{2+} and the lidocaine cation was probably the most likely mechanism.

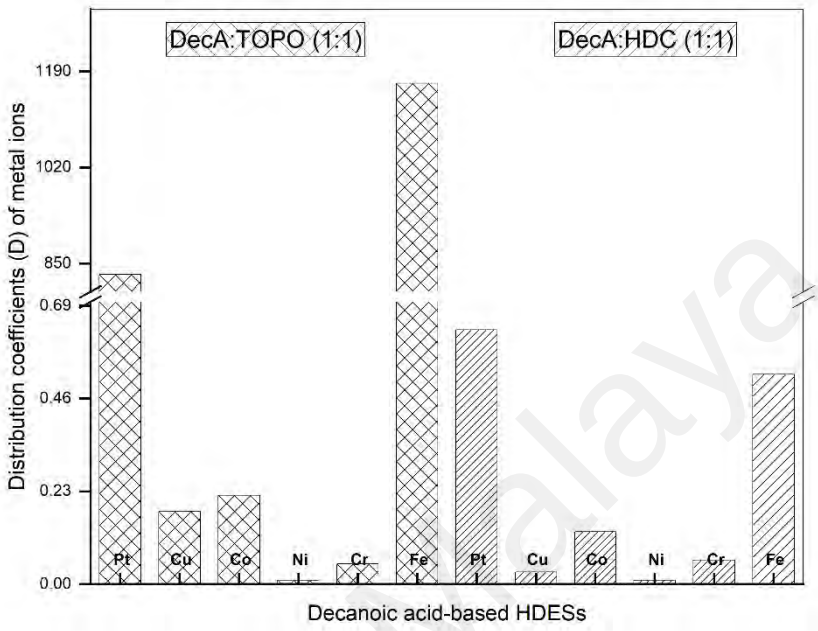

Figure 2.5: **Effect of HBA on the distribution coefficients of different metal ions. Data are extracted from (Schaeffer et al., 2020).**

Several authors investigated the performance of HDES in terms of enrichment factor (EF) and extraction recovery (ER) in the extraction process, as shown in Equations 2.3 and 2.4. Rad et al. (2019) studied the effect of pH on the extraction recovery of nickel for the pH range of 1-10. Lower recovery was observed at pH values below 7, which could be attributed to the competition between H^+ and Ni^{2+} in the formation of the complex (Rahnama & Najafi, 2016). Shi et al. (2020) investigated the effect of pH on the extraction of Cr (VI) from water using TOMC-based HDES. In the pH range of 2 to 5, the best extraction was obtained for Cr (VI). This could be due to the fact that when the pH was 2-5, $HCrO4^-$ was the predominant form and the electrostatic interaction between $HCrO^{4-}$ and N+(R3R') of TOMC favored the transfer of Cr (VI) from water to HDES. When the pH > 7, the extraction rate decreased due to too elevated level of OH^- which did not favor the interaction between $CrO4^{-2}$ and HDES. Figure 2.6 shows the effect of pH on the Cu(II)

distribution ratio in terpene-based HDES. As can be seen in Figure 2.6, the extraction of Cu(II) is inversely proportional to the concentration of hydrogen ions. Above pH 4.5, the distribution coefficient of Cu(II) increases due to the deprotonation of functional groups in the HDES and the formation of Cu(II) hydroxyl species, which increases the metal-ligand interactions. At low pH, excess H^+ ions compete with Cu(II) for coordination sites, reducing extraction efficiency. As pH increases, the reduced proton competition facilitates increased complex formation between Cu(II) and the HDES constituents, such as carboxyl or phosphate groups, resulting in improved extraction efficiency. In addition, the partial hydrolysis of Cu(II) to $Cu(OH)^+$ species at elevated pH values can increase its affinity for the hydrophobic phase and thus increase the distribution coefficient. For both HDES studied, little extraction occurs below pH 3 and reaches a maximum at pH 5.2. Further increase in pH is hindered by the hydrolysis of Cu(II).

$$ER(\%) = \frac{C_{set} \times V_{set}}{C_0 \times V_0} \times 100 = EF \times {}^{V_{set}}/_{V_0} \quad (2.3)$$

$$EF = {}^{C_{set}}/_{C_0} \quad (2.4)$$

Where C_{set} is the concentration and V_{set} is the volume of the extractant phase. C_0 and V_0 are the concentration and volume of the initial water phase, respectively.

HDES can also be used to remove metal ions from an unbuffered aqueous solution, which was first reported by Van Osch et al. (2016) They investigated the extraction of various metal chloride salts from water using HDES without changing the pH of the water streams. HDES were prepared by mixing DecA and lidocaine in different molar ratios.

Removal of all transition metal ions with high distribution ratios was demonstrated by an ion exchange mechanism, even at high Co^{2+} concentrations and low HDES/water mass ratios. It was possible to achieve maximum extraction and regeneration within 5s. Ruggeri et al. (2019) also found that buffered solutions are problematic for extraction

experiments: Cu(II), Ni(II), and Cr(III) are poorly soluble in phosphate buffer, and precipitation of hydroxides occurs under alkaline conditions. LLE is widely used for the extraction of metal ions from water medium as shown in Table 2.5. The extraction performance of various HDES for the extraction of metal ions was compared in terms of extraction efficiency or distribution ratio. Process and analysis methods were also mentioned for each system.

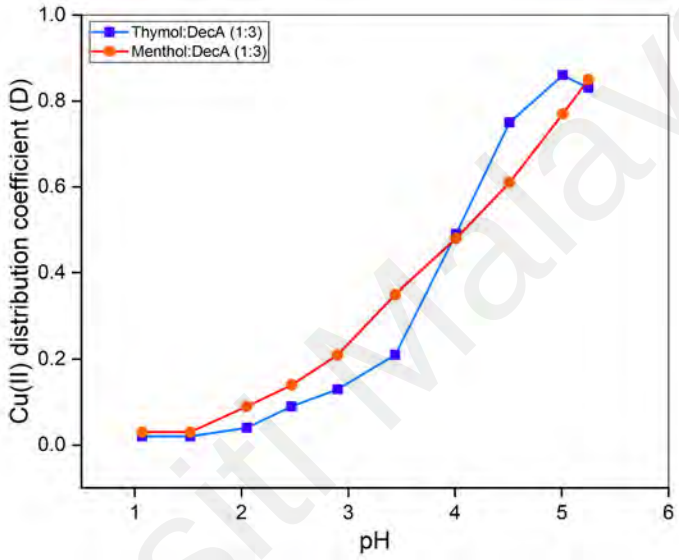

Figure 2.6: **Cu(II) distribution in HDES as a function of pH (T=20 °C, Na_2SO_4=0.1M).**

Table 2.5: Extraction of various metals from water solutions using HDES at optimum conditions.

HBA	HBD	Ratio	Analyte	Process	Method	EE (%) or D	Ref.
Lidocaine	DecA	2:1	Co	LLE	ICP-OES[a]	0.990-0.996	(Van Osch et al., 2016)
			Ni			>0.996	
			Zn			>0.995	
			Cu			>0.996	
			Na			0.195	
			K			0.211-0.457	
			Li			0.266	
			Cl			0.086-0.197	
			Mn			0.992	

Table 2.5, continued.

HBA	HBD	Ratio	Analyte	Process	Method	EE (%) or D	Ref.
Thymol	DecA	1:3	Cu	LLE	UV-Vis[b]	0.03-0.85	(Schaeffer et al., 2018)
Menthol	DecA	1:3	Cu	LLE	UV-Vis	0.02-0.86	(Schaeffer et al., 2018)
TOMC	BHB	1:3	Cr(IV)	LLE	UV-Vis	~100	(Shi et al., 2020)
L-menthol	SA	4:1	Ag^{+}	SLM	FAAS	90	(Shahrezaei et al., 2020)
Thymol	MPD	2:1	Boron	LLE	ICP-OES	90.1	(Almustafa et al., 2020)
Menthol	MPD	2:1		LLE	ICP-OES	83.2	
DL-Menthol	Lidocaine	5:5	Indium	LLE	ICP-OES	2.14	(Edgecomb et al., 2020)
	PS	7:3				4.1	
MAA	Lidocaine	9:1				28	
	PS	9:1				767	
TOPO	DecA	1:1	Pt^{4+}	LLE	UV-Vis	830.2	(Schaeffer et al., 2020)
			Pd^{2+}			25.04	
			Cu^{2+}			0.18	
			Co^{2+}			0.22	
			Ni^{2+}			<0.01	
			Cr^{3+}			0.05	
			Fe^{3+}			1169	
Thymol	TOPO	1:1	Pt^{4+}			327.6	
			Pd^{2+}			18.16	
			Cu^{2+}			0.05	
			Co^{2+}			<0.01	
			Ni^{2+}			<0.01	
			Cr^{3+}			0.02	
			Fe^{3+}			280.7	
HDC	DecA	1:1	Pt^{4+}			0.63	
			Pd^{2+}			0.18	
			Cu^{2+}			0.03	
			Co^{2+}			0.13	
			Ni^{2+}			<0.01	
			Cr^{3+}			0.06	
			Fe^{3+}			0.52	
TOPO	1-hexanol	1:1	Pt(IV)	LLE	ICP-OES	98.3	
	1-butanol	1:1	Pt(IV)			98.9	

Table 2.5, continued.

HBA	HBD	Ratio	Analyte	Process	Method	EE (%) or D	Ref.
	L-menthol	1:1	Pt(IV)			94.4	(Liu et al., 2021)
TOPO	TTFA	2:1	Li	LLE	ICP-OES	95.7	(Hanada & Goto, 2021)

[a]Inductively coupled plasma-optical emission spectrometer, [b]Ultraviolet–visible spectroscopy

Phelps et al. (2018) first reported the extraction of trace pertechnetate ($99mTcO_4^-$) from an aqueous medium using three HDES. They investigated the effect of the volumetric ratio of HDES to the aqueous phase on the extraction of $99mTcO_4^-$. The distribution ratios for 99mTcO4– extracted from a 0.15 M ReO_4^- aqueous solution using HDES as the extraction phase indicate that distribution ratio decreases monotonically as the volumetric ratio of HDES to the aqueous phase decreases. This is quite predictable since the perrhenate, which is a surrogate for TcO_4^-, effectively competes with the pertechnetate tracer levels and eventually outcompetes the ability of the HDES phase to take up tetra-oxo anions. The effect of HDES to aqueous volume ratio was also analyzed to remove lithium ions (Zante et al., 2020). When the ratio of HDES to aqueous phase increased, the EE improved. A non-negligible extraction of lithium was observed when the ratio was higher than 1. However, a 1:1 HDES to aqueous phase was suitable and economically feasible to achieve the desired efficiency.

Shahrezaei et al. (2020) used an HDES based on L-menthol and salicylic acid (SA) as an effective membrane fluid in a supported liquid membrane (SLM) extraction system to selectively separate silver ions without the need for a carrier ligand to form a highly selective complex with the metal ion for the first time. The HDES, consisting of L-menthol and SA (4:1), was used as an optimal membrane solvent and suitable carrier for the extraction of silver (Ag^+) ion. This technique is based on the formation of a

hydrophobic complex between Ag^+ ions and the HBD (SA) of HDES. Compared to existing SLM systems reported in the literature, the developed HDES-SLM system showed adequate permeability and enhanced selectivity for the transport of Ag^+ ion transport from aqueous solutions comprising Fe^{2+}, Mn^{2+}, Cu^{2+}, Ni^{2+}, Pb^{2+}, and Cd^{2+} as competing metal ions. The schematic diagram of the SLM cell and the system designed for the transfer of Ag^+ ions can be seen in Figure 2.7.

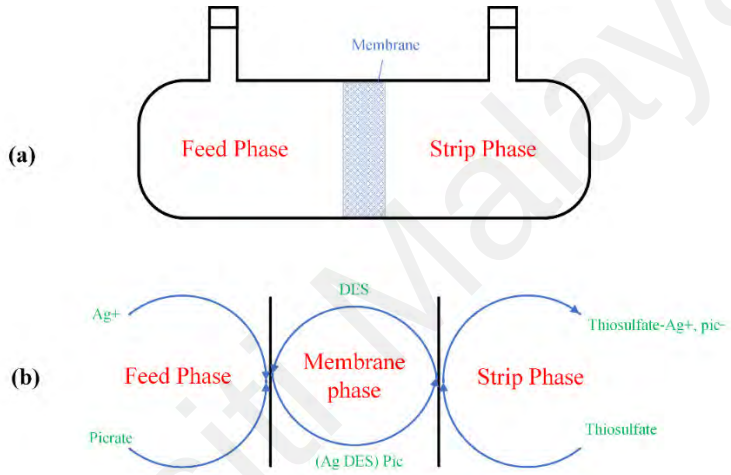

Figure 2.7: (a) Schematic of the SLM process, (b) SLM process for the transport of Ag^+ ions.

2.8.2 Removal of phenolic pollutants

Micropollutants have emerged as a new class of contaminants because, despite their relatively low concentration in water streams, their presence has been associated with a variety of adverse effects on human and animal health, including carcinogenic and endocrine-disrupting effects and antibiotic resistance in bacteria. Bisphenol-A (BPA) is a micropollutant of particular concern. It has been detected in an increasing number of water sources worldwide, despite the inability of conventional water treatment plants to eliminate it (Luo et al., 2014; Margot et al., 2015). Chlorophenols with covalently bonded chloride atoms are also considered organic pollutants (Karimiyan & Hadjmohammadi, 2016; Wang et al., 2019). Some nitrophenols are also classified as priority pollutants.

Table 2.6: Comparison of HDES with organic solvents and ILs for the removal of phenolic pollutants from water streams.

Solvent	Mole ratio	Phenol	Process	EE/ER (%)	Ref.
OctA:DdecA	3:1	BPA	LLE	76.04	(Florindo et al., 2018b)
NonA:DdecA	3:1			88.32	
DecA:DdecA	2:1			81.81	
OctA:NonA:DdecA	1:1:1			85.49	
OctA:decA:DdecA	1:1:1			82.77	
THAB[a]:OctA	1:2	BPA	LLE	94.91	(Florindo et al., 2020)
THAB:DecA	1:2			97.10	
TOAB[b]:OctA	1:2			90.48	
TOAB:DecA	1:2			97.61	
MTOAB[c]:OctA	1:2			84.24	
MTOAB:DecA	1:2			91.99	
MTOAB:DL-menthol	1:2			91.45	
DL-menthol:OctA	1:2			81.65	
DL-menthol:DecA	1:2			92.43	
MTOAC: OctA	1:2	4-CP[d]	DLLME	93.0	(An et al., 2020)
		2,4-DCP		90.8	
		2,4,6-TCP[e]		91.9	
DL-menthol:OctA	1:1	Phenol	LLE	up to 87.46	(Sas et al., 2019)
DL-menthol:DecA	1:1			up to 88.78	
DdecA:OctA	1:3			up to 75.78	
DdecA:decA	1:2			up to 67.84	
DL-menthol:OctA	1:1	*o*-Cresol	LLE	up to 96.49	
DL-menthol:decA	1:1			up to 96.80	
decA:OctA	1:3			up to 93.44	
decA:decA	1:2			up to 91.04	
DL-menthol:OctA	1:1	2-CP	LLE	up to 97.04	
DL-menthol:decA	1:1			up to 96.96	
DdecA:OctA	1:3			up to 98.42	
DdecA:decA	1:2			up to 98.00	
Menthol:PA[f]	1:1	BPA	LLE	98.2	(An & Row, 2021)
Menthol:FA[g]	1:1			99.0	
Menthol:DecA	1:2	2-CP	LLE	97.18	(Adeyemi et al., 2020)
		3-CP[h]		97.92	
		2,4-DCP		96.00	
[bmim][Tf2N]		3-CP	LLE	85.14	(Sulaiman et al., 2019)
[1,3bmPY][Tf2N]				89.33	
[1,3emPY][Tf2N]				87.02	
[Et2MeS][Tf2N]				74.83	
[C4mPip][Tf2N]				86.87	
Tributylphosphate		2,4-DCP	LLE	87.29	(Brinda Lakshmi et al., 2013)
Benzene				66.05	
MBK[i]				82.12	
Di-isopropylether				71.56	

[a]Tetraheptylammonium bromide, [b]Tetraoctylammonium bromide, [c]Methyltrioctylammonium bromide, [d]4-chlorophenol, [e]2,4,6-trichlorophenol, [f]propionic acid, [g]formic acid, [h]3-chlorophenol, [i]Methyl isobutylketone

Table 2.6 shows the list of various HDES used for the extraction of phenolic pollutants from aqueous streams. The results show that HDES have comparable extraction capabilities to the ILs tested. In some cases, HDES outperformed ILs such as [Et_2MeS][Tf_2N] in terms of extraction efficiency (Sulaiman et al., 2019). This is significant because HDES can replace ILs in the extraction of phenolic contaminants due to their better properties. Moreover, HDES showed higher extraction for 2,4-dichlorophenol (2,4-DCP) than organic solvents such as tributyl phosphate, benzene, methyl isobutyl ketone and di-isopropyl ether. However, the organic solvents required less time for the extraction process than HDES in terms of the duration of the process. For example, the extraction of chlorophenols with organic solvents took 10 minutes, while the extraction with HDES took 30 minutes (Adeyemi et al., 2020; Brinda Lakshmi et al., 2013).

Passos et al. (2012) studied the extraction of BPA from aqueous medium using aqueous biphasic systems consisting of 15% K_3PO_4 + 25% imidazolium or ammonium-based IL + 60% aqueous phase, and achieved extraction efficiencies up to 100% in a single step in most systems. Nevertheless, cross-contamination of the aqueous phase was not negligible, as the salt-rich phase in equilibrium with the IL -rich phase contains 22 wt% K_3PO_4 and 25 wt.% IL, posing further environmental concerns.

Florindo et al. (2018b) used sustainable fatty acid-based HDES for the first time to extract BPA from an aqueous environment. All of the fatty acid-based HDES studied are immiscible with water and do not require salting out agents, making them more economical and environmentally friendly. Very high EEs of up to 92% for BPA were obtained with the fatty acid-based HDES in one step. Three HDES were prepared entirely from fatty acids, including OctA, NonA, DecA and DdecA, all of which can behave as HBAs and HBDs simultaneously. The acquired EEs can be sorted in the following order:

OctA: DdecA HDES < DecA: DdecA HDES < NonA: DdecA HDES; this shows no obvious relationship between the EEs and the hydrophobicity of the DESs. This could be because DecA:DdecA HDES has a different molar ratio (2:1) than the other two HDES (3:1). Ternary DESs were also formed by adding a second HBD to OctA:DdecA, DecA:DdecA, and NonA:DdecA HDES and analyzed for the extraction of BPA. Overall, the EEs achieved with ternary HDES ranged from 79 to 91% (Figure 2.8), indicating that the addition of another component to binary DESs can help optimize the efficiency of BPA removal. Moreover, the lowest EE (76.04%) was obtained for binary DES OctA:DdecA, showing that increased hydrophobicity is beneficial in the removal of BPA. In other words, adding either NonA to OctA:NonA:DdecA or DecA to OctA:DecA:DdecA increases the EE of BPA. Conversely, decreasing the amount of OctA in ternary DESs contributes to an increase in EE.

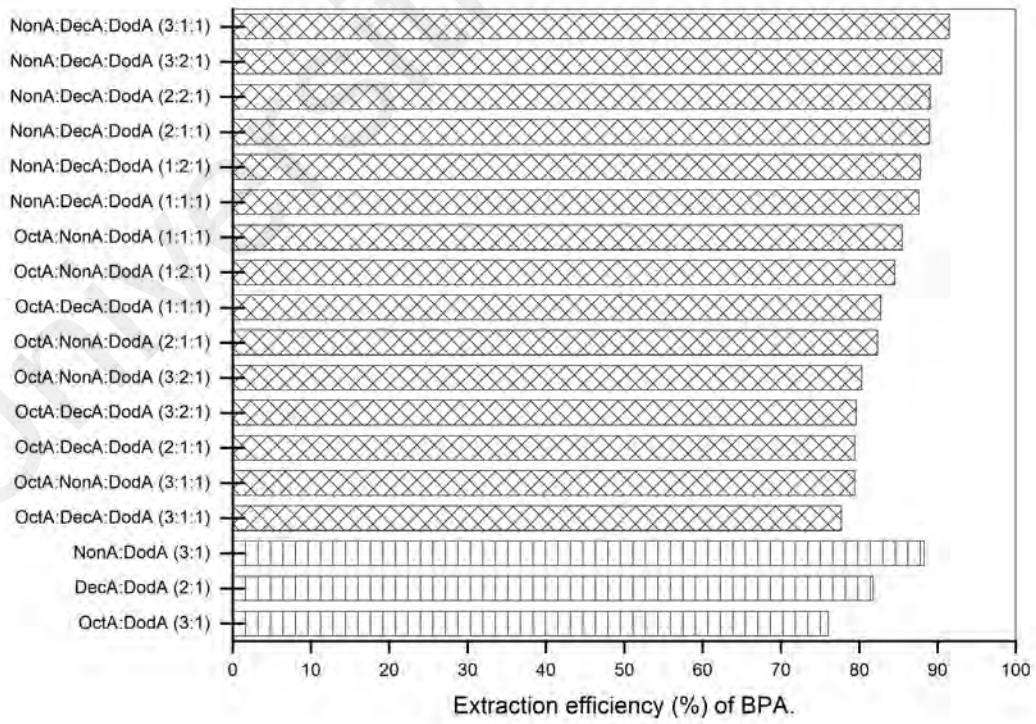

Figure 2.8: The extraction efficiency of BPA using binary and ternary fatty acid-based-HDES. Data are extracted from (Florindo et al., 2018b).

In another study, Florindo et al. (2020) prepared HDES by combining natural fatty acids (as HBD) with DL -menthol (as HBA or HBD) or quaternary ammonium salts (as HBA). They investigated the extraction of BPA from water. The performance of ionic HDES (quaternary ammonium-based DESs) and natural HDES (DL -menthol-based DESs) was compared to extract BPA. All HDES showed good EE up to 85%. It was observed that EE improved with increasing alkyl chain length of both fatty acid and quaternary ammonium salt. As for the HBA of DES, the trend of EE can be arranged in the following order: TOAB:HBD (~98%) > THAB:HBD (~95%) > MTOAB:HBD (~91%) > DL -menthol: HBD (~87%). The EE of BPA followed the HBD order as: THAB > TOAB > MTOAB > DL -menthol for OctA fatty acid, and THAB ~ TOAB > MTOAB > DL -menthol for DecA fatty acid.

The effect of different HBDs of HDES on the EE of BPA from environmental water was also studied by An and Row (2020). Different HBDs were mixed with DL -menthol in a 1:1 molar ratio (HBA: HBD) to form the HDES. For HBDs, the EE for BPA was as follows: Formic acid > Propionic acid > n-Butyl alcohol ~ Acetic acid > 1-Dodecanol > DecA > Oleyl alcohol > Hexanoic acid > OctA. For the hydroxylic acid HBD, the EE of the target decreased with increasing fatty acid chain length. A similar behavior was observed by Adeyemi et al. (2020) in the removal of chlorophenols from an aqueous medium. As the chain length of alkanoic acids (as HBD) increased from hexanoic acid to DecA, the extraction efficiency of 2- CP and 3- CP decreased (Adeyemi et al., 2020). This is plausible since the extraction capability of DES should improve with the increase of chlorine atoms in chlorophenols. The difference in hydrophobicity between the CPs and water is caused by an increase in the number of chlorine atoms (Sas et al., 2019). As a result, there is an interaction between the CPs and water that produces a driving force for the CPs to the DESs as more chlorine is bonded to the CPs' benzene ring. Similar behavior was observed in the work of Sas et al. (2019). Furthermore, ILs have been found

to display the similar behavior when the amount of chlorine atoms in the CPs increases (Deng et al., 2011; Huang et al., 2014).

As various researchers have noted, the molar ratio of HDES is a crucial element affecting the physicochemical aspects of DES. To investigate the effect of different molar ratios of HDES on EE of BPA, four molar ratios of HBA:HBD (1:2, 1:3, 1:4 and 1:5) were selected by Florindo et al. (2020) and used to prepare HDES belonging to quaternary ammonium salts and DL -menthol. The reason for using these particular molar ratios of the HDES is that larger ratios of salt to acid would not result in the formation of a liquid phase at room temperature. The effect of the molar ratio on the EE of BPA from an aqueous environment is shown in Figure 2.9. From Figure 2.9, it can be seen that the molar ratios do not have a significant effect on the extraction efficiency of the HDES studied, with TOAB:OctA showing the most significant changes in BPA extraction efficiency with the molar ratios of HBA:HBD. It can be concluded that increasing the acid concentration (from 1:2 to 1:5) does not improve the extraction efficiency of BPA for both neutral and ionic HDES. Similarly, the extraction of chlorophenols was not significantly affected for terpene-based HDES when the thymol concentration was increased. Additionally, Figure 2.9 illustrates the influence of the HBA/HBD molar ratio on the extraction efficiency of various chlorophenols. The mole of HBA (menthol) used was kept constant, while the mole of HBD (thymol) was altered to obtain a ratio ranging from 1:1 to 1:4.

In terms of the cost of an industrial extraction process, higher extraction efficiency with a minimum amount of solvent is desirable. The effect of HDES:water mass ratio on the extraction efficiency of chlorophenols was investigated, as shown in Figure 2.10 (a).

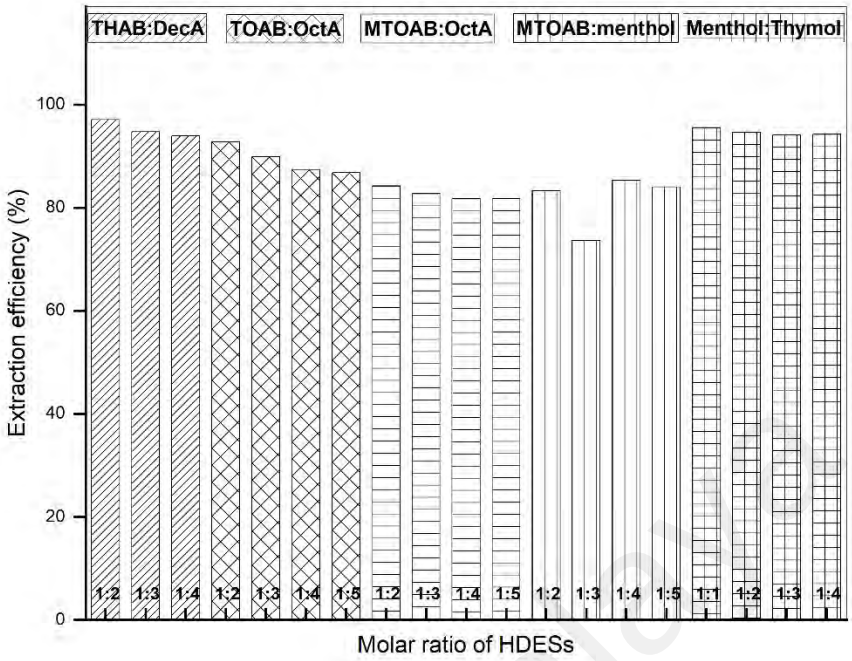

Figure 2.9: Influence of HBA: HBD ratio of different HDES on the EE of BPA and 2-CP. Menthol:thymol HDES used for the extraction of 2-CP. All other HDES were used to extract BPA. Data are taken from (Adeyemi et al., 2020; Florindo et al., 2020).

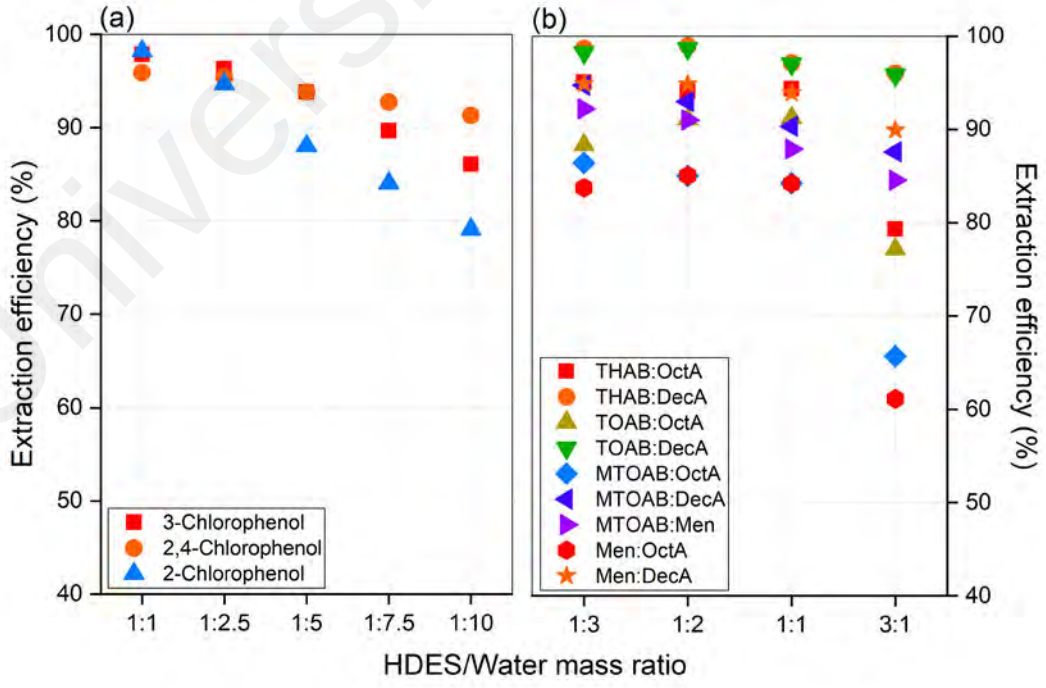

Figure 2.10: Effect of HDES/water mass ratio on the EEs of (a) chlorophenols using Menthol:thymol (1:2) HDES, (b) BPA using different HDES. Data are taken from (Adeyemi et al., 2020; Florindo et al., 2020).

Overall, the results show that extraction efficiency reduces with decreasing HDES:water mass ratio for all systems, although to different degrees. There was a slight decline in extraction capability with increasing mass ratio, such that substantial extraction could be achieved even with a HDES:water mass ratio mass ratio of 1:10. At a HDES:water mass ratio mass ratio of 1:10, the extraction efficiency of all systems was greater than 80% when 2 g of HDES and 20 g of the aqueous solution were mixed. This has huge economic implications as lower quantities of HDES exhibited considerable removal of chlorophenols from water.

Figure 2.11 shows the effects of different initial concentrations of phenolic compounds on extraction efficiency. It is observed that the extraction efficiency increases as the initial concentration of a phenolic compound increases. This is due to the ability of DES to remove phenols from water and the absence of DES saturation under working conditions. The lower extraction rate at low concentrations of phenolic compounds is due to the fact that the phenolic molecules may be completely surrounded by water molecules, which hinder the extraction process at this concentration. The influence of the initial concentration of phenolic compounds on extraction efficiency remains fairly stable after 50 ppm, as the HDES phase reaches a saturation threshold when all accessible sites for hydrogen bonding and hydrophobic interactions are occupied. At lower concentrations, the extraction efficiency improves as a larger number of phenolic molecules are accessible for interaction with HDES. Once a threshold concentration of about 50 ppm is reached, the system approaches equilibrium. At this point, additional phenolic molecules in the aqueous phase no longer contribute to improving extraction efficiency. This phenomenon is due to the finite number of active sites in the HDES phase, suggesting that beyond this concentration, the ability of HDES to solubilize new phenolic molecules remains constant, leading to a plateau in extraction efficiency. From Figure 2.11, the experimental data for extraction efficiency remains almost constant when the initial

concentration of phenolic compound is more than 50 mg L^{-1}. However, Adeyemi et al. (2020) reported that the extraction efficiency decreased after increasing the concentration of 2-CP in water. The removal of chlorophenols from aqueous medium is hindered by hydrophobic interactions between the chlorophenols and the HDES, hydrogen bonding between the HDES and the chlorophenols, and the placement of the chlorine atom on the benzene ring. For example, Deng et al. (2011) studied two dichlorophenols (3,4-dichlorophenol and 2,4-DCP) with different chlorine atom locations and identified substantial variations between the two. A distribution coefficient of 3500 was found for 2,4-DCP, while a distribution coefficient of 600 was found for 3,4-dichlorophenol. Two chlorine atoms were found in both chlorophenols, with one chlorine atom on the fourth carbon. In another experiment (Bekou et al., 2003), it was found that the IL 1-ethyl-3-methylimidazolium bis(perfluoroethylsulfonyl)imide had a higher extraction capability for 2,4-DCP compared to pentachlorophenol, which was contrary to the general trend of extraction increase with the increase of chlorine atoms.

Vortex-assisted liquid-liquid microextraction (VALLME) has also been used for the extraction of bisphenols from water (Ojeda & Rojas, 2018; Yang et al., 2014; Yiantzi et al., 2010). Li et al. (2020) presented the first report on the determination of bisphenols using TOMC-based HDES. In order to optimize the extraction of bisphenols, different techniques for dispersing HDES in water were investigated, including vortexing, shaking, and ultrasonic irradiation. Apart from vortexing, shaking and ultrasonic irradiation were found to be unable to disperse HDES into thousands of small droplets in water due to their high viscosity. The effect of different vortex times (1-6 min) on extraction efficiency was studied to determine the optimum vortex duration. The extraction efficiency increased progressively with increasing vortex duration from 1 to 4 minutes and then remained constant with increasing vortex duration, indicating that extraction equilibrium had already been reached. The effect of salt addition on extraction efficiency is often

evaluated throughout the LLE process, although it has not been clearly stated whether the effect is positive or negative (Ge et al., 2018). Li et al. (2020) investigated the effect of salt addition and reported that the peak area decreased with increasing amount of salt in the range of 0 to 0.5 g. The peak area decreased with the increasing amount of salt. This phenomenon is probably due to the addition of Cl^-, which could interfere with the hydrogen bonding between bisphenols and HDES due to its strong hydrogen bonding ability, resulting in a decrease in the extraction capability of HDES.

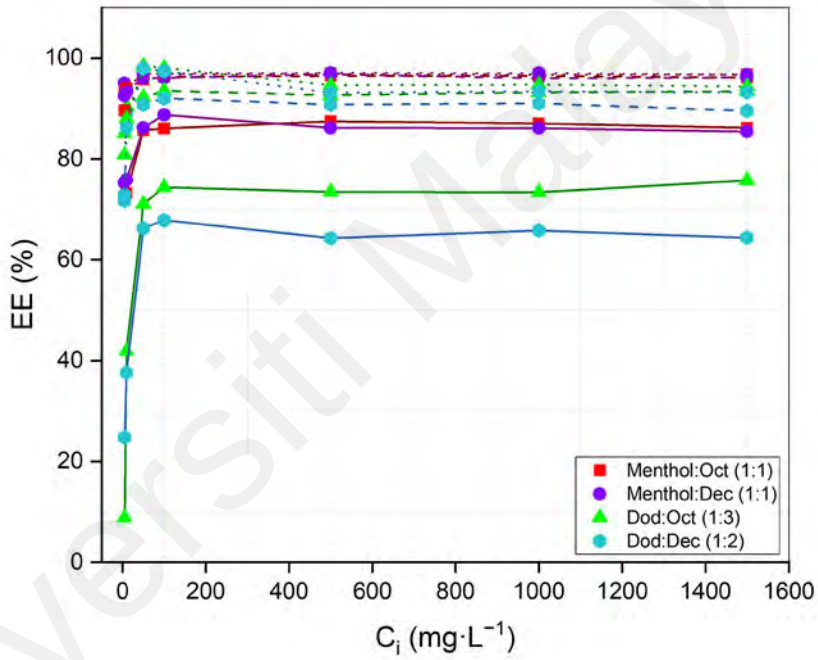

Figure 2.11: Effect of initial concentration of phenolic pollutants on the EE; solid, dash, and dot lines indicate the phenol, o-cresol, and 2-CP, respectively. Data are taken from (Sas et al., 2019).

Faraji et al. (2020) investigated ternary HDES for the extraction of nitrophenols from aqueous media using DLLME. They replaced binary HDES with ternary HDES to reduce their viscosity and used them in the VALLME process. The initial results showed relatively low extraction efficiency of nitrophenols for TBAB:thymol type HDES due to their relatively high viscosity and melting point. After addition of OctA to TBAB:thymol, the extraction efficiency was increased and the physicochemical properties of HDES were

improved. By increasing the molar ratio of OctA (TBAB:thymol:OctA from 1:1:1 to 1:1:3), the extraction efficiency increased and then remained constant (1:1:4). The study revealed that the low molar ratio of thymol in the HDES composition increases the extraction efficiency due to the strong π-π interactions. However, the extraction efficiency decreases at higher molar ratio of thymol in HDES. The various microextraction techniques used for the determination of different chlorophenols and nitrophenols in water samples are summarized in Table 2.7.

Table 2.7: Comparison of microextraction techniques used for the removal of phenols from water streams.

Method	Analyte	Matrix	Analysis	LR[a]	LOD[b]	RSD[c]	Ref.
DLLME	4-CP, 2,4-DCP, 2,4,6-TCP	Wastewater	HPLC	0.5-100	0.03-0.05	1.8-3.1	(An et al., 2020)
MMF-SPME[d]	4-NP[e], 2,4-DNP[f]	Tap water	HPLC	1.0-200	0.075-0.27	<10.0	(Mei et al., 2015)
DLLME	4-NP, 2,4-DNP	Tap water	HPLC-UV	1.0-500	0.2-0.3	≤ 5.0	(Faraji et al., 2020)
DLLME	2,4-DCP, 2,4,6-TCP	Environmental water	HPLC	0.1-50	0.016-0.024	1.5-3.0	(Tang et al., 2018)
MISPE[g]	4-CP, 2,4-DCP, 2,4,6-TCP	Seawater	HPLC-UV	0.5-50	0.05	1.0-3.3	(Ma & Row, 2018)
SPME[h]	2-CP, 4-CP, 2,3-CP[i], 3,4-CP[j]	Environmental water	HPLC-UV	0.1-100	0.01-0.03	4.4-6.1	(Hao et al., 2019)

[a]linear range in μg mL^{-1}, [b]limit of detection in μg mL^{-1}, [c]relative standard deviation in %, [d]multiple monolithic fiber-solid phase microextraction, [e]4-nitrophenol, [f]dinitrophenol, [g]Molecularly imprinted solid-phase extraction, [h]solid-phase microextraction, [i]2,3-chlorophenol, [j]3,4-chlorophenol

2.9 Summary of literature review

In order to reduce the use and production of hazardous compounds, the idea of green chemistry was launched in the mid to late 1990s, primarily through the promotion of innovative research towards the provision of innovative technologies. HDES meet green chemistry standards due to their low vapor pressure (Florindo et al., 2019a), high thermal

stability (Chen et al., 2021), wide liquid range (Gilmore et al., 2018b), and low flammability (Cao & Su, 2021). The use of HDES in the elimination of pollutants is constantly increasing. Due to their sustainability, ease of use, low vapor pressure, wide liquid spectrum, and negligible miscibility with water, HDES have great potential as sustainable solvents for the removal of pollutants from contaminated water. However, the most commonly used DES formulations contain solvents with hydrophilic properties. Despite an increased focus on HDES synthesis, their number is still small and additional efforts are needed to synthesize and investigate novel HDES as extraction solvents. This review highlights the extractive capabilities of these HDES, with particular emphasis on the extraction of heavy or toxic metals, phenolic pollutants, and PAHs from aqueous streams. The extraction efficiency could be improved by determining the optimum water content, viscosity, type of HBA/HBD, mass ratio of HDES to water, molar ratio of HDES, pH of the solution and initial concentration of the contaminant.

It is defined in the literature that the DESs can be formed by combining two or three low-cost components (Lee et al., 2019). However, this is not true for all DESs, especially not for HDES. Besides some fatty acids and terpenes (menthol and thymol) used as HBAs, the most commonly used quaternary ammonium salts with longer alkyl chains, such as TOAB, MTOAB, THAB, are expensive, which makes commercial application difficult. Several fundamental information gaps need to be filled, from the interactions driving the evolution of HDES to the involvement of water and the structure of the liquid phase. A more detailed understanding and interpretation of solid-liquid phase diagrams and eutectic melting point are also needed, as well as a systematic description of these solvents. Another critical aspect is the need for thermophysical property data, including densities and viscosities, as well as vapor pressure, polarity, and surface tension, which would facilitate the development of structure-property correlations for HDES. The polarity of HDES is an essential attribute for understanding their extractability and water

miscibility; yet little attention has been paid to this area. Therefore, systematic and comprehensive research on the polarity of HDES would be of great benefit. Moreover, to avoid the occurrence of emulsions, HDES must have a high surface tension. However, this parameter has not been sufficiently studied and further research is needed.

The type of HBA or HBD plays a crucial role in the formation and application of HDES in the extraction process. For example, in some studies (Gilmore et al., 2018a; Rad et al., 2019), phenol-based HBDs were chosen to form HDES for metal extraction. Phenol as HBD is suboptimal due to its possible corrosiveness and toxicity, as well as the possibility of nitration by concentrated nitric acid, which is often used as a digestion medium (Babich & Davis, 1981; Sato et al., 1973). To overcome these difficulties, it is recommended to use more chemically and environmentally friendly HBD components. The synthesis of HDES and the characterization of their physicochemical properties are still limited compared to hydrophilic DESs. Currently, there are no targeted studies on the toxicity of HDES. More diverse HDES need to be developed, especially those containing non-toxic, low-cost and biodegradable components as found in natural DESs. The use of naturally occurring components (both HBA and HBD) allows unprecedented customization of the properties of low-cost, non-renewable HDES, which is a critical goal of green chemistry.

The high viscosity of HDES impairs the separation and analysis of some extracts. Due to their high viscosity, HDES cannot be injected directly into GC or HPLC without dilution. In addition, HDES cannot be dispersed into thousands of small droplets in water by shaking and sonication due to their high viscosity. Therefore, one of the research fronts in the development of these solvents is the study and introduction of HDES with low viscosity and low melting point, which have strong and effective interactions with analytes. One solution to this problem is the development of three-component HDES,

because the third component lowers the viscosity and melting point but can also lead to stronger interactions (Faraji et al., 2020). Van Osch et al. (2019), one of the pioneering groups for HDES, presented four requirements for the sustainability of an HDES. One of the proposed requirements was that the viscosity should be less than 100 m.Pa.s. This requirement is more strict and practical than the one provided by Garcia et al. (2015) (<500 m.Pa.s).

Finally, it is important to use computational methods to select efficient HDES and understand the extraction mechanism for a particular application. This would play a crucial role in establishing a predictive framework to enable the "designer" attribute of HDES. However, there is little research in this regard. Therefore, a greater awareness of the critical importance of this topic should appeal to those who do not have access to or expertise in HDES and certain experimental methods for simulating systems and using aggregated raw data to complement experimental results.

CHAPTER 3: MATERIALS AND METHODOLOGY

This chapter presents the methodology, and materials used in this study. First, for the phenolic pollutant, COSMO-RS model was applied to select HDES based on their performance index. The HDES used in this work were prepared according to the method described by Abbott et al. (2004a), in which salt and HBD were mixed in a specific molar ratio. The synthesized HDES were characterized by various methods. The effects of various parameters including initial concentration, contact time, molar ratio of HDES, mass ratio of HDES to water solution, and pH were studied. COSMO-RS was also used to understand the extraction mechanism for the removal of phenolic pollutants. Consistency tests, including Hand and Othmer-Tobias correlations, were also performed. Several analytical techniques were used, including ^{1}HNMR, GC, and AAS. For the removal of cresols, HDES were prepared based on terpenes and carboxylic acids. Due to numerous advantages, HDES based on terpenes and carboxylic acids are ideal for the removal of phenolic impurities from water. Terpenes are a class of naturally occurring organic compounds derived from plants that confer biodegradability and low toxicity to HDES. In addition, various HDES were prepared and experimentally studied for the extraction of heavy metals, and parametric analysis was performed using the best HDES. The overall methodology of this research is shown in Figure 3.1.

3.1 Materials

The chemicals and materials utilized in this investigation are presented in Table 3.1, along with their Cas number, formula, supplier, molecular weight (MW) and purity. No additional purification was performed on any of the chemicals utilized.

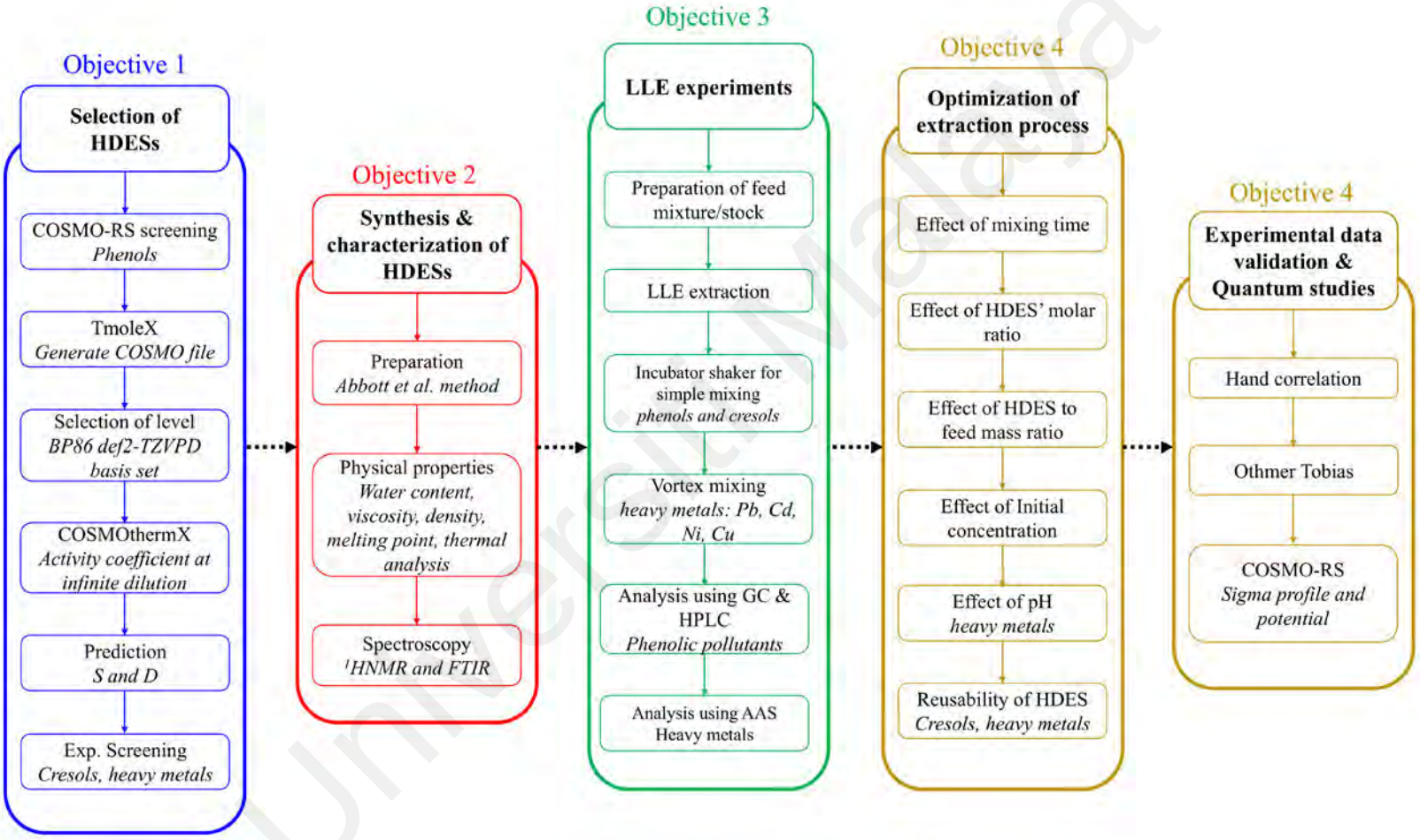

Figure 3.1: Overall research methodology

Table 3.1: List of chemicals used in this work.

Chemical	Formula	Cas Number	Supplier	MW (g/mole)	Purity (%)
Menthol	$C_{10}H_{20}O$	89-78-1	Sigma-Aldrich (USA)	156.27	≥95%
Thymol	$C_{10}H_{14}O$	89-83-8	BDH Laboratory (England)	150.22	≥99%
Decanoic acid	$C_{10}H_{20}O_2$	334-48-5	Sigma-Aldrich (Malaysia)	172.26	≥98%
Coumarin	$C_9H_6O_2$	91-64-5	Thermo Scientific (France)	146.14	≥99%
Camphor	$C_{10}H_{16}O$	76-22-2	Acros Organics (China)	152.23	≥96%
Hydrocinnamic acid	$C_9H_{10}O_2$	501-52-0	Sigma-Aldrich (USA)	150.17	≥99%
o-cresol	C_7H_8O	95-48-7	Acros Organics (India)	108.14	≥99%
m-cresol	C_7H_8O	108-39-4	Scarlau (Spain)	108.14	≥99%
Naphthalene	$C_{10}H_8$	91-20-3	Sigma-Aldrich (Germany)	128.17	≥99%
Toluene	C_7H_8	108-88-3	Scarlau (Spain)	92.14	≥99%
Deuterated Chloroform	$CDCl_3$	67-66-3	Sigma-Aldrich (USA)	119.38	≥99%
Ethanol	C_2H_6O	64-17-5	Sigma-Aldrich (Germany)	46.07	≥99.8%
1-hexanol	$C_6H_{14}O$	111-27-3	Fisher Scientific	102.16	99%
TOPO	$C_{24}H_{51}OP$	78-50-2	Thermo scientific	386.64	99%
Lead chloride	$PbCl_2$	7758-95-4	Techno Pharmchem (India)	278.11	99%
Cadmium nitrate tetrahydrate	$Cd(NO_3)_2.4H_2O$	10022-68-1	Scarlau (Spain)	308.48	≥98%

Table 3.1, continued.

Chemical	Formula	Cas Number	Supplier	MW (g/mole)	Purity (%)
Copper nitrate trihydrate	$Cu(NO_3)_2 \cdot 3H_2O$	10031-43-3	Sigma-Aldrich (USA)	24.60	99%
Iron chloride	$FeCl_3$	7705-08-0	Sigma-Aldrich (USA)	162.20	>97%
Nitric acid	HNO_3	7697-37-2	Fisher Scientific (UK)	63.01	≥65%
Hydrochloric Acid	$HCl.H_2O$	231-791-2	Fisher Scientific (UK)	36.46	~36%
Sodium hydroxide	NaOH	1310-73-2	Loba Chemie (India)	39.99	≥98%

3.2 COSMO-RS screening

TmoleX version 4.0 is a version of the TURBOMOLE program package for quantum chemistry with a graphical user interface. Using the BP86 level of density functional theory (DFT) and the triple zeta valence potential with diffuse functions (TZVPD), geometry optimizations were performed for each species involved (i.e., HDES constituent, phenol, water). The BP86 def2-TZVPD basis set was used for single point calculations.

The parameterization file BP _TZVPD_ FINE _ 19.ctd was used to import the .cosmo files into COSMOThermX version 19.0.5. The electroneutral approach was used. In this approach, each HDES is considered as three different compounds (cation, anion, HBD). Since HBD forms a complex with the salt halide anion in liquid form, reducing the interaction energy between the salt cation and the anion, HDES can be considered to consist of three different species in liquid form: cation, anion, and HBD.

The activity coefficient for phenol and water at infinite dilution ($\gamma\infty$) was determined in each HDES. The $\gamma\infty$ values were used to predict the capacity and selectivity of phenol

in HDES with respect to water at infinite dilution (C^{∞} and S^{∞}) as given in Equations 3.1 and 3.2. Equation 3.3 was used to determine performance index (PI). A total of 72 HDES were investigated. The list of HDES investigated in this study is given in Table 3.2.

$$C^{\infty}_{phenol} = \left(\frac{1}{\gamma^{\infty}_{phenol}}\right)_{DES\ phase} \quad (3.1)$$

$$S_{phenol/water,max} = S^{\infty}_{phenol/water} = \left(\frac{\gamma^{\infty}_{water}}{\gamma^{\infty}_{phenol}}\right)_{DES\ phase} \quad (3.2)$$

$$PI = C^{\infty}_{phenol}\ x\ S^{\infty}_{phenol/water} \quad (3.3)$$

Table 3.2: List of HDES screened.

HBA	HBD	ratio	Abbreviation
Benzoyltrifluoroacetone	Triphenyl phosphate	2:1	BTFA:TPP (2:1)
Decanoic acid	Lidocaine	2:1	DecA:Lid (2:1)
		3:1	DecA:Lid (3:1)
		4:1	DecA:Lid (4:1)
Dodecanoic acid	Octanoic acid	1:3	DdecA:OcA (1:3)
	Decanoic acid	1:2	DdecA:decA (1:2)
	Nonanoic acid	1:3	DdecA:NonA (1:3)
Hydrocinnamic acid	Decanoic acid	1:1	HDCA:DecA (1:1)
Menthol	Aliquat 336	7:3	Men:Alq (7:3)
	Lidocaine	5:5	Men:Lid (5:5)
	ibuprofen	7:3	Men:Ibp (7:3)
	Proton Sponge®	7:3	Men:PS (7:3)
	Octanoic acid	1:1	Men:OctA (1:1)
		1:2	Men:OctA (1:2)
	Decanoic acid	1:1	Men:DecA (1:1)
		1:2	Men:DecA (1:2)
		1:3	Men:DecA (1:3)
	methyl-2,4-pentanediol	2:1	Men:MPD (2:1)
	1-decanol	2:1	Men:1-dec (2:1)
	SA	4:1	Men:SA (4:1)
	Propionic acid	1:1	Men:PrpA (1:1)
	Formic acid	1:1	Men:FmA (1:1)
Methyl anthranilate	Lidocaine	9:1	Mal:Lid (9:1)
	ibuprofen	9:1	Mal:Ibp (9:1)
	Proton Sponge®	9:1	Mal:PS (9:1)
	DL-menthol	9:1	Mal:Men (9:1)
Methyltrioctylammonium bromide	Octanoic acid	1:2	MTOAB:OctA (1:2)
	Decanoic acid	1:2	MTOAB:DecA (1:2)

Table 3.2, continued.

HBA	HBD	ratio	Abbreviation
Methyltrioctylammonium chloride	Octanoic acid	1:2	MTOAC:OctA (1:2)
Tetrabutyl ammonium bromide	Thymol	1:2	TBAB:Thy (1:2)
	Octanoic acid	1:2	TBAB:OctA (1:2)
Thenoyltrifluoroacetone	Triphenyl phosphate	2:1	TTFA:TPP (2:1)
Thymol	Methyl-2,4-pentanediol	2:1	Thymol:MPD (2:1)
	1-decanol	2:1	Thymol:1-dec (2:1)
	Trioctylphosphine oxide	1:1	Thymol:TOPO (1:1)
	Decanoic acid	1:3	Thymol:DecA (1:3)
	Camphor	1:1	Thymol:Camp (1:1)
Trioctylmethylammonium chloride	Methyl 4-hydroxybenzoate	1:1	TOMAC:MHB (1:1)
		1:2	TOMAC:MHB (1:2)
		2:1	TOMAC:MHB (2:1)
	Butyl 4-hydroxybenzoate	1:1	TOMAC:BHB (1:1)
		1:2	TOMAC:BHB (1:2)
		1:3	TOMAC:BHB (1:3)
		2:1	TOMAC:BHB (2:1)
	isobutyl 4-hydroxybenzoate	1:1	TOMAC:iBHB (1:1)
		1:2	TOMAC:iBHB (1:2)
		1:3	TOMAC:iBHB (1:3)
		2:1	TOMAC:iBHB (2:1)
	2-Ethylhexyl 4-hydroxybenzoate	1:1	TOMAC:EHHB (1:1)
		1:2	TOMAC:EHHB (1:2)
		1:3	TOMAC:EHHB (1:3)
		2:1	TOMAC:EHHB (2:1)
	n-octyl 4-hydroxybenzoate	1:1	TOMAC:OHB (1:1)
		1:2	TOMAC:OHB (1:2)
		1:3	TOMAC:OHB (1:3)
		1:4	TOMAC:OHB (1:4)
		2:1	TOMAC:OHB (2:1)
	Decanoic acid	2:1	TOMAC:DecA (2:1)
		1:1	TOMAC:DecA (1:1)
		1:2	TOMAC:DecA (1:2)
	Ketoprofen	2:1	TOMAC:KPF (2:1)
		1:1	TOMAC:KPF (1:1)
		1:2	TOMAC:KPF (1:2)
	Gemfibrozil	1:1	TOMAC:GFB (1:1)
		1:2	TOMAC:GFB (1:2)
Trioctylphosphine oxide	Decanoic acid	1:1	TOPO:DecA (1:1)
	Menthol	1:1	TOPO:Men (1:1)
		1:3	TOPO:Men (1:3)
		1:4	TOPO:Men (1:4)
		1:5	TOPO:Men (1:5)
	1-hexanol	1:1	TOPO:Hex (1:1)
	3,5-Di-tertbutylcatechol	1:1	TOPO:DTBC (1:1)

3.3 Preparation of HDES

HDES are generally prepared by the same methods as DES. Components that are sparingly soluble or insoluble in water are used for the synthesis of HDES. The most intensively studied HDES are mainly composed of quaternary ammonium salts with longer alkyl chains. In this work, each HDES was prepared by mixing HBA and HBD in a specific molar ratio in a screw-capped bottle. Weighing was performed using an analytical balance (Fisher Scientific). The mixture was then stirred at 100 °C and 200 rpm with a magnetic stirrer on a hot plate until a homogeneous liquid phase was formed. The homogeneous HDES was allowed to stand overnight to ensure that no precipitate formed upon cooling. The chemical structures of the components of HDES are shown in Figure 3.2. The abbreviations of the HDES prepared in this work are presented in Table 3.3.

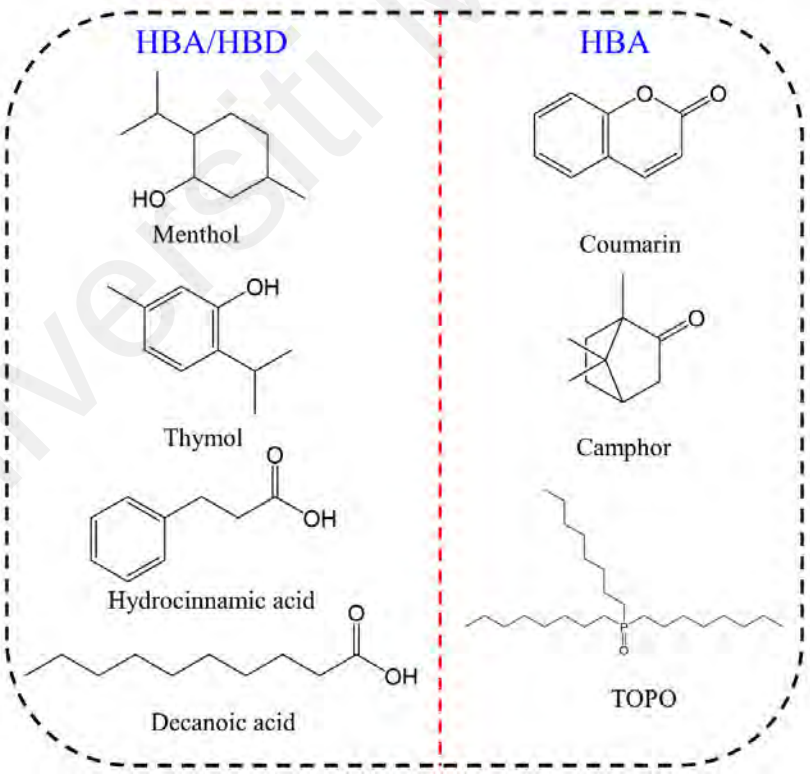

Figure 3.2: Chemical structure of the individual components of HDES.

Table 3.3: List of HDES prepared in this work along with their abbreviations.

Abbreviation	Component 1	Component 2	Molar ratio
Men:Thy	Menthol	Thymol	1:1
Men:DecA	Menthol	Decanoic acid	1:1
Thy:DecA	Thymol	Decanoic acid	1:1
HydA:DecA	Hydrocinnamic acid	Decanoic acid	1:1
Thy:Coum	Thymol	Coumarin	1:1
Thy:Camp	Thymol	Camphor	1:1
TOPO:Men	TOPO	Menthol	1:1
TOPO:Thy	TOPO	Thymol	1:1
TOPO:Hex	TOPO	1-Hexanol	1:1
TOPO:DecA	TOPO	Decanoic acid	1:1

3.3.1 Characteristics of HDES

3.3.1.1 Viscometer

An Anton Paar DMA 4100 M densiometer with repeatability and precision of 0.05 kg/m^3 and 0.1 kg/m^3, respectively, was used to measure the densities of HDES at 101.3 KPa. The approach described in the literature (Chirico et al., 2013) was used to determine the standard uncertainties of the densities considering the chemical purity. An Anton Paar Lovis 2000 M/ ME viscometer set at 101.3 kPa and with a relative accuracy of 0.005, was used to measure the viscosities of the DESs. The temperature was controlled with an accuracy of ± 0.02 K and the capillaries used were 1.59 and 1.8mm with an uncertainty of ± 0.005 and ± 0.03 m.Pa.s respectively. The falling ball concept is used to determine viscosity with the Lovis 2000 M/ ME. The sample was placed in the Lovis 2000 M/ ME to measure the falling time of the ball in a calibrated glass capillary with a steel ball as supplied by the manufacturer. The viscosities were calculated three times to obtain the average values, and the Guide to the Expression of Uncertainty in Measurement was used to report standard uncertainties of the viscosities using the equation given below (BIPM et al., 2008):

$$u = \frac{s}{\sqrt{n}} \tag{3.4}$$

Where u is standard uncertainty, s is the standard deviation of the measurements, and n is the number of measurements.

3.3.1.2 Karl Fisher

The water content of each HDES was measured by Karl Fischer titration (Aquamax Karl-Fischer, GR Scientific Ltd). The Aquamax Karl-Fischer titrator uses the Karl-Fischer method, a widely used technique for determining water content in various types of samples. In this method, water molecules react with a solution of iodine and sulfur dioxide to produce an intermediate that reacts with a titrant, such as sodium or potassium hydroxide. The amount of titrant required to reach the end point is proportional to the water content of the sample.

3.3.1.3 Melting point and thermal stability

Mettler Toledo's TGA/DSC 1 Star system was used to study the thermal properties of the HDES produced. Thermograms were recorded on a Mettler-Toledo TGA/DSC 1 STAR system in the temperature range of 25-400 °C with a ramp of 10 K/min under a synthetic air flow of 80 mL/min. Typically, 0.5-2 mg of sample was used per run.

3.3.1.4 Fourier transformation infrared (FTIR)

FTIR is a widely used analytical technique to identify organic, polymeric, and inorganic compounds in a sample by measuring the wavelengths of infrared light absorbed by the sample. In this study, a PerkinElmer Spectrum 100 FTIR spectrometer was used to analyze HDES. The spectrometer used infrared light in the range of 500 to 4000 cm^{-1} to obtain the spectra of the samples.

3.3.1.5 Proton nuclear magnetic resonance

^{1}HNMR spectra were recorded using a JEOL RESONANCE spectrometer (model ECX-500 II). Chloroform was used as solvent, and spectra were recorded at 24 ºC and a

magnetic field strength of 400 MHz. The JEOL RESONANCE spectrometer (model ECX-500 II) is a high-field nuclear magnetic resonance instrument used to analyze the structure and dynamics of HDES components. The peaks of the pure components and the mixture of known concentrations were used to select the identification peaks for computational purposes. Due to the multicomponent nature of the experiments, multiple peaks were selected for certain compounds to facilitate the calculation.

3.4 Preparation of feed mixture or stock solution

Phenol has higher solubility in water, so feed mixtures of phenol and water were prepared for phenol for different concentrations of phenol between 1 and 7 wt%. For the removal of cresol isomers from water, a stock solution of 15000 ppm was first prepared for the experimental screening of HDES. In the case of heavy metals, a 1000 ppm mixture of lead or iron and 100 ppm mixture of copper or cadmium in water were prepared to assess different HDES. The stock solutions were diluted to different concentrations by adding the appropriate amount of Milli-Q water. Calibration curves for the phenolic contaminants were recorded in GC, while calibration curves for the heavy metals were recorded at AAS. The calibration curves were prepared with standard solutions of the metal salts at a concentration of 1000 ppm.

3.5 LLE experiments

For the experimental screening of HDES, HDES were added to the feed mixture at a mass ratio of 1:1. The mixtures were stored in sealed bottles with screw caps. For the phenolic contaminants, the mixture was stirred in an incubator shaker at ambient temperature (298.15 K), atmospheric pressure (1 atm), and 200 rpm. The stirring time was 2 h, followed by a 24-h settling period to ensure that the phases were completely separated. A general experimental setup is illustrated in Figure 3.3.

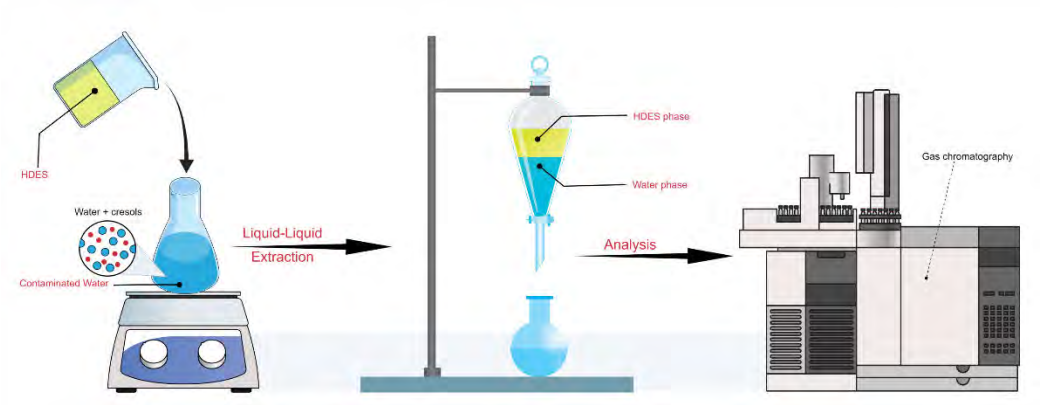

Figure 3.3: An illustration of the experimental setup.

The efficiency of the extracting solvents was evaluated using two important parameters: selectivity (S) and distribution ratio (D). Equations 3.5-3.7 were used to calculate the selectivity and distribution ratio:

$$D_{phenolic} = {x^B_{phenolic}}\Big/{x^T_{phenolic}} \tag{3.5}$$

$$D_{water} = {x^B_{water}}\Big/{x^T_{water}} \tag{3.6}$$

$$S = \frac{D_{phenolic}}{D_{water}} = {x^B_{phenolic}}\Big/{x^T_{phenolic}} \times {x^T_{water}}\Big/{x^B_{water}} \tag{3.7}$$

Where x is the concentration in mole fraction, phenolic stands for phenol or cresol. Superscripts *B* and *T* refer to the bottom and top phases, respectively.

For the heavy metals, the HDES were mixed with the stock solution at a mass ratio of 1:1. The mixtures were poured into the sealed screw-cap bottles. The mixtures were then placed in a thermoblock system (Thermomixer C, Eppendorf, Hamburg, Germany) and vortexed/mixed at room temperature (298.15 K), atmospheric pressure (1 atm), and 2000 rpm. The biphasic system was mechanically shaken at room temperature at 2000 rpm (unless otherwise specified) and then centrifuged at 3500 rpm for 10 minutes. Centrifugation relies on gravity to separate the components of a mixture based on their density and size. When a mixture is placed in a centrifuge and spun at high speed, the

force generated by the spinning causes the denser components of the mixture to settle to the bottom of the tube while the lighter components remain on top.

3.6 Compositional analysis

GC and HPLC instruments were used for the analysis of phenolic contaminants. For the extraction of phenolic pollutants from water, quantitative analysis was performed by GC. Table 3.4 lists the operating parameters for GC.

Table 3.4: Operating condition of GC.

Parameter	Value
Temperature of detector (K)	593.15
Temperature of injector (K)	593.15
Carrier gas total flow (mL/min)	134.15
Oven program	353.15 K for 2 min 353.15 K to 513.15 K Rate: 40 K/min

Raffinate phase and HDES phase compositions were determined using a GC-2010 Pro (Shimadzu) equipped with a flame ionization detector (FID) and a HP -5 column (5% diphenyl/95% dimethylpolysiloxane, 30 m, 0.32 mm ID, 0.25 m df). Helium served as the carrier gas in a split mode. To prevent contamination of the column with non-volatile chemicals (i.e., the HDES ingredients), the GC liner was cleaned after each system analysis. Each measurement was performed in triplicate, and average uncertainties were calculated.

It is not possible to use GC for the detection of HDES based on TOPO, so HPLC was used for this purpose. After phase separation, the raffinate phase was extracted into screw-thread bottles using a 1-mL needle syringe and syringe filter. Quantitative analysis of the raffinate phase was performed by HPLC. The specifications of the HPLC used are listed in Table 3.5.

Table 3.5: Specifications of HPLC used.

Device	HPLC Agilent
Column	Raptor ACR C-18 column (250 mm, 4.6 mm, 5µm)
Mobile phase	45 % water and 55 % acetonitrile
Mobile phase flow rate	0.6 mL/min
Absorbance wavelength of phenol	269 nm
Injection volume	10 µL

The extraction efficiency (EE %) of phenolic pollutants was evaluated using equation 3.8.

$$EE\ \% = \left(\frac{c_{phenolic}^{initial} - c_{phenolic}^{final}}{c_{phenolic}^{initial}}\right) \text{x } 100\ \% \tag{3.8}$$

Whereby $c_{phenolic}^{initial}$ = initial concentration of phenolic pollutant in aqueous phase

$c_{phenolic}^{final}$ = final concentration of phenolic pollutant in aqueous phase

By obtaining the concentration of each constituent in extract and raffinate phase, the mass of each constituent in extract and raffinate phase could be calculated. Following that, the composition was determined by using equation 3.9.

$$x_i = \frac{m_i}{m_{total}} \tag{3.9}$$

Whereby x_i = composition of each constituent

m_i = mass of each constituent

m_{total} = total mass of the phase

The extraction efficiency for the removal of heavy metals was obtained using the following equation:

$$EE(\%) = \frac{C_0 - C_1}{C_0} \times 100 \quad (3.10)$$

Where C_0 is the analyte concentration in the water phase before the extraction, and C_1 is the analyte concentration in the water phase after the extraction.

3.7 Parametric Analysis

To perform a parametric analysis, the effects of various parameters, including molar ratio of HDES, mass ratio of HDES to water, mixing time, initial concentration, and pH were studied.

3.7.1 Mixing time

When extracting target compounds from water using HDES, mixing time is an important factor in LLE. By increasing the contact between the two immiscible phases, mixing in LLE facilitates the transfer of the target component from the aqueous to the organic phase. Due to their low toxicity, biodegradability, and good selectivity, HDES are desirable replacements for conventional organic solvents in LLE. Certain HDES have low viscosity, which facilitates and speeds up mixing. However, longer mixing times do not always result in the formation of emulsions and do not always improve extraction efficiency. This may mean that equilibrium has already been reached and further mixing is not necessary. Therefore, a number of criteria, such as the properties of the HDES, the target compound, and the operating conditions, should be considered when determining the ideal mixing time. In this work, the effect of mixing time from 15 minutes to 2 hours on the removal of cresol contaminants from water was investigated. Mixing was performed in an incubator shaker at ambient temperature (298.15 K), atmospheric pressure (1 atm), and 200 rpm. For heavy metal extraction, vortex mixing was performed at room temperature (298.15 K) and 2000 rpm. The time was varied between 5 and 90 minutes.

3.7.2 HDES molar ratio

For the removal of cresol isomers, three HDES were selected to study the effects of their molar ratio on the extraction efficiency. The selected molar ratios ranged from 1:2 to 4:1 (HBA:HBD). For the removal of heavy metals, one HDES was used to investigate the effect of molar ratio.

3.7.3 HDES to feed mass ratio

The mass ratio of HDES to feed in LLE is a critical factor because it determines the amount of HDES required for successful extraction of the desired constituents from the feed. If the mass ratio of HDES to feed is too low, there may not be enough HDES to effectively extract the required ingredients from the feed. On the other hand, if the ratio is too high, there may be an unnecessary excess of HDES, which could increase process costs and reduce the effectiveness of the process. The optimal ratio depends on the density, viscosity and solubility of the HDES and the feed material, among other factors. For example, the selectivity of the extraction may be affected by the selected ratio. Therefore, in this work, the effect of the mass ratio was investigated using different HDES. The mass ratios were usually varied between 1:1 and 1:6 (ratio of HDES to feed).

3.7.4 Initial concentration

When performing a parametric analysis, it is important to consider the initial phenolic contaminant/heavy metal content of the water for several reasons.

1. Extraction efficiency: the initial concentration of contaminants can affect how well HDES are able to remove the contaminants.

2. Real world application: in the real world, the number of phenolic impurities in water can vary greatly. Studying how the extraction process behaves under different conditions is facilitated by considering the effects of initial concentration.

3. Saturation point: There is a maximum amount of solute that can be dissolved in a given solvent, and this saturation point varies from solvent to solvent. To avoid supersaturation of the solvent and ensure effective extraction, it is important to understand how the initial concentration of phenolic impurities/heavy metal affects the saturation point of the HDES.

4. Mass transfer rate: the initial concentration of impurities can affect the mass transfer rate between the water and the HDES phase. The time required to extract a compound can be shortened if the concentration is increased at the beginning, as this leads to an increase in the mass transfer rate. Analyzing the effects of the initial concentration can lead to an improvement in the efficiency of the process.

5. Optimization of the process: studying the effect of initial concentration on extraction efficiency, mass transfer rate and other process factors allows fine-tuning of the plant for optimum performance.

Various concentrations of phenol between 1 and 7 wt% were considered. Concentrations between 1500 ppm and 15000 ppm were studied for the cresol isomer. Low concentrations of cresol are common in all types of water, including surface water, groundwater, and drinking water, and are often below the detection limit down to a few micrograms per liter (g/L) or parts per billion (ppb). However, cresol concentrations in water bodies may be higher in regions with heavy industrial activity or inadequate wastewater treatment. A range between 100 ppm and 1000 ppm was chosen for the concentration of lead in water. For heavy metals, concentrations varied between 10 to 1000 ppm depending on the type of heavy metal.

3.7.5 Effect of pH

The effect of pH was studied for the removal of heavy metals from water. The pH varied between 3 and 7.

3.8 Reusability

It is of utmost importance to have a solvent that can be used for many extractions without decreasing its extractability, especially from an economic point of view. To determine if HDES could be reused, a series of consecutive extraction cycles were performed. In each cycle, exactly the same DES was contacted with a "new" contaminated water phase.

3.9 Consistency test

For {Phenol/cresol + water + HDES} ternary system, the Hand (1930) (equation 3.12) and Othmer and Tobias (1942) (equation 3.13) correlations were employed to determine the accuracy of the LLE data:

$$ln\left(\frac{w''_{phenol}}{w''_{water}}\right) = a + b\,ln\left(\frac{w'_{phenol}}{w'_{HDES}}\right) \quad (3.12)$$

$$ln\left(\frac{1 - w''_{water}}{w''_{water}}\right) = c + d\,ln\left(\frac{1 - w'_{HDES}}{w'_{HDES}}\right) \quad (3.13)$$

Where w_{phenol}, w_{water}, and wH_{DES} represent the concentrations of phenolic pollutant, water, and HDES, respectively. The fitting parameters for the Othmer-Tobias correlations are "*c*" and "*d*," whereas the fitting parameters for the Hand correlation are "*a*" and "*b*." Superscripts ' and " denote the extract and raffinate layers, respectively. The linearity of each function, as evidenced by the values of the regression coefficients R^2, which are close to unity for both systems, is an indication of how consistent the LLE experimental data are.

3.10 Safety aspects

Throughout the process of removing phenolic contaminants and heavy metals from the water, the laboratory adhered very closely to all safety requirements and regulations to ensure a safe working environment for the researchers and staff. Personal protective equipment was always worn, including lab coats, gloves, and safety glasses when there was a risk of coming into contact with chemicals. Because the lab was equipped with the proper ventilation systems and fume hoods, the likelihood of someone inhaling harmful fumes or having an adverse reaction to volatile chemicals was very low. It was also ensured to keep the workplace clean, well-organized and equipped with properly labeled reagent containers and waste disposal devices. This significantly reduced the risk of mishaps and cross-contamination. By strictly adhering to these safety procedures, potential hazards were successfully reduced and ensured the proper conduct of studies to remove phenolic contaminants and heavy metals from the water.

CHAPTER 4: RESULTS AND DISCUSSION

4.1 COSMO-RS screening results

Capacity, selectivity, and performance index are important characteristics to consider when selecting an HDES for a separation process. Phenol selectivity can be described as the ratio between the phenol concentration in the extract phase and that in the raffinate phase. High selectivity means that the HDES interacts better with the phenol compared to water. By using an HDES with high phenol selectivity, fewer stages are required to extract phenol, which in turn reduces investment costs. Subsequently, the capacity at infinite dilution can be described as the largest amount of phenol that can dissolve in the HDES. Therefore, by using a high capacity HDES, a smaller amount of HDES is required to remove phenol from the water. This is beneficial because the solvent to feedstock ratio is lowered, resulting in a smaller extraction column and lower operating costs. Both parameters are critical, and the performance index is the product of maximum selectivity and maximum capacity.

The thermodynamic model known as COSMO-RS is applied in liquid-liquid systems to provide predictions about the physicochemical characteristics of solvents and solutes, as well as the miscibility of these two types of molecules. It has been effectively utilized in the solution of a broad range of problems, one of which was the development of DES. Nevertheless, when dealing with low concentrations of solutes in the system or trace levels of solutes, there are various obstacles and constraints to consider. Predictions made with COSMO-RS are often more accurate for systems in which the components have structures or characteristics that are comparable to one another. Due to the constraints of the underlying quantum chemical computations and the COSMO-RS model itself, it is possible that the predictions will be less accurate for systems that include very low concentrations of the substance being studied. The behavior of solutes present in extremely minute quantities is susceptible to being impacted by a wide variety of

circumstances, including the presence of other components in the system, the temperature, or the pressure. Because of these characteristics, utilizing COSMO-RS to produce a prediction regarding the usefulness of a solvent for a certain activity might be a more difficult endeavor. The performance of various HDES for the removal of phenol form water in terms of C^{∞}, S^{∞}, and PI are depicted in Table 4.1.

Table 4.1: COSMO-RS screening results

HBA	HBD	Molar ratio	C^{∞}	S^{∞}	PI
Benzoyltrifluoroacetone	Triphenyl phosphate	2:1	1.979	128.6	254.4
Decanoic acid	Lidocaine	2:1	1.987	1.511	3.001
		3:1	1.648	1.372	2.262
		4:1	1.485	1.374	2.041
Dodecanoic acid	Octanoic acid	1:3	1.008	0.899	0.907
	Decanoic acid	1:2	0.998	8.129	8.112
	nonanoic acid	1:3	1.038	7.328	7.607
Hydrocinnamic acid	Decanoic acid	1:1	2.546	10.08	25.67
Menthol	Aliquat 336	7:3	6.360	51.72	328.9
	Lidocaine	5:5	3.949	6.694	26.44
	ibuprofen	7:3	1.259	20.62	25.97
	Proton Sponge®	7:3	1.229	46.69	57.40
	Octanoic acid	1:1	1.283	14.24	18.30
		1:2	1.223	10.67	13.05
	Decanoic acid	1:1	1.179	14.77	17.42
		1:2	1.105	11.87	13.13
		1:3	1.072	10.58	11.35
	methyl-2,4-pentanediol	2:1	2.129	15.23	32.43
	1-decanol	2:1	1.832	25.92	47.49
	SA	4:1	1.286	7.565	9.73
	Propionic acid	1:1	1.400	9.405	13.17
	Formic acid	1:1	1.198	7.537	9.04
Methyl anthranilate	Lidocaine	9:1	1.529	7.814	11.90
	ibuprofen	9:1	1.269	30.58	38.82
	Proton Sponge®	9:1	1.236	53.00	65.50
	DL-menthol	9:1	1.520	40.84	62.07
Methyltrioctylammonium bromide	Octanoic acid	1:2	6.734	36.95	248.8
	Decanoic acid	1:2	7.892	43.66	344.6
	Menthol	1:2	25.50	41.49	1057.9
Methyltrioctylammonium chloride	Octanoic acid	1:2	2.895	13.15	38.08
Tetrabutyl ammonium bromide	Thymol	1:2	5.788	14.48	83.81
	octanoic acid	1:2	9.555	32.59	311.4
	Octanoic acid	1:1	29.39	49.25	1447.1

Table 4.1, continued.

HBA	HBD	Molar ratio	C^{∞}	S^{∞}	PI
Tetraheptyl ammonium bromide	Decanoic acid	1:1	33.05	51.94	1716.9
Tetraoctyl ammonium bromide	Octanoic acid	1:1	34.53	36.86	1272.8
	Decanoic acid	1:1	40.53	40.76	1651.9
Thenoyltrifluoroacetone	triphenyl phosphate	2:1	1.950	126.1	245.8
Thymol	methyl-2,4-pentanediol	2:1	1.239	3.302	4.091
	1-decanol	2:1	1.006	4.541	4.569
	Trioctylphosphine oxide	1:1	6.704	138.0	925.3
	Decanoic acid	1:3	0.863	4.445	3.836
	Camphor	1:1	1.679	8.910	14.959
Trioctylmethylammonium chloride	Methyl 4-hydroxybenzoate	1:1	3.781	5.350	20.23
		1:2	2.382	3.085	7.351
		2:1	4.817	10.31	49.68
	butyl 4-hydroxybenzoate	1:1	4.295	8.062	34.63
		1:2	2.628	5.344	14.04
		1:3	1.873	3.684	6.90
		2:1	5.310	13.58	72.13
	isobutyl 4-hydroxybenzoate	1:1	3.867	5.844	22.60
		1:2	2.349	3.557	8.36
		1:3	1.671	2.359	3.9432
		2:1	4.882	10.98	53.60
	2-Ethylhexyl 4-hydroxybenzoate	1:1	4.433	7.864	34.86
		1:2	2.547	5.401	13.75
		1:3	1.740	3.696	6.43
		2:1	5.475	13.11	71.79
	n-octyl 4-hydroxybenzoate	1:1	4.465	9.815	43.82
		1:2	2.561	7.134	18.27
		1:3	1.748	4.959	8.669
		1:4	1.779	3.344	5.949
		2:1	5.508	15.39	84.79
	Decanoic acid	2:1	5.479	28.20	154.5
		1:1	4.658	20.91	97.40
		1:2	3.020	17.92	54.11
	Ketoprofen	2:1	6.059	26.03	157.7
		1:1	5.346	20.13	107.6
		1:2	3.685	17.70	65.21
	Gemfibrozil	1:2	3.085	16.58	51.15
		1:1	4.893	19.80	96.91
Trioctylphosphine oxide	Decanoic acid	1:1	9.698	256.0	2483.2
	menthol	1:1	14.89	215.7	3211.7
		1:3	3.884	135.8	527.6
		1:4	3.194	99.82	318.8
		1:5	2.775	80.29	222.77
	1-butyric acid	1:1	11.31	243.3	2753.6
	1-hexanoic acid	1:1	10.64	249.2	2651.1

Table 4.1, continued.

HBA	HBD	Molar ratio	C^{∞}	S^{∞}	PI
	1-butanol	1:1	19.36	187.6	3630.8
	1-hexanol	1:1	18.39	186.1	3422.9
	1-octanol	1:1	17.55	193.3	3392.2
	Dodecanoic acid	1:1	9.264	265.4	2459.1
	N,N′-dihexylthiourea	1:1	14.01	76.80	1075.6
	1,2-Decanediol	1:1	17.24	146.3	2522.8
	3,5-Di-tertbutylcatechol	1:1	5.696	80.45	458.3

4.2 Characteristics of HDES

4.2.1 FTIR analysis

The formation of a eutectic mixture is the result of a variety of intermolecular interactions between the substances involved. ChCl, sugars, and organic acids form eutectic mixtures due to the development of hydrogen bonds between the two molecules, one acting as HBD and the other as HBA. According to studies by Narishetty and Panchagnula (2005) on eutectic mixtures of ceramide and cholesterol, the terpene interacts with both the lipid alkyl tails and the polar head groups of the mixture, lowering its melting temperature and breaking the inter- and interlamellar hydrogen bonding network. Therefore, it is important to know how terpenes (menthol or thymol) interact with the other compounds in a eutectic mixture. The FTIR spectra of different HDES formed by combining HBA and HBD are shown in Figures 4.1 and 4.2.

For Men:Thy, a hydroxyl group can be observed in the range of 3200-3300 cm^{-1} for both menthol and thymol. After the formation of a eutectic mixture, this band was shifted to the higher value of 3388 cm^{-1}, confirming the formation of hydrogen bonds. Men:DecA and Thy:DecA, eutectic mixtures, have a carboxyl group (decanoic acid) in their structure, which shows a representative band (carbonyl group) around 1700 cm^{-1} in the spectra. However, in the FTIR spectra of HBA thymol or menthol, only a single band

is observed at about 3250 cm^{-1} which corresponds to the hydroxyl group. The formation of hydrogen bonds between the terpenes and HBDs was further confirmed by FTIR spectra. The intermolecular hydrogen bonding interaction between the HBDs and HBAs is observed in the carboxyl group region of the FTIR spectra of the eutectic mixtures.

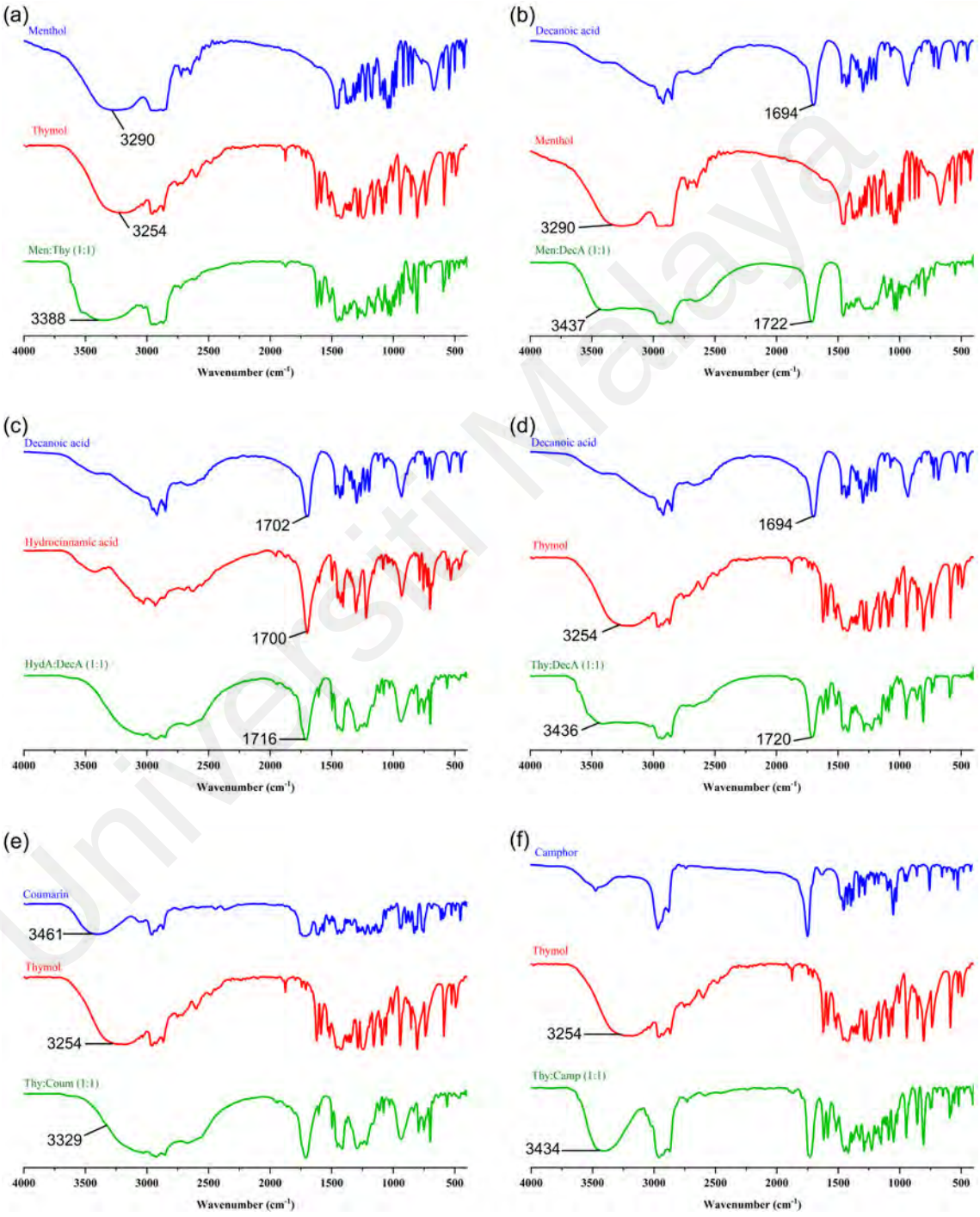

Figure 4.1: FTIR analysis of terpenes and carboxylic acid based-HDES and their individual components. (a) Men:Thy (1:1), (b) Men:DecA (1:1), (c) HydA:DecA (1:1), (d) Thy:DecA (1:1), (e) Thy:Coum (1:1), (f) Thy:Camp (1:1).

Figure 4.1 shows that the carbonyl band of the HBDs, previously located at low wave numbers (1694 cm^{-1}) for Men:DecA, becomes broader and migrates to the highest values (1722 cm^{-1} for menthol and 1720 cm^{-1} for thymol). This proves the presence of new hydrogen bonds and the development of a compound. These data can be further supported by the physical states of the compounds. For example, the eutectic combination of menthol and decanoic acid initially has a solid state, but after HDES formation, a liquid is formed. Moreover, the peaks of the hydroxyl group also shifted to higher values (from 3290 to 3437 cm^{-1} for Men:DecA and 3254 to 3436 cm^{-1} for Thy:DecA). In HydA:DecA, both components forming a eutectic mixture are carboxylic acids. The representative bands (carbonyl group) for both components are around 1700 cm^{-1}. After HDES formation, a shift to higher values confirming the formation of a new compound.

For Thy:Coum, the peak of the hydroxyl group is located at different positions in the FTIR spectra of pure thymol and coumarin due to their different molecular structures and functional groups. While both thymol and coumarin have a hydroxyl group (-OH) attached to an aromatic ring, the hydroxyl group of thymol is in a more basic chemical environment. Therefore, the hydroxyl peak appears at different locations in the FTIR spectra of the different compounds. In the FTIR spectrum of the resulting HDES, a shift of the hydroxyl peak is observed when thymol and coumarin are combined in the molar ratio of 1:1; the hydroxyl peak in the FTIR spectrum of pure thymol and coumarin is at different wavelengths. The shift in the hydroxyl peak is an indication that a new chemical species has been formed. The shift was also observed in Thy:Camp HDES.

Interactions between thymol and coumarin or camphor molecules may be the cause of the shift of the hydroxyl peak in the HDES spectrum. A change in the position of the hydroxyl peak can occur when these two compounds are combined, due to the formation of hydrogen bonds that affect the electrical environment of the hydroxyl groups.

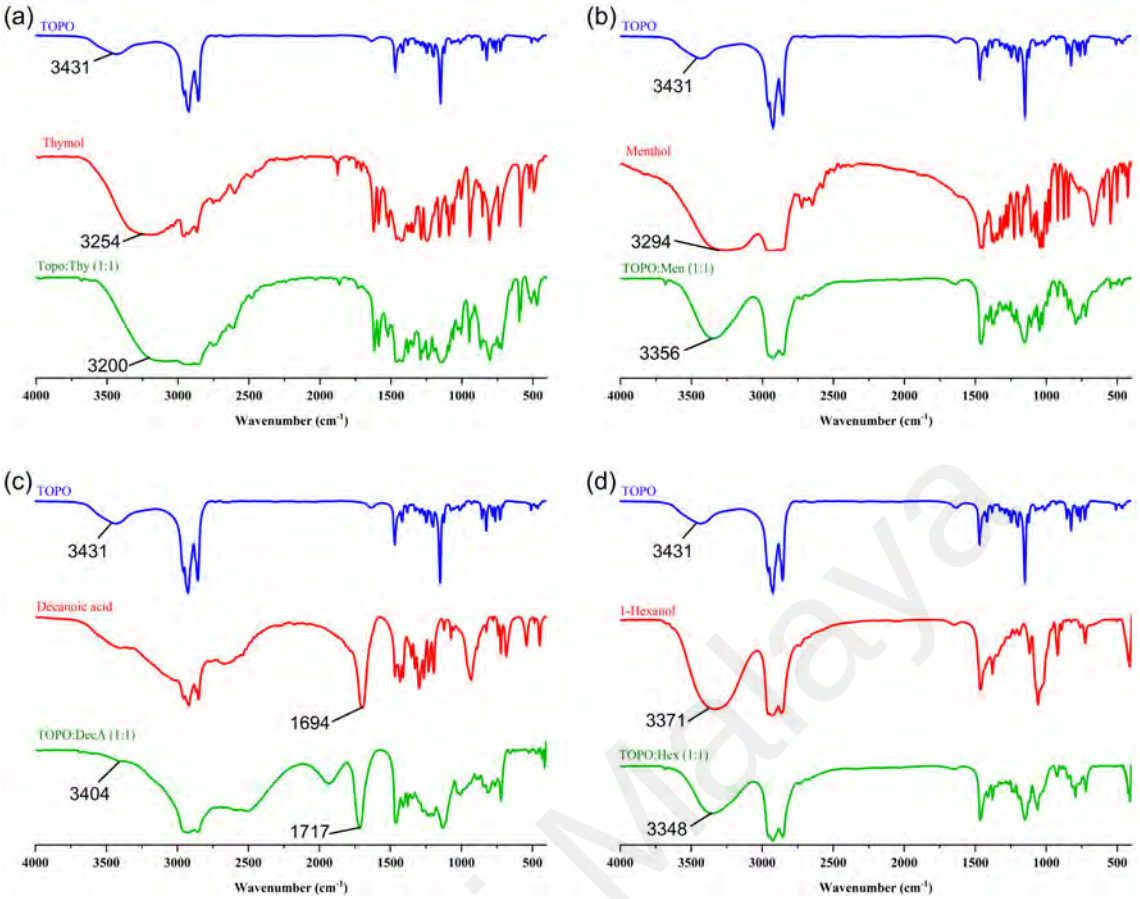

Figure 4.2: FTIR analysis of TOPO-based HDES and their individual components. (a) TOPO:Thy (1:1), (b) TOPO:Men (1:1), (c) TOPO:DecA (1:1), (d) TOPO:Hex (1:1).

Figure 4.2 shows the FTIR spectra of TOPO-based HDES. The presence of a broad band at 3356 cm^{-1} in the FTIR spectrum of TOPO:Men, which lies between the O-H stretching frequencies of TOPO and menthol, indicates that hydrogen bonding has occurred between the two components, confirming the evolution of the HDES complex. The frequency change of the O-H stretching vibration in HDES may be related to the formation of hydrogen bonds between the O-H group of TOPO and the hydroxyl group in menthol, resulting in a weakening of the O-H bond and a shift to lower frequencies.

Because of the larger size of the TOPO molecule, which makes it less susceptible to hydrogen bonding with the smaller menthol molecule, the change in the O-H stretching frequency of TOPO might be less obvious in the HDES spectrum. In addition, the extent of the O-H stretching band in the HDES spectrum compared to the individual components

might indicate that the O-H group of TOPO is involved in numerous hydrogen bonding interactions with the hydroxyl group of menthol. The observation of an intermediate O-H stretching frequency in the FTIR spectrum of the HDES mixture and changes in the shape and intensity of the peaks compared to the individual components are consistent with the formation of hydrogen bonds between the components and confirm the formation of the HDES complex.

The prominent peak at 3404 cm^{-1} in the TOPO:DecA spectrum shows a slight shift compared to the TOPO spectrum, indicating a change in hydrogen bonding environment. This phenomenon may be attributed to the interaction between TOPO and decanoic acid, where the hydroxyl group of the acid forms a hydrogen bond with the oxygen of the phosphine oxide group in TOPO. The peak observed in the DES spectra at 1717 cm^{-1} shows a shift from 1694 cm^{-1} in the decanoic acid spectrum. The observed shift to a higher wavenumber in the DES can be attributed to the formation of a complex between the carboxylic acid group of decanoic acid and TOPO. The interaction is due to hydrogen bonding, which affects the C=O stretching vibration and leads to a change in peak position. The changes in the FTIR peaks observed during the formation of the DES indicate that molecular interactions take place between TOPO and the decanoic acid, supporting the idea that a DES is formed.

4.2.2 Thermal analysis

Quantifying the degradation of HDES is useful. Thermograms were measured to evaluate the degradation temperatures of HDES. They show the weight loss of HDES as a function of temperature. As can be seen in Figures 4.3 and 4.4, all selected HDES except TOPO:Men and TOPO:Hex show a one-step decay of weight loss. The decomposition temperatures (T_{deg}) from the thermograms of the HDES are summarized in Table 4.2.

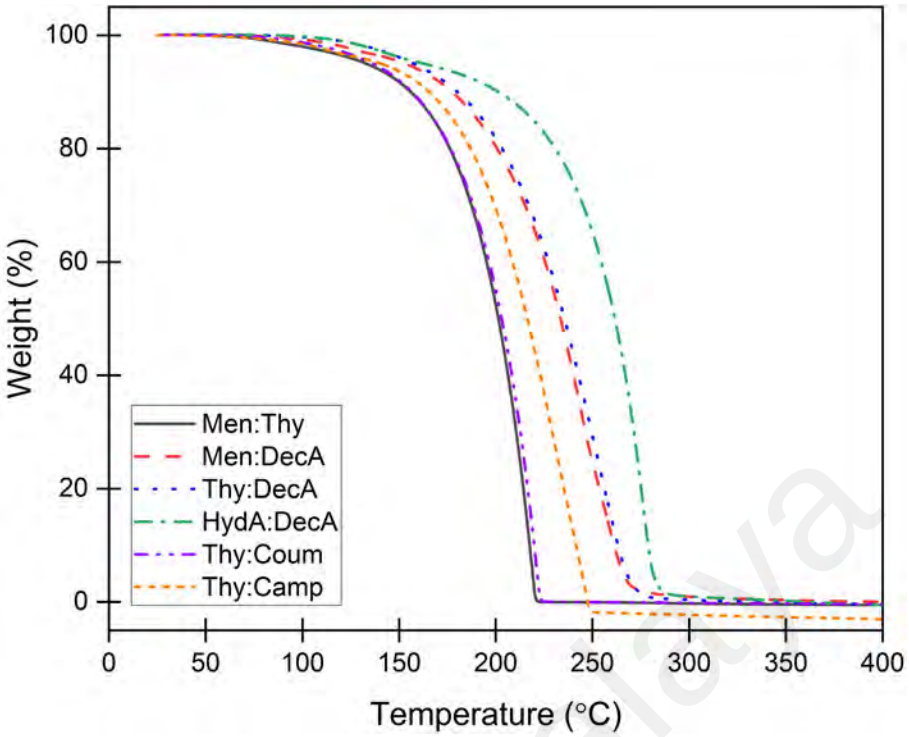

Figure 4.3: TGA analysis of terpenes and carboxylic acid-based HDES.

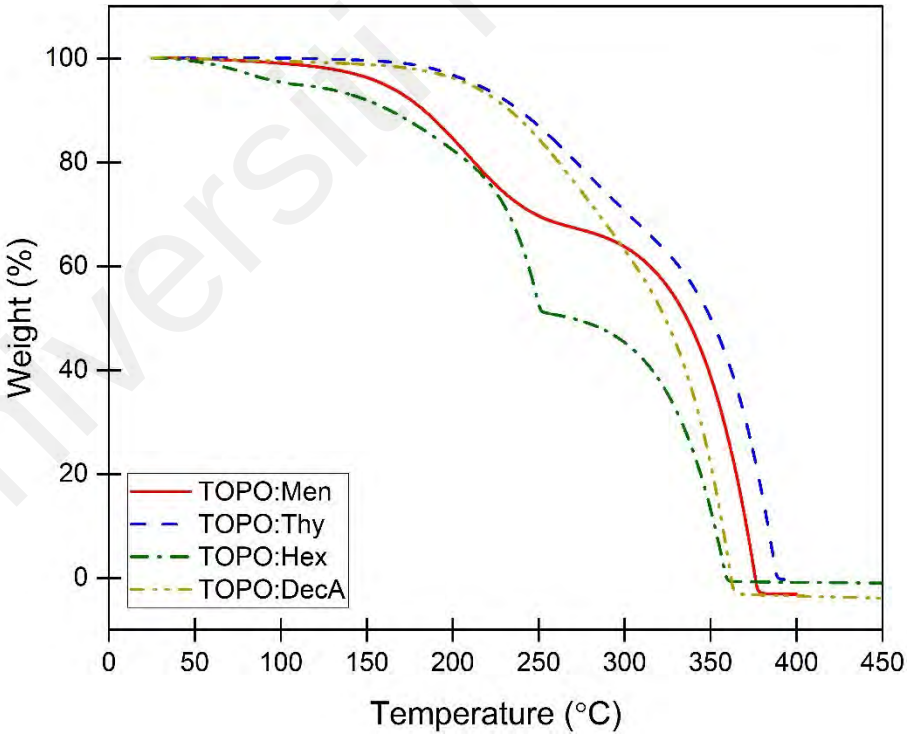

Figure 4.4: TGA analysis of TOPO-based HDES.

The T_{deg} values are lower than those previously reported for HDES based on decanoic acid and quaternary ammonium salts. It is believed that these lower T_{deg} values do not

indicate degradation, but rather represent sublimation/evaporation of the DES constituents. Components with a strong odor, such as menthol, thymol, and coumarin can sublimate. These data indicate that the degradation temperature and volatility are highly dependent on the constituents. This is an essential factor to consider when designing a DES for a particular application and applies to both hydrophilic and hydrophobic DESs. The melting points of all HDES produced were also measured and are listed in Table 4.2.

Table 4.2: Melting point (T_m) and degradation temperature (T_{deg}) of the selected HDES.

HDES	T_m (ºC)	T_{deg} (ºC)
Men:Thy	-15.38	122.6
Men:DecA	2.45	133.2
Thy:DecA	14.01	152
HydA:DecA	14.07	144.5
Thy:Coum	-34.7	136.6
Thy:Camp	-43.89	116.7
TOPO:Men	25.27	125.8
TOPO:Thy	-25.77	162.5
TOPO:Hex	-56.9	105.6
TOPO:DecA	31.49	154.6

4.2.3 Rheological properties

The viscosity and density of HDES were measured at temperatures ranging from 298.15 to 318.15 K and at 101.3 kPa atmospheric pressure. Water content was also measured for all HDES. Density and viscosity are essential properties of any solvent, as they affect mass transfer processes and thus usability for specific purposes. The viscosity and density data measured in this work showed good agreement with literature data (Table 4.3). At 298.15 K, the viscosities of all HDES were < 70 m.Pa.s. These values are much lower than those of some conventional hydrophilic DES (Abbott et al., 2004b; Zhang et al., 2012), IL (Rooney et al., 2010), and some categories of HDES (Van Osch et al., 2015). Previously, the viscosities of DES presented by Van Osch et al. (2015) ranged from 173 to 783 m.Pa.s, while those presented by Ribeiro et al. (2015) ranged from 10 to 220

m.Pa.s. In another study, Van Osch et al. (2019) reported viscosities of 17 HDES that ranged from 20 to 86800 m.Pa.s. The authors also suggested that viscosities as low as 100 m.Pa.s are suitable for industrial applications. The HDES investigated in this study met this viscosity requirement. Some researchers have noted that the increased viscosities of DESs are due to their unusual behavior resulting from the intensity of hydrogen bonding association (Adeyemi et al., 2020; Van Osch et al., 2019).

Table 4.3: Water content, Viscosity and density of HDES at 298.15 K temperature and 101.3 kPa pressure.[a]

HDES	Water content (wt%)	Density (kg/m^3)	Viscosity (m.Pa.s)	Density (kg/m^3)	Viscosity (m.Pa.s)
		This work		Literature	
Men:Thy	0.011	932.9±2	36.1±0.04	936.5(Van Osch et al., 2019) 931.6 (Adeyemi et al., 2020)	53.14 (Van Osch et al., 2019)
Men:DecA	0.213	896.1±2	18.85±0.01	899.77 (Van Osch et al., 2019)	20.03 (Van Osch et al., 2019) 22 (Dietz et al., 2019)
Thy:DecA	0.018	929.9±2	12.02±0.01	943.7 (Makoś et al., 2018)	11.2 (Makoś et al., 2018) 16 (Dietz et al., 2019)
HydA:DecA	0.049	978.6±2	11.46±0.02	NA	NA
Thy:Coum	0.017	1087.9±2	21.97±0.02	1091.80 (Van Osch et al., 2019)	29.16 (Van Osch et al., 2019)
Thy:Camp	0.079	966.9±2.0	20.71±0.01	987.3 (Makoś et al., 2018)	25.8 (Makoś et al., 2018)
TOPO:Men	0.078	877.6±2.0	43.16±0.11	NA	NA
TOPO:Thy	0.097	898.1±2.0	68.39±0.38	NA	NA
TOPO:Hex	0.112	862.2±2.0	23.35±0.35	NA	NA
TOPO:DecA	0.083	881.2±2.0	44.26±0.74	NA	NA

[a]Standard uncertainties are u(T) = 0.1 K, u(P) = 1 kPa, u(η) and u(ρ) are reported inside the table following the ±sign. The water contents were measured at 298.15 ± 1 K.

Figure 4.5 shows the effect of temperature on viscosity for all HDES prepared in this work. The figure shows that the viscosity of all HDES decreases with increasing temperature. TOPO:Thy has the highest viscosity at any temperature, while the mixture

of decanoic acid and hydrocinnamic acid has the lowest viscosity. The observed differences in viscosity can be explained by the molecular structures and hydrogen bonding properties of the compounds contained in each mixture. Men:Thy has both hydrogen bonding donating and accepting properties, resulting in strong intermolecular hydrogen bonding and high viscosity. In contrast, the mixture of decanoic acid and hydrocinnamic acid in the 1:1 molar ratio has low viscosity because the intermolecular hydrogen bonding is weak.

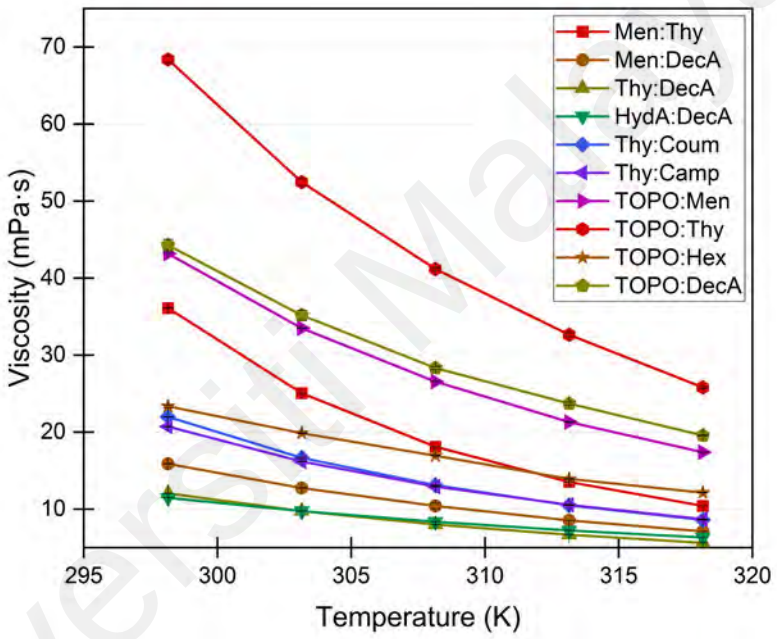

Figure 4.5: Effect of temperature on the viscosity of all prepared HDES.

Density is a crucial physicochemical characteristic of DES because it is determined by the molecular packaging and the interaction strength between the constituents. Therefore, it is a crucial factor to consider when evaluating the suitability of DES as an extraction medium. The density of HDES reported in the literature varies between 0.85 to 1.5 $g \cdot cm^{-3}$ (Van Osch et al., 2020; Wazeer et al., 2022), but is generally close to that of water. However, the combined density is greater than that of water when both HDES components have a higher density than water, or vice versa. Figure 4.6 shows how temperature affects the density of each HDES. As the temperature increases, the density

of all HDES decreases. Comparing the densities of the different HDES at the same temperature, it can be seen that Thy:Coum has the highest density. The density of these HDES is critical when they are used to extract contaminants from water. HDES with higher density have a greater tendency to separate pollutants from water, resulting in better separation of contaminants into the HDES phase (Sportiello et al., 2022). This would lead to more efficient extraction and subsequent elimination of contaminants. When contaminants are added to the water-HDES mixture, they have different affinities for the two phases, which cannot be mixed. Pollutants with higher hydrophobicity or greater affinity for the HDES will separate into the HDES phase, while pollutants with higher hydrophilicity will remain in the water phase. The number of pollutants removed from the water and transferred to the HDES phase is determined by the partition coefficient between the two phases.

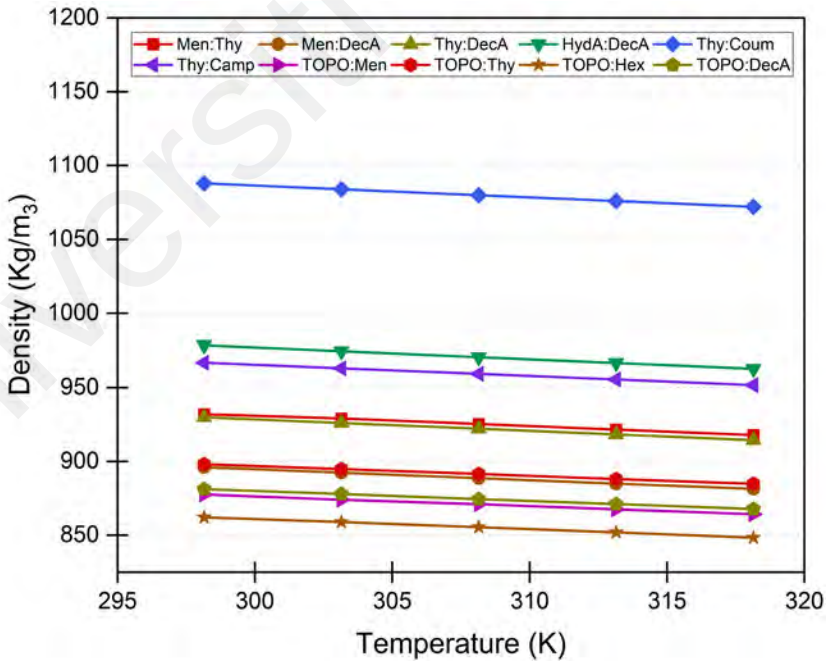

Figure 4.6: Effect of temperature on the density of all prepared HDES.

4.2.4 ^{1}HNMR analysis

The structure and purity of HDES can be characterized by ^{1}HNMR spectroscopy. Different functional groups in HDES can be identified and characterized by examining the proton signals

in the NMR spectra. These data are important to verify the composition of the solvent and to gain insight into its chemistry. In addition, NMR spectroscopy allows scientists to assess the quality of the HDES sample and check for the presence of impurities that could affect the accuracy or repeatability of the experiments. The ^{1}HNMR spectra of all HDES are shown in Figures 4.7 and confirm the presence of all components.

The ^{1}HNMR spectra for various HDES provides a comprehensive understanding of the proton environments and interactions within these mixtures. The spectrum highlights the unique peaks corresponding to the different compounds. For example, the spectra of pure menthol, pure thymol and Men:Thy HDES provide valuable information for identifying the individual compounds and understanding their interactions. The spectrum of menthol shows peaks at higher ppm values (about 3-4 ppm) corresponding to protons near the hydroxyl group, while the peaks at lower ppm values (0.5-1 ppm) represent the methyl groups. The spectrum of thymol shows clear peaks for the aromatic protons at 6.8-7.1 ppm, while the methyl groups on the aromatic ring can be seen at 1-2 ppm. The spectrum of Men:Thy HDES shows a combination of features of both menthol and thymol, confirming the presence of both compounds.

In the case of Men:DecA and Thy:DecA, the peaks of decanoic acid can be observed at 2.0-2.5 ppm for protons near the carboxyl group and at 0.5-1.5 ppm for protons of the alkyl chain. These peaks merge with the aromatic and hydroxyl-related peaks of thymol or menthol. This integration improves understanding of the synergistic effects and potential interactions between the components of these HDESs.

Other mixtures such as hydrocinnamic acid, coumarin and camphor have their own spectral properties. The spectrum of HydA:DecA shows peaks originating from the hydrocinnamic acid at around 6.5-7.5 ppm, indicating the presence of aromatic protons. In addition, the spectrum shows clear peaks that can be assigned to decanoic acid. The aromatic peaks of thymol and coumarin in Thy:Coum HDES combine in a way that suggests interactions between these molecules, as evidenced by specific shifts and

splitting patterns. The spectrum of Thy:Camp HDES shows peaks originating from thymol and camphor, providing insight into the proton environments of both the aromatic and alkyl chains.

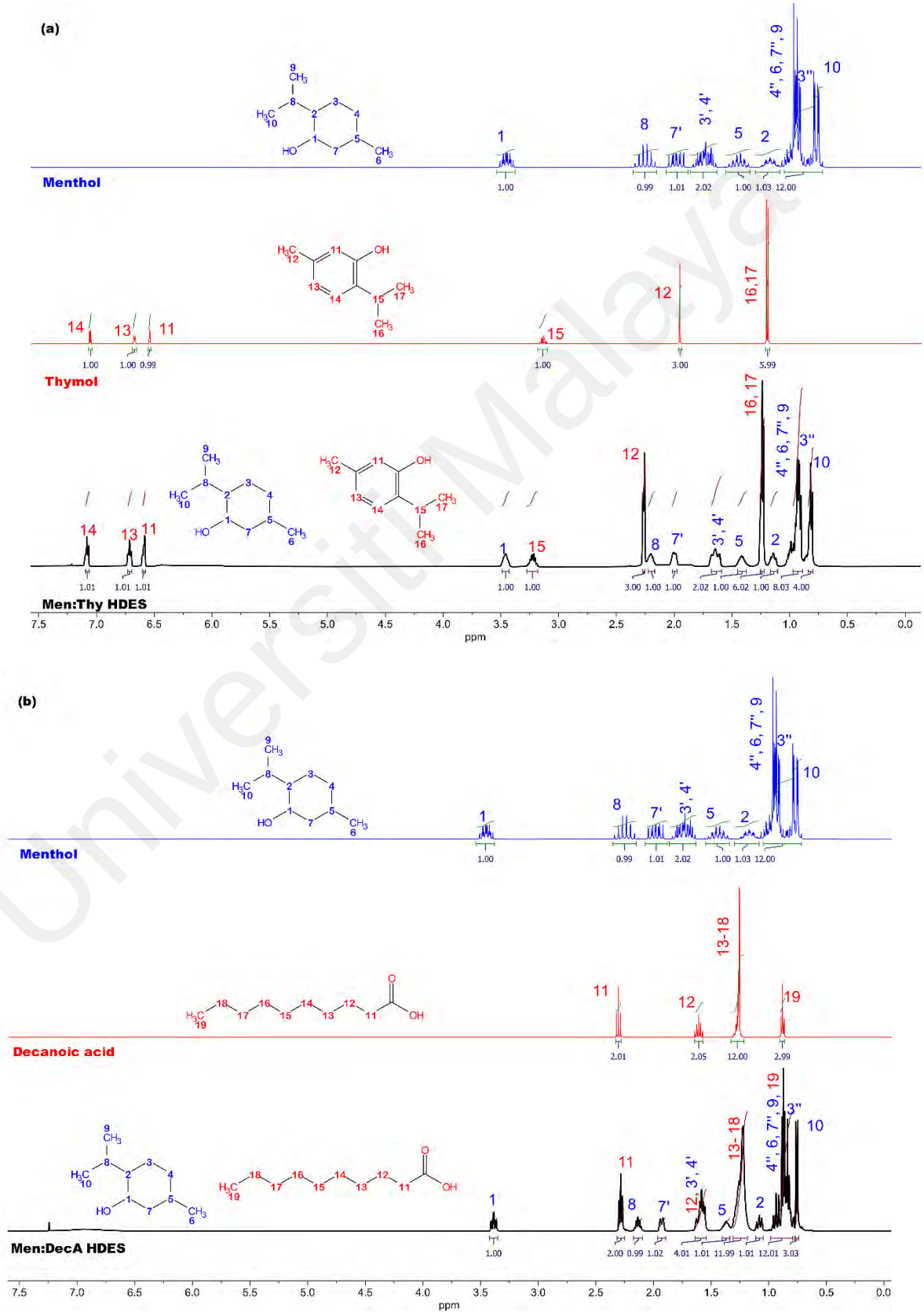

Figure 4.7, continued.

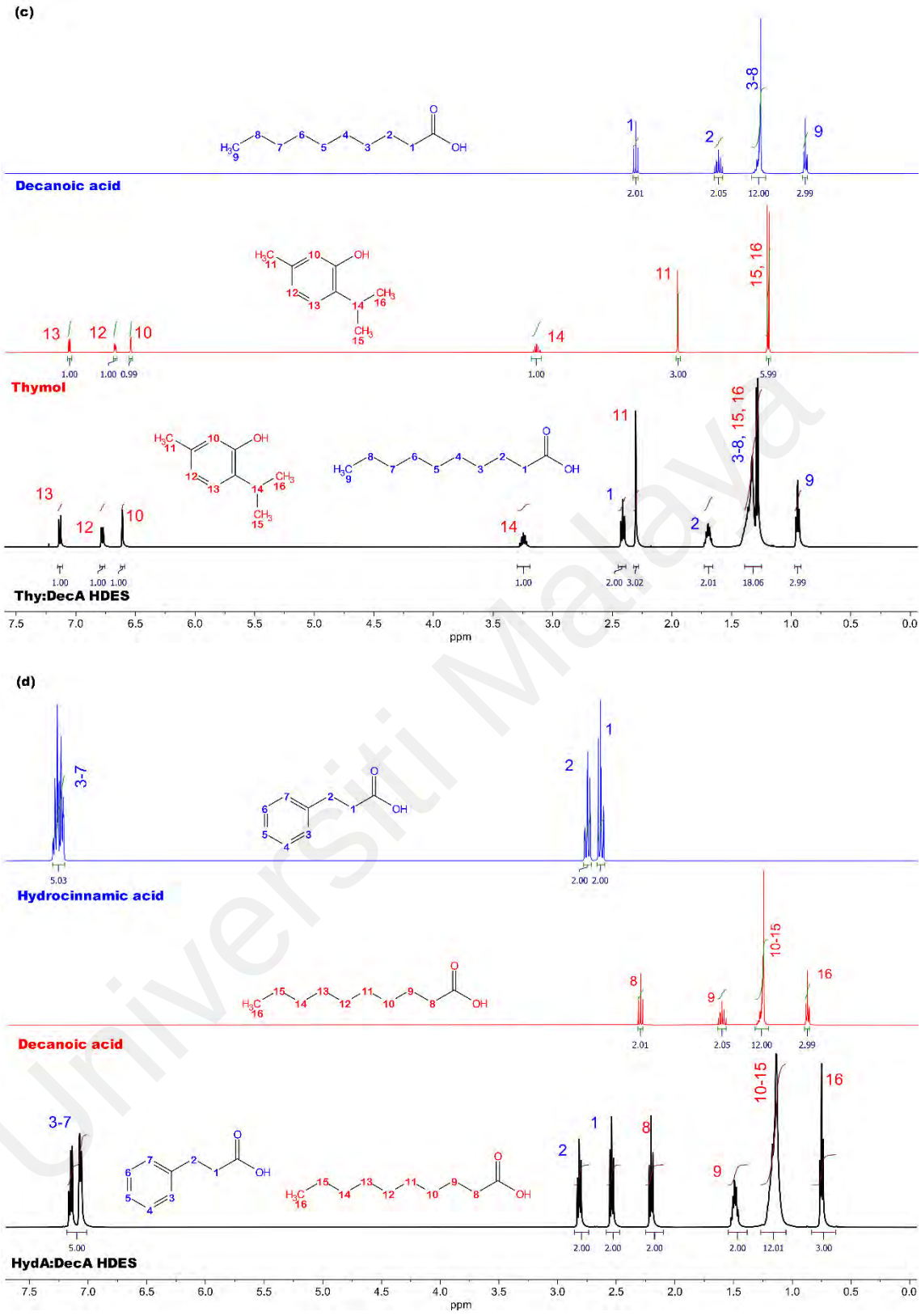

Figure 4.7, continued.

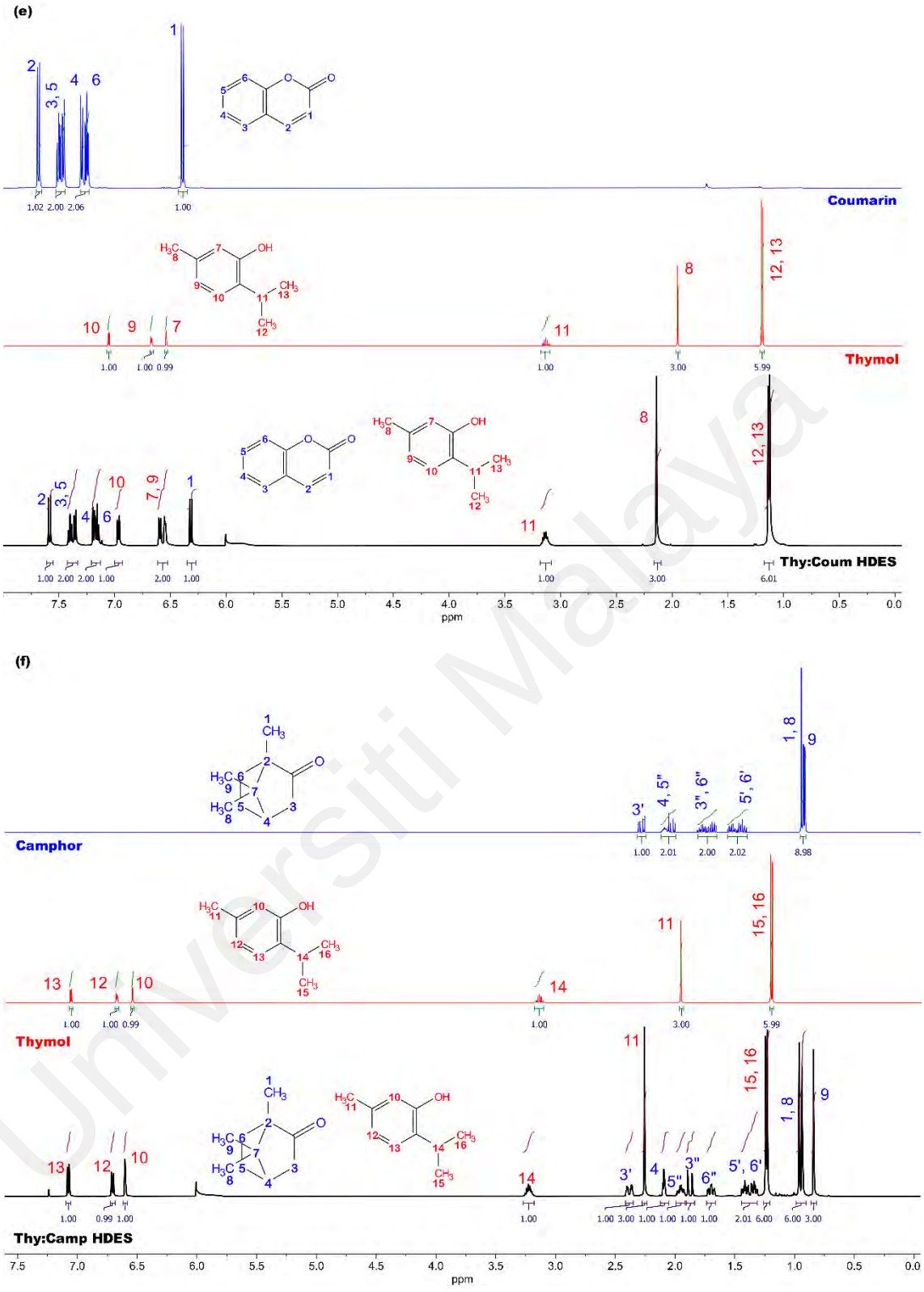

Figure 4.7, continued.

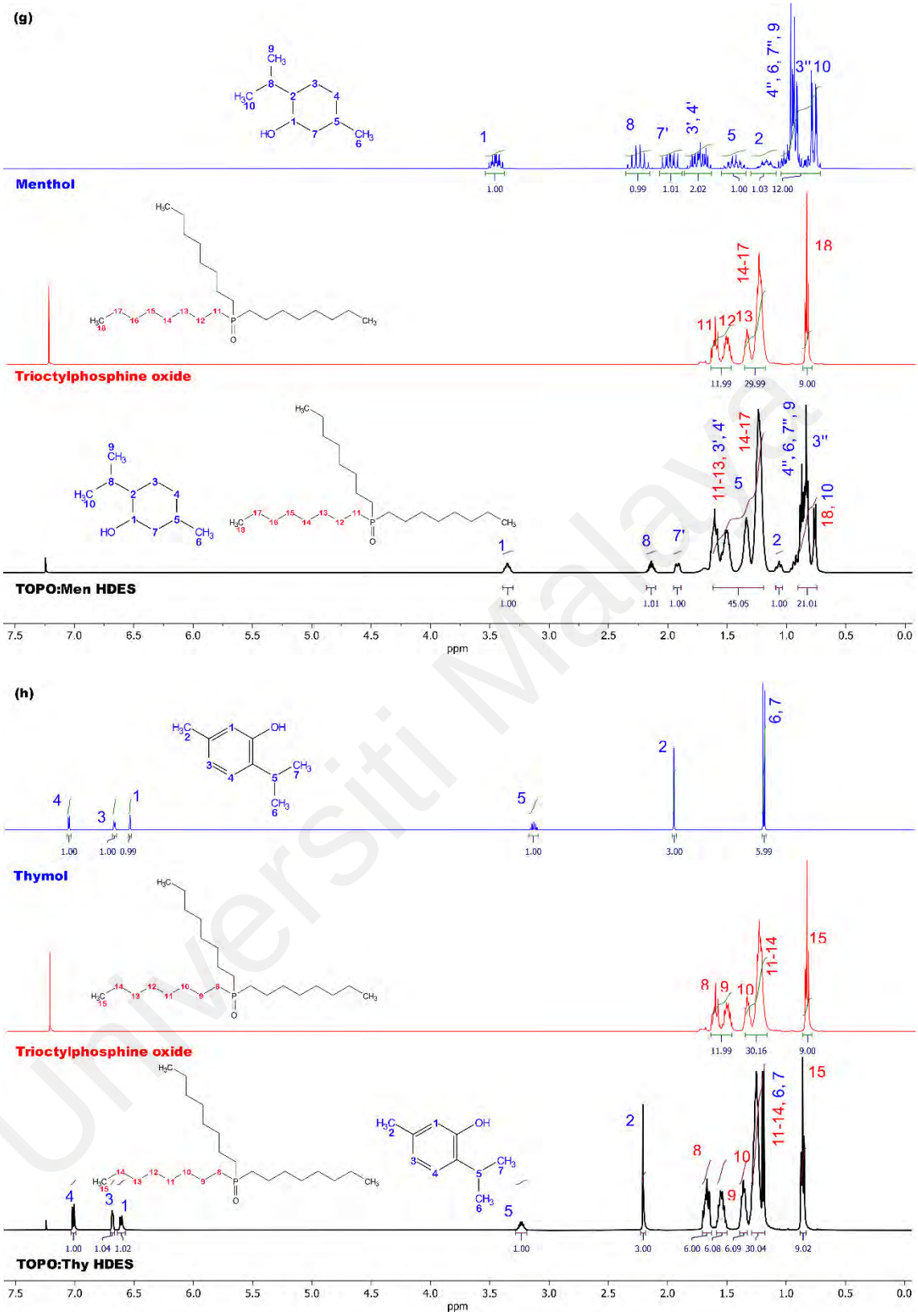

Figure 4.7, continued.

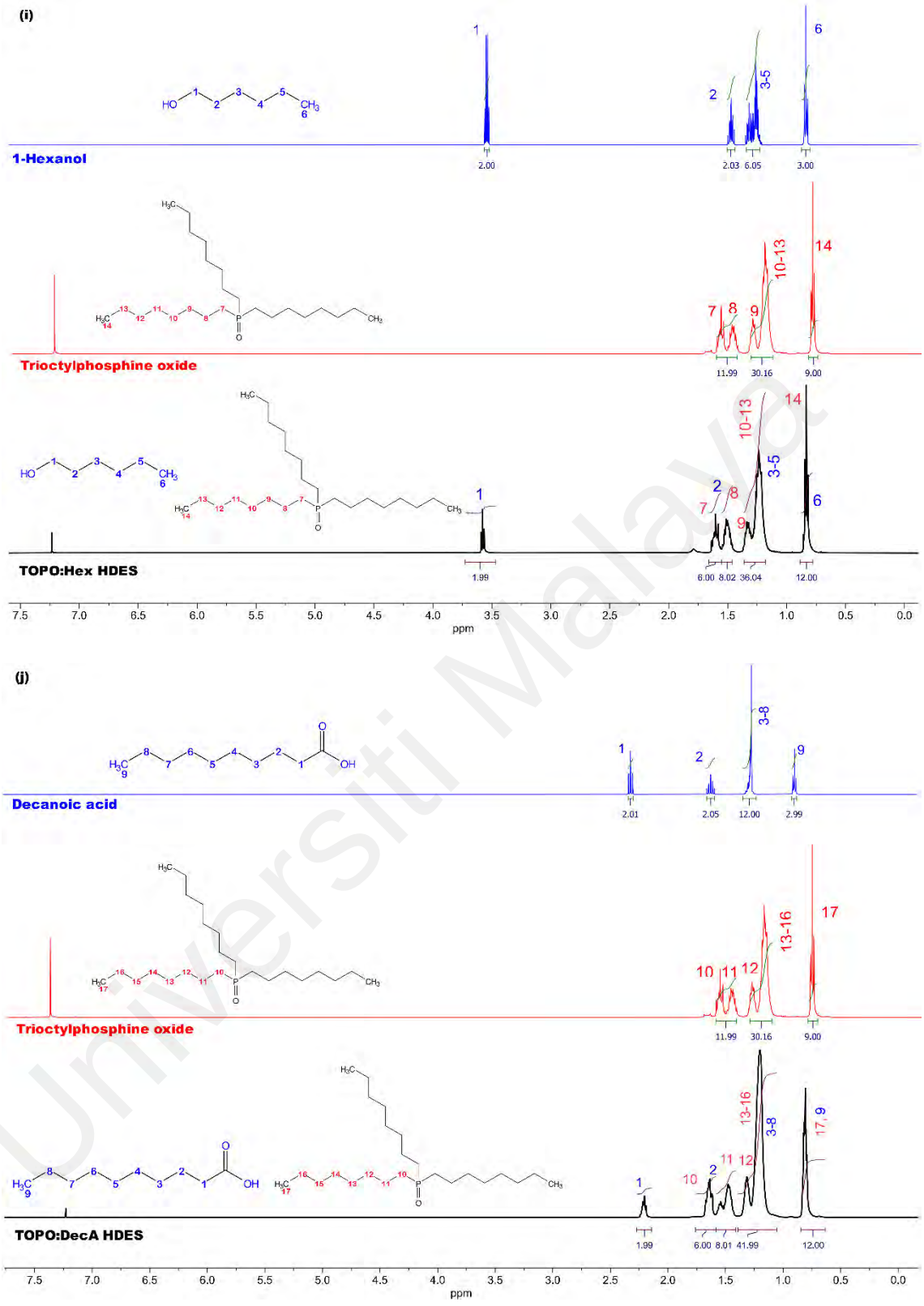

Figure 4.7: ^{1}H NMR spectra of all HDES and their individual components in $CDCl_3$. (a) Men:Thy, (b) Men:DecA, (c) Thy:DecA, (d) HydA:DecA, (e) Thy: Coum, (f) Thy:Camp, (g) TOPO:Men, (h) TOPO:Thy, (i) TOPO:Hex, (j) TOPO:DecA. The peak around 7.3 ppm is the solvent residual peak of $CDCl_3$.

In addition, the spectra of TOPO-based HDES exhibit unique features due to the presence of TOPO. For example, the peaks in the TOPO:Men HDES spectrum correspond

to the presence of menthol and the long alkyl chain of TOPO. The peaks around 0.9 ppm represent the terminal methyl groups (CH_3) of TOPO. The peaks between 1.2-1.7 ppm correspond to the methylene (CH_2) groups in the long alkyl chains of TOPO.

Overall, the ^{1}HNMR spectra of these HDESs provide a comprehensive understanding of the proton environments and interactions present in these mixtures. The peaks and their chemical shifts provide a thorough insight into the contribution of each component and reveal the different chemical environments formed by these HDES. The analysis is crucial for identifying the presence and interactions of each compound in the HDES. This helps in the characterization and exploration of potential applications of these unique solvent systems.

4.3 Removal of phenol from water

In the present study, the application of HDES for the removal of phenol from aqueous solutions with phenol concentrations ranging from 1 to 7 wt% is investigated. Understanding the effectiveness of HDES in eliminating phenol can help in developing environmentally friendly and effective approaches to wastewater treatment. This can ensure the protection of ecosystems and the promotion of human health and welfare. The results of this study will facilitate the improvement of phenol elimination techniques and provide perspectives on the potential use of HDES as a viable approach to reduce phenol contamination in water reservoirs. Based on the COSMO-RS screening (Section 4.1), four HDES with the highest PI were selected for experimental analysis.

4.3.1 COSMO-RS evaluation

A comprehensive examination of the findings revealed a diverse array of values among the 72 HDES in relation to the parameters under investigation. The study revealed a significant link between capacity and PI, as well as selectivity and PI. This finding emphasizes that HDES systems with higher capacity and selectivity tend to provide

superior performance. The analysis conducted indicated an apparent trend in which HDES containing higher molecular weight components and exhibiting balanced HBA-HBD ratios exhibited superior performance in terms of phenol removal effectiveness. The observed phenomenon can be ascribed to the capacity of HDES to establish stable and efficient interactions with phenolic compounds. The results of HDES' screening in terms of capacity, selectivity and PI are shown in Figures 4.8-4.10.

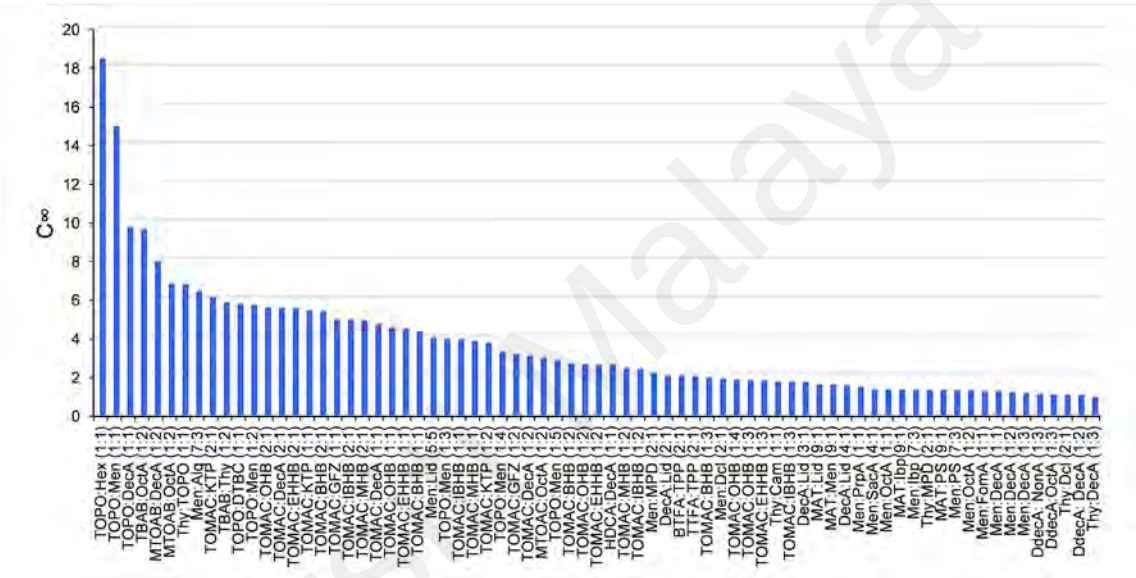

Figure 4.8: Capacity of HDES for the removal of phenol from water at infinite dilution.

The ability of HDES to remove phenol at infinite dilution, as seen in Figure 4.8, indicates its significant affinity for phenolic chemicals, even at minimal levels. This property suggests that the proposed HDES-based LLE method can be efficiently used for the treatment of wastewater whose phenolic content varies greatly. In practical applications, HDES can be adapted for large-scale extraction by optimizing operating parameters such as solvent-to-feed ratio, contact time, and phase separation efficiency. The immiscibility of HDES with water minimizes solvent loss, while its adjustable selectivity enables the targeted extraction of phenols without affecting other important water components. The study shows that the reusability of HDES makes this approach

sustainable and economically feasible for industrial wastewater treatment. Future research should focus on combining HDES extraction with complementary techniques such as membrane filtration or adsorption to improve the overall efficiency of wastewater treatment.

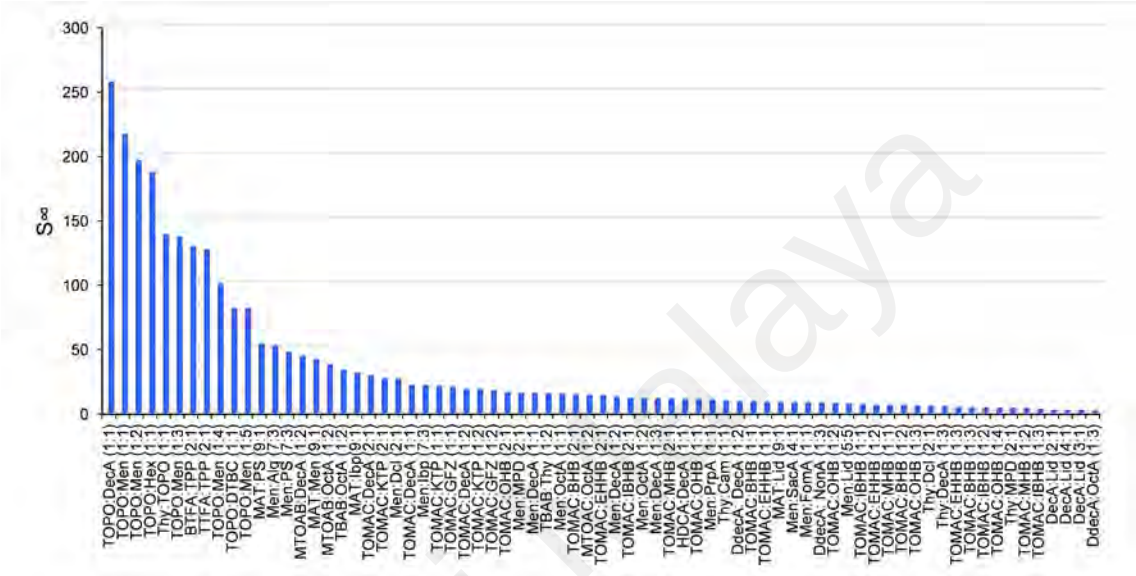

Figure 4.9: Selectivity of HDES for the removal of phenol from water at infinite dilution.

It can be seen from Figures 4.8-4.10 that the selection of HBA and HBD is crucial in the formation of HDES. HBAs and HBDs that possess larger molecular weight and complex structures exhibit a tendency to generate HDES that possess superior capacity and selectivity towards phenol. This phenomenon can be attributed to the enhanced interaction between these HBAs and HBDs and phenol molecules.

An example of a notable outcome is the combination of TOPO with decanoic acid in a 1:1 molar ratio, resulting in a significantly high PI value of 2483.17. It can also be observed that the molar ratio has a noticeable effect on the effectiveness of phenol removal. For instance, a change in the molar ratio of the DecA:Lid HDES results in a decrease in the PI from 3.01 to 2.04. This pattern suggests that the solvent's affinity for phenol may be improved by a larger ratio of HBA to HBD. Effective extraction depends

on the solvent's polarity and, consequently, its affinity towards phenol molecules, which are influenced by the intricate balance between the HBA and HBD components in the HDES.

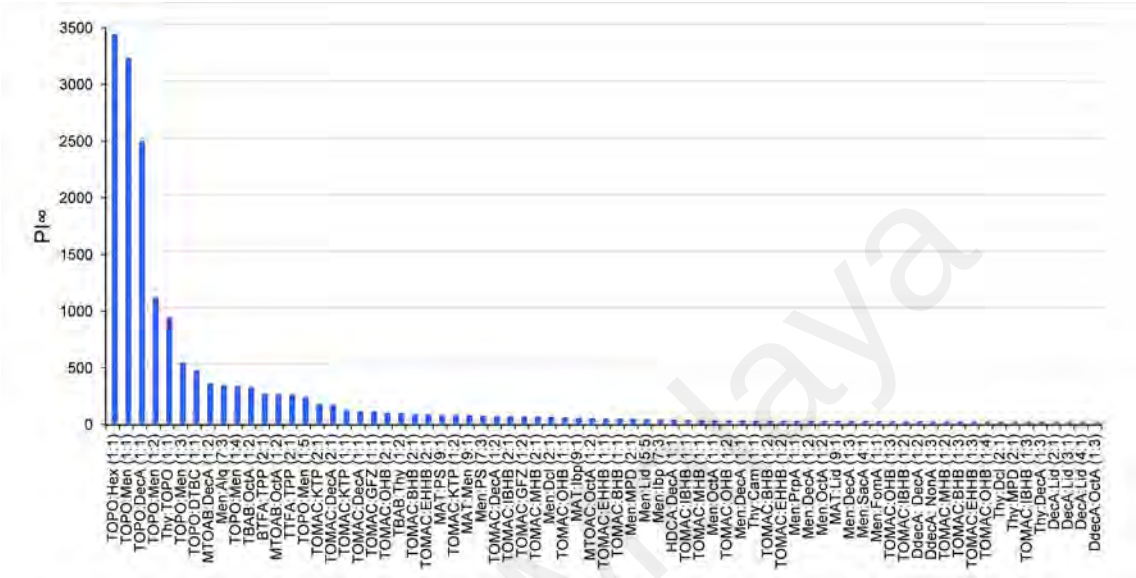

Figure 4.10: Performance index of HDES for the removal of phenol from water at infinite dilution.

The four HDES TOPO:Men, TOPO:Thy, TOPO:Hex, and TOPO:DecA (all at 1:1 molar ratio) demonstrated significantly higher PI values compared to other HDES in the study, making them superior candidates for further investigation in phenol removal applications. While TOPO:DecA showed superior selectivity (Figure 4.9), suggesting a higher specificity towards phenol over water, TOPO:Men and TOPO:Hex, in particular, displayed high-capacity values, reflecting their ability to dissolve larger quantities of phenol. The carboxylic acid group in decanoic acid may have contributed to TOPO:DecA's high PI by promoting hydrogen bonding with phenol. The high PI seen in TOPO:Men system may be attributed to a synergistic interaction between capacity and selectivity, which might potentially be ascribed to the chemical interactions occurring among TOPO:Men HDES and phenol. Similarly, TOPO:Hex has a high PI value, indicating enhanced phenol elimination effectiveness, due to the longer alkyl chain

encouraging favorable interactions. TOPO:Thy demonstrated substantial PI, indicating favorable interactions with phenol molecules, owing to thymol's aromatic ring promoting π-π interactions.

The chosen HDES have a combination of favorable attributes such as a balanced molar ratio, a high PI, and diverse molecular structures. They have the potential to provide critical insights into the mechanics of phenol extraction, necessitating additional experimental investigation. The subsequent experimental screening attempts to confirm the computational findings and elaborate on the fundamental factors governing phenol ex-traction efficiency.

4.3.2 Experimental validation

The experimental LLE data for ternary systems was investigated at a temperature of 298.15 K and a pressure of 101 kPa to assess the effectiveness of HDES in extracting phenol from wastewater. The GC calibration curve is shown in Figure 4.11. The obtained LLE data is reported in Table 4.4 and the extraction efficiency is shown in Figure 4.12.

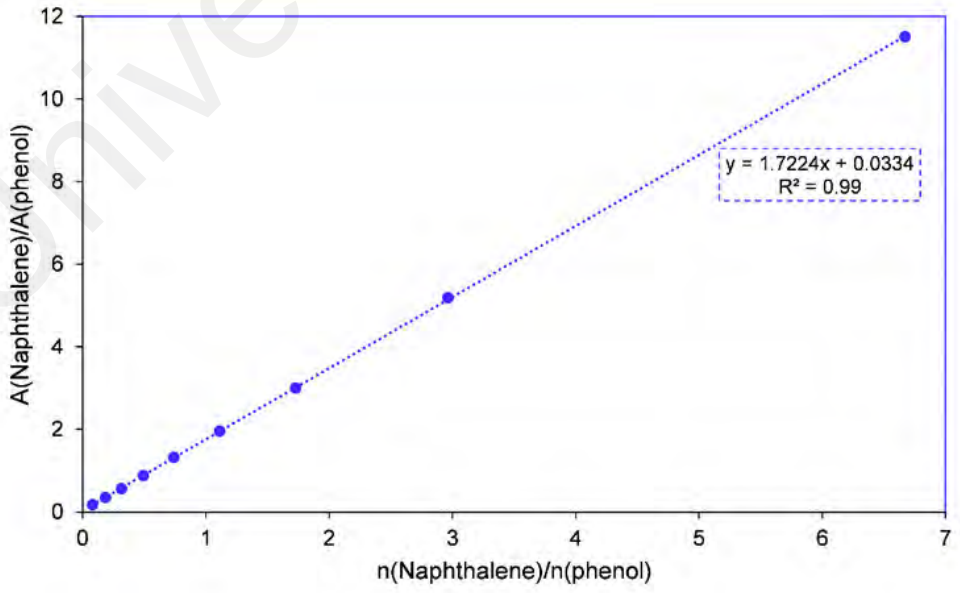

Figure 4.11: GC calibration curve of naphthalene/phenol.

Table 4.4: Composition of the experimental tie-lines (mole fraction), phenol distribution ratio (D), and selectivity (S) for the ternary systems {water (1) + phenol (2) + HDES (3)} at 298.15 K and 101.325 kPa.*

Water-rich phase			HDES-rich phase			D	S
x'_1	x'_2	x'_3	x''_1	x''_2	x''_3		
{water (1) + phenol (2) + TOPO:Men (3)}							
0.9987	0.0007	0.0005	0.4707	0.0225	0.5068	30.7	65.1
0.9983	0.0008	0.0010	0.4576	0.0497	0.4927	64.8	141.3
0.9990	0.0008	0.0003	0.4478	0.0700	0.4822	91.3	203.6
0.9988	0.0007	0.0005	0.4376	0.0911	0.4712	128.0	292.2
0.9991	0.0006	0.0004	0.4235	0.1204	0.4561	208.0	490.7
0.9991	0.0008	0.0002	0.4148	0.1384	0.4467	178.2	429.2
0.9987	0.0005	0.0008	0.4034	0.1623	0.4344	331.1	819.7
{water (1) + phenol (2) + TOPO:Hex (3)}							
0.9978	0.0007	0.0015	0.5210	0.0192	0.4598	27.8	53.3
0.9974	0.0013	0.0013	0.5114	0.0372	0.4514	29.7	57.9
0.9978	0.0011	0.0012	0.4976	0.0633	0.4392	59.0	118.4
0.9981	0.0010	0.0009	0.4879	0.0815	0.4306	79.2	162.0
0.9985	0.0009	0.0006	0.4773	0.1014	0.4213	109.6	229.3
0.9975	0.0011	0.0014	0.4674	0.1201	0.4125	104.7	223.5
0.9982	0.0011	0.0007	0.4602	0.1337	0.4062	125.8	272.8
{water (1) + phenol (2) + TOPO:Thy (3)}							
0.9985	0.0007	0.0008	0.2270	0.0323	0.7406	43.7	192.2
0.9993	0.0007	0.0000	0.2185	0.0686	0.7128	105.4	482.2
0.9989	0.0007	0.0004	0.2108	0.1014	0.6877	153.4	726.8
0.9991	0.0008	0.0001	0.2048	0.1273	0.6679	169.5	827.3
0.9987	0.0009	0.0004	0.1978	0.1570	0.6452	170.3	859.6
0.9988	0.0009	0.0003	0.1905	0.1883	0.6213	200.5	1051.6
0.9986	0.0008	0.0006	0.1847	0.2130	0.6023	270.7	1463.9
{water (1) + phenol (2) + TOPO:DecA (3)}							
0.9989	0.0007	0.0005	0.3136	0.0388	0.6477	58.7	187.1
0.9988	0.0009	0.0003	0.3053	0.0642	0.6305	74.1	242.3
0.9988	0.0008	0.0004	0.2953	0.0949	0.6098	118.1	399.6
0.9989	0.0008	0.0003	0.2881	0.1170	0.5950	142.1	492.8
0.9987	0.0008	0.0005	0.2758	0.1547	0.5695	193.3	699.9
0.9988	0.0008	0.0004	0.2707	0.1703	0.5591	201.3	742.9
0.9991	0.0008	0.0001	0.2610	0.1999	0.5391	256.0	979.7

*Standard uncertainties : u(x) = 0.013, u(T) = 0.5 K, u(P) = 1 kPa.

The experimental results indicate that as the concentration of phenol is varied from 1% to 7%, there is a slight rise in the phenol composition in the water-rich phase, but the phenol concentration in the HDES-rich phase experiences a significant increase. This

observation suggests that the affinity of phenol towards HDES becomes stronger as the concentration of phenol increases. This suggests the hydrophobic characteristics of phenol, as it tends to favor the HDES phase over the aqueous phase. Furthermore, with a rise in the concentration of phenol, both the distribution ratio and the selectivity exhibit an upward trend across all the HDES. This suggests that higher phenol concentrations lead to improved extraction efficiency. The observed correlation between improved efficiency and increasing phenol content indicates that higher concentrations of phenol are favorable to more effective extraction. The observed phenomenon may be attributed to the increased driving force for mass transfer that occurs at higher phenol concentrations.

The relationship between extraction efficiency and phenol concentration demonstrates a positive correlation across all HDES, indicating an improvement in extraction efficiency as phenol concentration increases. The extraction efficiencies of TOPO:Men, TOPO:Hex, and TOPO:DecA were seen to be higher at elevated phenol concentrations in comparison to TOPO:Thy. At 7% phenol content, TOPO:Men exhibited the highest extraction efficiency (~96%). This indicates that the extraction efficiency is influenced by the type of HDES. The data clearly indicates that there is a notable variation in the composition of phases among various HDES. This observation implies that the selection of HDES has an impact on the equilibrium partitioning of phenol between the aqueous and DES phases. The interaction between phenol and the solvent, and therefore the extraction efficiency, may be influenced by the nature of the HDES. Table 4.4 indicates that the concentration of HDES in the water phase is significantly low, underscoring the hydrophobic properties of HDES. This minimal presence may be attributed to slight solubility or dispersion of HDES in the water phase. The obtained LLE data is graphically rendered as triangular ternary diagrams in Figure 4.13. Figure 4.13 demonstrates that all ternary systems exhibit Type I phase behavior, characterized by a singular immiscibility zone.

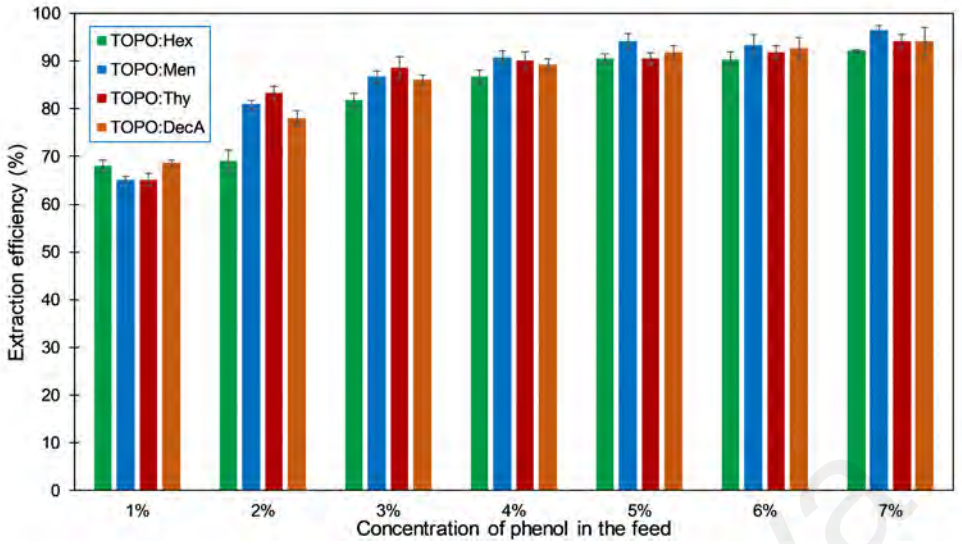

Figure 4.12: Effect of phenol concentration on the extraction efficiency of HDES.

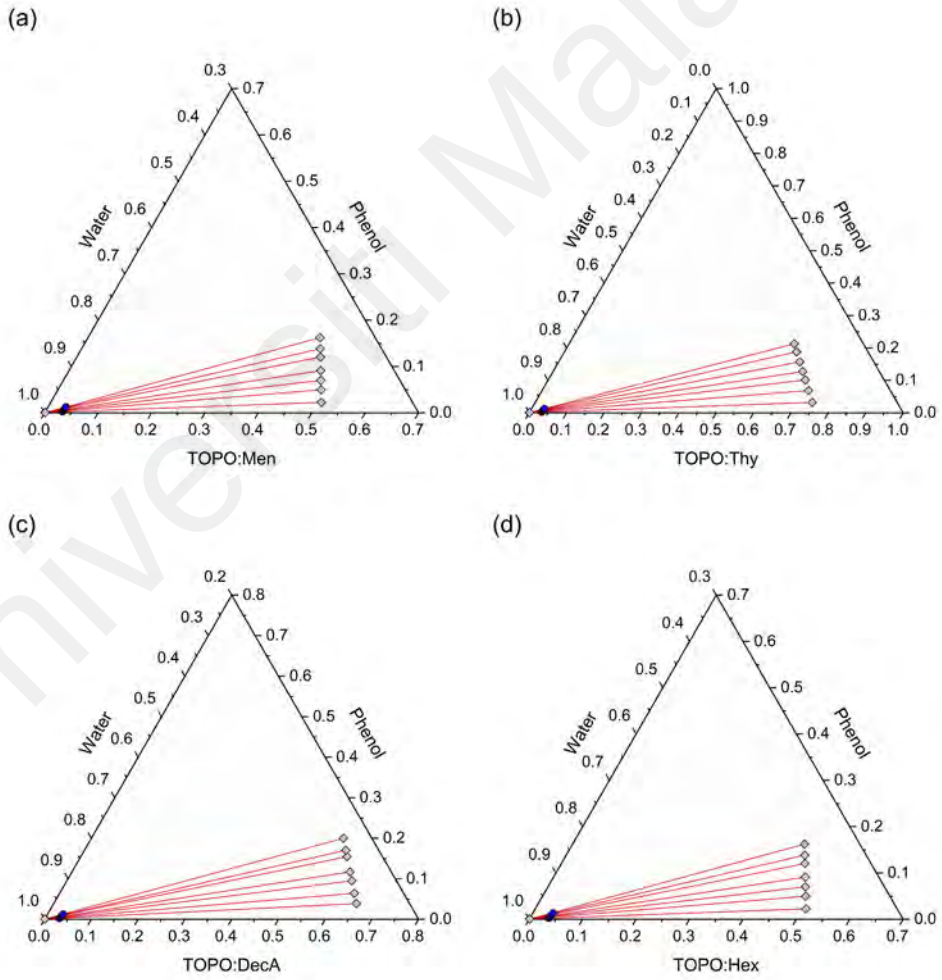

Figure 4.13: Ternary liquid–liquid equilibrium diagram in mole fraction for (a) water (1) + phenol (2) + TOPO:Men (3); (b) water (1) + phenol (2) + TOPO:Thy (3); (c) water (1) + phenol (2) + TOPO:DecA (3); and (d) water (1) + phenol (2) + TOPO:Hex (3).

The observation in Figure 4.13 reveals that all of the systems exhibit positive tie-line slopes, which signifies that the HDES-rich phase has a higher quantity of phenol compared to the water-rich phase at equilibrium. This suggests that a smaller quantity of solvent is required to achieve a significant level of extraction. In addition, it can be observed that the slopes of the data increase as the concentration of phenol (the solute) increases. This implies that when the solute concentration decreases, there is an increase in the concentration of solvent (HDES) needed to extract the solute from the solution. Figure 4.13 demonstrates a positive correlation between the length of the tie-lines and the degree of immiscibility.

4.3.3 Consistency test

The reliability of ternary system {Phenol+ water + HDES} was checked using the Hand and Othmer–Tobias correlations. Both correlations show a linear regression >0.93. This indicates a high degree of reliability and consistency in the experimental tie-line data. The correlation data for all four HDES is shown in Table 4.5.

Table 4.5: Othmer-Tobias and Hand correlations for the separation of phenol and water via HDES.

HDES	Othmer-Tobias			Hand		
	a	**b**	R^2	**c**	**d**	R^2
TOPO:Men	-10.08	-2.212	0.956	-5.416	0.029	0.969
TOPO:Thy	0.767	1.744	0.941	5.067	0.147	0.936
TOPO:DecA	-6.596	-0.703	0.930	-4.918	0.160	0.947
TOPO:Hex	-5.724	-0.891	0.957	-6.140	-0.26	0.979

4.4 Removal of cresol isomers from water

Cresols have distinct effects on the environment and human health. For instance, o-cresol is considered a toxic isomer and can cause severe health problems. Cresol isomers tend to cause adverse effects on the environment since they can be hazardous to aquatic

creatures and may bioaccumulate in food chains. The introduction of these chemical substances has the potential to perturb the equilibrium of ecological systems by diminishing the concentration of oxygen in aqueous environments, thereby influencing the viability and procreative capacity of aquatic organisms. In this work, six HDES were prepared and employed for the liquid extraction of m-cresol and o-cresol from wastewater. The HDES include Men:Thy, Men:DecA, Thy:DecA, HydA:DecA, Thy:Coum, and Thy:Camp. All HDES were prepared at 1:1 molar ratio. The effect of various parameters such as contact time, HDES to water mass ratio, HDES' molar ratio, and initial concentration was examined. The experimental results indicated excellent efficiency for the removal of cresols from wastewater using all HDES. The extraction efficiency of >94% was achieved for the removal of cresol isomers from wastewater using all the prepared HDES. Furthermore, the COSMO-RS was employed to understand the extraction procedure. This model offers an in-depth understanding of the interactions between the HDES and the cresols.

4.4.1 HDES cross-contamination with water

To ensure the stability of HDES and water during the LLE procedure (2 h), they were mixed in a ratio of 50% v/v. These mixtures were prepared in sealed bottles with screw caps. To ensure proper contact between the two phases, they were stirred for 4 h before allowing them to settle for 24 h. After mixing and settling, a sample of the HDES phase was taken. This was used to measure the amount of water contained in the HDES phase using the Aquamax Karl Fischer titrator. Only traces of water were detected in the pure HDES (0.011–0.213 wt%). Figure 4.14 shows the water solubility of six HDES after mixing with the aqueous phase.

Thy:DecA showed highest solubility (3.639%), while the other HDES showed a water solubility in the range of 1.668–3.059%. A similar behavior was observed in the literature

for the terpene-based HDES (Almustafa et al., 2020; Martins et al., 2018; Ribeiro et al., 2015). With the exception of Thy:DecA, all other HDES behaved like neutral HDES due to their water solubility of less than 3 wt% (Florindo et al., 2019b).

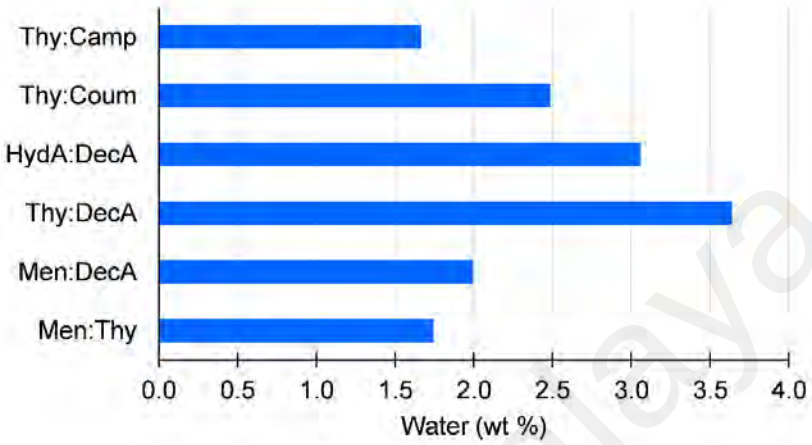

Figure 4.14: Water solubility of six HDES used for the removal of cresols.

4.4.2 Extraction analysis

The solubility limit for o-cresol and m-cresol in water is set at 2.5 and 2.4 g/100 ml, respectively.

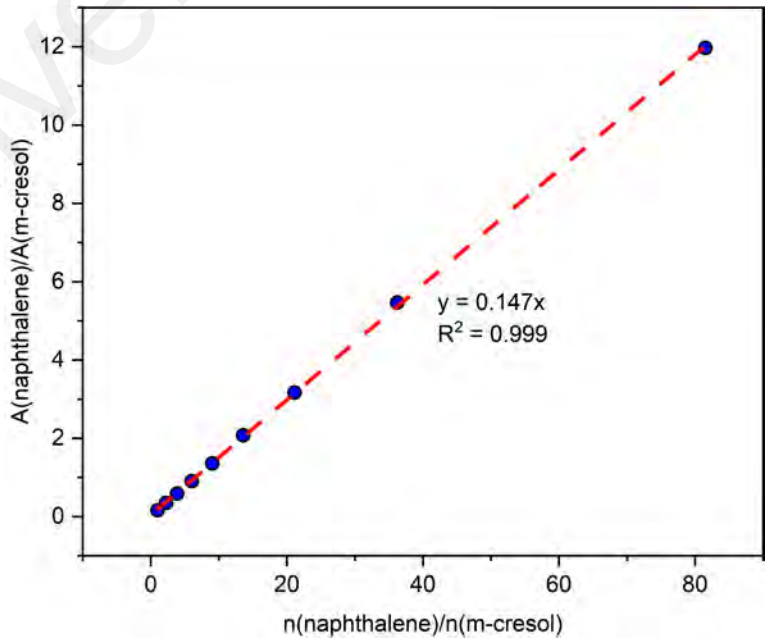

Figure 4.15: GC calibration curve of m-cresol and naphthalene.

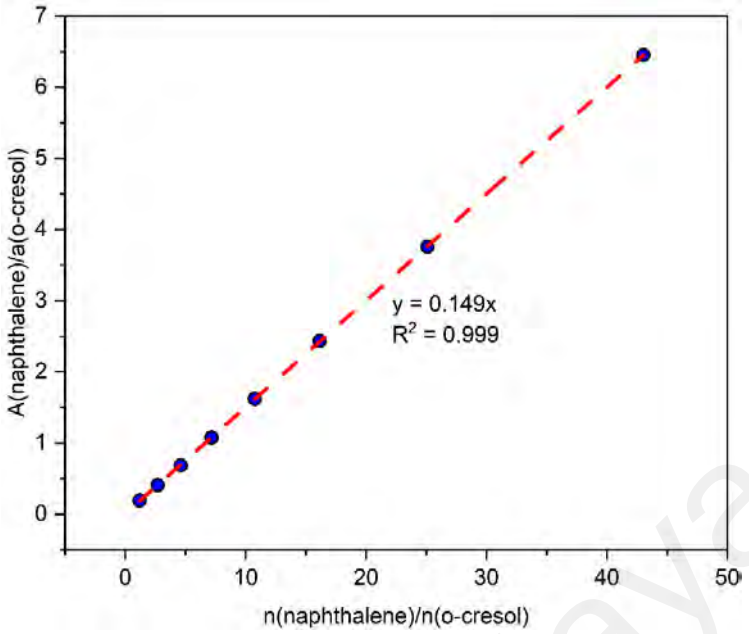

Figure 4.16: GC calibration curve of o-cresol and naphthalene.

Cresols, such as o-cresol and m-cresol, are frequently used as disinfectants and solvents and in the manufacture of resins, plastics and pesticides. Industries such as chemical industry, coal processing and petroleum refining can produce effluents with elevated concentrations of cresols, particularly o-cresol and m-cresol (Chen et al., 2017). For the experimental screening of HDES, a model solution of 1.5 g/100 ml cresol was prepared gravimetrically. A calibration curve of m-cresol/naphthalene and o-cresol/naphthalene was established for the determination of the composition (Figures 4.15 and 4.16).

As can be seen in Figure 4.17, all prepared HDES were able to achieve an extraction efficiency of over 94% in the removal of cresol isomers from water. In terms of performance index, Men:Thy and Thy:Coum yielded higher values as shown in Table 4.6. The high efficiency of Men:Thy and Thy:Coum can be attributed to the strong interaction between the individual components of the HDES, culminating in an increased affinity for cresol isomers.

Table 4.6: The performance of six HDES in terms of selectivity (S) and distribution ratio (D) for the removal of o-cresol and m-cresol from water at 298.15 K and 101.325 kPa.*

HDES	m-cresol		o-cresol	
	D	S	D	S
Men:Thy	387.86±28.4	1821.4±188.5	450.99±33.0	2118.50±219.3
Men:DecA	374.60±27.4	1309.1±135.5	460.63±33.7	1627.27±168.4
Thy:DecA	182.56±13.4	405.3±41.94	253.77±18.6	562.36±58.20
HydA:DecA	246.16±18.0	693.6±71.79	338.27±24.8	952.64±98.60
Thy:Coum	566.76±41.5	1949.4±201.8	494.30±36.2	1724.46±178.5
Thy:Camp	361.03±26.4	1727.4±178.9	393.57±28.8	1885.44±195.2

*Standard uncertainties are u(x) = 0.0014, u(T) = 0.5 K and u(P) = 1.0 kPa.

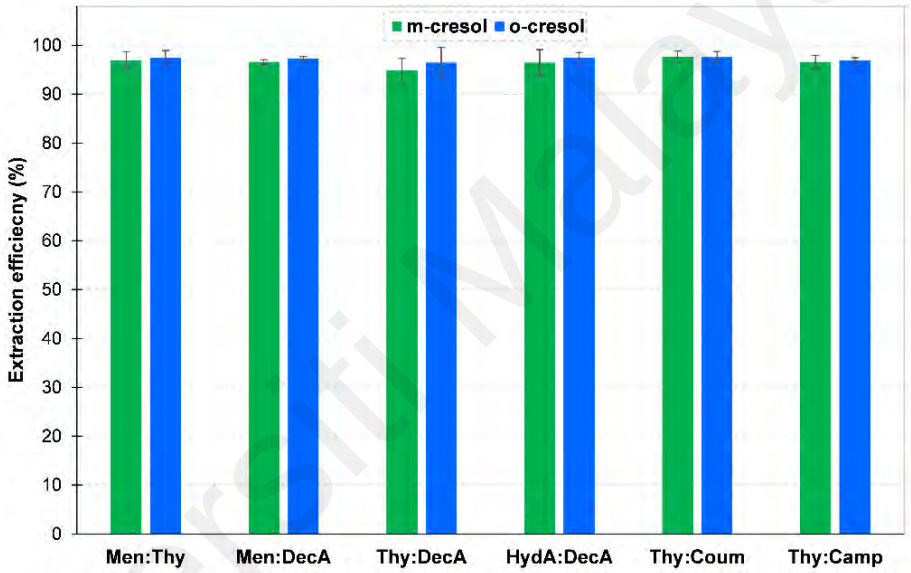

Figure 4.17: Extraction efficiency of cresols in 6 HDES.

Thy:Coum was found to be the best HDES, both in terms of efficiency and performance index. One reason for this could be the lowest solubility of coumarin in water compared to all other individual components of the HDES used in this work. The partition coefficient indicates the efficiency of the HDES in distributing cresols between the aqueous and organic phases. Based on the distribution ratio, it can be deduced that Thy:Coum has the best performance in the elimination of cresols from water, as it has the highest distribution ratio. In HydA:DecA HDES, the hydrocinnamic acid has a carboxylic acid group, which has the ability to form hydrogen bonds with water molecules

and make them more polar, reducing the hydrophobicity and extraction performance of the compound.

One of the critical factors in the industrial implementation of a process is the optimization of experimental parameters. This is due to the fact that these characteristics have a major influence on the cost-efficiency ratio. In the next section, the influence of different experimental variables on extraction efficiency is analyzed. These variables include the contact time, the mass ratio of HDES to aqueous phase, the molar ratio of HDES, and the initial concentration. Three HDES (Men:Thy, Thy:DecA, and Thy:Coum) were selected for the parametric analysis. Men:Thy and Thy:Coum were selected because they showed the highest efficiency in extracting cresols from water, while Thy:DecA showed the lowest extraction efficiency.

4.4.2.1 Effect of contact time

An important indicator for determining the kinetics of an extraction process is the contact time. A longer extraction time leads to a better dispersion and uniform distribution of the HDES in the sample solution. Consequently, the efficiency is increased by an improved dispersion of the extractant. In general, however, a shorter contact time is required to achieve faster kinetics. Therefore, the effect of extraction time on efficiency was investigated by changing the mixing time between 15-120 minutes (Figure 4.18).

It can be observed that the extraction process of cresols using the selected HDES reached a complete equilibrium between 15 and 30 minutes. The extraction efficiency remained almost constant with increasing contact time. To ensure equilibrium, the contact time was set at 30 minutes for further studies. The extraction efficiency remains almost constant with prolonged contact time as the system quickly reaches equilibrium, generally within 15–30 minutes, as can be seen in Figure 4.18. This indicates that the mass transfer of cresols from the aqueous phase to the HDES phase is extremely efficient and a longer

mixing time does not significantly improve the extraction process. The rapid attainment of equilibrium means that the interaction between cresols and HDES components, mainly through hydrogen bonding and hydrophobic interactions, occurs rapidly and leads to saturation of the accessible binding sites. Once equilibrium is reached, extraction is not improved by further mixing as phase equilibrium between the HDES and the aqueous medium is reached.

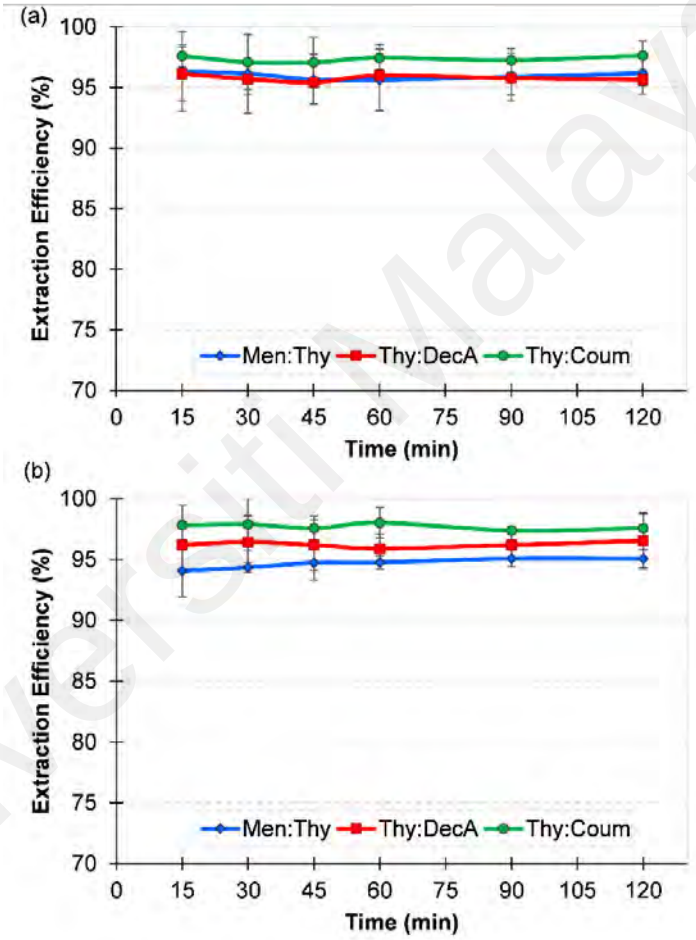

Figure 4.18: The Effect of contact time on the extraction efficiency of (a) m-cresol, (b) o-cresol.

4.4.2.2 Effect of HDES to water phase mass ratio

The use of extraction solvents in LLE should be kept as low as possible from an industrial point of view in order to minimize costs and environmental impact. Optimizing the mass ratio between HDES and water phase mass ratio in LLE is one way to achieve

this goal, as it influences how effective the extraction process is while controlling the amount of solvent required (Figure 4.19).

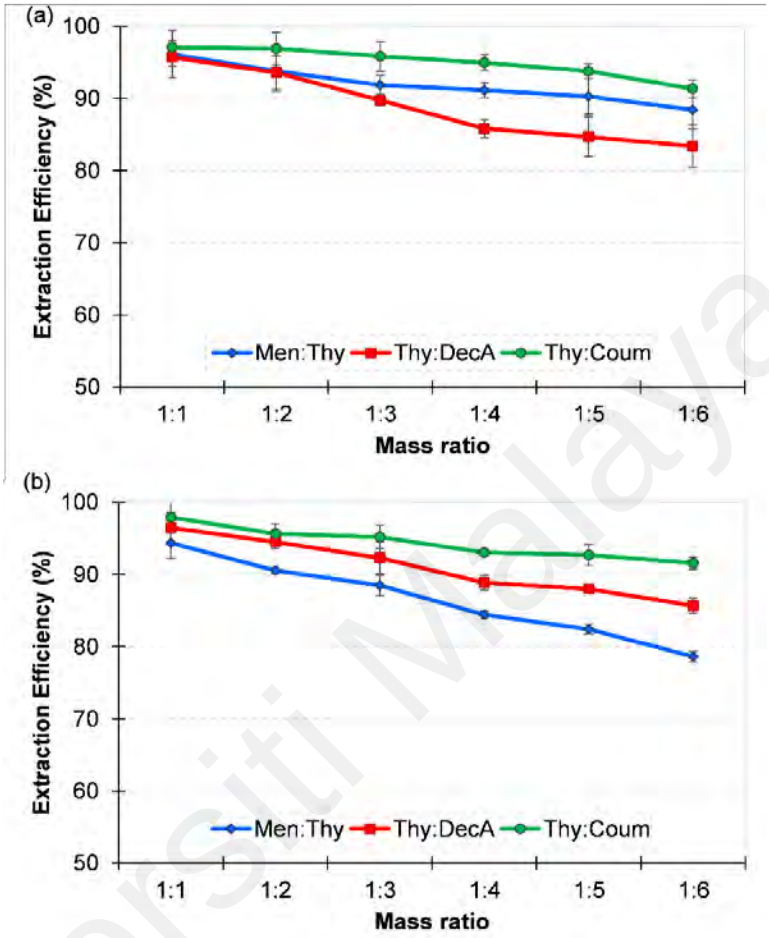

Figure 4.19: The effect of HDES:water mass ratio on the extraction efficiency of (a) m-cresol, and (b) o-cresol.

To find the optimal ratio between HDES and water phase, an HDES:water mass ratio of 1:1 to 1:6 was investigated. As can be seen in Figure 4.19, the extraction performance of all three HDES decreased with decreasing amount of HDES. However, for Thy:Coum, there was only a slight decrease in efficiency from 1:1 to 1:3. Based on the results from Figure 4.19, optimal ratios for all three HDES were found. A mass ratio of 1:1 was chosen for Men:Thy, while a ratio of 1:2 was chosen for Thy:DecA and a mass ratio of 1:3 was chosen for Thy:Coum. By considering HDES, the consumption of extraction solvents was reduced, and the environmental impact of the extraction process was minimized while

maintaining high extraction efficiency with a lower amount of HDES. Even at a mass ratio of 1:6, considerable extraction was achieved because the rate at which extraction capacity decreased was so low. ≥ 80% extraction efficiency was achieved for all systems at a phase ratio of 1:6. As significant extraction of cresols was observed at lower HDES mass ratio; this has significant economic benefits.

4.4.2.3 Effect of HDES' molar ratio

According to various researchers, the physicochemical properties of HDES are significantly influenced by the molar ratio of HBA to HBD (Florindo et al., 2020; Zhang et al., 2012). For this reason, the effect of molar ratio of three selected HDES on the extraction efficiency of cresols was investigated (Figure 4.20).

As for Men:Thy, the results presented in Figure 4.20 show that the molar ratio of menthol to thymol has no significant effect on the efficiency of extraction of cresol from water. Although there is some small variation in the extraction efficiency values, the overall trends suggest that there is no obvious relationship between extraction efficiency and molar ratio. A likely reason for this lack of dependence is that menthol and thymol have similar chemical structures and therefore their ability to form a homogeneous solution is not affected by the molar ratio. As a result, the extraction efficiency could be generally constant for all molar ratios studied.

The extraction efficiency of Thy:DecA decreases when the molar ratio of Thy:DecA increases from 1:1 to 4:1. The extraction efficiency of cresol decreases as the molar ratio of thymol to decanoic acid increases. This can be explained by the fact that the amount of decanoic acid in HDES decreases as the molar ratio of thymol to decanoic acid increases from 1:1 to 4:1, resulting in a less polar solvent system. As the polarity decreases, the extraction of the polar cresol molecule becomes less efficient, resulting in lower extraction efficiency. In addition, at higher thymol to decanoic acid molar ratios,

the thymol molecules begin to aggregate due to their high surface activity, resulting in a reduction in the total surface area of the extracting solvent. The reduced surface area reduces the interaction between the extracting solvent and the aqueous phase, which decreases the efficiency of cresol extraction.

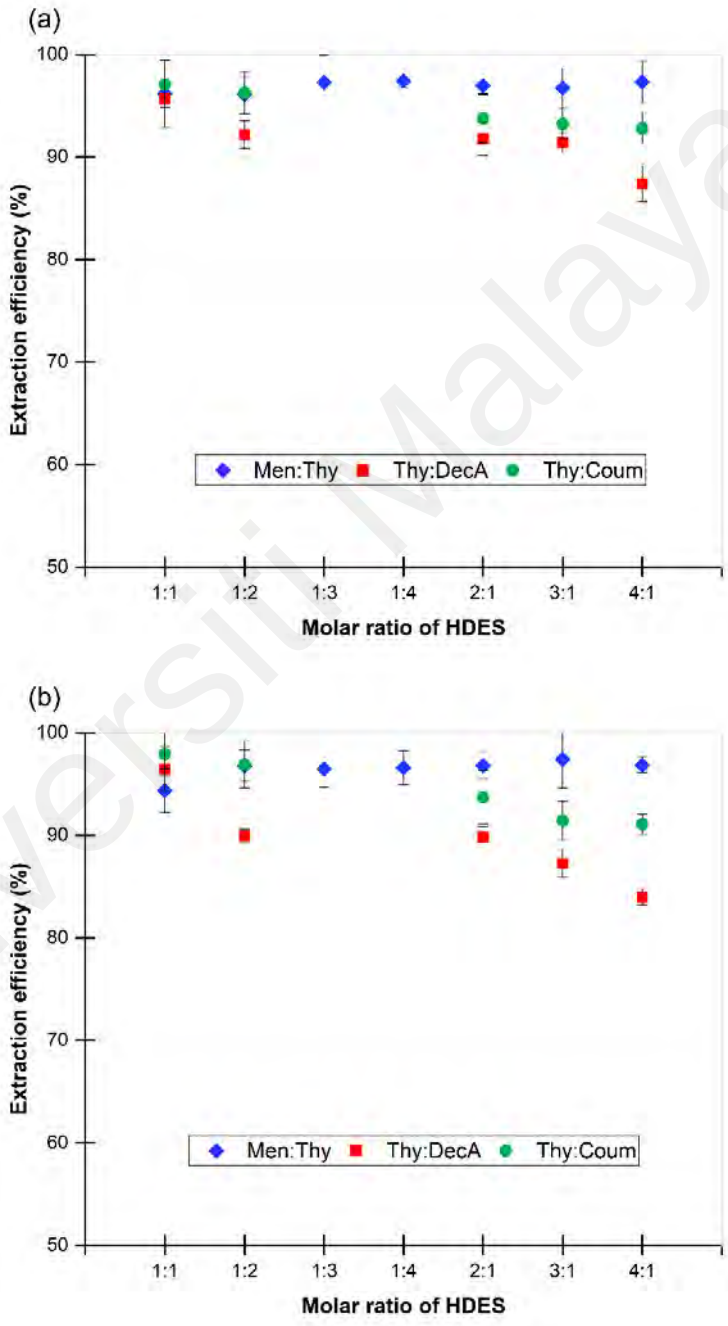

Figure 4.20: The effect of changing molar ratio of HDES on the extraction of (a) m-cresol, and (b) o-cresol from water.

An increase in the thymol content in Thy:Coum leads to a higher concentration of thymol in the HDES phase and a lower concentration of coumarin. Due to its higher polarity, thymol has a higher affinity for water molecules than coumarin. Therefore, in Thy:Coum HDES, a higher amount of thymol in the HDES phase leads to a reduction in the extraction efficiency of cresols.

4.4.2.4 Effect of initial concentration of cresols

The study focused on the effect of the initial concentration of cresols (between 0.15 g/ml and 1.5 g/ml) in aqueous solutions on the extraction efficiency. The results presented in Figure 4.21 show that the extraction efficiency of cresols decreases with increasing cresol concentration in water. In fact, the cresol extraction efficiency depends on the HDES type and the initial cresol concentration in the water.

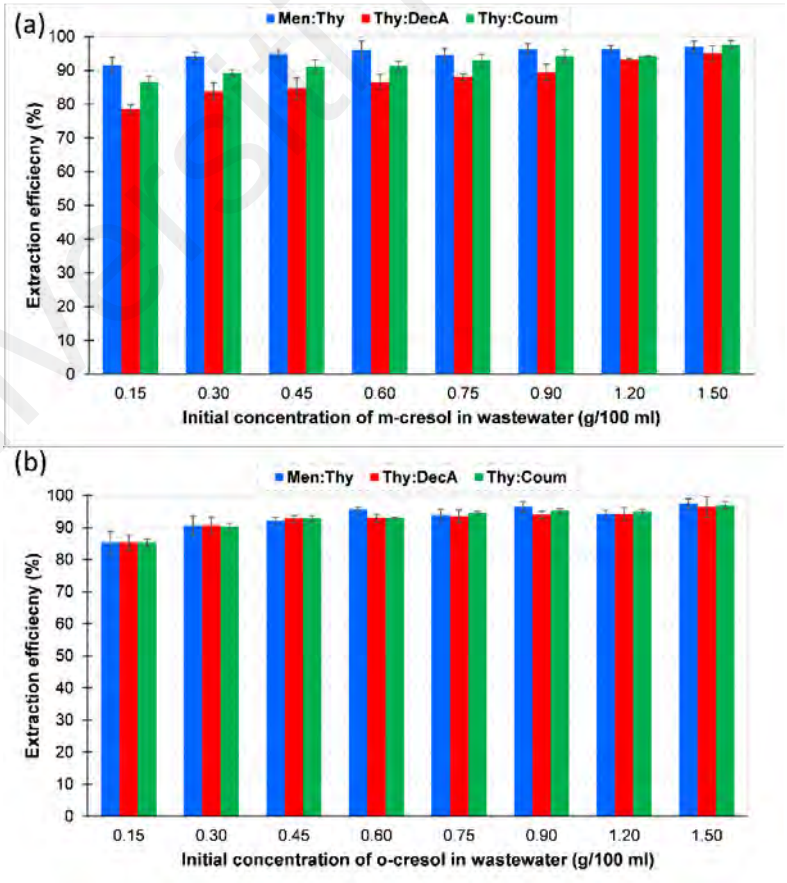

Figure 4.21: The effect of initial concentration of (a) m-cresol, and (b) o-cresol on the extraction efficiency.

The extraction efficiency of all three HDES improves with increasing initial cresol concentration. This trend is due to the increase in the initial concentration of cresol, which leads to a higher driving force for mass transfer and thus to a higher extraction efficiency. A similar trend has already been observed when using DESs for other phenolic pollutants (Adeyemi et al., 2020; Florindo et al., 2020; Sas et al., 2019). The Thy:DecA HDES has the lowest extraction efficiency for cresol compared to the other two HDES, regardless of the initial concentrations. This can be attributed to the lower polarity of the Thy:DecA system compared to the other two systems. The long hydrophobic tail of decanoic acid reduces the polarity of the system and thus reduces the solubility of cresol.

4.4.2.5 Reuse of HDES

The reusability of the HDES was investigated by performing successive extraction cycles in which the same HDES was continuously in contact with "fresh" contaminated water phase (Figure 4.22). Thy:Coum was selected due to its superior performance index. The study focused on the reuse of Thy:Coum in the extraction of m-cresol in six consecutive cycles at 1:3 mass ratio of Thy:Coum to the aqueous solution of m-cresol.

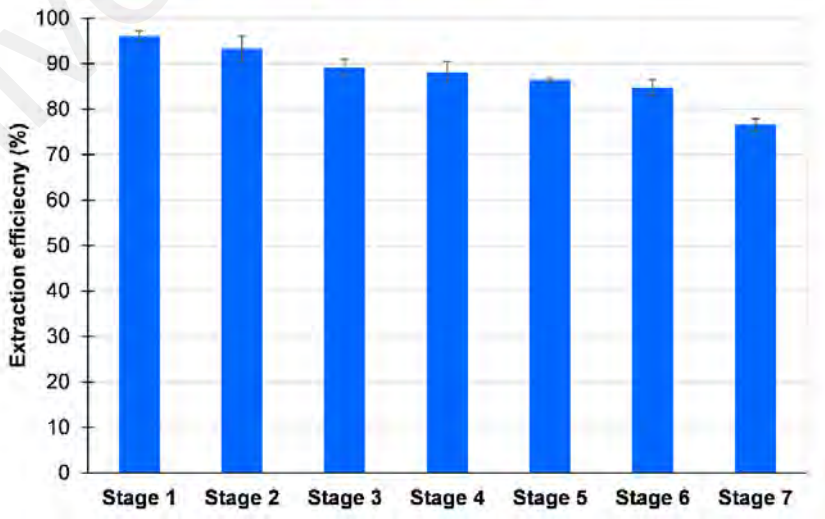

Figure 4.22: Reuse of Thy:Coum after several cycles of extraction of m-cresol from water at 1:3 HDES to water mass ratio and 30 mins of contact time.

The present study shows that there is an inverse relationship between the number of cycles of the DES employed and its extraction capacity. The higher the number of cycles, the lower the ability of the HDES to extract cresols. The observed phenomenon can possibly be attributed to the presence of cresol in the dissolved HDES. It is plausible that the dissolution of equivalent amounts of cresol in cresol-contaminated HDES is more challenging compared to freshly extracted HDES in the same time interval. In addition, the observed decrease in efficiency can be attributed to several factors, including loss of HDES constituents, accumulation of impurities, and changes in physical properties. To optimize the effectiveness of HDES in the removal of cresol, it is essential to consider the reusability of the solvent and to regularly replace or regenerate the HDES when necessary. Nevertheless, even after 6 cycles, Thy:Coum was able to extract m-cresol with an extraction efficiency of ~80%.

4.4.3 Consistency test

The reliability of ternary system {cresol + water + HDES} was checked using the Hand and Othmer–Tobias correlations. The linear regression data and fitting parameters for both correlations are shown in Table 4.7. Both correlations show a linear regression >0.90. However, Hand correlation exhibited better linearity than Othmer-Tobias.

Table 4.7: Othmer-Tobias and Hand correlations for the separation of cresols and water via three HDES.

HDES	Othmer-Tobias			Hand		
	a	**b**	R^2	**c**	**d**	R^2
m-cresol						
Men:Thy	8.636	3.686	0.948	-5.379	0.543	0.957
Thy:DecA	-13.41	-3.092	0.982	-5.026	0.463	0.967
Thy:Coum	2.674	2.622	0.905	-5.291	0.546	0.984
o-cresol						
Men:Thy	5.189	2.433	0.910	-5.684	0.415	0.980
Thy:DecA	-6.417	0.518	0.900	-4.998	0.606	0.984
Thy:Coum	-9.169	-1.230	0.890	-6.955	0.250	0.950

4.4.4 Understanding extraction mechanism

COSMO-RS was used to simulate the extraction of cresol isomers from aqueous solution using HDES. The model served as a tool to understand how the phenolic pollutants were extracted. There are essentially two possible methods for extracting phenols from the aqueous phase. The first mechanism is based on the hydrophobic contact between the phenols present in the aqueous phase and the HDES. The second process involves the formation of hydrogen bonds between the phenols and the HDES. The sigma profile calculations yield a specific threshold value for hydrogen bonding, denoted as $\sigma hb = \pm 0.0084$ e/A^2. Chemical substances that exhibit a significant peak at $\sigma < \sigma hb$ are often identified as hydrogen bond donors. Conversely, peaks with a standard deviation (σ) greater than the hydrogen bond strength (σhb) are characterized by their tendency to accept hydrogen bonds.

Both m-cresol and o-cresol have a hydroxyl group (-OH) and a methyl group (-CH_3) bound to a benzene ring in their molecular structure. Cresols are classified as phenols and tend to donate hydrogen bonds, which is reflected in the sigma profile of these molecules as a region of increased electron density near the hydroxyl group. Since the oxygen atom in the hydroxyl group is more electronegative than the hydrogen atom, a sigma hole is produced as a result. This is due to the fact that a partial negative charge is created on the oxygen atom while a partial positive charge is created on the hydrogen atom. The sigma profile, on the other hand, would not show a region of high electron density near the methyl group, which would correlate with the propensity of the molecule to accept hydrogen bonds. This is due to the fact that the carbon atoms that make up the methyl group have a lower electronegative potential than the carbon atoms that make up the benzene ring, and therefore they do not generate a significant partial negative charge.

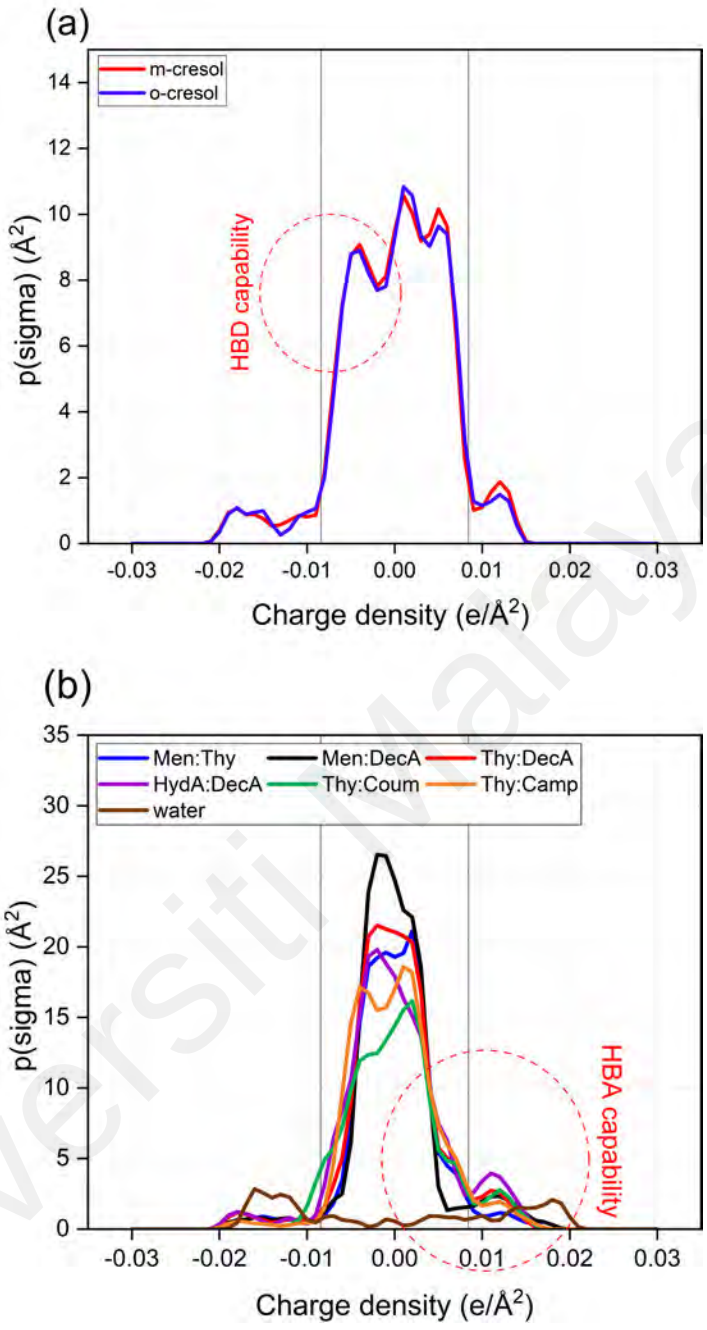

Figure 4.23: Sigma profiles of (a) cresols and (b) HDES used in this work.

According to the sigma profile Figure 4.23 (a), the cresols can be characterized as hydrogen bond donors due to an obvious peak on the left side of the threshold. This would cause the cresols to move towards the hydrogen bond acceptors, the HDESs, as they have notable peaks on the right side of the threshold Figure 4.23 (b). Consequently, there would be a mechanism for the transport of organic pollutants from the aqueous phase to the HDES phase. Several research groups (Brinda Lakshmi et al., 2013; Deng et al., 2011;

Fan et al., 2008) have made comparable findings regarding the transfer of phenolic pollutants from an aqueous phase into hydrophobic ionic liquids by hydrogen bonding.

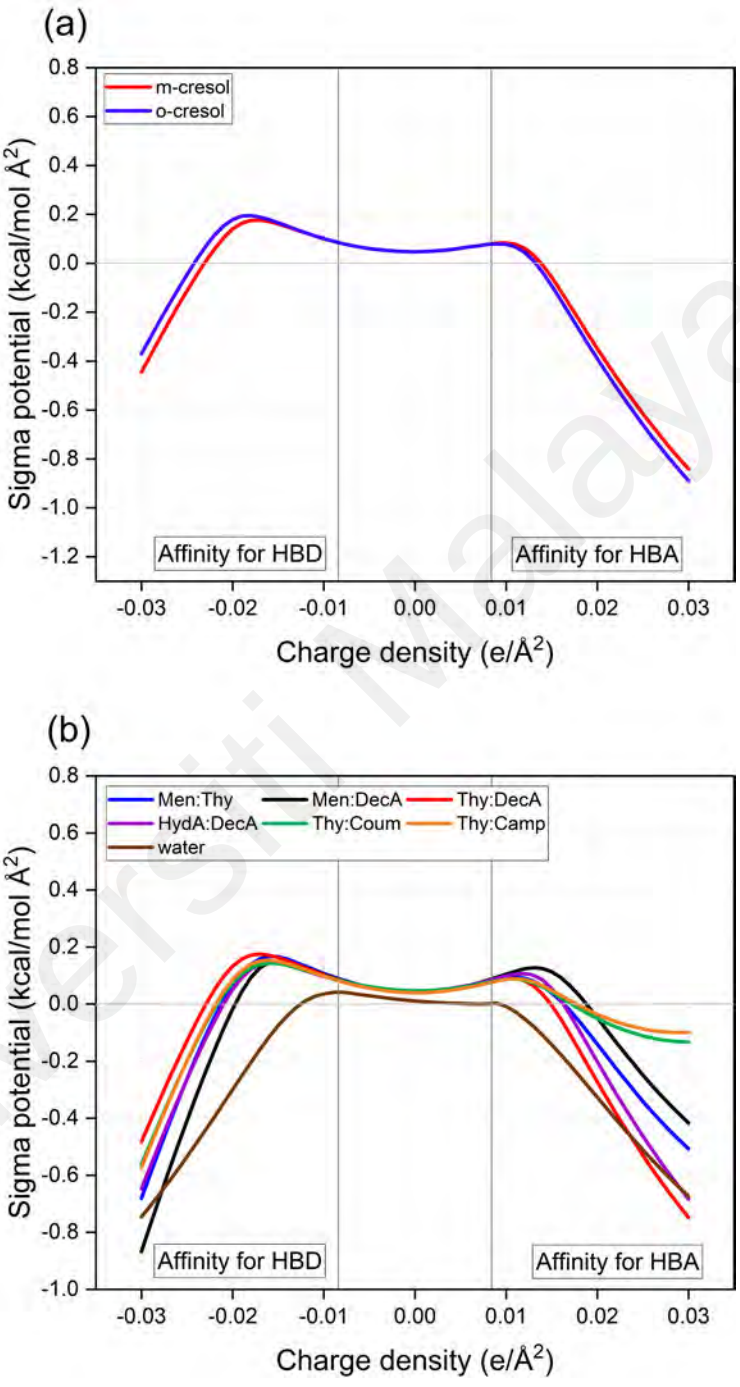

Figure 4.24: Sigma potential of (a) cresols and (b) HDES used in this work.

The relationship between the selectivity of the system and a surface of polarity σ is measured by the σ-potential in COSMO-RS. The distribution of the σ-potential on the surface of the molecule can be roughly divided into three regions: the affinity to the HBA

region, the non-polar region and the affinity to the HBD region. Figure 4.24 (a) shows that both the m-cresol and o-cresol models have a high capacity to release hydrogen. This is due to the presence of a higher negative σ-potential in the region that accepts hydrogen bonds and a more positive σ-potential in the region that donates hydrogen bonds.

However, Men:Thy, Thy:DecA and Thy:Coum showed the ability to accept hydrogen bonds as they had a larger negative σ-potential in the affinity to the HBD region and a more positive σ-potential in the affinity for HBA region, as shown in Figure 4.24 (b). Furthermore, Figures 4.23 (b) and 4.24 (b) also show the comparison between the sigma profile and sigma potential of HDES and water. From the sigma profile of the HDES and water, it can be observed that the interaction between the HDES and water is not favorable. Water shows peaks at both the HBA and HBD capabilities regions, whereas the HDES only shows some noticeable peaks at the HBA capability region.

For all the HDES, the peaks are mainly in the nonpolar region, indicating immiscibility with water. This is also in agreement with what have been reported by (Cheng & Qi, 2021; Jiang et al., 2021) where it was mentioned that the peaks of DES at the nonpolar region is an important factor indicating the hydrophobicity of the DES in extracting the targeted solutes from aqueous medium. Having said that, the HDESs that contain DecA have larger mutual solubility with water than other HDESs because it has a stronger peak in HBA and HBD regions, which results in stronger HBA and HBD affinities. Comparing the sigma potentials of the HDES and water in Figure 4.24 (b), water shows stronger affinity towards both HBA and HBD due to the more negative values of their sigma potentials on both sides of the graph. All other HDES, although showing affinity towards both HBA and HBD, are not as strong as water based on their less negative values.

The Thy:Coum HDES system for the extraction of cresol is primarily determined by hydrogen bonds between the hydroxyl group (-OH) of thymol and the functional ether

group (-O-) of coumarin. This interaction creates a stable eutectic mixture in which cresol, which contains a hydroxyl functional group (-OH), participates in further hydrogen bonding with thymol and coumarin, improving its solubility and selective extraction. Figure 4.25 clearly shows the incorporation of cresol molecules into the hydrogen bonding network of HDES, with the hydroxyl group of cresol forming robust donor-acceptor interactions with the pre-existing hydrogen bonding structure of the solvent.

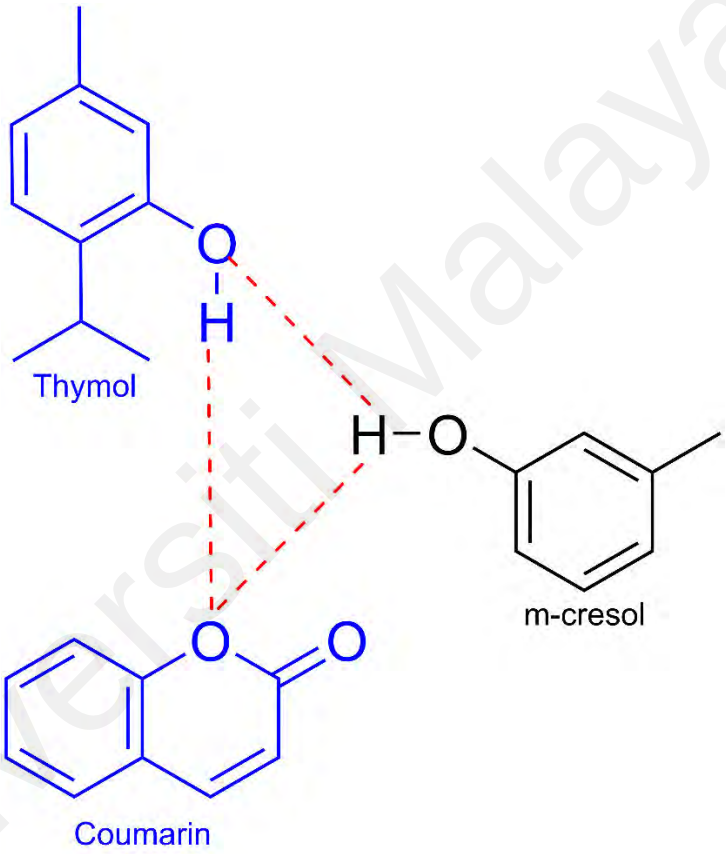

Figure 4.25: Molecular interactions in Thy:Coum HDES for m-cresol extraction.

In addition, π-π stacking interactions between the aromatic rings of coumarin and cresol enhance the solubilization and thus the attraction of HDES for cresol molecules. The hydrophobic properties of thymol and coumarin ensure that the HDES remains insoluble in water, minimizing solvent loss and maintaining phase stability. This behavior corresponds to the main hydrophobic solvation principles, in which non-polar and slightly polar organic molecules preferentially pass into a hydrophobic solvent phase. The robust

but selective hydrogen bonding and π-π stacking make thymol-coumarin HDES an effective medium for cresol extraction, providing excellent selectivity while reducing co-extraction of other aqueous impurities.

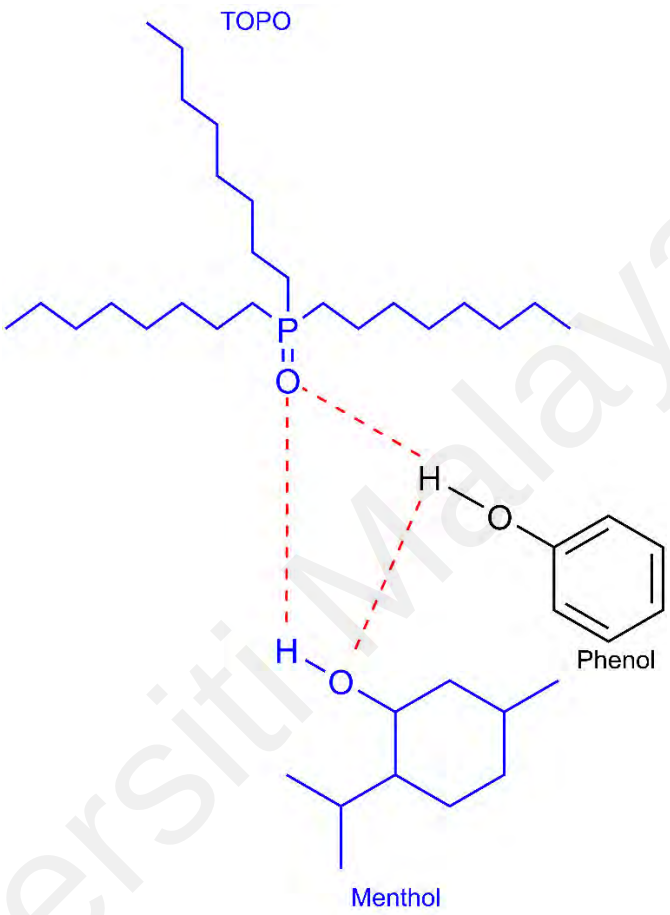

Figure 4.26: Molecular interactions in TOPO:Men HDES for phenol extraction.

The TOPO:Men HDES system for phenol extraction depends primarily on the hydrogen bonding between the phosphoryl group (-P=O) in TOPO and the hydroxyl group (-OH) in phenol, as shown in Figure 4.26. The highly electronegative phosphoryl group serves as a potent hydrogen bond acceptor, forming permanent donor-acceptor bonds with phenol molecules and thus increasing their solubility in the HDES phase. In addition, the hydroxyl group (-OH) of menthol strengthens the hydrogen bonds, thereby reinforcing the structural integrity of the eutectic system and increasing its attraction to phenol. The hydrogen bonds are crucial for the solvation of phenol. They allow the HDES

to preferentially extract the phenol while reducing interference from other less polar or non-hydrogen bonded moieties.

The hydrophobic structure of menthol provides improved stability, ensuring that the HDES remains phase-separated from water and prevents unwanted solvent loss. Furthermore, Lewis acid-base interactions between the phosphoryl group of TOPO and the hydroxyl functional group of phenol introduce an additional dimension of selectivity that makes TOPO:Men HDES very efficient for the extraction of phenol from aqueous solutions. The interplay of robust hydrogen bonding, dipole-dipole interactions and hydrophobic solvation guarantees effective and selective extraction of phenol, which supports the use of these HDES in wastewater treatment.

4.5 Heavy metal removal from wastewater

To the best of our knowledge, this is the first study in which HDES have been used for the removal of some heavy metals such as lead and cadmium from non-buffered water. LLE is a widely used method for the removal of metal ions from water. In comparison to other approaches, extraction has a number of benefits, including the ability to perform the removal process in a continuous manner, the utilization of equipment that is relatively easy to run, and the requirement of just a small quantity of the extractant (Wellens et al., 2012).

Dodecane, toluene, and kerosene are examples of some of the traditional organic water-immiscible solvents that have been the focus of the majority of research into the process of extracting metal salts from aquatic environments (Dietz, 2006). The fact that these solvents are toxic, volatile, and flammable are the primary drawbacks associated with their use. ILs have been put to use in the process of removing metal salts from water (Parmentier et al., 2013). Salts having a melting point lower than 100 °C, which are normally liquid at room temperature, are referred to as ILs (Hallett & Welton, 2011).

These salts are made up of a cation and an anion that interact with each other by electrostatic forces. ILs are a type of designer solvent that, in comparison to traditional solvents, have several benefits, including lower vapor pressures. On the other hand, the extended synthesis and purifying processes required for ILs are one of its primary drawbacks. Because of this, the manufacturing of ILs is quite costly.

DESs, also known as designer solvents, consist of two or more components that are linked through hydrogen bonding and potentially van der Waals interactions (Francisco et al., 2013). The intermolecular attractions that occur between various molecules serve to stabilize the liquid configurations, resulting in a reduction of the mixture's melting temperature in comparison to the melting temperature of the individual components. The initial reported DESs were comprised of amides and ChCl (Abbott et al., 2003). The physicochemical characteristics of DESs can be adjusted by selecting the constituents of the DES based on their chemical ratio and nature, molecular structure, and water content. One significant benefit of DESs in comparison to ILs is their uncomplicated preparation process. The present study centers on the utilization of HDES for the purpose of eliminating metal salts from a water-based milieu, in contrast to the extensive array of hydrophilic DESs that have been previously reported.

This section is further divided into two major parts. One part includes the extraction of lead and cadmium since they are toxic metals even at low concentrations, while second part will deal with the extraction of iron and copper since these two metals are known as essential trace elements.

4.5.1 Extraction of lead and cadmium

Eight HDES were prepared and investigated for the extraction of lead and cadmium from aqueous solutions. The HDES were characterized with respect to their physical and thermal properties. In addition, the effects of various parameters such as contact time, pH,

the mass ratio of water to HDES, and HDES' molar ratio on extraction performance of lead and cadmium were investigated using the best HDES. FTIR spectra were recorded before and after extraction of lead and cadmium to better understand the extraction mechanism. The study investigated the sustainability of HDES through regeneration, multi-stage extraction and reuse and demonstrated the longevity of solvents and the minimal loss of efficiency over multiple cycles. The results represent an important contribution to environmental remediation by presenting a scalable and environmentally friendly approach to tackling heavy metal pollution.

4.5.1.1 Potential of HDES for lead and cadmium extraction

To select suitable HBA and HBD for the intended purpose (heavy metal extraction), natural, biodegradable components were used that can form a liquid DES at room temperature and extract lead or cadmium from an aqueous phase without becoming substantially soluble in it. Various combinations of HBA and HBD were then investigated. The HBA, namely TOPO, thymol and menthol, were selected from a group of components whose ability to form stable hydrophobic DES had already been reported in the literature. The ability of eight HBD and HBA combinations to form a liquid eutectic mixture at room temperature was investigated at a 1:1 molar ratio. The inclusion of terpene-based components leads to lower viscosity, which in turn promotes improved mass transfer. This is a crucial element for successful phase separation and metal recovery. Efficient separation of phases from water is facilitated by the hydrophobic nature of these HDES, especially in combination with hydrocinnamic acid or decanoic acid. This results in less solvent loss and enables better recovery after extraction. This choice reflects the values of green chemistry, which promotes sustainable processes by prioritizing natural sources and components that have less impact on the environment. HDES formulations chosen are expected to exert a strong attraction on lead and cadmium by utilizing the metal complexing capabilities of carboxylic acids such as decanoic acid.

4.5.1.2 Extraction analysis

Eight HDES were prepared and studied for their ability to extract lead and cadmium from water, taking advantage of their hydrophobic properties. Figure 4.27 presents the distribution ratios of all HDES.

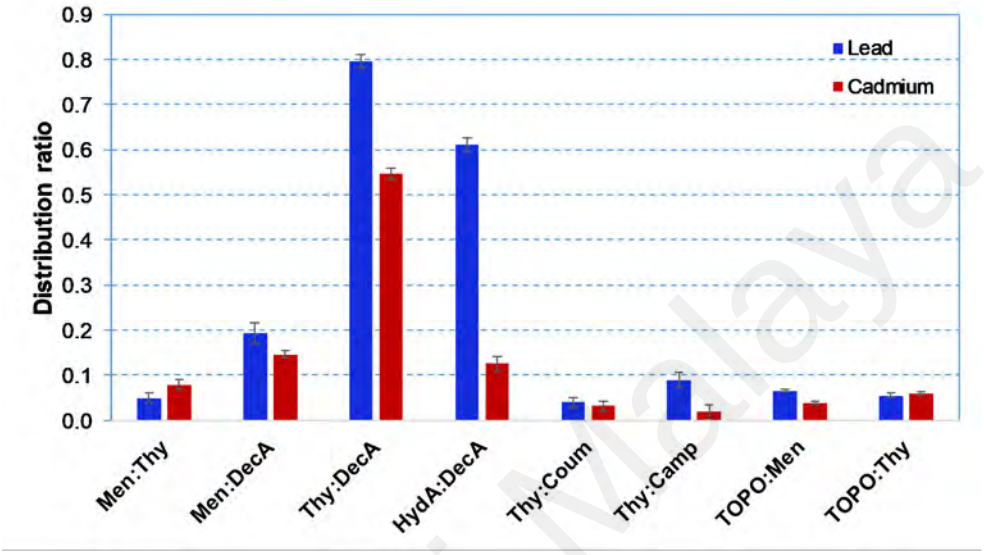

Figure 4.27: Distribution ratio of lead and cadmium by various HDES. Initial concentration of lead is 1000 ppm and 100 ppm of cadmium; vortex mixing, 2000 rpm for 30 min at 298.15 K; centrifugation time, 10 min.

The decision to use initial concentrations of 1000 ppm for lead and 100 ppm for cadmium in the extraction experiments with HDES was motivated by the goal of assessing the efficiency of HDES at higher concentrations. Throughout the study, extractions were carried out at the natural pH of the stock solutions, unless specified otherwise. Figure 4.27 reveals significant variations in the distribution ratio among the different HDES.

The differences in the distribution ratio of lead and cadmium when using different HDES are due to the particular physicochemical interactions between the metal ions and the HDES components. The HDES consisting of Men:DecA (1:1), Thy:DecA (1:1), and HydA:DecA (1:1) exhibited significantly higher D-values for both metals, suggesting increased attraction to these metal ions. The presence of decanoic acid with its long

carbon chain promotes hydrophobic interactions with metal ions, thus supporting their transfer into the HDES phase. The increased D-value for lead in the Thy:DecA combination could be due to the formation of more stable complexes with thymol, which is known for its ability to generate π–π interactions and hydrogen bonding, thus improving the solubility of the metal in HDES. Thymol is a hydrophobic molecule, which means it tends to associate with other non-polar or slightly polar species. In a HDES, the environment around the metal ions can be more favorable for interaction with hydrophobic molecules like thymol compared to more polar or aqueous environments. This enhances the likelihood of complex formation with Pb^{2+} and Cd^{2+}. Extracting Pb^{2+} and Cd^{2+} contaminants from water using eutectic solvents involves overcoming the hydration energy barrier, where metal ions are surrounded by a hydration shell due to their charge. Eutectic solvents, composed of two or more components that form mixtures with lower melting points than their individual parts, effectively disrupt this hydration shell through complexation and partitioning mechanisms. Complexation involves forming complexes between the solvent components and metal ions, reducing their solubility in water. Meanwhile, partitioning drives the metal ions from the aqueous phase into the eutectic solvent phase, influenced by differences in solvation energy and complex formation. This selective extraction can be tailored based on the coordination chemistry of the metal ions and the solvent mixture's composition, enhancing efficiency. Additionally, the lower melting point of eutectic solvents facilitates phase separation, aiding in the recovery of extracted metal ions. Overall, eutectic solvents offer a promising method to efficiently extract Pb^{2+} and Cd^{2+} contaminants from water by effectively overcoming the hydration energy barrier through specialized solvent properties and mechanisms.

On the other hand, systems such as Thy:Camp and Thy:Coum showed lower D values, possibly due to weaker interactions between the metal ions and solvent components. The

chemical structures of camphor and coumarin are less interactive/rigid than that of decanoic acid, which could result in a less effective solvation environment for metal ions. The difference in the distribution ratios of all HDES can be attributed to the different ionic radii of the metals and the physicochemical properties of the HDES. In addition, the higher ionic radii of lead (compared to cadmium) may lead to different extraction efficiencies. This behavior is justified by the existing literature, which shows that the extraction of metals with HDES is significantly influenced by the physicochemical properties of the HDES components and metal ions. The selectivity and solvation ability of HDES are determined by interactions such as π–π interactions, hydrogen bonding, and hydrophobicity.

The TOPO-based HDES were not able to efficiently extract lead and cadmium from water. This can be attributed to the molecular interactions in these systems. TOPO is known for its ability to extract various transition and rare earth metals; however, it was not able to form strong complexes with lead and cadmium as compared to other HDES that were tested in this study. Another possible reason could be the steric hindrance generated by bulky TOPO. While the phosphine oxide in TOPO has the ability to interact with some metal ions, it is not able to coordinate or interact strongly with the lead and cadmium ions.

It is obvious that Thy:DecA showed a higher D-value compared to the other HDES (Figure 4.27). This is possible because thymol contains a hydroxyl (–OH) group, which can serve as a ligand for metal ions in the event of hydrogen dynamics. The lone pairs of electrons on the oxygen atom of the hydroxyl group can coordinate with the metal ions, forming a stable complex. This interaction is particularly strong with metal ions like Pb^{2+} and Cd^{2+} due to their ability to accept electron pairs from donor atoms (such as oxygen). Moreover, the aromatic ring in thymol can also interact with metal ions. The delocalized

π-electrons of the aromatic ring can interact with the metal ions, enhancing the overall binding affinity. This type of interaction is known as π-cation interaction and can contribute to the stability of the metal-thymol complex. The relatively small size and specific structural configuration of thymol allow it to effectively interact with metal ions. This spatial arrangement can facilitate better coordination and binding with Pb^{2+} and Cd^{2+} compared with other larger or more rigid molecules. The electronegativity and polarizability of thymol can create a more favorable interaction environment for Pb^{2+} and Cd^{2+}. The ability of thymol to polarize and accommodate the electron density around the metal ions can enhance the binding strength. Hence, after the initial screening of HDES for extraction of lead and cadmium from water, Thy:DecA was selected for further optimization to improve the extraction efficiency for lead and cadmium. Various parameters including contact time, water to HDES mass ratio, and HDES molar ratio were investigated for the efficient extraction of lead and cadmium using the Thy:DecA system. This study also investigated the effect of pH on the speciation of metal ions. An evaluation of multi-stage extraction was performed to improve the extraction efficiency, while regeneration of HDES was investigated to determine the solvent reusability and economic feasibility of the process. With this optimized technique, the extraction process for lead and cadmium should be improved to increase the efficiency, sustainability and practical use of HDES in the remediation of heavy metals. The study also investigated the effect of the initial concentration and recognized its critical role in influencing the extraction efficiency and understanding the performance of the HDES system under different loading conditions.

4.5.1.3 Effect of water to HDES mass ratio

The mass ratio of water to HDES had a considerable influence on the extraction of lead and cadmium, as shown by the variations in the distribution ratios (Figure 4.28). Increasing the amount of HDES from 1:1 to 1:4 improves the extraction efficiency for

both metals, possibly due to the increased number of complexation sites and a stronger hydrophobic driving force.

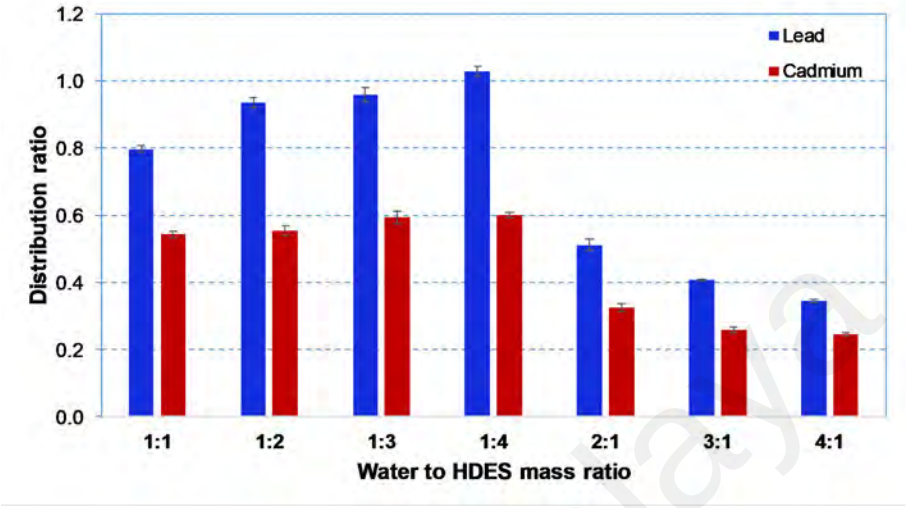

Figure 4.28: Effect of water to HDES mass ratio on the extraction of lead and cadmium. Initial concentration, lead = 1000 ppm and cadmium = 100 ppm; Thy:DecA (1:1) HDES; vortex mixing, 2000 rpm for 30 min at 298.15 K; centrifugation time, 10 min.

The distribution coefficient for lead increases from 0.79 at a ratio of 1:1 to 1.02 at a ratio of 1:4, which represents a considerable improvement in extraction efficiency. The increase in the distribution coefficient for cadmium from 0.54 to 0.59 at the same ratios indicates that the extraction of cadmium is also improved by a greater proportion of HDES. The increase in the distribution ratio is due to the improved ability of HDES to dissolve metals and the stronger interactions between the metals and HDES components when the amount of HDES is higher.

The highest extraction efficiency was achieved at a mass ratio of 1:4 between water and the HDES. However, this means that a larger amount of HDES is required than water. This raises the question of whether the use of a significant amount of HDES is feasible and financially viable, particularly in large-scale applications or scenarios where resource efficiency is critical. The use of a large amount of HDES can lead to higher operating costs and difficulties in regenerating and recovering the HDES. On the other hand,

choosing a 1:1 mass ratio (water to HDES) for the extraction of both metals makes a balance between increased efficiency and economy. Even with a 1:1 mass ratio, better extraction efficiency was achieved while minimizing concerns regarding the over-utilization of HDES. This choice considers both the immediate extraction results and wider impact of solvent consumption on the overall effectiveness and sustainability of the remediation strategy.

4.5.1.4 Effect of contact time

The extraction kinetics were investigated in terms of contact time. The effect of the contact time on the extraction performance of lead and cadmium using Thy:DecA (1:1) HDES in terms of the distribution ratio is shown in Figure 4.29. The results showed that the maximum extraction was achieved after about 15-20 min for lead and increased more slowly for cadmium, with less noticeable effects after 15 min.

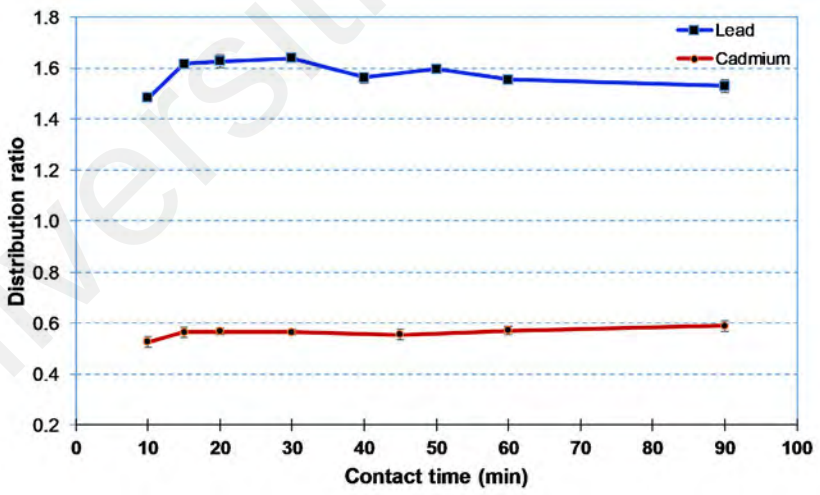

Figure 4.29: Effect of contact time on the extraction of lead and cadmium. Initial concentration, lead = 1000 ppm and cadmium = 100 ppm; Thy:DecA (1:1) HDES; vortex mixing, 2000 rpm at 298.15 K; centrifugation time, 10 min.

An increase in the distribution ratio of lead from 1.48 to 1.62 from 10 to 15 min indicate a rapid extraction process. This is followed by a plateau effect where the distribution ratio remains constant after 15 min, demonstrating that equilibrium is

achieved. After 30 min, the slight decline in the D value could be due to the redistribution of lead ions back into the water phase or saturation of the organic phase (HDES). For cadmium, the increase in D values was negligible after 15 min, indicating that equilibrium was reached. A 15-minute contact period for both metals was chosen based on the trade-off between operational feasibility and extraction efficiency. Studies have shown that extraction efficiency can increase rapidly before reaching a plateau, which is consistent with the trends reported in a previous study (Martins et al., 2019).

4.5.1.5 Effect of molar ratio

Figure 4.30 shows the effect of molar ratio of Thy:DecA HDES on the extraction of lead and cadmium in terms of distribution ratio. The extraction performance of Thy:DecA was increased with the increasing concentration of decanoic acid in the HDES.

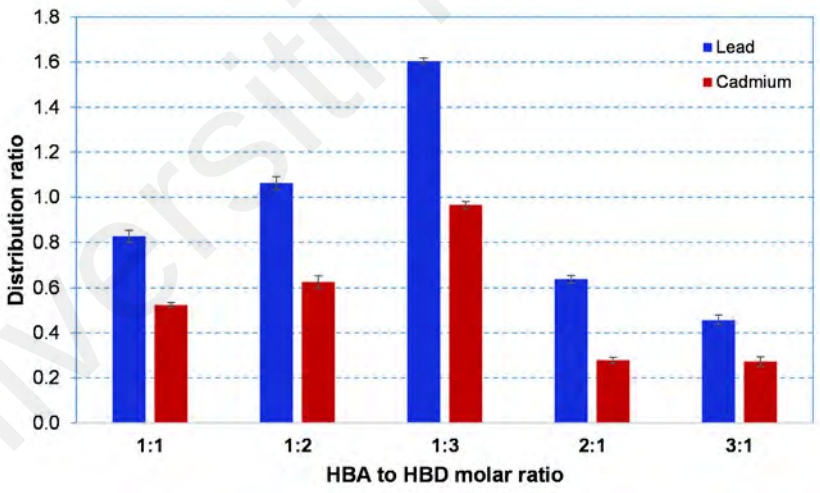

Figure 4.30: Effect of HDES' molar ratio on the extraction of lead and cadmium. Initial concentration, lead = 1000 ppm and cadmium = 100 ppm; vortex mixing, 2000 rpm for 15 mins at 298.15 K; centrifugation time, 10 min.

The maximum D-values for lead (1.6) and cadmium (0.96) were obtained at a 1:3 Thy:DecA molar ratio. This could be due to the increased solvation capacity of decanoic acid at higher concentrations which resulted in the improved interaction between the metals and Thy:DecA. Furthermore, the presence of carboxyl groups and hydrophobic

nature of decanoic acid also play an important role in in the increased extraction efficiency of HDES. This behavior is coherent with the literature that signify the importance of solvent concentration in the formation of complexes with metals (Morais et al., 2020). The lower distribution ratios for lead and cadmium were obtained at 2:1 and 3:1 Thy:DecA molar ratios. Therefore, after adjusting the composition of HDES, 1:3 Thy:DecA was selected to further improve the extraction of metal from aqueous solution.

4.5.1.6 Effect of pH

The effect of pH on the distribution ratio of lead and cadmium is shown in Figure 4.31. At pH 5 and 6, the best extraction performance was obtained using Thy:DecA for lead and cadmium, respectively. The ideal pH values largely correspond to the natural pH conditions for the extraction processes, which are 5.29 for lead and 6.20 for cadmium. At pH 3 and 4, the extraction efficiency for both metals decreased because of the increased competition between protons and metal ions for the binding sites in the DES as well as the protonation of the functional groups in thymol and decanoic acid. The ability of DES to efficiently complex and solvate metal ions can be impaired by this competition. Increased acidity can promote the formation of metal species that are less easily extracted by DES.

When the pH reaches ideal values (5 for lead and 6 for cadmium), the conditions become more favorable for the extraction of metal ions. This improvement is due to less proton competition, improved deprotonation of the acidic groups in the DES, and the abundance of metal ion species that are easier to extract. These ideal pH values most likely correspond to the natural speciation patterns of lead and cadmium in aqueous solutions, where the metal ion forms interacting with the DES clearly predominate. The extraction efficiency began to decrease at pH values above the optimal range, particularly at pH 7. This decrease could be due to the formation of hydroxide complexes with the

metal ions, which have lower solubility in the DES phase, or an increase in the competition of hydroxide ions for the metal ions, reducing their transfer to the DES phase.

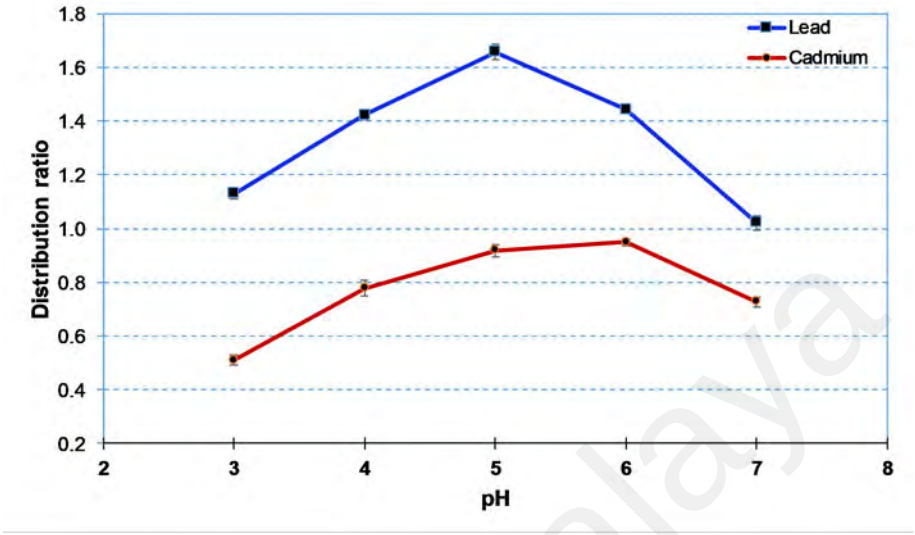

Figure 4.31: Effect of pH on the extraction of lead and cadmium. Initial concentration, lead = 1000 ppm and cadmium = 100 ppm; Thy:DecA (1:3) HDES; vortex mixing, 2000 rpm for 15 mins at 298.15 K; centrifugation time, 10 min.

The presence of other divalent contaminants in water poses significant challenges for the extraction of Pb^{2+} and Cd^{2+} using eutectic solvents, primarily due to competition for binding sites and varying chemical affinities. Similar ions such as Zn^{2+}, Cu^{2+}, and Ni^{2+} can compete with Pb^{2+} and Cd^{2+} for complexation or partitioning into the eutectic solvent phase, forming complexes with solvent components or sharing similar solvation energies, thereby reducing extraction selectivity and efficiency. Additionally, the chemical properties of contaminants like Fe^{2+} or Mn^{2+} can undergo oxidation or reduction reactions, altering their extraction behavior compared to Pb^{2+} and Cd^{2+}. Moreover, fluctuations in water pH influence the speciation of these ions, potentially affecting their interaction with eutectic solvent components. Adjusting pH levels becomes crucial to optimize Pb^{2+} and Cd^{2+} extraction efficiency while minimizing interference from other contaminants. To effectively address these challenges in practical applications, strategies such as solvent optimization and screening are essential for maximizing the efficacy of

eutectic solvents in selectively removing Pb^{2+} and Cd^{2+} from water contaminated with diverse divalent ions.

4.5.1.7 Effect of initial concentration

There is a noticeable pattern in the data regarding the effect of initial concentration on the efficiency of extraction of lead and cadmium with Thy:DecA HDES (Figure 4.32). As the initial concentration of the two metals increases, the extraction efficiency decreases. The efficiency of lead reduced to 61.78% (at 1000 ppm) from 93.46% (at 100 ppm) while for cadmium, the efficiency was dropped to 49.20% (at 100 ppm) from 91.21% (at 10 ppm). There is a possibility of more efficient solvation of individual ions at lower concentrations of metals due to higher ratio of HDES constituents to metal ions. At higher metal concentrations, there may not be enough HDES molecules to interact with the metals, resulting in a reduction of removal efficiency. This behavior is in-line with the principles of solubility and complexation theory, which confirms that the ability of any solvent to interact or dissolve solutes is limited and is affected by the properties of both the solute and the solvent.

With increasing metal concentrations, the decrease in efficiency could be attributed to the reduced interactions between the components of HDES and metal ions. These results are consistent with research results on metal extraction using different solvents, such as HDES and IL (Liu et al., 2021; Schaeffer et al., 2018). Although the dynamics and interactions in HDES systems may be different, the basic principles that determine how the initial concentration affects extraction efficiency are generally applicable to different solvent systems. It is important to optimize the amount of HDES used in relation to the metal ion concentration to achieve efficient extraction, especially in applications with high metal contamination.

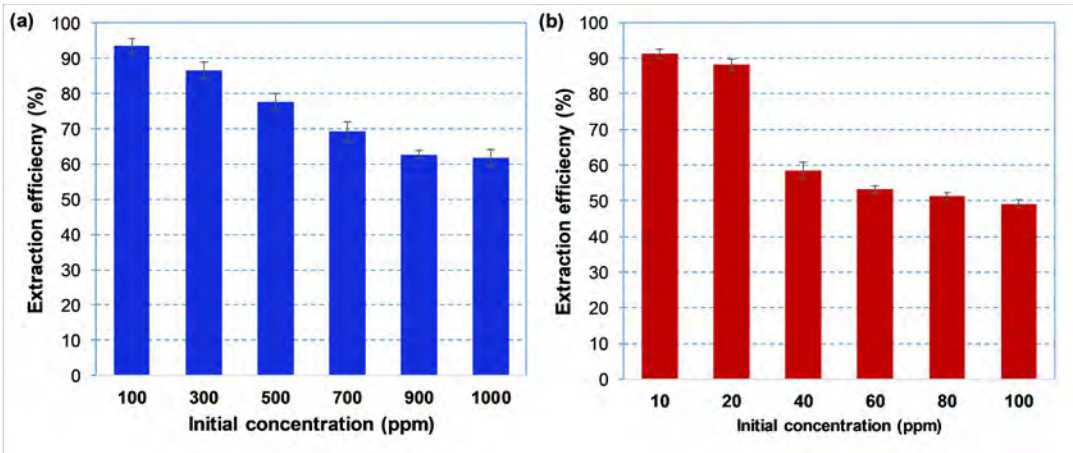

Figure 4.32: Effect of initial concentration of (a) lead and (b) cadmium on the extraction efficiency. Thy:DecA (1:3) HDES; vortex mixing, 2000 rpm for 15 mins at 298.15 K; centrifugation time, 10 min.

4.5.1.8 Reuse of HDES

Thy:DecA was reused for five consecutive stages to investigate the effects of reusability on the extraction process to remove lead and cadmium. After 5 stages, the D-values of both metals were reduced (from 1.66 to 1.04 for lead and from 0.99 to 0.64 for cadmium), as shown in Figure 4.33. This shows that the efficiency of the selected HDES decreased after each cycle in recovering these heavy metal contaminants. The ability of the HDES to efficiently dissolve additional metal ions may be reduced by the accumulation of these ions in the solvents during repeated cycles, leading to saturation.

The components of HDES may partially deteriorate or change after repeated interaction with water and metal ions, reducing their ability to dissolve metals and consequently their effectiveness in extracting metals. This is particularly important for systems containing organic acids and substances that may be hydrolyzed or oxidized, including decanoic acid and thymol. Even after 5-stages, Thy:DecA was still able to extract significant amounts of lead and cadmium from aqueous media. For cadmium, the D value was reduced from 0.99 to 0.64 while for lead it was reduced to 1.04 from 1.66 after 5 stages using Thy:DecA system. Clearly, there is a substantial drop in the extraction

efficiency of both metals, however, Thy:DecA was still able to exhibit D value of greater than 1 for lead and significant value for cadmium in the 5th stage. This indicates that the selected solvent is still efficient in removing these metals from water.

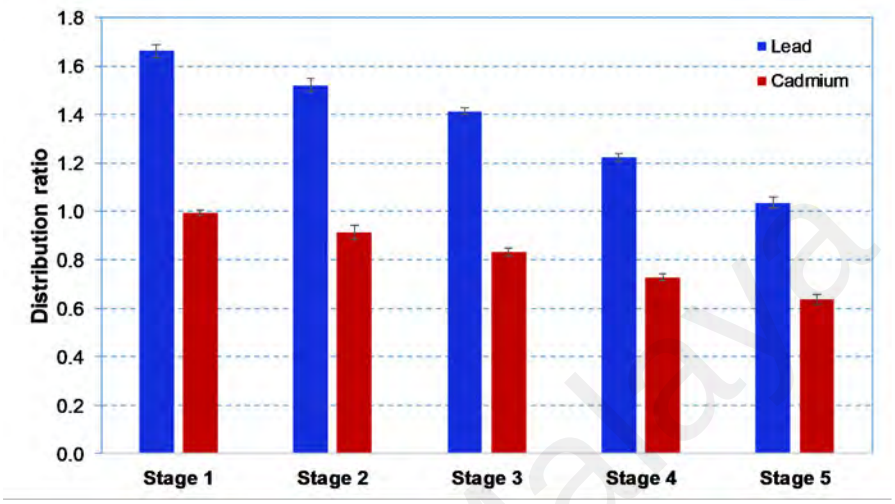

Figure 4.33: HDES reuse over 5 stages. Initial concentration, lead = 1000 ppm and cadmium = 100 ppm; Thy:DecA (1:3) HDES; vortex mixing, 2000 rpm for 15 mins at 298.15 K; centrifugation time, 10 min.

4.5.1.9 Multistage extraction

The study of extraction of lead and cadmium at high concentrations using a multistage extraction process with Thy:DecA aimed to evaluate the effectiveness of DES in removing these metals from highly contaminated water (Figure 4.34).

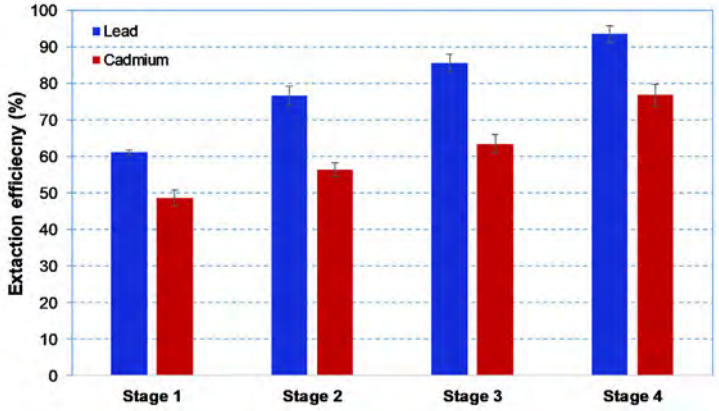

Figure 4.34: Multistage extraction of lead and cadmium. Initial concentration, lead = 1000 ppm and cadmium = 100 ppm; Thy:DecA (1:3) HDES; vortex mixing, 2000 rpm for 15 mins at 298.15 K; centrifugation time, 10 min.

The results show a remarkable improvement in extraction efficiency for lead, reaching almost maximum efficiency after four stages, in contrast to the lower efficiency observed for cadmium. This highlights the particular behavior of DES towards these metals in high concentration scenarios.

After 4 stages, the extraction efficiency of lead was reached to 93.49%. This could be due to the larger ionic radius of lead in comparison to cadmium, resulting in a more stable complexes with the Thy:DecA. On the other hand, the extraction efficiency of cadmium was lower (76.70%) after 4 stages. This suggests weak interactions of cadmium ions with the Thy:DecA as compared to lead. It is crucial to consider the chemical properties and behavior of both the target metals and the extracting solvent, as shown by the different extraction efficiencies between lead and cadmium at high concentrations. Although DES has the potential to effectively remove heavy metals, in this case primarily lead, from polluted water, the results suggest that refinement of DES composition, extraction conditions and possibly the development of metal-specific DES formulations may be required to achieve comparable efficacy for other metals such as cadmium.

4.5.1.10 Regeneration of HDES

Two potential aqueous stripping solutions including NaOH (an alkaline solution) and HCl (an acidic solution) were used to investigate the stripping efficiency of metals in the HDES phase. With NaOH, precipitation occurred, possibly due to the saponification reaction between decanoic acid and NaOH, resulting in the formation of sodium decanoate and water. This highlights unfavorable changes in the physical properties of HDES constituents and their ability to remove metals due to their reaction with strong bases.

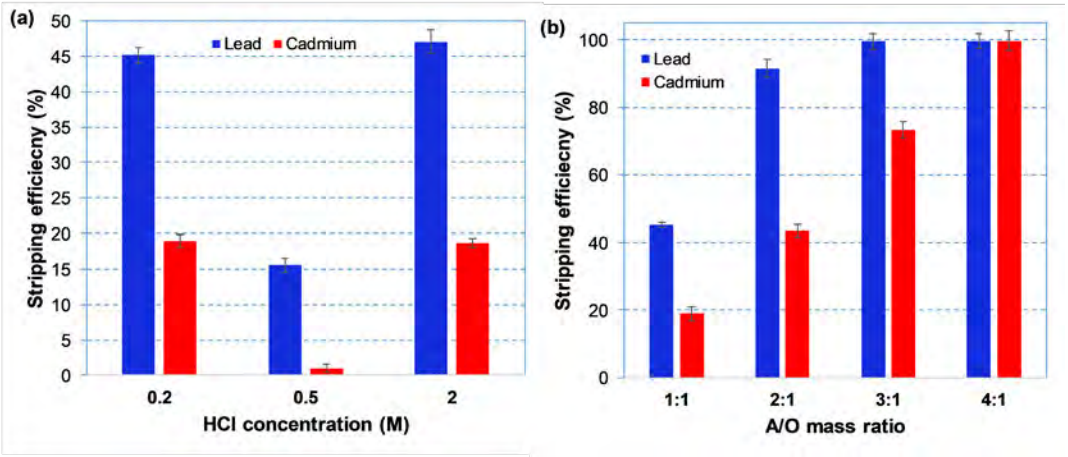

Figure 4.35: (a) Stripping efficiency using HCl as stripping agent at various concentrations, (b) effect of aqueous HCl to HDES (A/O) mass ratio on stripping efficiency. HCl concentration = 0.2 M; Initial concentration, lead = 1000 ppm and cadmium = 100 ppm; Thy:DecA (1:3) HDES.

To perform stripping, HCl was mixed with HDES phase at different concentrations at 500 rpm for 6 hours followed by a settling time of 24 hours. Figure 4.35 (a) shows the effect of HCl concentration on the effectiveness of lead and cadmium stripping. It was observed that almost comparable results were obtained for 0.2 M and 2 M HCl concentrations, however, 0.5 M HCl concentrations exhibited significantly lower performance. This indicates a non-linear correlation between the concentration of HCl and stripping efficiency. This could be due to the changes in the acidity of the solution affecting the solubility of metals. Figure 4.35 (b) shows the effect of HCl to HDES (A/O) mass ratio on the stripping efficiency. At higher A/O ratios (3:1 for lead, and 4:1 for cadmium), almost complete recovery of both metals was achieved.

4.5.2 Extraction of iron and copper

Terpene-based HDES were investigated for the extraction of iron and copper from aqueous environments. This work presents an environmentally friendly and efficient technique for the extraction of iron and copper ions by using HDES formed by mixing terpenes and carboxylic acids. Five HDES were experimentally investigated for their efficiency in extracting iron and copper from aqueous environments. The effects of

experimental parameters such as mixing time, mass ratio of organic to aqueous phase, molar ratio of HDES, pH and the initial metal concentration in the water phase on the extraction behavior of ions and copper were investigated. FTIR spectra were recorded before and after extraction of iron and copper from water. In addition, the sustainability of DES through reuse and regeneration was also investigated. DES was reused for five consecutive stages of metal extraction. The stripping efficiency of iron extraction was also investigated with HNO_3.

4.5.2.1 Prospective of using HDES

Natural, biodegradable components were used to form liquid HDES at room temperature that extract iron or copper from an aqueous phase without substantially dissolving in it. Subsequently, several combinations of HBA and HBD were investigated. Terpenes known for their ability to form stable hydrophobic DES were selected based on previous literature. An investigation was conducted to determine the capacity of five combinations of HBD and HBA to prepare a liquid eutectic mixture at 25 ºC in a 1:1 molar ratio. The addition of terpene-based components such as menthol and thymol reduce viscosity, which leads to improved mass transfer. The hydrophobic properties of these DES, especially in combination with carboxylic acid, help to effectively separate the phases from the water. This decision is in line with the principles of green chemistry, which advocates sustainable practices by components with low environmental impact.

4.5.2.2 Selection of HDES

The choice of solvent plays an important role in the extraction of pollutants from water medium. For the extraction of iron and copper, five HDES were experimentally tested for their extraction efficiency. In this study, the pH of the stock solutions was not adjusted unless otherwise stated. The natural pH of the stock solutions of iron (1000 ppm) and

copper (100 ppm) were 2.478 and 5.77, respectively. Figure 4.36 shows the performance comparison of five HDES for the extraction of iron and copper from water.

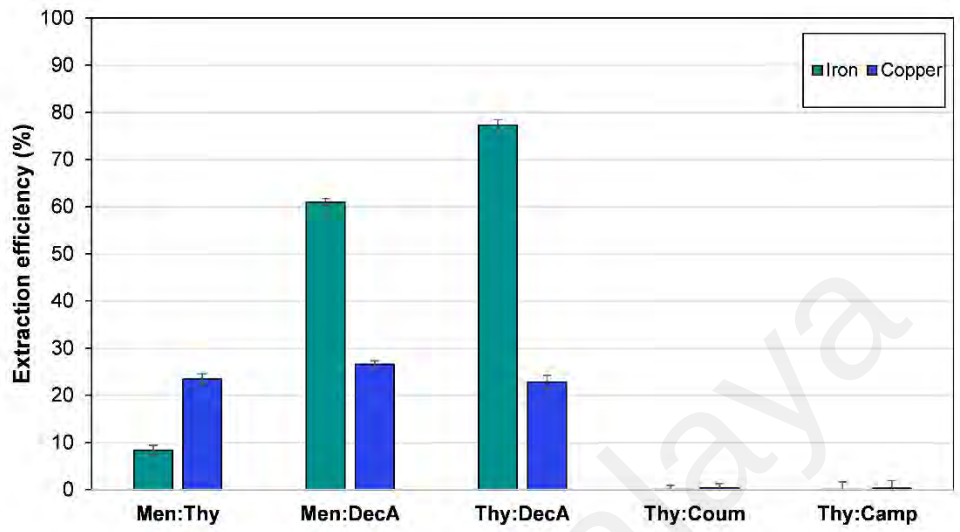

Figure 4.36: Extraction performance of five HDES for the removal of copper and iron. Initial concentration, iron = 1000 ppm, copper = 100 ppm; vortex mixing at 2000 rpm for 30 min; centrifuge for 10 min.

Men:Thy exhibited low extraction efficiency for both metals, probably due to weak interactions between the solvent and the metal ions. Thy:DecA showed the highest extraction efficiency (77.2 %) for iron. This is an indication of the formation of a stable complex between the decanoic acid of Thy:DecA and iron.

Due to the carboxylate coordination and the longer aliphatic chain of decanoic acid, it improves solvation. On the other hand, thymol as a phenolic component can further stabilize the iron complex due to additional hydrogen bonding or π-π interactions. In addition, the solubility of metals in solvents also plays an important role. Decanoic acid can act as a ligand, and it is known that iron forms more stable complexes with ligands. This could explain the lower extraction efficiency of copper compared to iron. No HDES was able to significantly remove copper from water. Among the HDES tested, Men:DecA showed the highest extraction efficiency (26.5 %) for the extraction of copper from water. Thy:Coum and Thy:Camp were not able to extract iron and copper from water, which

could be due to the weaker interactions of camphor and coumarin with metal ions. The extraction efficiency of iron with decanoic acid based HDES was higher compared to copper. This could be due to the shape and smaller radii of copper, which was unable to form a strong complex with the long chain decanoic acid. On the other hand, ions with higher coordination numbers and larger ionic radii were able to form more stable complexes with the decanoic acid based HDES.

4.5.2.3 Effect of mixing time

In order to determine the optimum contact time for the extraction of iron and copper from an aqueous medium, the extraction efficiency of the two metals was investigated as a function of the equilibrium time (Figure 4.37). The effect of mixing time was investigated for the extraction of iron and copper with Thy:DecA and Men:DecA, respectively.

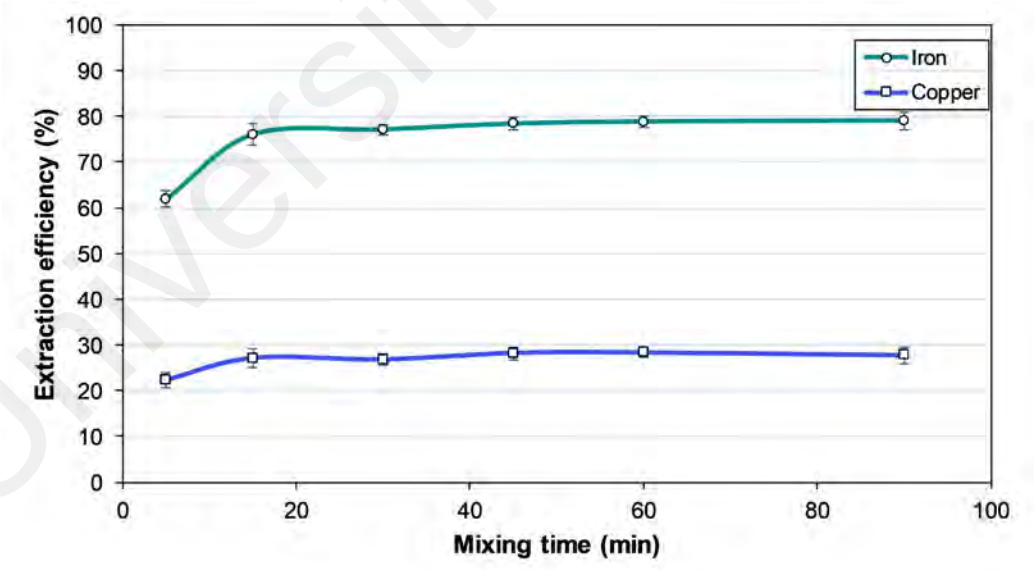

Figure 4.37: Effect of mixing time on the extraction efficiency of iron and copper. Initial concentration, iron = 1000 ppm, copper = 100 ppm; vortex mixing at 2000 rpm; centrifuge for 10 min.

Figure 4.37 shows the effect of mixing time on the extraction efficiency of iron and copper. It can be seen from the figure that the extraction efficiency of the metals increased

rapidly up to 15 minutes. For example, the extraction efficiency of iron increased from 61.95% to 75.94% when the time was increased from 5 to 15 minutes. Equilibrium was reached within 15 minutes and the percentage of extraction of both metals did not change significantly. Therefore, the 15-minute time period was chosen for subsequent studies on the extraction of both metals.

4.5.2.4 Effect of O/A mass ratio

From an industrial point of view, it is important to use less solvent in the LLE process in order to reduce costs and environmental concerns. One way to achieve this goal is to optimize the O/A mass ratio. The effects of the O/A mass ratio in the range of 2:1 to 1:5 was investigated. Figure 4.38 shows the effect of the O/A mass ratio on the extraction of iron and copper.

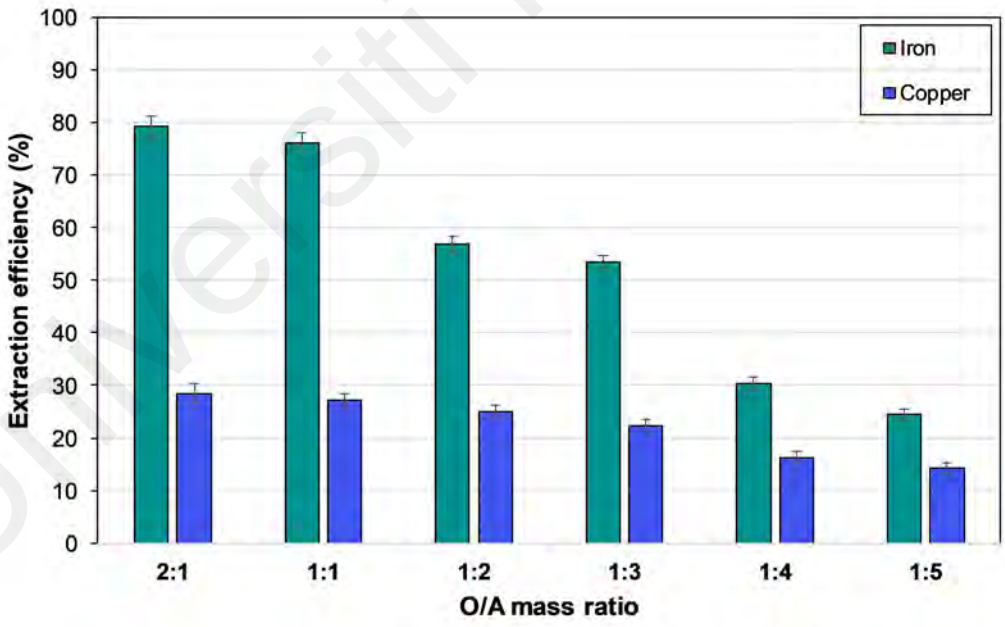

Figure 4.38: Effect of O/A mass ratio on the extraction efficiency of iron and copper. Initial concentration, iron = 1000 ppm, copper = 100 ppm; vortex mixing at 2000 rpm for 15 min; centrifuge for 10 min.

The O/A mass ratio has a significant effect on the extraction of iron and copper. With increasing amount of HDES, the extraction efficiency was increased. The increase in

extraction efficiency could be due to the improved ability of the HDES to dissolve metals and stable interactions between the HDES and the metal ions at higher concentrations of HDES. The extraction efficiency decreased from 79.17% to 24.54% when the O/A mass ratio was changed from 2:1 to 1:5. The highest extraction efficiency was achieved at an O/A mass ratio of 2:1, however, indicating that a higher HDES concentration is required, which is not practical for industrial applications. At a mass ratio of 1:1, the change in extraction efficiency was small. For example, the extraction efficiency of iron with Thy:DecA decreased from 79.17% to 75.97%, while the extraction efficiency of copper with Men:DecA decreased from 28.49% to 27.29%. Therefore, an O/A mass ratio of 1:1 was selected for the extraction of both metals.

4.5.2.5 Effect of molar ratio of HDES

A higher extraction efficiency has already been achieved in the extraction of iron from water at a molar ratio of 1:1 of HDES. Therefore, in this section, the effect of molar ratio for the extraction of copper from water with Men:DecA was investigated.

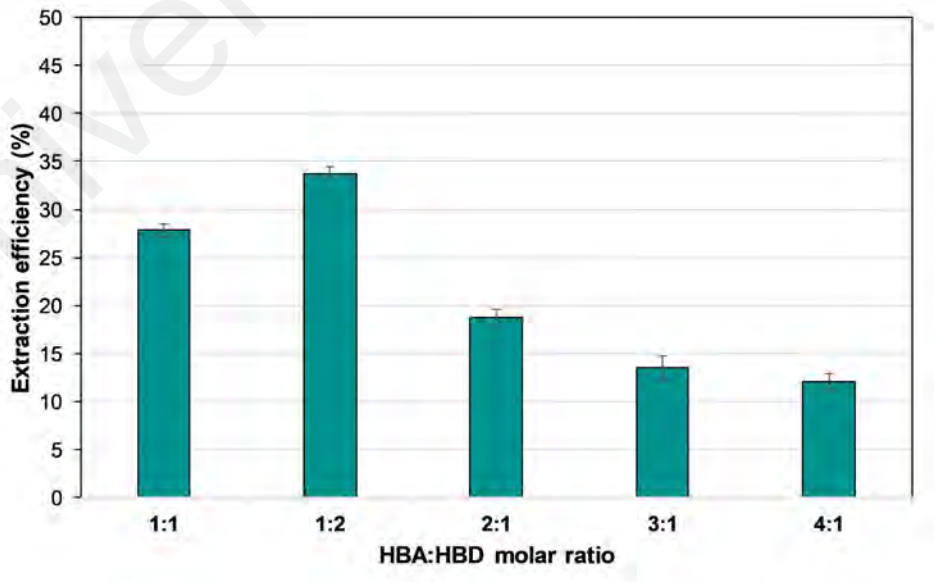

Figure 4.39: Effect of molar ratio of Men:DecA on the extraction efficiency of copper. Initial concentration, copper = 100 ppm; vortex mixing at 2000 rpm for 15 min; centrifuge for 10 min.

Various researchers have reported that the physicochemical properties of HDES are affected by the molar ratio of HBA to HBD of HDES (Florindo et al., 2020; Zhang et al., 2012). Therefore, the influence of the molar ratio of HDES on the extraction efficiency of copper from water was investigated. Figure 4.39 illustrates the influence of HDES molar ratio on the extraction efficiency of copper from water.

The highest extraction efficiency was obtained at a HDES molar ratio of 1:2 between HBA and HBD. This could be due to the increased amount of decanoic acid, which can form more stable complexes with the copper. However, this efficiency is still low and at all molar ratios the extraction efficiency is significantly lower compared to iron. The extraction efficiency further decreased when the amount of menthol was increased at 2:1 and 3:1 molar ratio between HBA and HBD. A possible reason for this could be the functional group of the alcohol and the heavier structure, which may not be efficient in solvating copper ions. Therefore, after adjusting the molar ratio of HDES, a ratio of 1:2 HBA to HBD was chosen to further improve the extraction of copper from an aqueous medium.

4.5.2.6 Effect of pH

The effect of pH on the extraction of iron and copper from an aqueous solution is shown in figure 4.40. The effect of pH on the extraction of iron was investigated in a range of 1 to 2.5. At a higher pH value (above 2.5), precipitation occurred. For copper, the pH ranged from 1 to 6. At pH of 2 and 6, the highest extraction efficiencies were achieved for iron and copper, respectively. In acidic solutions, iron is normally present as Fe^{3+}. At a pH of 2, it forms more stable complexes with HDES because the carboxyl group in the decanoic acid is more strongly protonated, which improves its ability to coordinate with iron ions. In acidic solutions, the iron is normally present as Fe^{3+}. At a pH of 2, it forms more stable complexes with the HDES, as the carboxyl group of the

decanoic acid is more strongly protonated, which improves its ability to coordinate with iron ions. Considering the pH, the small improvement in extraction efficiency from 76.08% to 79.80% indicates that the HDES is already very effective at the natural pH of the iron solution of 2.47. On the other hand, the copper extraction efficiency increases to 37% at pH 6, compared to 33.77% at the natural pH of 5.77, suggesting that a slightly less acidic environment enhances the solubility of the copper-decanoic acid complex, possibly due to less competition for binding sites on the HDES from excess hydrogen ions and improved charge distribution on the copper ion. Both metals show trends indicating that the protonation states of the HDES components and the charge properties of the metal ions are critical to the extraction process. The optimal pH values correspond to the stability and solubility of the resulting metal-HDES complexes.

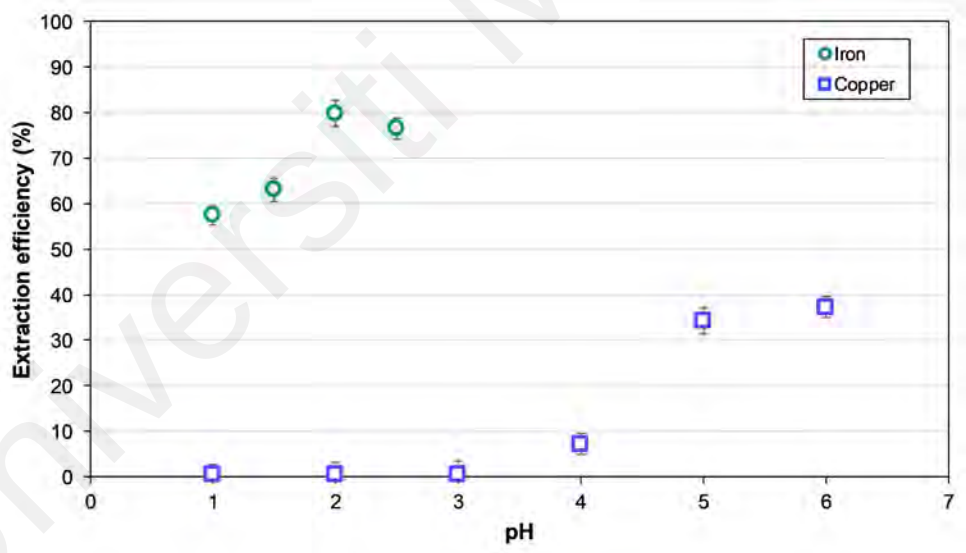

Figure 4.40: Effect of pH on the extraction efficiency of iron and copper. Initial concentration, iron = 1000 ppm, copper = 100 ppm; vortex mixing at 2000 rpm for 15 min; centrifuge for 10 min.

4.5.2.7 Effect of initial concentration of metals

Figure 4.41 shows the influence of the initial concentration of the metals on the extraction efficiency. The study shows that the extraction efficiency of both metals

depends on the type of DES and the initial concentration of the metals in the water medium.

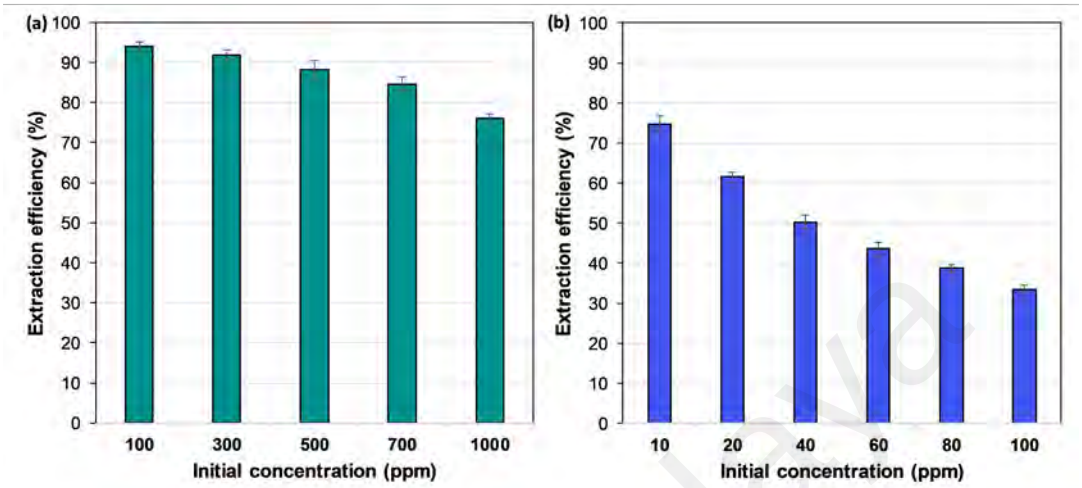

Figure 4.41: Effect of initial concentration of (a) iron and (b) copper on the extraction efficiency. vortex mixing, 2000 rpm for 15 mins at 298.15 K; centrifuge for10 min.

The extraction efficiency increases with the decrease of the initial concentration of both metals. The extraction efficiency of iron increases from 75.97% (at 1000 ppm) to 93.91% (at 100 ppm), while for copper it increased from 33.42% (at 100 ppm) to 74.69% (at 10 ppm). This indicates that solvation of metals could be more efficient at low concentrations due to the higher proportion of HDES components compared to metals. On the other hand, at higher concentrations of metals, there may not be enough HDES molecules to interact with the metal ions, resulting in lower extraction efficiency.

4.5.2.8 Reuse and regeneration of the HDES

In a separation process, it is crucial to minimize the use of solvents from both an economic and a sustainability perspective. The reuse of HDES for 5 consecutive cycles of extraction of metals from the water medium was investigated as shown in Figure 4.42.

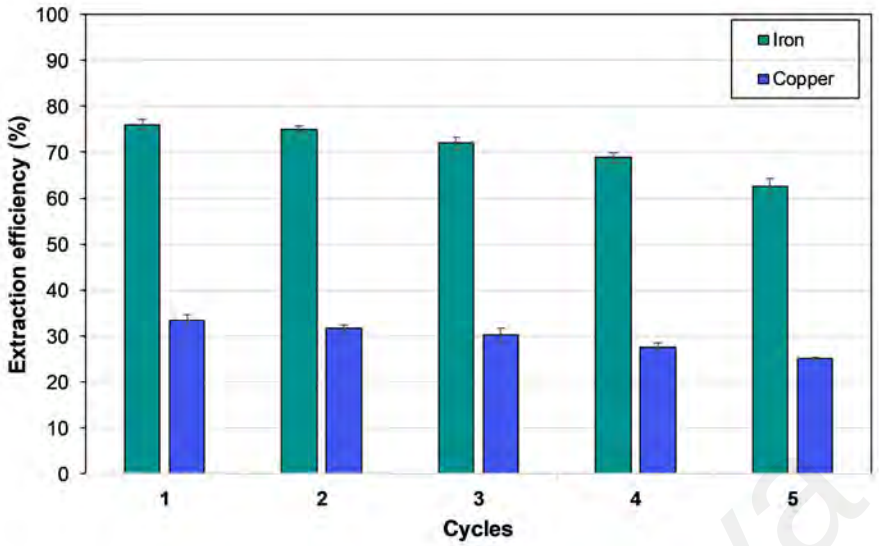

Figure 4.42: HDES reuse over 5 cycles. Initial concentration, iron = 1000 ppm, copper = 100 ppm; vortex mixing at 2000 rpm for 15 min; centrifuge for 10 min.

The HDES phase was collected after complete phase separation and then remixed with the metal-containing stock solution. The HDES showed consistent efficiency in removing both metals from the aqueous solution over four cycles. It was observed that it was not until the fifth cycle that the HDES extraction capacity began to gradually decrease, indicating that the HDES was approaching saturation. For example, after the fifth cycle, the extraction capacity of iron decreased from 76.08% to 62.64%.

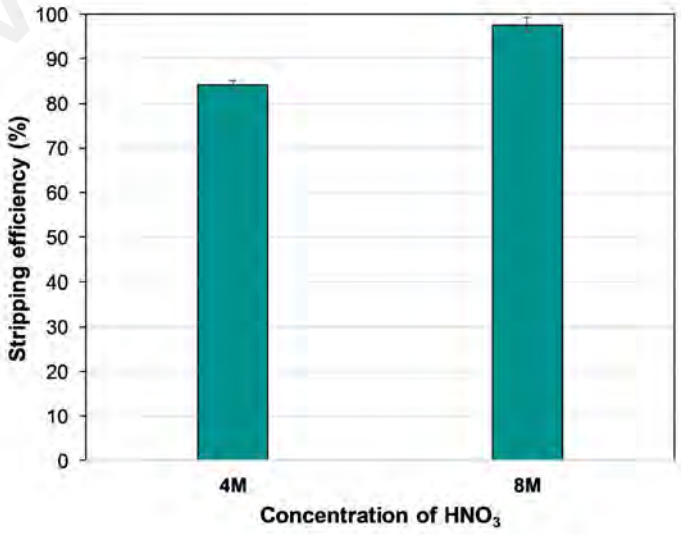

Figure 4.43: Stripping efficiency using HNO_3 as stripping agent at various concentrations.

With Thy:DecA, a high extraction efficiency of iron was achieved, even at high concentrations. Therefore, the stripping efficiency of iron was also investigated using an aqueous solution of HNO_3. To perform stripping, HNO_3 was mixed with HDES at different concentrations at 300 rpm for 8 hours, followed by a settling period of one day. Precipitation took place with 2M HNO_3 solution. Figure 4.43 shows the effect of HNO_3 concentration on the efficiency of iron stripping. Stripping efficiencies of 84.06% and 97.66% were achieved with 4M and 8M HNO_3 solution, respectively, when mixed with the DES phase at a mass ratio of 1:4 HDES to aqueous phase.

4.5.3 Understanding the extraction mechanism

Regarding the mechanism of extraction of metals, carboxylic acid forms coordination complexes with the metal ions by acting as a ligand. The decanoic acid in the HDES has several binding sites for metals so that they can form coordination complexes. In the organic phase, these metal complexes have greater stability. The formation of metal complexes leads to the sequestration of metal ions from the water phase into the organic phase. Another factor that influences the transfer of metal ions from the aqueous to the organic phase is the different affinity between the HDES under investigation and water. In addition, the hydrophobic property of HDES further enhances the extraction of metal ions. This process prevents the mixing of water with the solvent and thus creates a favorable condition for the extraction of metal ions. Ensuring this property is crucial for optimizing the extraction process by maintaining the preferential binding of metal ions to carboxylic acids in HDES (Majidi & Bakhshi, 2024). Thy:DecA HDES offers a unique approach for extracting heavy metals from aqueous solutions. This DES consisted of thymol, a naturally occurring compound with phenolic properties, and decanoic acid, a medium-chain fatty acid. A graphical illustration of the extraction mechanism is shown in Figure 4.44. The mechanism of heavy metals extraction using Thy:DecA HDES involves at least five interrelated steps:

(i) **Complexation and Partitioning**: For instance, the Thy:DecA DES operates by forming complexes with metal ions present in water. The phenolic hydroxyl group of thymol and carboxylic group of decanoic acid can coordinate with metal ions through ligand exchange reactions, where water molecules in the hydration shell surrounding the metal ions are replaced. This complexation process is driven by the affinity of the HDES components for the metal ions, which disrupts the equilibrium of metal ion solvation in water.

(ii) **Hydrophobic Interaction**: The hydrophobic nature of the Thy:DecA HDES plays a crucial role in the extraction mechanism. Decanoic acid, being hydrophobic, forms a non-polar environment within the HDES mixture. This environment enhances the solvation of the metal complexes due to the shielding effect from water molecules, which preferentially interact with each other rather than with the hydrophobic interior of the HDES. This hydrophobic interaction aids the extraction of lead and cadmium from the aqueous phase into the DES phase.

(iii) **Phase Separation**: After complexation, the metal-loaded Thy:DecA DES formed a distinct phase separate from the aqueous phase. This phase separation can be facilitated by differences in density or solubility between the HDES and aqueous phases. The ability to separate these phases allows for easy recovery of the metal-laden Thy:DecA DES for subsequent processing or regeneration.

(iv) **Regeneration and Recycling**: One of the advantages of the Thy:DecA DES is its potential for regeneration and recycling. Once saturated with metal ions, the DES can undergo regeneration processes such as pH adjustment or solvent extraction to release the bound metal ions. For example, adjusting the pH of the HDES-water mixture can disrupt metal-carboxyl bonds, allowing for the

desorption of metal ions back into the aqueous phase. Alternatively, competitive ligands or thermal treatments can facilitate metal ion release, enabling the HDES to be reused multiple times without significant loss of extraction efficiency.

(v) **Selectivity and Efficiency**: Thy:DecA HDES exhibits selectivity towards metal ions due to the specific interaction between their hydrated forms and the DES components. This selectivity can be further enhanced by optimizing the composition of the DES mixture and adjusting operational parameters such as pH and temperature. High extraction efficiency is achievable through these tailored conditions, ensuring effective removal of heavy metals from water while minimizing interference from other ions.

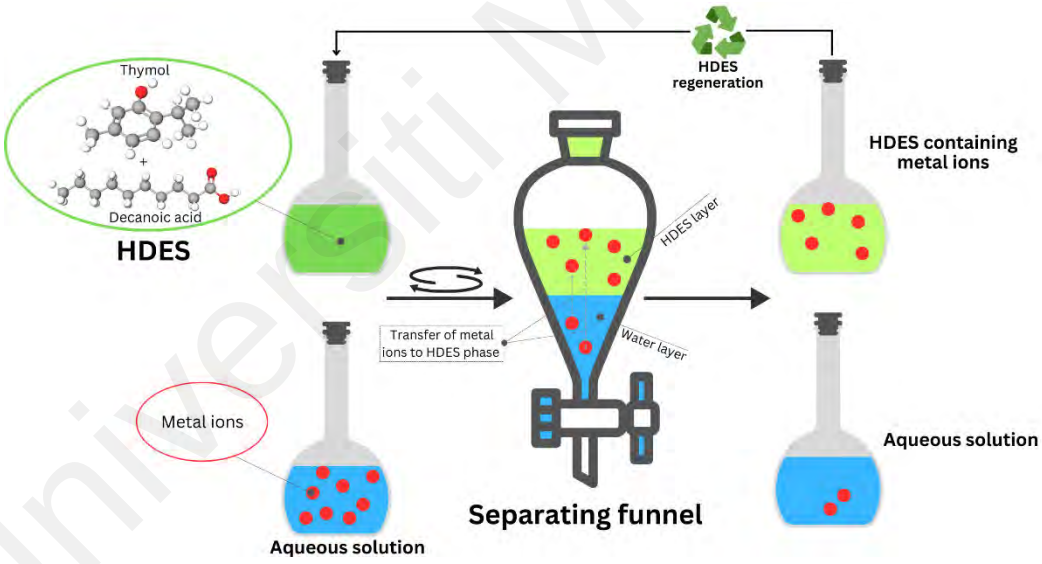

Figure 4.44: Schematic of the extraction process of heavy metal ions using Thy:DecA HDES.

HDES such as the Thy:DecA, are well suited to extract heavy metals such as lead and cadmium due to their robust hydrogen bonding, hydrophobic properties and π-π interactions. The ability of HDES to solubilize and stabilize heavy metal ions is primarily determined by the hydrogen bonds between the carboxyl (-COO-) and hydroxyl (-OH) functional groups within the solvent system. Decanoic acid, which acts as a HBA,

provides carboxylate groups that robustly bond with Pb^{2+} and Cd^{2+}, resulting in ion-pair complexes that increase their solubility in the organic phase. Thymol acts as a HBD and provides phenolic hydroxyl groups (-OH) that enhance the stabilization of the extracted metal ions via additional hydrogen bonding and weak cation-π interactions. Figure 4.45 shows the interaction of metals with aromatic π-systems. It suggests that Pb^{2+} and Cd^{2+} prefer an off-center or π-coordinated conformation due to electrostatic forces rather than significant orbital hybridization. This discovery supports the notion that Pb^{2+} and Cd^{2+} within HDESs are likely held by a synergy of hydrogen bonding with carboxyl groups and secondary cation-π interactions with the aromatic ring of thymol. The hydrophobic properties of HDES contribute significantly to metal extraction by reducing water solubility and facilitating the phase transfer of Pb^{2+} and Cd^{2+}, enhancing their selective removal from aquatic environments.

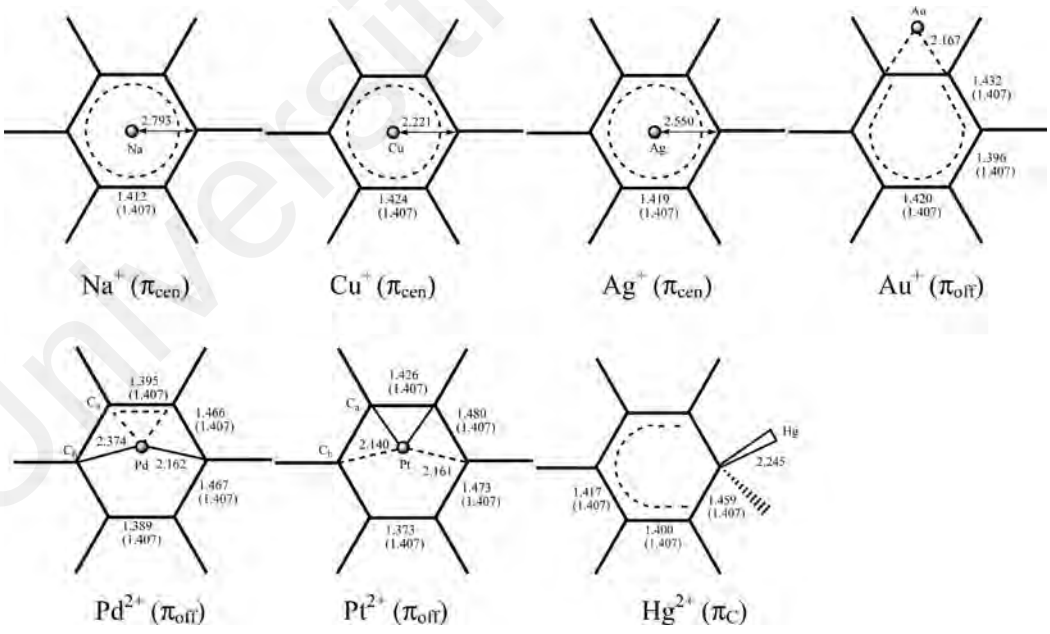

Figure 4.45: Structures of the metals−benzene complexes (Yi et al., 2009).

The binding properties of metal cations with benzene, as described in the previous work (Yi et al., 2009), serve as a valuable comparison for understanding the interactions of heavy metals in HDES. Figure 4.46 illustrates that the metals exhibit multiple bonding

conformations, with some preferring π-centered bonding, while others prefer eccentric π- or direct coordination with carbon atoms. In HDES, Pb^{2+} and Cd^{2+} are thought to undergo ion-dipole interactions with the carboxyl groups of decanoic acid, while they undergo mild π-interactions with the aromatic system of thymol. This method differs from transition metals such as Pd^{2+} and Pt^{2+}, which exhibit enhanced π-backdonation and covalent-like interactions with benzene. The differences in contact strength and binding mode emphasize the need to select an HDES system that has an ideal balance between hydrogen bond strength and hydrophobicity for the efficient extraction of Pb^{2+} and Cd^{2+}. Metals with lower charge density, such as Pb^{2+} and Cd^{2+}, exhibit less structural distortion in their coordination complexes, resulting in weaker binding to solvent molecules compared to transition metals (Yi et al., 2009). This observation highlights the effectiveness of HDES in the extraction of Pb^{2+} and Cd^{2+}, as the metal ions are effectively stabilized by the carboxyl groups without being so tightly bound that they cannot undergo a phase transition into the organic solvent. Understanding the π-π interactions, the influences of hydrogen bonding and the charge transfer properties of Pb^{2+} and Cd^{2+} in HDES therefore provides a more systematic method for improving solvent formulations aimed at the selective and effective extraction of heavy metals from polluted water.

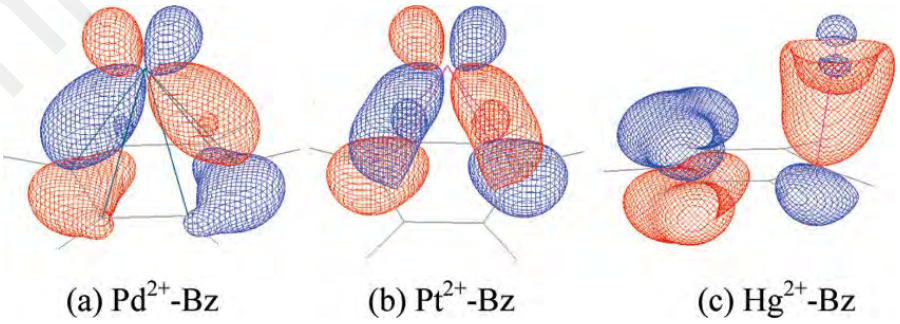

Figure 4.46: Occupied molecular orbitals of the metals dication attached to benzene ring (Yi et al., 2009).

To confirm the mechanistic step explained earlier, FTIR spectra of HDES were recorded before and after the extraction of lead, cadmium, and iron from the aqueous

medium to understand the complexation step. The FTIR spectra of Thy:DecA (1:1) before and after lead and cadmium extraction are shown in Figure 4.47.

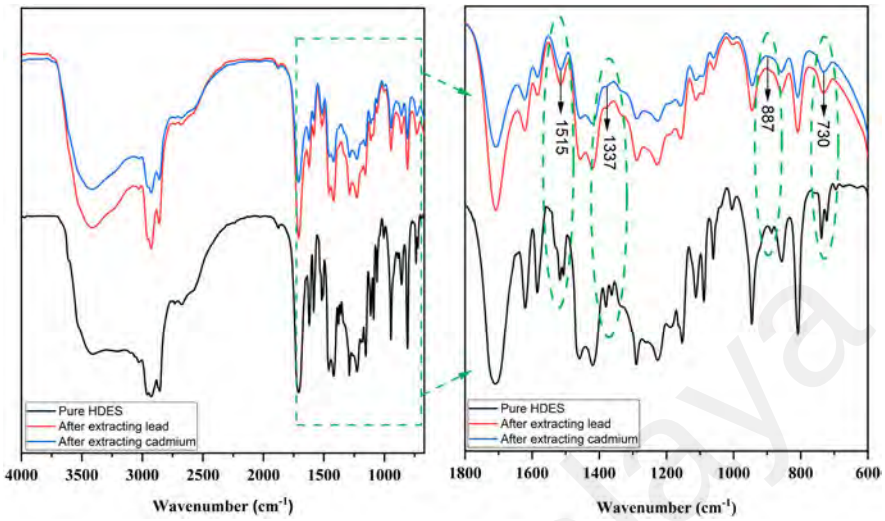

Figure 4.47: FTIR spectra of Thy:DecA before and after the extraction of lead and cadmium from water.

The peaks at 730 cm^{-1} and 1515 cm^{-1} can be used to understand the complexation implication of lead and cadmium ions with Thy:DecA HDES. In the blank Thy:DecA spectrum and at 730 cm^{-1} and 1515 cm^{-1}, two split peaks can be observed. Upon complexation with lead and cadmium ions, the two split peaks changed to singles for Thy:DecA/Pb^{2+} and Cd^{2+} ions harmonics. There was another peak at 1337 cm^{-1}, whose intensity decreased with the complexation of Thy:DecA with lead and cadmium ions.

Figure 4.48 shows the FTIR spectra before and after extraction of iron from the water medium. The peak of pure DES at 696 cm^{-1} disappears after the extraction of iron, which is related to the C-H stretching vibration of decanoic acid. The disappearance of this peak indicates that the molecules of decanoic acid are involved in the extraction. Two peaks associated with the C=O stretching vibrations of thymol and decanoic acid were observed in the 740 cm^{-1} region.

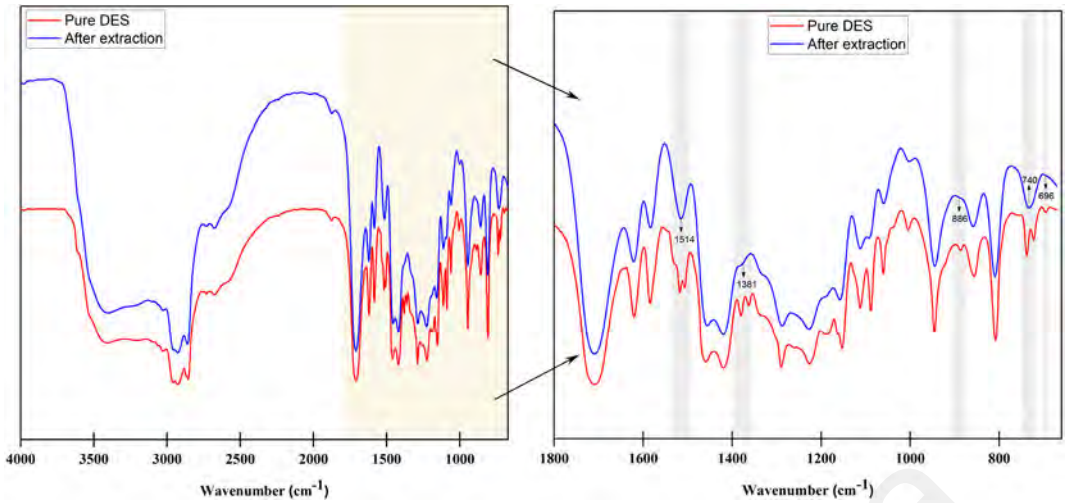

Figure 4.48: FTIR spectra of Thy:DecA DES before and after the extraction of iron from water.

The disappearance of one of these peaks indicates that the molecules of decanoic acid are no longer in the same form. At 886 cm^{-1} the peak disappears after the extraction of iron ions. This peak is associated with the C-H vibration of the thymol molecules. The disappearance of this peak indicates that the C-H bonds of thymol are no longer in the same form as in pure DES. In addition, the conversion of two peaks at 1381 cm^{-1} into one peak indicates that the thymol molecules are not in the same form, as these peaks are associated with the C-O-C stretching vibrations of the molecules of thymol and decanoic acid. The remaining peak could be due to the C-O-C stretching vibration of the molecules of decanoic acid. A similar trend was observed in 1514 cm^{-1} region. Finally, there was a broad peak at 3614 cm^{-1} that disappeared after extraction of the iron ions. This peak is probably related to the OH stretching of water. The absence of this peak suggests that the hydroxyl group is involved in the extraction process, possibly through the formation of hydrogen bonds with the iron ions. Due to the hydrophobic nature of the DES, the DES was able to form complexes with the iron ions.

In summary, the properties of HDES used in the extraction of phenols and heavy metals are closely linked to their molecular interactions, as demonstrated by FTIR and ^{1}HNMR. These spectroscopic techniques provide insights into hydrogen bond formation,

intermolecular interactions and structural changes during the extraction process. The FTIR spectra of HDES, especially terpenes and carboxylic acids, show remarkable shifts in the hydroxyl (-OH) stretching bands after the formation of HDES, indicating the formation of hydrogen bonds between the HBD and the HBA. In Men:Thy and Thy:DecA, the hydroxyl group bands shifted from approximately 3200–3300 cm^{-1} to higher values, indicating the formation of stronger hydrogen bonds. In TOPO-based HDES, the changes in the O-H stretching vibration confirmed the formation of hydrogen bonds between the oxygen-containing functional groups and hydrogen donors such as menthol and thymol.

The effectiveness of HDES in removing heavy metals is evidenced by the FTIR spectra before and after extraction, which show significant changes indicating complexation between metal ions and functional groups in HDES. Analysis of Thy:DecA shows that the peaks at 730 cm^{-1} and 1515 cm^{-1}, which were originally identified as split peaks, merged into single peaks upon interaction with Pb^{2+} and Cd^{2+} ions, indicating direct coordination between the solvent and the metal ions. The absence of a peak at 696 cm^{-1} after iron extraction indicates the involvement of decanoic acid molecules in the removal process. In addition, a shift in the C=O stretching vibrations at 740 cm^{-1} emphasizes the interaction between iron ions and HDES. The structural changes indicate that metal removal occurs via selective coordination with the active functional groups in HDES, highlighting the importance of molecular interactions in influencing extraction efficiency.

The ^{1}H NMR analysis results confirm the FTIR spectroscopy results by showing specific peak shifts indicative of changes in the molecular environments as a result of complex formation. In Men:DecA and Thy:DecA, the protons near the carboxyl group (2.0–2.5 ppm) and the protons associated with the alkyl chains (0.5–1.5 ppm) exhibited significant shifts compared to the pure components, suggesting enhanced intermolecular

interactions. The aromatic peaks of thymol and coumarin in Thy:Coum HDES showed significant fusion, indicating robust molecular interactions and a stable HDES structure. The extraction process resulted in the disappearance or displacement of characteristic peaks, especially those associated with hydroxyl (-OH) and carbonyl (-COOH) groups, indicating metal chelation and binding of organic pollutants.

The relationship between these spectroscopic results and extraction efficiency emphasizes the essential role of intermolecular interactions in the removal of contaminants. Strong hydrogen bonding and metal complexation significantly influence the selectivity and performance of HDES. These interactions improve the extraction capacity of HDES while ensuring their reusability and efficiency over multiple extraction cycles. The observed spectral shifts indicate that the stability and functionality of HDES are maintained during the extraction process, making them a viable alternative to conventional solvents for environmental remediation.

CHAPTER 5: CONCLUSION

5.1 Conclusion

Water contamination by hazardous pollutants remains a critical challenge for human health and environmental sustainability. Regulatory bodies such as WHO and EPA classify heavy metals and phenolic pollutants as priority contaminants. This study successfully demonstrated the feasibility of using HDES for their removal via LLE. HDES offer an environmentally friendly alternative to conventional VOCs due to their high extraction efficiencies, immiscibility in water, and tunable properties. The ability of HDES to selectively remove contaminants from aqueous solutions presents a major advancement in the field of green chemistry and water treatment technologies.

The selection of HDES was based on COSMO-RS screening and the availability of laboratory chemicals. Their physical properties were characterized through melting point, stability, viscosity, and density measurements. FTIR confirmed hydrogen bonding interactions among HDES components. The experimental screening of six HDES for cresol extraction demonstrated efficiencies above 94%. The order of extraction efficiency for m-cresol was Thy:Coum > Men:Thy > Thy:Camp > Men:DecA > HydA:DecA > Thy:DecA, while for o-cresol, it followed Thy:Coum > Men:Thy > HydA:DecA > Men:DecA > Thy:Camp > Thy:DecA. These findings reinforce the importance of molecular interactions and solvent-solute compatibility in the successful extraction of organic pollutants.

For phenol removal, 72 HDES were screened using COSMO-RS, and four TOPO-based HDES were selected for experimental validation. Among them, TOPO:Men showed the highest extraction efficiency of 96% at 7% phenol content. This confirms that TOPO-based HDES are promising solvents for phenol extraction. The results highlight

the effectiveness of integrating computational solvent screening with experimental validation to optimize solvent selection.

HDES also exhibited effective heavy metal extraction. Thy:DecA showed the best performance, achieving distribution ratios of 1.61 for lead and 0.965 for cadmium, attributed to the carboxyl group in decanoic acid forming strong metal-ligand bonds. Multi-stage extraction and reusability tests confirmed the robustness of HDES, with optimized extraction efficiencies of 93.49% for lead and 76.70% for cadmium. Additionally, terpene-based HDES successfully extracted iron and copper, with Men:DecA and Thy:DecA showing the highest efficiencies. The iron stripping efficiency using 8M HNO3 reached 97.66%. The extraction mechanism was validated through FTIR analysis before and after metal extraction. Furthermore, the ability of HDES to be regenerated and reused over multiple cycles without significant loss in efficiency underscores their sustainability and cost-effectiveness.

This research highlights the ability of HDES to act as efficient and sustainable solvents for removing both heavy metals and phenolic pollutants from water. The study underscores the importance of systematic solvent screening, characterization, and process optimization in achieving high extraction yields. The findings contribute to the development of greener water treatment technologies that mitigate pollution while ensuring environmental and human health protection. Future applications of HDES could extend to industrial wastewater treatment, recovery of valuable metals, and removal of emerging contaminants.

All research objectives were systematically addressed, encompassing solvent selection and characterization, mechanistic validation and process optimization. By combining experimental and computational methods, a strong framework for solvent development was established that promotes high efficiency and sustainability. The results enrich the

field of green chemistry and water purification technologies by providing scalable solutions for environmental remediation.

5.2 Significance of This Research

This research makes significant contributions to the advancement of sustainable and efficient water treatment methods. The use of HDES as an alternative to conventional solvents aligns with green chemistry principles, offering reduced toxicity, volatility, and environmental impact. By systematically screening and experimentally validating HDES, this study provides a robust framework for solvent selection in LLE applications. Furthermore, this research highlights the importance of solvent screening using computational tools such as COSMO-RS, which allows for more efficient and targeted solvent design. The integration of experimental validation with computational predictions enhances the reliability and applicability of HDES in real-world scenarios. The insights gained from this study help bridge the gap between theoretical solvent modeling and practical applications, paving the way for further innovations in environmentally friendly solvent technologies.

The research also establishes the feasibility of HDES for multi-pollutant extraction. The successful removal of phenol, cresols, lead, cadmium, iron, and copper demonstrates the versatility of HDES in addressing diverse water contamination challenges. Unlike conventional solvents, which often pose environmental and health risks, HDES provide a greener alternative with high selectivity and efficiency. The study further enhances the understanding of HDES-metal interactions, which is crucial for optimizing extraction efficiency and designing future solvent systems. These findings contribute to the growing body of knowledge on HDES and their potential applications beyond wastewater treatment, including in metal recovery and industrial separations. Additionally, the superior performance of TOPO-based HDES for phenol extraction suggests that HDES

can be customized for specific target pollutants, making them highly adaptable to different treatment needs.

Additionally, the demonstrated reusability of HDES supports their economic and practical viability for industrial applications. The findings pave the way for scaling up HDES-based extraction systems for real-world wastewater treatment. The ability to recycle and reuse HDES without significant loss in extraction efficiency ensures cost-effectiveness and sustainability in industrial applications. This research also provides a foundation for future work in optimizing HDES formulations, exploring additional pollutant removal applications, and integrating HDES-based processes into existing water treatment infrastructures. The results also emphasize the potential of HDES to play a vital role in addressing global water security challenges by offering a scalable and environmentally friendly alternative to conventional extraction methods. Overall, this work contributes to the broader goal of developing eco-friendly, high-performance separation technologies to ensure water safety and environmental sustainability.

5.3 Future Outlook and Recommendations

In order to reduce the use and production of hazardous compounds, the idea of green chemistry was launched in the mid to late 1990s, primarily through the promotion of innovative research towards the provision of innovative technologies. HDES meet green chemistry standards due to their low vapor pressure (Florindo et al., 2019a), high thermal stability (Chen et al., 2021), wide liquid range (Gilmore et al., 2018b), and low flammability (Cao & Su, 2021; Warrag & Kroon, 2019). The use of HDES in the elimination of pollutants is constantly increasing. Due to their sustainability, ease of use, low vapor pressure, wide liquid spectrum, and negligible miscibility with water, HDES have great potential as sustainable solvents for the removal of pollutants from contaminated water. However, the most commonly used DES formulations contain

solvents with hydrophilic properties. Despite an increased focus on HDES synthesis, their number is still small and additional efforts are needed to synthesize and investigate novel HDES as extraction solvents. The extractive capabilities of these HDES were highlighted in this work, with particular emphasis on the extraction of heavy or toxic metals, and phenolic pollutants from aqueous streams. The extraction efficiency could be improved by determining the optimum water content, viscosity, type of HBA/HBD, mass ratio of HDES to water, molar ratio of HDES, pH of the solution and initial concentration of the contaminant.

5.3.1 Challenges and Limitations

While the results of this research are promising, it is important to note some limitations:

The high viscosity of HDES presents handling, separation and analysis challenges for many prepared samples. This can affect liquid-liquid extraction performance and reduce efficiency. Viscosity affects mass transfer rates and the solubility of impurities, leading to inefficiencies during the extraction process. The development of novel formulations that have lower viscosity while ensuring high selectivity and stability is essential.

The limited availability of low-cost, non-toxic HDES components poses a challenge. Although HDES are considered environmentally friendly, the high cost of commonly used hydrogen bond donors (HBDs) and hydrogen bond acceptors (HBAs), especially quaternary ammonium salts, limits their wide application. In addition, many HBDs are not biodegradable, raising concerns about their impact on the environment after several reuse cycles. Additional research on bio-based hydrogen bond donors and acceptors is needed to improve cost-effectiveness and sustainability.

The lack of comprehensive data on thermophysical properties is notable. Properties such as polarity, surface tension, vapor pressure and hydrophobicity are crucial for the development of efficient extraction processes, but are not yet sufficiently explored for HDES. Further research is needed to develop comprehensive phase diagrams and improve HDES formulations for targeted industrial applications.

The long-term effects of HDES on the environment, particularly in terms of biodegradability and ecotoxicity, have not yet been sufficiently researched. Further studies are needed to assess the fate of HDES in aquatic systems, soil and the atmosphere to mitigate potential environmental impacts. Toxicity studies need to include effects on microbial communities and aquatic organisms to fully assess potential risks.

Scalability study was conducted at laboratory scale, so considerable effort was required to modify the HDES extraction processes for industrial implementation. Exploring the feasibility of synthesis, process optimization and automation on a large scale is essential to combine laboratory experiments with practical industrial applications.

There are gaps in computational modeling. Although COSMO-RS has been used for solvent selection, further refinement is needed to improve the predictive accuracy of computational models for HDES applications. It is critical to develop more robust theoretical frameworks for the dynamic assessment of solvent-pollutant interactions that allow better tuning of HDES properties to specific pollutants.

5.3.2 Future Work

Future research should focus on the following critical areas to address these challenges:

Initiatives need to focus on synthesizing HDES with lower viscosity while maintaining high extraction efficacy. This could be achieved by developing ternary HDES or

modifying the chemical architectures to improve flowability. Exploring different HBA and HBD combinations that reduce viscosity while maintaining favorable solvent properties is critical.

Ecotoxicological assessments need to be carried out to determine the biodegradability and lasting effects of HDES in different environmental systems. This includes assessing their degradation in different environmental matrices and identifying potential degradation products that may be of concern.

Further studies need to investigate the use of HDES for a broader range of contaminants, including pharmaceuticals, microplastics and novel organic pollutants. The ability of HDES to selectively extract and recover high value-added chemicals from industrial waste should be investigated.

Both pilot-scale and large-scale studies need to be conducted to assess the feasibility of HDES in large-scale wastewater treatment, integrating techno-economic and life-cycle assessments to evaluate cost-effectiveness and environmental impact. Process intensification strategies, such as the integration of HDES extraction with membrane filtration or adsorption technologies, need to be investigated to improve efficiency.

Enhancing the predictive capabilities of COSMO-RS and other computational tools will be critical to improving HDES formulation and facilitating effective contaminant extraction. The development of machine learning based models for solvent selection can increase efficiency and minimize trial and error.

Exploring the fusion of HDES with other advanced separation methods, such as membrane filtration, adsorption or catalytic degradation, can improve overall removal efficiency and process sustainability. Hybrid approaches that combine HDES with

electrochemical and photochemical processes can provide innovative solutions for persistent pollutants.

The regeneration and long-term performance of existing HDES applications are significantly impacted by their reuse capacity. Future research should focus on improving regeneration methods that reduce solvent loss while maintaining extraction efficacy over numerous cycles. Understanding the molecular degradation processes of HDES after repeated applications would improve their long-term viability. Future studies should focus on improving the extraction of HDES from treated wastewater to ensure thorough phase separation and reduce solvent loss. Although HDES have low water solubility, their low mutual solubility in some formulations requires improved separation methods, including membrane filtration, sophisticated adsorption techniques and solvent regeneration by selective strippers. Investigating the application of hydrophobic adsorbents, such as modified activated carbon or polymeric resins, may improve the recovery of HDES and mitigate the environmental impact. In addition, investigating the use of advanced oxidation processes for the controlled degradation of HDES residues could provide an alternative method where solvent reuse is impractical. Subsequent investigations into the long-term stability and recyclability of HDES during multiple extraction cycles will be crucial for industrial scalability, as will the assessment of their environmental impact through life cycle analyzes.

The disposal of spent HDES requires careful study to mitigate environmental impact while ensuring sustainability. A basic method is regeneration and reuse, where exhausted HDES are subjected to a stripping process using acidic (e.g. HCl) or alkaline (e.g. NaOH) solutions to recover the extracted impurities and rejuvenate the solvent for repeated cycles. This work shows that some HDES, such as Thy:DecA, maintain considerable extraction performance after five reuse cycles, while performance gradually declines due

to solvent saturation and degradation. When regeneration is no longer practical, thermal treatment serves as a viable disposal strategy in which HDES are incinerated under controlled conditions to ensure thorough degradation of the organics without releasing harmful by-products. Biodegradation studies should be conducted on naturally occurring HDES to evaluate microbial decomposition under environmental conditions, especially for solvents containing biodegradable components such as menthol and thymol. Another effective technique is chemical treatment, where HDES are subjected to oxidation or hydrolysis to break down complex organic compounds into environmentally safe products. Disposal of HDES containing persistent organic structures or metallic pollutants as hazardous waste in licensed facilities may be essential to prevent soil and water pollution. In addition, the integration of HDES disposal into the circular economy, e.g. the conversion of spent solvents into secondary raw materials for industrial use, could improve sustainability. Future research needs to focus on improving solvent regeneration methods and assessing the long-term environmental impact of HDES disposal in order to develop more sustainable and efficient disposal strategies.

By exploring these potential research avenues, HDES could be further developed into a scalable and efficient solution for environmental remediation and sustainable chemical processing. The results of this study provide a solid foundation for further advances in sustainable solvent technology. The future prospects for HDES are extremely favorable as they can transform industrial wastewater treatment and resource recovery through their selective and sustainable extraction capacities.

REFERENCES

Abbas, A., Al-Amer, A. M., Laoui, T., Al-Marri, M. J., Nasser, M. S., Khraisheh, M., & Atieh, M. A. (2016). Heavy metal removal from aqueous solution by advanced carbon nanotubes: critical review of adsorption applications. *Separation and Purification Technology, 157,* 141-161.

Abbott, A. P., Boothby, D., Capper, G., Davies, D. L., & Rasheed, R. K. (2004a). Deep eutectic solvents formed between choline chloride and carboxylic acids: versatile alternatives to ionic liquids. *Journal of the American Chemical Society, 126*(29), 9142-9147.

Abbott, A. P., Capper, G., Davies, D. L., & Rasheed, R. (2004b). Ionic liquids based upon metal halide/substituted quaternary ammonium salt mixtures. *Inorganic chemistry, 43*(11), 3447-3452.

Abbott, A. P., Capper, G., Davies, D. L., Rasheed, R. K., & Tambyrajah, V. (2003). Novel solvent properties of choline chloride/urea mixtures. *Chemical Communications*(1), 70-71.

Abdi, K., Ezoddin, M., & Pirooznia, N. (2020). Temperature-controlled liquid–liquid microextraction using a biocompatible hydrophobic deep eutectic solvent for microextraction of palladium from catalytic converter and road dust samples prior to ETAAS determination. *Microchemical Journal, 157,* 104999.

Abdullah, N., Yusof, N., Lau, W., Jaafar, J., & Ismail, A. (2019). Recent trends of heavy metal removal from water/wastewater by membrane technologies. *Journal of Industrial and Engineering Chemistry, 76,* 17-38.

Adeyemi, I., Sulaiman, R., Almazroui, M., Al-Hammadi, A., & AlNashef, I. (2020). Removal of chlorophenols from aqueous media with hydrophobic deep eutectic solvents: Experimental study and COSMO RS evaluation. *Journal of Molecular Liquids, 311,* 113180.

Aghav, R., Kumar, S., & Mukherjee, S. (2011). Artificial neural network modeling in competitive adsorption of phenol and resorcinol from water environment using some carbonaceous adsorbents. *Journal of Hazardous materials, 188*(1-3), 67-77.

Akpor, O., & Muchie, M. (2010). Remediation of heavy metals in drinking water and wastewater treatment systems: processes and applications. *International Journal of Physical Sciences*, *5*(12), 1807-1817.

Al-Dawsari, J. N., Bessadok-Jemai, A., Wazeer, I., Mokraoui, S., AlMansour, M. A., & Hadj-Kali, M. K. (2020). Fitting of experimental viscosity to temperature data for deep eutectic solvents. *Journal of Molecular Liquids*, *310*, 113127.

Al-Mutaz, I. S., & Wazeer, I. (2016). Optimization of location of thermo-compressor suction in MED-TVC desalination plants. *Desalination and Water Treatment*, *57*(55), 26562-26576.

Almustafa, G., Sulaiman, R., Kumar, M., Adeyemi, I., Arafat, H. A., & AlNashef, I. (2020). Boron extraction from aqueous medium using novel hydrophobic deep eutectic solvents. *Chemical Engineering Journal*, *395*, 125173.

An, Y., Ma, W., & Row, K. H. (2020). Preconcentration and determination of chlorophenols in wastewater with dispersive liquid–liquid microextraction using hydrophobic deep eutectic solvents. *Analytical Letters*, *53*(2), 262-272.

An, Y., & Row, K. H. (2020). Evaluation of Menthol-Based Hydrophobic Deep Eutectic Solvents for the Extraction of Bisphenol A from Environment Water. *Analytical Letters*, 1-13.

An, Y., & Row, K. H. (2021). Evaluation of Menthol-Based Hydrophobic Deep Eutectic Solvents for the Extraction of Bisphenol A from Environment Water. *Analytical Letters*, *54*(9), 1533-1545.

Anku, W. W., Mamo, M. A., & Govender, P. P. (2017). Phenolic compounds in water: sources, reactivity, toxicity and treatment methods. *Phenolic compounds-natural sources, importance and applications*, 419-443.

Archana, V., Begum, K. M. S., & Anantharaman, N. (2016). Studies on removal of phenol using ionic liquid immobilized polymeric micro-capsules. *Arabian Journal of Chemistry*, *9*(3), 371-382.

Arcon, D. P., & Franco Jr, F. C. (2020). All-fatty acid hydrophobic deep eutectic solvents towards a simple and efficient microextraction method of toxic industrial dyes. *Journal of Molecular Liquids, 318*, 114220.

Azimi, A., Azari, A., Rezakazemi, M., & Ansarpour, M. (2017). Removal of heavy metals from industrial wastewaters: a review. *ChemBioEng Reviews*, *4*(1), 37-59.

Babich, H., & Davis, D. (1981). Phenol: A review of environmental and health risks. *Regulatory Toxicology and Pharmacology*, *1*(1), 90-109.

Baker, M., & Mayfield, C. (1980). Microbial and non-biological decomposition of chlorophenols and phenol in soil. *Water, Air, and Soil Pollution, 13*, 411-424.

Bandosz, T. J., Policicchio, A., Florent, M., Li, W., Poon, P. S., & Matos, J. (2020). Solar light-driven photocatalytic degradation of phenol on S-doped nanoporous carbons: The role of functional groups in governing activity and selectivity. *Carbon, 156*, 10-23.

Barakat, M. (2011). New trends in removing heavy metals from industrial wastewater. *Arabian Journal of Chemistry*, *4*(4), 361-377.

Bazrafshan, E., Amirian, P., Mahvi, A. H., & Ansari-Moghaddam, A. (2016). Application of adsorption process for phenolic compounds removal from aqueous environments: a systematic review. *Global NEST Journal, 18*(1), 146-163.

Bekou, E., Dionysiou, D. D., Qian, R.-Y., & Botsaris, G. D. (2003). Extraction of chlorophenols from water using room temperature ionic liquids. *Ion. Liq. as Green Solvents Prog. Prospect., 856*, 544-560.

BIPM, I., Ifcc, I., Iso, I., & Iupap, O. (2008). Evaluation of measurement data—guide to the expression of uncertainty in measurement, JCGM 100: 2008 GUM 1995 with minor corrections. *Joint Committee for Guides in Metrology*.

Blanco-Pedrekhon, A., Shibanov, I., Motuzenko, N., & Kagramanov, G. (2021). Extraction-membrane technology for processing oil-based mud. IOP Conference Series: Earth and Environmental Science,

Bodzek, M., Konieczny, K., & Kwiecińska, A. (2011). Application of membrane processes in drinking water treatment–state of art. *Desalination and Water Treatment, 35*(1-3), 164-184.

Bolisetty, S., Peydayesh, M., & Mezzenga, R. (2019). Sustainable technologies for water purification from heavy metals: review and analysis. *Chemical Society Reviews, 48*(2), 463-487.

Brinda Lakshmi, A., Balasubramanian, A., & Venkatesan, S. (2013). Extraction of phenol and chlorophenols using ionic liquid [Bmim]+[BF4]− dissolved in tributyl phosphate. *CLEAN–Soil, Air, Water, 41*(4), 349-355.

Busca, G., Berardinelli, S., Resini, C., & Arrighi, L. (2008). Technologies for the removal of phenol from fluid streams: a short review of recent developments. *Journal of Hazardous materials, 160*(2-3), 265-288.

Caetano, M., Valderrama, C., Farran, A., & Cortina, J. L. (2009). Phenol removal from aqueous solution by adsorption and ion exchange mechanisms onto polymeric resins. *Journal of Colloid and Interface Science, 338*(2), 402-409.

Cai, F., Zhao, M., Wang, Y., Wang, F., & Xiao, G. (2015). Phosphoric-based ionic liquids as solvents to separate the azeotropic mixture of ethanol and hexane. *The Journal of Chemical Thermodynamics, 81*, 177-183.

Cao, J., & Su, E. (2021). Hydrophobic deep eutectic solvents: The new generation of green solvents for diversified and colorful applications in green chemistry. *Journal of Cleaner Production*, 127965.

Černá, M. (1995). Use of solvent extraction for the removal of heavy metals from liquid wastes. *Environmental monitoring and assessment, 34*(2), 151-162.

Chaemiso, T. D., & Nefo, T. (2019). Removal methods of heavy metals from laboratory wastewater. *Journal of Natural Sciences Research, 9*(2), 36-42.

Chang, S. H., Teng, T. T., & Ismail, N. (2010). Extraction of Cu (II) from aqueous solutions by vegetable oil-based organic solvents. *Journal of Hazardous Materials, 181*(1-3), 868-872.

Chang, S. H., Teng, T. T., & Ismail, N. (2011). Screening of factors influencing Cu (II) extraction by soybean oil-based organic solvents using fractional factorial design. *Journal of environmental management, 92*(10), 2580-2585.

Chen, C.-C., Huang, Y.-H., Hung, S.-M., Chen, C., Lin, C.-W., & Yang, H.-H. (2021). Hydrophobic deep eutectic solvents as attractive media for low-concentration hydrophobic VOC capture. *Chemical Engineering Journal, 424*, 130420.

Chen, Y., Lv, R., Li, L., & Wang, F. (2017). Measurement and thermodynamic modeling of ternary (liquid+ liquid) equilibrium for extraction of o-cresol, m-cresol or p-cresol from aqueous solution with 2-pentanone. *The Journal of Chemical Thermodynamics, 104*, 230-238.

Chen, Y., Meng, Y., Yang, J., Li, H., & Liu, X. (2012). Phenol distribution behavior in aqueous biphasic systems composed of ionic liquids–carbohydrate–water. *Journal of Chemical & Engineering Data, 57*(7), 1910-1914.

Cheng, H., & Qi, Z. (2021). Applications of deep eutectic solvents for hard-to-separate liquid systems. *Separation and Purification Technology, 274*, 119027.

Chirico, R. D., Frenkel, M., Magee, J. W., Diky, V., Muzny, C. D., Kazakov, A. F., Kroenlein, K., Abdulagatov, I., Hardin, G. R., & Acree Jr, W. E. (2013). Improvement of quality in publication of experimental thermophysical property

data: Challenges, assessment tools, global implementation, and online support. *Journal of Chemical & Engineering Data, 58*(10), 2699-2716.

Clark, J. H., & Tavener, S. J. (2007). Alternative solvents: shades of green. *Organic process research & development, 11*(1), 149-155.

Crini, G., & Lichtfouse, E. (2019). Advantages and disadvantages of techniques used for wastewater treatment. *Environmental Chemistry Letters, 17*, 145-155.

Cunha, S. C., & Fernandes, J. O. (2018). Extraction techniques with deep eutectic solvents. *TrAC Trends in Analytical Chemistry, 105*, 225-239.

Dai, Y., van Spronsen, J., Witkamp, G.-J., Verpoorte, R., & Choi, Y. H. (2013). Natural deep eutectic solvents as new potential media for green technology. *Analytica chimica acta, 766*, 61-68.

Debadatta, D., & Susmita, M. (2015). Study of individual and simultaneous degradation of chromium (vi) and phenol using two potent indigenous microorganisms. *Journal of Environmental Research And Development, 9*(3), 530.

Deng, N., Li, M., Zhao, L., Lu, C., de Rooy, S. L., & Warner, I. M. (2011). Highly efficient extraction of phenolic compounds by use of magnetic room temperature ionic liquids for environmental remediation. *Journal of Hazardous materials, 192*(3), 1350-1357.

Dietz, C. H., Creemers, J. T., Meuleman, M. A., Held, C., Sadowski, G., van Sint Annaland, M., Gallucci, F., & Kroon, M. C. (2019). Determination of the total vapor pressure of hydrophobic deep eutectic solvents: experiments and perturbed-chain statistical associating fluid theory modeling. *ACS Sustainable Chemistry & Engineering, 7*(4), 4047-4057.

Dietz, M. L. (2006). Ionic liquids as extraction solvents: where do we stand? *Separation Science and Technology, 41*(10), 2047-2063.

dos Santos Junior, G. A., Fortunato, V. D., Silva, G. G., Ortega, P. F., & Lavall, R. L. (2019). High-performance Li-ion hybrid supercapacitor based on LiMn2O4 in ionic liquid electrolyte. *Electrochimica Acta, 325*, 134900.

Edgecomb, J. M., Tereshatov, E. E., Zante, G., Boltoeva, M., & Folden III, C. M. (2020). Hydrophobic amine-based binary mixtures of active pharmaceutical and food grade ingredients: characterization and application in indium extraction from aqueous hydrochloric acid media. *Green Chemistry, 22*(20), 7047-7058.

Espino, M., de los Ángeles Fernández, M., Gomez, F. J., & Silva, M. F. (2016). Natural designer solvents for greening analytical chemistry. *TrAC Trends in Analytical Chemistry, 76*, 126-136.

Fan, J., Fan, Y., Pei, Y., Wu, K., Wang, J., & Fan, M. (2008). Solvent extraction of selected endocrine-disrupting phenols using ionic liquids. *Separation and Purification Technology, 61*(3), 324-331.

Faraji, M., Noormohammadi, F., & Adeli, M. (2020). Preparation of a ternary deep eutectic solvent as extraction solvent for dispersive liquid-liquid microextraction of nitrophenols in water samples. *Journal of Environmental Chemical Engineering, 8*(4), 103948.

Flett, D. S. (2005). Solvent extraction in hydrometallurgy: the role of organophosphorus extractants. *Journal of Organometallic Chemistry, 690*(10), 2426-2438.

Florindo, C., Branco, L. C., & Marrucho, I. M. (2019a). Quest for green-solvent design: from hydrophilic to hydrophobic (deep) eutectic solvents. *ChemSusChem, 12*(8), 1549-1559.

Florindo, C., Celia-Silva, L. G., Martins, L. F., Branco, L. C., & Marrucho, I. M. (2018a). Supramolecular hydrogel based on a sodium deep eutectic solvent. *Chemical Communications, 54*(54), 7527-7530.

Florindo, C., Lima, F., Branco, L. s. C., & Marrucho, I. M. (2019b). Hydrophobic deep eutectic solvents: a circular approach to purify water contaminated with ciprofloxacin. *ACS Sustainable Chemistry & Engineering, 7*(17), 14739-14746.

Florindo, C., Monteiro, N. V., Ribeiro, B. D., Branco, L., & Marrucho, I. (2020). Hydrophobic deep eutectic solvents for purification of water contaminated with Bisphenol-A. *Journal of Molecular Liquids, 297*, 111841.

Florindo, C., Romero, L., Rintoul, I., Branco, L. C., & Marrucho, I. M. (2018b). From phase change materials to green solvents: hydrophobic low viscous fatty acid–based deep eutectic solvents. *ACS Sustainable Chemistry & Engineering*, *6*(3), 3888-3895.

Francisco, M., van den Bruinhorst, A., & Kroon, M. C. (2013). Low-transition-temperature mixtures (LTTMs): A new generation of designer solvents. *Angewandte Chemie international edition*, *52*(11), 3074-3085.

Galadima, A., Garba, Z., Leke, L., Almustapha, M., & Adam, I. (2011). Domestic water pollution among local communities in Nigeria-causes and consequences. *European journal of scientific research*, *52*(4), 592-603.

Garcia, G., Aparicio, S., Ullah, R., & Atilhan, M. (2015). Deep eutectic solvents: physicochemical properties and gas separation applications. *Energy & Fuels*, *29*(4), 2616-2644.

Ge, D., Zhang, Y., Dai, Y., & Yang, S. (2018). Air-assisted dispersive liquid–liquid microextraction based on a new hydrophobic deep eutectic solvent for the preconcentration of benzophenone-type UV filters from aqueous samples. *Journal of separation science*, *41*(7), 1635-1643.

Gilmore, M., McCourt, E. a. N., Connolly, F., Nockemann, P., Swadźba-Kwaśny, M., & Holbrey, J. D. (2018a). Hydrophobic deep eutectic solvents incorporating trioctylphosphine oxide: advanced liquid extractants. *ACS Sustainable Chemistry & Engineering*, *6*(12), 17323-17332.

Gilmore, M., McCourt, E. N., Connolly, F., Nockemann, P., Swadźba-Kwaśny, M., & Holbrey, J. D. (2018b). Hydrophobic deep eutectic solvents incorporating trioctylphosphine oxide: Advanced liquid extractants. *ACS Sustainable Chemistry & Engineering*, *6*(12), 17323-17332.

Gjineci, N., Boli, E., Tzani, A., Detsi, A., & Voutsas, E. (2016). Separation of the ethanol/water azeotropic mixture using ionic liquids and deep eutectic solvents. *Fluid Phase Equilibria, 424*, 1-7.

Gunatilake, S. (2015). Methods of removing heavy metals from industrial wastewater. *Methods, 1*(1), 14.

Gupta, S., Ashrith, G., Chandra, D., Gupta, A. K., Finkel, K. W., & Guntupalli, J. S. (2008). Acute phenol poisoning: a life-threatening hazard of chronic pain relief. *Clinical Toxicology, 46*(3), 250-253.

Habibi, E., Ghanemi, K., Fallah-Mehrjardi, M., & Dadolahi-Sohrab, A. (2013). A novel digestion method based on a choline chloride–oxalic acid deep eutectic solvent for determining Cu, Fe, and Zn in fish samples. *Analytica chimica acta*, *762*, 61-67.

Hadj-Kali, M. K., Althuluth, M., Mokraoui, S., Wazeer, I., Ali, E., & Richon, D. (2020). Screening of ionic liquids for gas separation using COSMO-RS and comparison between performances of ionic liquids and aqueous alkanolamine solutions. *Chemical Engineering Communications, 207*(9), 1264-1277.

Hadj-Kali, M. K., Hizaddin, H. F., Wazeer, I., Mulyono, S., & Hashim, M. A. (2017). Liquid-liquid separation of azeotropic mixtures of ethanol/alkanes using deep eutectic solvents: COSMO-RS prediction and experimental validation. *Fluid Phase Equilibria, 448*, 105-115.

Haider, M. B., Dwivedi, M., Jha, D., Kumar, R., & Sivagnanam, B. M. (2021). Azeotropic separation of isopropanol-water using natural hydrophobic deep eutectic solvents. *Journal of Environmental Chemical Engineering, 9*(1), 104786.

Hajipour, A. R., & Rafiee, F. (2015). Recent progress in ionic liquids and their applications in organic synthesis. *Organic Preparations and Procedures International, 47*(4), 249-308.

Hallett, J. P., & Welton, T. (2011). Room-temperature ionic liquids: solvents for synthesis and catalysis. 2. *Chemical reviews, 111*(5), 3508-3576.

Hanada, T., & Goto, M. (2021). Synergistic deep eutectic solvents for lithium extraction. *ACS Sustainable Chemistry & Engineering, 9*(5), 2152-2160.

Hand, D. B. (1930). Dineric distribution. *The Journal of Physical Chemistry, 34*(9), 1961-2000.

Hao, L., Liu, W., Wang, C., Wu, Q., & Wang, Z. (2019). Novel porous Fe3O4@ C nanocomposite from magnetic metal-phenolic networks for the extraction of chlorophenols from environmental samples. *Talanta, 194*, 673-679.

Hernández-Francisco, E., Peral, J., & Blanco-Jerez, L. (2017). Removal of phenolic compounds from oil refinery wastewater by electrocoagulation and Fenton/photo-Fenton processes. *Journal of Water Process Engineering, 19*, 96-100.

Hollenbach, R., Ochsenreither, K., & Syldatk, C. (2020). Enzymatic synthesis of glucose monodecanoate in a hydrophobic deep eutectic solvent. *International journal of molecular sciences, 21*(12), 4342.

Huang, F., Berton, P., Lu, C., Siraj, N., Wang, C., Magut, P. K., & Warner, I. M. (2014). Surfactant-based ionic liquids for extraction of phenolic compounds combined with rapid quantification using capillary electrophoresis. *Electrophoresis, 35*(17), 2463-2469.

Hubicki, Z., & Kołodyńska, D. (2012). Selective removal of heavy metal ions from waters and waste waters using ion exchange methods. *Ion exchange technologies, 7*, 193-240.

Ji, Y., Meng, Z., Zhao, J., Zhao, H., & Zhao, L. (2020). Eco-friendly ultrasonic assisted liquid–liquid microextraction method based on hydrophobic deep eutectic solvent for the determination of sulfonamides in fruit juices. *Journal of Chromatography A, 1609*, 460520.

Jiang, C., Cheng, H., Qin, Z., Wang, R., Chen, L., Yang, C., Qi, Z., & Liu, X. (2021). COSMO-RS prediction and experimental verification of 1, 5-pentanediamine extraction from aqueous solution by ionic liquids. *Green Energy & Environment, 6*(3), 422-431.

Joshi, N. C., Sharma, R., & Singh, A. (2017). Biosorption: A review on heavy metal toxicity and advances of biosorption on conventional methods. *J. Chem. Chem. Sci, 7*(9), 714-724.

Karimi, S., Shekaari, H., & Ahadzadeh, I. (2020). Effect of some deep eutectic solvents based on choline chloride on thermodynamic properties of 5-hydroxymethylfurfural at T=(288.15 to 318.15) K. *Journal of the Taiwan Institute of Chemical Engineers, 117*, 1-9.

Karimiyan, H., & Hadjmohammadi, M. (2016). Ultrasound-assisted supramolecular-solvent-based microextraction combined with high-performance liquid chromatography for the analysis of chlorophenols in environmental water samples. *Journal of separation science, 39*(24), 4740-4747.

Khan, A. S., Ibrahim, T. H., Jabbar, N. A., Khamis, M. I., Nancarrow, P., & Mjalli, F. S. (2021). Ionic liquids and deep eutectic solvents for the recovery of phenolic compounds: effect of ionic liquids structure and process parameters. *Rsc Advances, 11*(20), 12398-12422.

Khasawneh, O. F. S., & Palaniandy, P. (2021). Removal of organic pollutants from water by Fe2O3/TiO2 based photocatalytic degradation: A review. *Environmental Technology & Innovation, 21*, 101230.

Kumar, A., Kumar, S., & Kumar, S. (2005). Biodegradation kinetics of phenol and catechol using Pseudomonas putida MTCC 1194. *Biochemical Engineering Journal, 22*(2), 151-159.

Lee, H., Kang, S., Jin, Y., Jung, D., Park, K., Li, K., & Lee, J. (2020). Systematic investigation of the extractive desulfurization of fuel using deep eutectic solvents from multifarious aspects. *Fuel, 264*, 116848.

Lee, J., Jung, D., & Park, K. (2019). Hydrophobic deep eutectic solvents for the extraction of organic and inorganic analytes from aqueous environments. *TrAC Trends in Analytical Chemistry, 118*, 853-868.

Li, T., Song, Y., Dong, Z., Shi, Y., & Fan, J. (2020). Hydrophobic deep eutectic solvents as extractants for the determination of bisphenols from food-contacted plastics by high performance liquid chromatography with fluorescence detection. *Journal of Chromatography A, 1621*, 461087.

Li, X., Sun, L., Lv, X., Qi, J., Lu, H., & Wu, Y. (2021). Sustainable separation of petroleum hydrocarbons pollutant using hydrophobic deep eutectic solvents regulated by CO2. *Journal of Environmental Chemical Engineering, 9*(5), 106280.

Lima, F., Branco, L. C., Silvestre, A. J., & Marrucho, I. M. (2021). Deep desulfurization of fuels: Are deep eutectic solvents the alternative for ionic liquids? *Fuel, 293*, 120297.

Liu, R., Geng, Y., Tian, Z., Wang, N., Wang, M., Zhang, G., & Yang, Y. (2021). Extraction of platinum (IV) by hydrophobic deep eutectic solvents based on trioctylphosphine oxide. *Hydrometallurgy, 199*, 105521.

Liu, X., Chen, M., Meng, Z., Qian, H., Zhang, S., Lu, R., Gao, H., & Zhou, W. (2020). Extraction of benzoylurea pesticides from tea and fruit juices using deep eutectic solvents. *Journal of Chromatography B, 1140*, 121995.

Longeras, O., Gautier, A., Ballerat-Busserolles, K., & Andanson, J.-M. (2020). Deep Eutectic Solvent with Thermo-Switchable Hydrophobicity. *ACS Sustainable Chemistry & Engineering, 8*(33), 12516-12520.

Loos, G., Scheers, T., Van Eyck, K., Van Schepdael, A., Adams, E., Van der Bruggen, B., Cabooter, D., & Dewil, R. (2018). Electrochemical oxidation of key pharmaceuticals using a boron doped diamond electrode. *Separation and Purification Technology, 195*, 184-191.

Loyon, L. (2017). Overview of manure treatment in France. *Waste management, 61*, 516-520.

Luo, Y., Guo, W., Ngo, H. H., Nghiem, L. D., Hai, F. I., Zhang, J., Liang, S., & Wang, X. C. (2014). A review on the occurrence of micropollutants in the aquatic environment and their fate and removal during wastewater treatment. *Science of the total environment, 473*, 619-641.

Ma, W., & Row, K. H. (2018). Solid-phase extraction of chlorophenols in seawater using a magnetic ionic liquid molecularly imprinted polymer with incorporated silicon dioxide as a sorbent. *Journal of Chromatography A, 1559*, 78-85.

Madoni, P., & Romeo, M. G. (2006). Acute toxicity of heavy metals towards freshwater ciliated protists. *Environmental Pollution, 141*(1), 1-7.

Majidi, E., & Bakhshi, H. (2024). Hydrophobic deep eutectic solvents characterization and performance for efficient removal of heavy metals from aqueous media. *Journal of Water Process Engineering, 57*, 104680.

Makoś, P., Przyjazny, A., & Boczkaj, G. (2018). Hydrophobic deep eutectic solvents as “green” extraction media for polycyclic aromatic hydrocarbons in aqueous samples. *Journal of Chromatography A, 1570*, 28-37.

Makoś, P., Słupek, E., & Gębicki, J. (2020). Hydrophobic deep eutectic solvents in microextraction techniques–A review. *Microchemical Journal, 152*, 104384.

Manoli, E., & Samara, C. (2008). The removal of polycyclic aromatic hydrocarbons in the wastewater treatment process: experimental calculations and model predictions. *Environmental Pollution, 151*(3), 477-485.

Margot, J., Rossi, L., Barry, D. A., & Holliger, C. (2015). A review of the fate of micropollutants in wastewater treatment plants. *Wiley Interdisciplinary Reviews: Water, 2*(5), 457-487.

Martin, T., & Holdich, D. (1986). The acute lethal toxicity of heavy metals to peracarid crustaceans (with particular reference to fresh-water asellids and gammarids). *Water research, 20*(9), 1137-1147.

Martins, M. A., Crespo, E. A., Pontes, P. V., Silva, L. P., Bülow, M., Maximo, G. J., Batista, E. A., Held, C., Pinho, S. P., & Coutinho, J. A. (2018). Tunable hydrophobic eutectic solvents based on terpenes and monocarboxylic acids. *ACS Sustainable Chemistry & Engineering, 6*(7), 8836-8846.

Martins, M. A., Pinho, S. P., & Coutinho, J. A. (2019). Insights into the nature of eutectic and deep eutectic mixtures. *Journal of Solution Chemistry, 48*, 962-982.

McNeice, P., Marr, A. C., Marr, P. C., Earle, M. J., & Seddon, K. R. (2018). Binary alkoxide ionic liquids. *ACS Sustainable Chemistry & Engineering, 6*(11), 13676-13680.

Mei, M., Huang, X., Yu, J., & Yuan, D. (2015). Sensitive monitoring of trace nitrophenols in water samples using multiple monolithic fiber solid phase microextraction and liquid chromatographic analysis. *Talanta, 134*, 89-97.

Mohammadi, S., Kargari, A., Sanaeepur, H., Abbassian, K., Najafi, A., & Mofarrah, E. (2015). Phenol removal from industrial wastewaters: a short review. *Desalination and Water Treatment, 53*(8), 2215-2234.

Molden, D., Oweis, T., Steduto, P., Bindraban, P., Hanjra, M. A., & Kijne, J. (2010). Improving agricultural water productivity: Between optimism and caution. *Agricultural water management, 97*(4), 528-535.

Morais, E. S., Lopes, A. M. d. C., Freire, M. G., Freire, C. S., Coutinho, J. A., & Silvestre, A. J. (2020). Use of ionic liquids and deep eutectic solvents in polysaccharides dissolution and extraction processes towards sustainable biomass valorization. *Molecules, 25*(16), 3652.

Mulyono, S., Hizaddin, H. F., Wazeer, I., Alqusair, O., Ali, E., Hashim, M. A., & Hadj-Kali, M. K. (2019). Liquid-liquid equilibria data for the separation of

ethylbenzene/styrene mixtures using ammonium-based deep eutectic solvents. *The Journal of Chemical Thermodynamics*, *135*, 296-304.

Narishetty, S. T., & Panchagnula, R. (2005). Effect of L-menthol and 1, 8-cineole on phase behavior and molecular organization of SC lipids and skin permeation of zidovudine. *Journal of Controlled Release*, *102*(1), 59-70.

Nasrullah, A., Saad, B., Bhat, A., Khan, A. S., Danish, M., Isa, M. H., & Naeem, A. (2019). Mangosteen peel waste as a sustainable precursor for high surface area mesoporous activated carbon: Characterization and application for methylene blue removal. *Journal of Cleaner Production*, *211*, 1190-1200.

Ngo, H. H., Guo, W., Zhang, J., Liang, S., Ton-That, C., & Zhang, X. (2015). Typical low cost biosorbents for adsorptive removal of specific organic pollutants from water. *Bioresource technology*, *182*, 353-363.

Ojeda, C. B., & Rojas, F. S. (2018). Vortex-assisted liquid–liquid microextraction (VALLME): the latest applications. *Chromatographia*, *81*(1), 89-103.

Ola, P. D., & Matsumoto, M. (2019). Use of deep eutectic solvent as extractant for separation of Fe (III) and Mn (II) from aqueous solution. *Separation Science and Technology*, *54*(5), 759-765.

Ongondo, F. O., Williams, I. D., & Cherrett, T. J. (2011). How are WEEE doing? A global review of the management of electrical and electronic wastes. *Waste management*, *31*(4), 714-730.

Othmer, D., & Tobias, P. (1942). Liquid-liquid extraction data-the line correlation. *Industrial & Engineering Chemistry*, *34*(6), 693-696.

Parmentier, D., Metz, S. J., & Kroon, M. C. (2013). Tetraalkylammonium oleate and linoleate based ionic liquids: promising extractants for metal salts. *Green Chemistry*, *15*(1), 205-209.

Passos, H., Sousa, A. C., Pastorinho, M. R., Nogueira, A. J., Rebelo, L. P. N., Coutinho, J. A., & Freire, M. G. (2012). Ionic-liquid-based aqueous biphasic systems for improved detection of bisphenol A in human fluids. *Analytical Methods*, *4*(9), 2664-2667.

Pena-Pereira, F., & Namieśnik, J. (2014). Ionic liquids and deep eutectic mixtures: sustainable solvents for extraction processes. *ChemSusChem*, *7*(7), 1784-1800.

Phelps, T. E., Bhawawet, N., Jurisson, S. S., & Baker, G. A. (2018). Efficient and selective extraction of 99mTcO4–from aqueous media using hydrophobic deep eutectic solvents. *ACS Sustainable Chemistry & Engineering*, *6*(11), 13656-13661.

Rad, A. S., Rahnama, R., Zakeri, M., & Jamali, M. R. (2019). Dispersive liquid–liquid microextraction based on green type solvents—" deep eutectic solvents"—for highly selective separation and efficient preconcentration of nickel in water samples. *Journal of the Iranian Chemical Society*, *16*(8), 1715-1722.

Rahnama, R., & Najafi, M. (2016). The use of rapidly synergistic cloud point extraction for the separation and preconcentration of trace amounts of Ni (II) ions from food and water samples coupling with flame atomic absorption spectrometry determination. *Environmental monitoring and assessment*, *188*(3), 150.

Rashed, M. N. (2013). Adsorption technique for the removal of organic pollutants from water and wastewater. *Organic pollutants-monitoring, risk and treatment*, *7*, 167-194.

Ribeiro, B. D., Florindo, C., Iff, L. C., Coelho, M. A., & Marrucho, I. M. (2015). Menthol-based eutectic mixtures: hydrophobic low viscosity solvents. *ACS Sustainable Chemistry & Engineering*, *3*(10), 2469-2477.

Rodríguez-Llorente, D., Cañada-Barcala, A., Muñoz, C., Pascual-Muñoz, G., Navarro, P., Santiago, R., Águeda, V. I., Álvarez-Torrellas, S., García, J., & Larriba, M. (2020). Separation of phenols from aqueous streams using terpenoids and hydrophobic eutectic solvents. *Separation and Purification Technology*, *251*, 117379.

Rooney, D., Jacquemin, J., & Gardas, R. (2010). Thermophysical properties of ionic liquids. *Ionic liquids*, 185-212.

Rosman, N., Salleh, W. N. W., Ismail, A. F., Jaafar, J., Harun, Z., Aziz, F., Mohamed, M. A., Ohtani, B., & Takashima, M. (2018). Photocatalytic degradation of phenol over visible light active ZnO/Ag2CO3/Ag2O nanocomposites heterojunction. *Journal of Photochemistry and Photobiology A: Chemistry, 364*, 602-612.

Ruggeri, S., Poletti, F., Zanardi, C., Pigani, L., Zanfrognini, B., Corsi, E., Dossi, N., Salomäki, M., Kivelä, H., & Lukkari, J. (2019). Chemical and electrochemical properties of a hydrophobic deep eutectic solvent. *Electrochimica Acta, 295*, 124-129.

Salleh, M. Z. M., Hadj-Kali, M., Wazeer, I., Ali, E., & Hashim, M. A. (2019). Extractive separation of benzene and cyclohexane using binary mixtures of ionic liquids. *Journal of Molecular Liquids, 285*, 716-726.

Sarmad, S., Mikkola, J. P., & Ji, X. (2017). Carbon dioxide capture with ionic liquids and deep eutectic solvents: a new generation of sorbents. *ChemSusChem, 10*(2), 324-352.

Sas, O. G., Castro, M., Domínguez, Á., & González, B. (2019). Removing phenolic pollutants using deep eutectic solvents. *Separation and Purification Technology, 227*, 115703.

Sas, O. G., Domínguez, I., González, B., & Domínguez, Á. (2018). Liquid-liquid extraction of phenolic compounds from water using ionic liquids: Literature review and new experimental data using [C2mim] FSI. *Journal of environmental management, 228*, 475-482.

Sas, O. G., Sanchez, P. B., González, B., & Domínguez, Á. (2020). Removal of phenolic pollutants from wastewater streams using ionic liquids. *Separation and Purification Technology, 236*, 116310.

Sato, T., Nishida, T., & Yamatake, M. (1973). The extraction of uranium (VI) and thorium (IV) from nitric acid solutions by tri-n-octyl phosphine oxide. *Journal of Applied Chemistry and Biotechnology, 23*(12), 909-917.

Schaeffer, N., Conceição, J. H., Martins, M. A., Neves, M. C., Pérez-Sánchez, G., Gomes, J. R., Papaiconomou, N., & Coutinho, J. A. (2020). Non-ionic hydrophobic eutectics–versatile solvents for tailored metal separation and valorisation. *Green Chemistry, 22*(9), 2810-2820.

Schaeffer, N., Martins, M. A., Neves, C. M., Pinho, S. P., & Coutinho, J. A. (2018). Sustainable hydrophobic terpene-based eutectic solvents for the extraction and separation of metals. *Chemical Communications, 54*(58), 8104-8107.

Schäfer, A., Broeckmann, A., & Richards, B. (2005). Membranes and renewable energy—a new era of sustainable development for developing countries. *Membrane Technology, 2005*(11), 6-10.

Shabani, E., Zappi, D., Berisha, L., Dini, D., Antonelli, M. L., & Sadun, C. (2020). Deep eutectic solvents (DES) as green extraction media for antioxidants electrochemical quantification in extra-virgin olive oils. *Talanta, 215*, 120880.

Shahrezaei, F., Shamsipur, M., Gholivand, M. B., Zohrabi, P., Babajani, N., Abri, A., Zonouz, A. M., & Shekaari, H. (2020). A highly selective green supported liquid membrane by using a hydrophobic deep eutectic solvent for carrier-less transport of silver ions. *Analytical Methods, 12*(38), 4682-4690.

Shi, Y., Xiong, D., Zhao, Y., Li, T., Zhang, K., & Fan, J. (2020). Highly efficient extraction/separation of Cr (VI) by a new family of hydrophobic deep eutectic solvents. *Chemosphere, 241*, 125082.

Shishov, A., Bulatov, A., Locatelli, M., Carradori, S., & Andruch, V. (2017). Application of deep eutectic solvents in analytical chemistry. A review. *Microchemical Journal, 135*, 33-38.

Shishov, A., Pochivalov, A., Nugbienyo, L., Andruch, V., & Bulatov, A. (2020). Deep eutectic solvents are not only effective extractants. *TrAC Trends in Analytical Chemistry*, 115956.

Silva, N. H., Pinto, R. J., Freire, C. S., & Marrucho, I. M. (2016). Production of lysozyme nanofibers using deep eutectic solvent aqueous solutions. *Colloids and Surfaces B: Biointerfaces, 147*, 36-44.

Smith, E. L., Abbott, A. P., & Ryder, K. S. (2014). Deep eutectic solvents (DESs) and their applications. *Chemical reviews, 114*(21), 11060-11082.

Sorouraddin, S. M., Farajzadeh, M. A., & Dastoori, H. (2020). Development of a dispersive liquid-liquid microextraction method based on a ternary deep eutectic solvent as chelating agent and extraction solvent for preconcentration of heavy metals from milk samples. *Talanta, 208*, 120485.

Sorouraddin, S. M., Farajzadeh, M. A., Dastoori, H., & Okhravi, T. (2021). Development of an air-assisted liquid-liquid microextraction method based on a ternary solidified deep eutectic solvent in extraction and preconcentration of Cd (II) and Zn (II) ions. *International Journal of Environmental Analytical Chemistry, 101*(11), 1567-1580.

Sportiello, L., Favati, F., Condelli, N., Di Cairano, M., Caruso, M. C., Simonato, B., Tolve, R., & Galgano, F. (2022). Hydrophobic Deep Eutectic Solvents in the food sector: focus on their use for the extraction of bioactive compounds. *Food Chemistry*, 134703.

Sulaiman, R., Adeyemi, I., Abraham, S., Hasan, S., & AlNashef, I. (2019). Liquid-liquid extraction of chlorophenols from wastewater using hydrophobic ionic liquids. *Journal of Molecular Liquids, 294*, 111680.

Tadesse, H., & Luque, R. (2011). Advances on biomass pretreatment using ionic liquids: an overview. *Energy & environmental science, 4*(10), 3913-3929.

Tang, B., Zhang, H., & Row, K. H. (2015). Application of deep eutectic solvents in the extraction and separation of target compounds from various samples. *Journal of separation science, 38*(6), 1053-1064.

Tang, W., Dai, Y., & Row, K. H. (2018). Evaluation of fatty acid/alcohol-based hydrophobic deep eutectic solvents as media for extracting antibiotics from environmental water. *Analytical and bioanalytical chemistry, 410*(28), 7325-7336.

Tchinsa, A., Hossain, M. F., Wang, T., & Zhou, Y. (2021). Removal of organic pollutants from aqueous solution using metal organic frameworks (MOFs)-based adsorbents: A review. *Chemosphere, 284*, 131393.

Tereshatov, E., Boltoeva, M. Y., & Folden, C. (2016). First evidence of metal transfer into hydrophobic deep eutectic and low-transition-temperature mixtures: indium extraction from hydrochloric and oxalic acids. *Green Chemistry, 18*(17), 4616-4622.

Thasneema, K., Dipin, T., Thayyil, M. S., Sahu, P. K., Messali, M., Rosalin, T., Elyas, K., Saharuba, P., Anjitha, T., & Hadda, T. B. (2021). Removal of toxic heavy metals, phenolic compounds and textile dyes from industrial waste water using phosphonium based ionic liquids. *Journal of Molecular Liquids, 323*, 114645.

Thirunavukkarasu, A., Nithya, R., & Sivashankar, R. (2020). A review on the role of nanomaterials in the removal of organic pollutants from wastewater. *Reviews in Environmental Science and Bio/Technology, 19*(4), 751-778.

Tomai, P., Lippiello, A., D'Angelo, P., Persson, I., Martinelli, A., Di Lisio, V., Curini, R., Fanali, C., & Gentili, A. (2019). A low transition temperature mixture for the dispersive liquid-liquid microextraction of pesticides from surface waters. *Journal of Chromatography A, 1605*, 360329.

Torres, E., Bustos-Jaimes, I., & Le Borgne, S. (2003). Potential use of oxidative enzymes for the detoxification of organic pollutants. *Applied Catalysis B: Environmental, 46*(1), 1-15.

Tsai, W.-T. (2006). Human health risk on environmental exposure to Bisphenol-A: a review. *Journal of Environmental Science and Health Part C, 24*(2), 225-255.

Van der Bruggen, B., Vandecasteele, C., Van Gestel, T., Doyen, W., & Leysen, R. (2003). A review of pressure-driven membrane processes in wastewater treatment and drinking water production. *Environmental progress, 22*(1), 46-56.

Van Osch, D. J., Dietz, C. H., van Spronsen, J., Kroon, M. C., Gallucci, F., van Sint Annaland, M., & Tuinier, R. (2019). A search for natural hydrophobic deep eutectic solvents based on natural components. *ACS Sustainable Chemistry & Engineering, 7*(3), 2933-2942.

Van Osch, D. J., Dietz, C. H., Warrag, S. E., & Kroon, M. C. (2020). The Curious Case of Hydrophobic Deep Eutectic Solvents: A Story on the Discovery, Design, and Applications. *ACS Sustainable Chemistry & Engineering, 8*(29), 10591-10612.

Van Osch, D. J., Parmentier, D., Dietz, C. H., van den Bruinhorst, A., Tuinier, R., & Kroon, M. C. (2016). Removal of alkali and transition metal ions from water with hydrophobic deep eutectic solvents. *Chemical Communications, 52*(80), 11987-11990.

Van Osch, D. J., Zubeir, L. F., van den Bruinhorst, A., Rocha, M. A., & Kroon, M. C. (2015). Hydrophobic deep eutectic solvents as water-immiscible extractants. *Green Chemistry, 17*(9), 4518-4521.

Vardhan, K. H., Kumar, P. S., & Panda, R. C. (2019). A review on heavy metal pollution, toxicity and remedial measures: Current trends and future perspectives. *Journal of Molecular Liquids, 290,* 111197.

Vasiljevic, T., & Harner, T. (2021). Bisphenol A and its analogues in outdoor and indoor air: Properties, sources and global levels. *Science of the total environment, 789,* 148013.

Vekariya, R. L. (2017). A review of ionic liquids: Applications towards catalytic organic transformations. *Journal of Molecular Liquids, 227,* 44-60.

Verevkin, S. P., Sazonova, A. Y., Frolkova, A. K., Zaitsau, D. H., Prikhodko, I. V., & Held, C. (2015). Separation performance of BioRenewable deep eutectic solvents. *Industrial & engineering chemistry research, 54*(13), 3498-3504.

Verma, R., & Banerjee, T. (2018). Liquid–liquid extraction of lower alcohols using menthol-based hydrophobic deep eutectic solvent: experiments and COSMO-SAC predictions. *Industrial & engineering chemistry research, 57*(9), 3371-3381.

Villegas, L. G. C., Mashhadi, N., Chen, M., Mukherjee, D., Taylor, K. E., & Biswas, N. (2016). A short review of techniques for phenol removal from wastewater. *Current Pollution Reports, 2*(3), 157-167.

Wang, H., Hu, L., Liu, X., Yin, S., Lu, R., Zhang, S., Zhou, W., & Gao, H. (2017). Deep eutectic solvent-based ultrasound-assisted dispersive liquid-liquid microextraction coupled with high-performance liquid chromatography for the determination of ultraviolet filters in water samples. *Journal of Chromatography A, 1516,* 1-8.

Wang, J., & Chen, H. (2020). Catalytic ozonation for water and wastewater treatment: recent advances and perspective. *Science of the total environment, 704,* 135249.

Wang, J., Jing, W., Tian, H., Liu, M., Yan, H., Bi, W., & Chen, D. D. Y. (2020). Investigation of deep eutectic solvent-based microwave-assisted extraction and efficient recovery of natural products. *ACS Sustainable Chemistry & Engineering, 8*(32), 12080-12088.

Wang, Q., & Yang, Z. (2016). Industrial water pollution, water environment treatment, and health risks in China. *Environmental Pollution, 218,* 358-365.

Wang, Q., Yao, L., Hao, L., Li, Y., Wang, C., Wu, Q., & Wang, Z. (2019). Ferrocene-based nanoporous organic polymer as solid-phase extraction sorbent for the extraction of chlorophenols from tap water, tea drink and peach juice samples. *Food chemistry, 297,* 124962.

Wang, X., Lu, Y., Shi, L., Yang, D., & Yang, Y. (2020). Novel low viscous hydrophobic deep eutectic solvents liquid-liquid microextraction combined with acid base induction for the determination of phthalate esters in the packed milk samples. *Microchemical Journal, 159*, 105332.

Warrag, S. E., & Kroon, M. C. (2019). Hydrophobic deep eutectic solvents. *Deep Eutectic Solvents: Synthesis, Properties, and Applications*, 83-93.

Wasi, S., Tabrez, S., & Ahmad, M. (2013). Toxicological effects of major environmental pollutants: an overview. *Environmental monitoring and assessment, 185*(3), 2585-2593.

Wazeer, I., AlNashef, I. M., Al-Zahrani, A. A., & Hadj-Kali, M. K. (2021a). The subtle but substantial distinction between ammonium-and phosphonium-based deep eutectic solvents. *Journal of Molecular Liquids*, 115838.

Wazeer, I., Hadj-Kali, M. K., & Al-Nashef, I. M. (2021b). Utilization of Deep Eutectic Solvents to Reduce the Release of Hazardous Gases to the Atmosphere: A Critical Review. *Molecules, 26*(1), 75.

Wazeer, I., Hayyan, M., & Hadj-Kali, M. K. (2018a). Deep eutectic solvents: designer fluids for chemical processes. *Journal of Chemical Technology & Biotechnology, 93*(4), 945-958.

Wazeer, I., Hizaddin, H. F., El Blidi, L., Ali, E., Hashim, M. A., & Hadj-Kali, M. K. (2018b). Liquid–liquid equilibria for binary azeotrope mixtures of benzene and alcohols using choline chloride-based deep eutectic solvents. *Journal of Chemical & Engineering Data, 63*(3), 613-624.

Wazeer, I., Hizaddin, H. F., Hashim, M. A., & Hadj-Kali, M. K. (2022). An overview about the extraction of heavy metals and other critical pollutants from contaminated water via hydrophobic deep eutectic solvents. *Journal of Environmental Chemical Engineering*, 108574.

Wellens, S., Thijs, B., & Binnemans, K. (2012). An environmentally friendlier approach to hydrometallurgy: highly selective separation of cobalt from nickel by solvent

extraction with undiluted phosphonium ionic liquids. *Green Chemistry, 14*(6), 1657-1665.

Wen, J., Lu, Y., Shi, L., & Yang, Y. (2020). A novel cloud point extraction based on fatty acid deep eutectic solvent combined with high-performance liquid chromatography for determination of ultraviolet absorbent in food packaging bags. *Microchemical Journal, 153*, 104466.

Wenzl, T., Simon, R., Anklam, E., & Kleiner, J. (2006). Analytical methods for polycyclic aromatic hydrocarbons (PAHs) in food and the environment needed for new food legislation in the European Union. *TrAC Trends in Analytical Chemistry*, *25*(7), 716-725.

Wimalawansa, S. J. (2013). Purification of contaminated water with reverse osmosis: effective solution of providing clean water for human needs in developing countries. *International journal of emerging technology and advanced engineering, 3*(12), 75-89.

Wu, Y., Xu, J., Mumford, K., Stevens, G. W., Fei, W., & Wang, Y. (2020). Recent advances in carbon dioxide capture and utilization with amines and ionic liquids. *Green Chemical Engineering*, *1*(1), 16-32.

Xiao, J., Xie, Y., & Cao, H. (2015). Organic pollutants removal in wastewater by heterogeneous photocatalytic ozonation. *Chemosphere, 121*, 1-17.

Yagub, M. T., Sen, T. K., Afroze, S., & Ang, H. M. (2014). Dye and its removal from aqueous solution by adsorption: a review. *Advances in colloid and interface science*, *209*, 172-184.

Yang, M., Hong, K., Li, X., Ge, F., & Tang, Y. (2017). Freezing temperature controlled deep eutectic solvent dispersive liquid–liquid microextraction based on solidification of floating organic droplets for rapid determination of benzoylureas residual in water samples with assistance of metallic salt. *Rsc Advances, 7*(89), 56528-56536.

Yang, X., Diao, C. P., Sun, A. L., & Liu, R. M. (2014). Rapid pretreatment and determination of bisphenol A in water samples based on vortex-assisted liquid–liquid microextraction followed by high-performance liquid chromatography with fluorescence detection. *Journal of separation science, 37*(19), 2745-2750.

Yang, Z., Zhou, Y., Feng, Z., Rui, X., Zhang, T., & Zhang, Z. (2019). A review on reverse osmosis and nanofiltration membranes for water purification. *Polymers, 11*(8), 1252.

Yi, H.-B., Lee, H. M., & Kim, K. S. (2009). Interaction of benzene with transition metal cations: theoretical study of structures, energies, and IR spectra. *Journal of chemical theory and computation, 5*(6), 1709-1717.

Yiantzi, E., Psillakis, E., Tyrovola, K., & Kalogerakis, N. (2010). Vortex-assisted liquid–liquid microextraction of octylphenol, nonylphenol and bisphenol-A. *Talanta, 80*(5), 2057-2062.

Zahoor, I., & Mushtaq, A. (2023). Water pollution from agricultural activities: A critical global review. *Int. J. Chem. Biochem. Sci, 23*(1), 164-176.

Zainal-Abidin, M. H., Hayyan, M., & Wong, W. F. (2021). Hydrophobic deep eutectic solvents: Current progress and future directions. *Journal of Industrial and Engineering Chemistry, 97*, 142-162.

Zante, G., Braun, A., Masmoudi, A., Barillon, R., Trebouet, D., & Boltoeva, M. (2020). Solvent extraction fractionation of manganese, cobalt, nickel and lithium using ionic liquids and deep eutectic solvents. *Minerals Engineering, 156*, 106512.

Zhang, Q., Vigier, K. D. O., Royer, S., & Jérôme, F. (2012). Deep eutectic solvents: syntheses, properties and applications. *Chemical Society Reviews, 41*(21), 7108-7146.

Zheng, T., Wang, J., Wang, Q., Nie, C., Smale, N., Shi, Z., & Wang, X. (2015). A bibliometric analysis of industrial wastewater research: current trends and future prospects. *Scientometrics, 105*(2), 863-882.